ASTRON REPORT 7114-02

VIBRATION TEST PROCEDURES FOR ORBITER SIDEWALL MOUNTED PAYLOADS PHASE II FINAL REPORT

A. G. Piersol
P. H. White
E. G. Wilby
J. F. Wilby

Astron Research and Engineering
3228 Nebraska Avenue
Santa Monica, CA 90404

February 1, 1989

Contract F04701-87-C-0010

Prepared for:
USAF/AFSC
HQ Space Division
P.O. Box 92960
Los Angeles, CA 90009-2960

UNCLASSIFIED
SECURITY CLASSIFICATION OF THIS PAGE

REPORT DOCUMENTATION PAGE

Form Approved
OMB No. 0704-0188

1a. REPORT SECURITY CLASSIFICATION UNCLASSIFIED	1b. RESTRICTIVE MARKINGS NONE
2a. SECURITY CLASSIFICATION AUTHORITY	3. DISTRIBUTION/AVAILABILITY OF REPORT UNLIMITED DISTRIBUTION
2b. DECLASSIFICATION/DOWNGRADING SCHEDULE	
4. PERFORMING ORGANIZATION REPORT NUMBER(S) 7114-02	5. MONITORING ORGANIZATION REPORT NUMBER(S)
6a. NAME OF PERFORMING ORGANIZATION Astron Research & Engineering 6b. OFFICE SYMBOL (If applicable)	7a. NAME OF MONITORING ORGANIZATION USAF/AFSC
6c. ADDRESS (City, State, and ZIP Code) 3228 Nebraska Avenue Santa Monica, CA 90404	7b. ADDRESS (City, State, and ZIP Code) HQ Space Division P.O. Box 92960 Los Angeles, CA 90009-2960
8a. NAME OF FUNDING/SPONSORING ORGANIZATION USAF/AFSC 8b. OFFICE SYMBOL (If applicable)	9. PROCUREMENT INSTRUMENT IDENTIFICATION NUMBER
8c. ADDRESS (City, State, and ZIP Code) HQ Space Division P.O. Box 92960 Los Angeles, CA 90009-2960	10. SOURCE OF FUNDING NUMBERS PROGRAM ELEMENT NO. / PROJECT NO. / TASK NO / WORK UNIT ACCESSION NO

11. TITLE (Include Security Classification)

Vibration Test Procedures for Orbiter Sidewall-Mounted Payloads, Phase II Final Report

12. PERSONAL AUTHOR(S)

Piersol, Allan G., White, Pritchard H., Wilby, Emma G., Wilby, John F.

13a. TYPE OF REPORT	13b. TIME COVERED	14. DATE OF REPORT (Year, Month, Day)	15. PAGE COUNT
FINAL	FROM _____ TO JAN 89	1989 - JAN - 13	

16. SUPPLEMENTARY NOTATION

17. COSATI CODES			18. SUBJECT TERMS (Continue on reverse if necessary and identify by block number)
FIELD	GROUP	SUB-GROUP	

19. ABSTRACT (Continue on reverse if necessary and identify by block number)

Mechanical vibration tests of payloads mounted on the Space Shuttle Vehicle (SSV) cargo bay sidewall are currently performed in compliance with USAF Space Division Document SD-CF-0206, which specifies an acceleration level at the input to the payload. This procedure does not take into account the "loading" of the sidewall structure by the payload at the resonance frequencies of the payload where the payload apparent weight becomes large. The result is potentially severe overtesting of payloads at their resonance frequencies where payload damage is most likely. In this study, a new mechanical vibration test procedure has been developed that takes into account the mounting point impedance of the sidewall structure, and allows a well defined reduction or "notching" of the input acceleration levels at payload resonances based upon an input force limit to the payload. The validity and practicality of the procedure has been demonstrated by experiments on a simulated OASIS payload with an Adaptive Payload Carrier (APC). A complete vibration test specification detailing the procedure is presented.

20. DISTRIBUTION/AVAILABILITY OF ABSTRACT ☒ UNCLASSIFIED/UNLIMITED ☐ SAME AS RPT. ☐ DTIC USERS	21. ABSTRACT SECURITY CLASSIFICATION UNCLASSIFIED
22a. NAME OF RESPONSIBLE INDIVIDUAL	22b TELEPHONE (Include Area Code) / 22c OFFICE SYMBOL

DD Form 1473, JUN 86 *Previous editions are obsolete.* SECURITY CLASSIFICATION OF THIS PAGE

TABLE OF CONTENTS

List of Figures

1. INTRODUCTION

Mechanical vibration tests on payloads mounted on the Space Shuttle Vehicle (SSV) sidewall are currently tested in compliance with the U.S. Air Force Space Division Document SD-CF-0206 [1]. This document requires a conventional input motion controlled vibration test, where the input to the payload at its attachment points is specified in terms of a smoothed acceleration power spectral density (PSD) function in g^2/Hz over a frequency range from 20 to 2000 Hz. The specified input acceleration PSD must be applied over the full frequency range of interest, independent of the dynamic response of the payload; i.e., the specification does not allow for interaction or "loading" of the payload mounting structure by payload resonant responses. The result is a potentially severe overtest at the resonance frequencies of the payload, where the force applied by the shaker to drive the payload to the specified acceleration levels is very large, larger, in fact, than that which could be applied in the real service environment,(see [2] for details and illustrations). This problem is a historic one that arises in the vibration testing of all components that mount on resilient structures.

In Phase I of this study [2], several approaches to alleviate the above problem were investigated, and a new vibration testing procedure for SSV sidewall mounted payloads was formulated where limits on the input force to the payload are specified in conjunction with the desired input acceleration PSD. Specifically, it is recommended that vibration tests be performed in compliance with [1], except the input acceleration PSD is reduced at certain frequencies as required to prevent the input force to the payload from exceeding specified force limits. The force limits are derived from the so called "blocked force" of the SSV sidewall structure, which represents the maximum force that the sidewall can input to an attached payload. The purpose of the Phase II study reported herein is to demonstrate the new test procedure on a simulated SSV sidewall mounted payload, and to finalize a detailed test specification for all SSV sidewall mounted payloads using this procedure.

This report is divided into five sections, including this introductory section, plus two Appendices and an Attachment. Section 2 summarizes relevant background material that is developed and presented in greater depth in [1]. Section 3 details the formulation of mounting point apparent weight functions for the SSV sidewall, from which the applicable force limits for sidewall mounted payloads are derived. Section 4 covers the results of the vibration tests performed on a simulated SSV sidewall mounted payload to verify and demonstrate the new test procedures. Conclusions and recommendations are presented in Section 5. OV-101 apparent weight data and blocked force calculations are presented in Appendix A, and supporting plots and data from the vibration tests are included in Appendix B. The final, recommended vibration test procedure for SSV sidewall mounted payloads is detailed in an Attachment to this report.

2. BACKGROUND

The full theoretical background for the proposed vibration testing procedure is detailed in the Phase I Final Report [2]. The key analytical relationships behind the procedure, and approximations that simplify the implementation of the procedure are reviewed here.

2.1 Review of Recommended Testing Procedure

Assume a vibration test is performed on a shaker with a wire-wound armature such that the armature current has a linear relationship to the armature force. It follows that the Fourier transform (per unit time) of the interface force applied to a payload during a vibration test along any one of the three orthogonal axes of the payload is given by

$$F(f) = K(f)\, C(f) - W_T\, A(f) \tag{1}$$

where

$F(f)$ = Fourier transform of the interface force, lb.
$C(f)$ = Fourier transform of shaker armature current, amp.
$A(f)$ = Fourier transform of the shaker table acceleration, g.
$K(f)$ = Shaker armature force calibration factor, lb/amp.
W_T = Total weight of shaker armature and fixtures, lb.

In terms of spectral density functions, the autospectrum (PSD) of the interface force is given by

$$G_{FF}(f) = |K(f)|^2\, G_{CC}(f) + W_T^2\, G_{AA}(f) - 2W_T\, \mathrm{Re}[K(f)\, G_{CA}(f)] \tag{2}$$

where

$G_{FF}(f)$ = PSD of the interface force, lb^2/Hz.
$G_{CC}(f)$ = PSD of the armature current, amp^2/Hz.
$G_{AA}(f)$ = PSD of the shaker table acceleration, g^2/Hz.
$G_{CA}(f)$ = Cross-spectrum of armature current and shaker table acceleration, amp-g/Hz.
$\mathrm{Re}[\ ]$ = Real part of the complex number in [ ].

and all other terms are as defined in Equation (1). The procedure to establish the shaker current to force calibration factor, $K(f)$, is detailed in [2] and repeated with an illustration in Section 4 to follow. Theoretically, this calibration procedure need be accomplished only once for a given shaker since $K(f)$ is a function only of the shaker armature configuration (number of windings, magnetic field gap and flexure design), which should not change significantly over the life of an undamaged shaker. In practice, however, it

would be prudent to check the calibration of the shaker at least once a year, or after any test that might have caused shaker damage.

In a conventional, motion controlled vibration test, the PSD of the shaker table acceleration is made equal to a specified input PSD provided by a test specification document; e.g., [1]. That is,

$$G_{AA}(f) = G_{TT}(f) \tag{3}$$

where $G_{TT}(f)$ is the input PSD stated in the test specification document. This is done no matter what input force PSD may be required to achieve the specified input acceleration PSD. As detailed and demonstrated in [2], this test procedure commonly results in a severe overtest of the payload at its resonance frequencies where the input force required to achieved the specified input acceleration becomes unrealistically large; i.e., larger than the maximum force that can be delivered from the payload mounting structure in service.

The recommended testing procedure introduces a limit on the input acceleration delivered by the shaker table to the payload, based upon the interface force defined in Equation (1). Specifically, the input acceleration PSD is limited such that the interface force PSD never exceeds the "blocked force" capabilities of the payload mounting structure in its service environment, in this case, the SSV sidewall structure. The blocked force for a mounting structure is defined by

$$F_B(f) = W_S(f)\, A_0(f) \tag{4}$$

where

$F_B(f)$ = blocked force of the mounting structure, lb.

$W_S(f)$ = Apparent weight (reciprocal of accelerance) of the mounting structure, lb/g.

$A_0(f)$ = Free acceleration of the unloaded mounting structure, g.

The blocked force represents the maximum force that the mounting structure (i.e., the SSV sidewall) can deliver to the payload [2]. To obtain an appropriate blocked force limit for a vibration test, assume the free acceleration response of the unloaded mounting structure is equal to the specified input acceleration for the vibration test (this assumption is justified in [2]). In terms of PSD functions, it follows that

$$G_{BB}(f) = |W_S(f)|^2\, G_{TT}(f) \tag{5}$$

where $G_{BB}(f)$ is the PSD of the blocked force and the other quantities are as defined in Equations (3) and (4). The determination of appropriate mounting point apparent weights, $W_S(f)$, for the SSV sidewall along the three orthogonal axes is detailed in Section 3 to follow.

Based upon the forgoing considerations and assumptions, the recommended vibration test procedure is as follows. Apply an input acceleration PSD from the shaker to the payload of

$$G_{AA}(f) = G_{TT}(f) \text{ where } G_{FF}(f) \leq G_{BB}(f) \tag{6}$$

At those frequencies where $G_{FF}(f) > G_{BB}(f)$, limit the input acceleration PSD to the payload to

$$G_{AA}(f) \text{ such that } G_{FF}(f) = G_{BB}(f) \tag{7}$$

2.2 Real Time Implementation

Ideally, the recommended test procedure would be implemented in real time using a test shaker equalization system with a dual control, as follows:

1. One equalizer channel using a shaker table acceleration signal to establish an input acceleration spectrum to the payload that is equal to a specified acceleration spectrum, as is currently done in conventional, motion controlled vibration tests.

2. A second equalizer channel using a combination of shaker armature current signal and acceleration signal to establish an input force spectrum to the payload that is bounded by a specified maximum interface force spectrum, as defined by the blocked force for the payload mounting structure.

The first equalization operation using a table acceleration input signal is presently accomplished by modern, FFT equalizer systems for vibration test shakers. These equalizers generally operate on unit time Fourier transforms of signals, computed using an FFT algorithm, rather than an actual PSD function. Hence, the first equalization operation involves making

$$|A(f)| = [G_{TT}(f)]^{1/2} \tag{8}$$

where $A(f)$ and $G_{TT}(f)$ are as defined in Equations (1) and (3), respectively.

The second equalization operation could be readily achieved by a second equalizer channel using an input force signal computed from the shaker table acceleration signal and the power amplifier current signal via Equation (1). The equalization of the shaker table acceleration spectrum would be controlled by the first

channel, except at those frequencies where the spectrum of the force signal monitored by the second channel exceeds the blocked force spectrum. At such frequencies, the second equalization channel would govern, and the shaker table acceleration spectrum would be reduced as required to make the interface force spectrum equal to the specified force spectrum limit; i.e., from Equations (1), (4), and (5),

$$|F(f)| = |K(f)\, C(f) - W_T\, A(f)| = |F_B(f)| = |W_S(f)|\, [G_{TT}(F)]^{1/2} \qquad (9)$$

where all terms are as defined in Equations (1) through (4). Note that all quantities, excluding W_T, on the left side of Equation (9) are complex Fourier transforms (involving both magnitude and phase).

The dual channel real time equalization procedure defined in Equations (8) and (9) is schematically illustrated in Figure 1. The procedure could be implemented with minor modifications to present FFT shaker equalization systems. Such modifications undoubtedly will be introduced by the manufacturers of shaker equalization systems in the future, if the demand for a combined force and acceleration test procedure becomes sufficiently wide spread.

2.3 Quasi-Real Time Implementation

A dual channel equalization procedure in near real time can be accomplished with present shaker equalization systems using an approximation for the interface force that allows the necessary force calculations to be accomplished using a single channel spectrum analyzer. Specifically, if Equation (1) is written as

$$K(f)\, C(f) = F(f) + W_T\, A(f) \qquad (10)$$

It follows that, in terms of PSD functions

$$G_{FF}(f) = |K(f)|^2\, G_{CC}(f) - W_T^2\, G_{AA}(f) - 2W_T\, Re[G_{FA}(f)] \qquad (11)$$

where $G_{FA}(f)$ is the cross-spectrum between the interface force and the acceleration into the payload, and all other terms are as defined in Equation (2). Now, at the undamped natural frequency of each normal mode of the payload, the phase between the applied force and input acceleration to the payload must theoretically be 90 degrees [3]. Hence, at the undamped natural frequencies of the payload, the last term in Equation (11) should be nil (i.e., $Re[G_{FA}(f)] = 0$), and the input force is given by

$$G_{FF}(f) \approx |K(f)|^2\, G_{CC}(f) - W_T^2\, G_{AA}(f) \qquad (12)$$

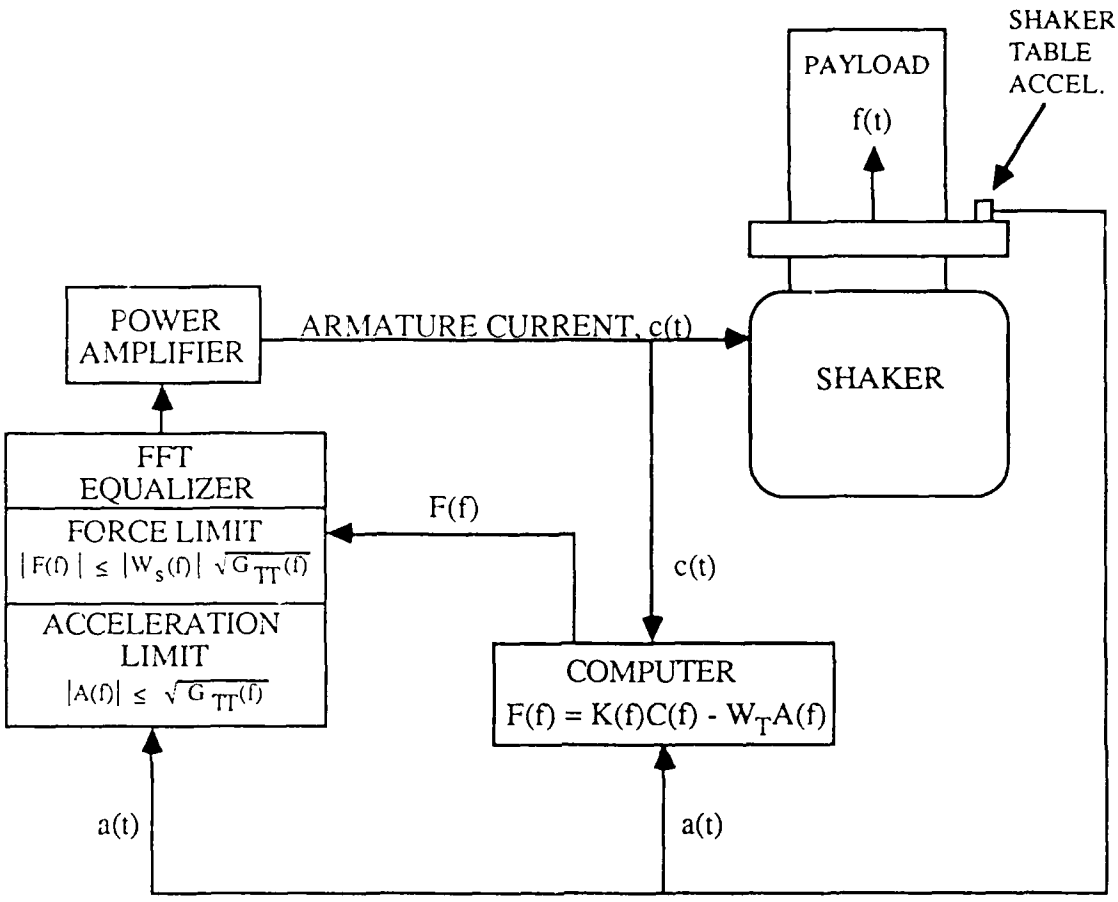

Figure 1. Schematic Diagram of Dual Controlled Shaker-Equalizer System.

where all terms are as defined in Equation (2). Of course, the resonance frequency associated with each normal mode of the payload is always a little less than the undamped natural frequency (by a factor of $[1 - \eta^2]^{1/2}$, where η is the damping ratio [4]). Nevertheless, at the resonance frequencies where the input force becomes excessive, Equation (12) should a reasonable approximation for the input force. This approximation greatly simplifies the equalization procedure because a limiting PSD for the armature current can now be calculated directly from Equations (5) and (12) to be

$$\text{Limit } [G_{CC}(f)] \approx [W_T^2 G_{AA}(f) + |W_S(f)|^2 G_{TT}(f)]/|K(f)|^2 \tag{13}$$

where all terms are as defined in Equations (2) through (4). In Equation (13), $G_{AA}(f) \leq G_{TT}(f)$ and, for the SSV sidewall, $W_T < W_S(f)$ (see Appendix A). Hence, the first term in the brackets is generally very small compared to the second term in the brackets. A further simplification of Equation (13) is achieved by letting $G_{AA}(f) = G_{TT}(f)$, so that

$$\text{Limit } [G_{CC}(f)] \approx [W_T^2 + |W_S(f)|^2] G_{TT}(f)/|K(f)|^2 \tag{14}$$

This PSD for the limiting current can be calculated in advance of the test, and compared to the PSD of the actual armature current calculated on-line as the shaker input vibration to the payload is brought up to the specified input acceleration PSD. As those frequencies where the computed PSD of the armature current reaches the limiting value in Equation (13), the PSD of the input acceleration is not increased further. The application of this quasi-real time equalization procedure is fully demonstrated in Section 4.

To evaluate the accuracy of the approximation for the input force in Equation (14) at resonance frequencies, consider the exact solution of the limiting current given from Equations (5) and (11) by

$$G_{CC}(f) = |W_S(f)|^2 G_{TT}(f) + W_T^2 G_{AA}(f) + 2W_T \, Re[G_{FA}(f)]/|K(f)|^2 \tag{15}$$

It is known that the phase between the input force and the input acceleration to the payload through the normal mode of the payload (approximating a simple oscillator) will pass from 0 to 180 degrees with increasing frequency [4], reaching 90 degrees at the undamped natural frequency. Since the resonance frequency is always less than the undamped natural frequency [3], the phase at resonance will be less than 90 degrees for the first mode. For higher order modes, however, the phase at resonance might be greater than 90 degrees. To evaluate the potential error for either case, consider the extreme limits where the phase at resonance is (a) 0 degrees, and (b) 180 degrees.

2.3.1 Approximation Error With 0 Degree Force to Acceleration Phase

For a zero degree phase shift between the applied force and the input acceleration, assuming the coherence between the force and acceleration is unity, it follows that

$$G_{FA}(f) = [G_{FF}(f)\, G_{AA}(f)]^{1/2} \tag{16}$$

To obtain comparable results, let $G_{AA}(f) = G_{TT}(f)$ in Equation (15), as was done in Equation (14). Noting that the limiting force is $G_{FF}(f) = |W_S(f)|^2\, G_{TT}(f)$, Equation (15) then reduces to

$$G_{CC}(f) = [W_T^2 + |W_S(f)|^2 + 2W_T\, |W_S(f)|]\, G_{TT}(f) \,/\, |K(f)|^2 \tag{17}$$

A direct comparison of the simple approximation in Equation (14) with the result in Equation (17) for a zero degree phase shift suggests that Equation (14) could yield a limiting current for a vibration test that is too low, raising the possibility of an undertest condition at resonance. The magnitude of the undertest is plotted as a function of the ratio, $R_W(f) = W_T/|W_S(f)|$, in Figure 2. In Section 3.4 to follow, it will be seen that the apparent weight of the SSV sidewall structure will generally be very much larger than the weight of the test shaker armature and fixture used for payload tests ($R_W(f) << 1$), at least at frequencies below 200 Hz. It follows from Figure 2 that the potential undertest introduced by the approximation, even at this lower limiting phase condition, should be small compared to the various sources of conservatism inherent in vibration test specifications.

2.3.2 Approximation Error With 180 Degree Force to Acceleration Phase

Now consider the case of a 180 degree phase shift between the applied force and the input acceleration. Again assuming the coherence between the force and acceleration is unity, it follows that

$$G_{FA}(f) = -[G_{FF}(f)\, G_{AA}(f)]^{1/2} \tag{18}$$

Letting $G_{AA}(f) = G_{TT}(f)$, and again noting that the limiting force is $G_{FF}(f) = |W_S(f)|^2\, G_{TT}(f)$, Equation (15) reduces to

$$G_{CC}(f) = [W_T^2 + |W_S(f)|^2 - 2W_T\, |W_S(f)|]\, G_{TT}(f) \,/\, |K(f)|^2 \tag{19}$$

A direct comparison of the simple approximation in Equation (14) with the result in Equation (19) for a 180 degree phase shift suggests that Equation (14) could now yield a limiting current for a vibration test that is too

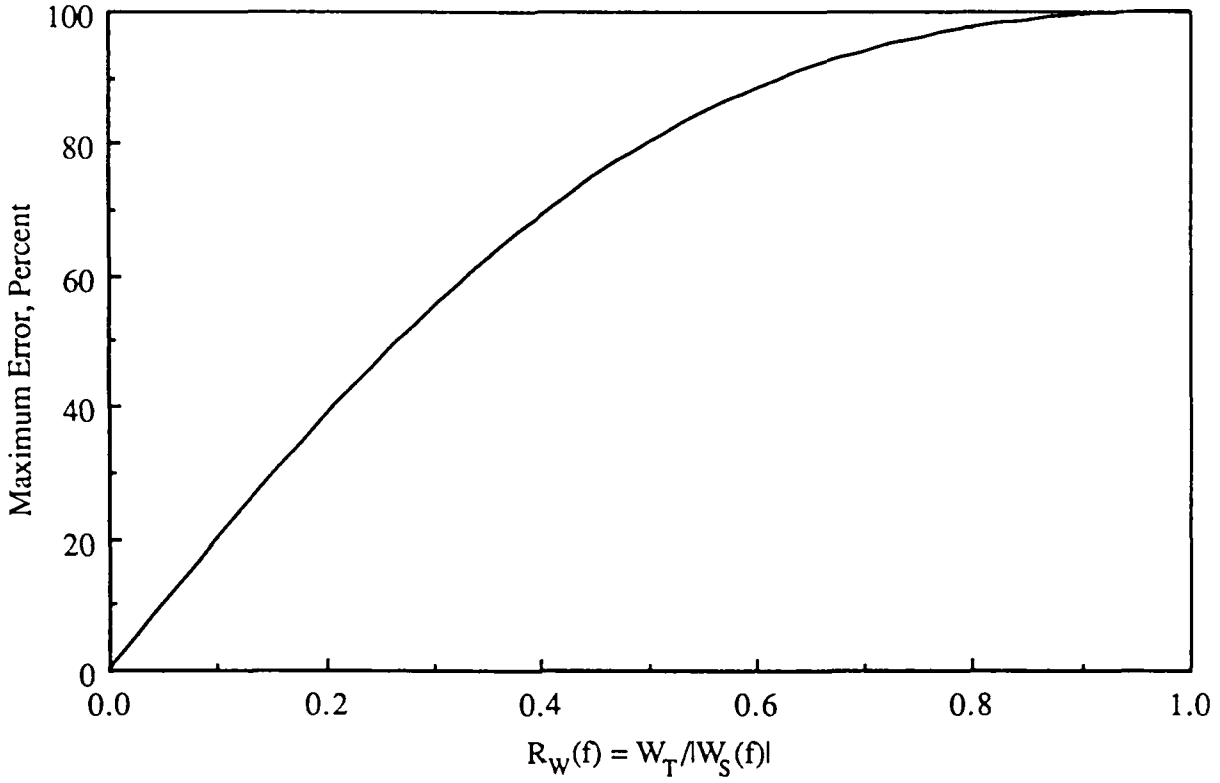

Figure 2. Maximum Undertest or Overtest Error For Simplified Alternate Vibration Test Procedure Using Equation (14) Approximation For Limit Current.

high, leading to a potential overtest. The magnitude of the potential overtest error is the same as the undertest error detailed for the 0 degree phase condition in Figure 2. In this case, however, the potential error is of less concern, since it would simply add additional conservatism to the test procedure. Based upon the arguments presented in Section 2.3.1, the added conservatism of the test will not be unreasonable for the usual case where $R_W(f) << 1$.

2.4 Total Armature Weight Determination

Referring to Equations (9), (11) and (12), the total armature-fixture weight, W_T, is a key parameter in establishing the interface force to the payload during a vibration test. Specifically, when multiplied by the shaker table acceleration, it is essentially a force that must be subtracted from the armature electromagnetic force to obtain the interface force to the payload. It follows that, as W_T becomes large compared to the apparent weight of the payload, a small error in W_T will translate into a large error in the interface force to the payload. Hence, it is desirable for W_T to be as small as feasible for a given payload. In practical terms, this means the shaker and fixtures (including "slip tables") used for a vibration test of a given payload should not be substantially larger than is necessary to achieve the desired test levels. As a rule of thumb, it is desirable to have a W_T that is no larger than the dead weight of the payload being tested.

3. SOURCE APPARENT WEIGHT FUNCTIONS

In developing a bound for the force which could be applied to the payload by the supporting structure in service, the concept of apparent weight has been introduced. Restating Equation (5), the maximum force to be applied to the component under test is

$$G_{BB}(f) = |W_S(f)|^2 G_{TT}(f) \tag{20}$$

It is therefore critical that a reliable estimate of the support structure apparent weight be developed.

A payload will normally be attached to the SSV sidewall at several points. Unless these points are very close together on an extremely stiff structure, there may be sufficient differences in vibration characteristics at the attachment points to produce input forces to the payload that are of different magnitude and phase. This will, in turn, lead to rocking or out-of-plane motion of the payload. When tested on a shaker table, however, the payload is forced to vibrate uniformly in a single direction. Therefore, in defining the apparent weight for purposes of establishing a vibration test specification, it is necessary to consolidate information regarding the dynamic characteristics of the support structure at each of the mounting points into a single function for motion along just one axis. This is equivalent to describing the characteristics of the structure when all the mounting points are constrained to vibrate with uniform motion, i.e., all with the same amplitude and phase.

In this section, an analytical development for appropriately defining an apparent weight is presented. The validity of the procedure is evaluated by an experiment on a simple structure with multiple mounting points. Finally, the OV-101 accelerance measurements are discussed, and the SSV sidewall apparent weight set forth.

3.1 Analytical Considerations

The dynamic characteristics of a linear, multi-degree of freedom system may be described by such attributes as stiffness, compliance, impedance, mobility, accelerance, or apparent weight. These functions relate to the response (in displacement, velocity, or acceleration) at one point on the structure as a result of an excitation (force or moment) at another point. The relations are illustrated in Table 1.

TABLE 1. SYSTEM RESPONSE CHARACTERISTICS

DESCRIPTOR	RELATION	SYMBOL
Stiffness	Force/Displacement	K
Compliance	Displacement/Force	C
Impedance	Force/Velocity	Z
Mobility	Velocity/Force	M
Apparent Weight	Force/Acceleration	W
Accelerance	Acceleration/Force	I

The compliance, mobility, or accelerance of a structure may be directly measured by applying a single force (or moment) to the structure at one point, and measuring the corresponding response quantity at other locations of interest. The force location is then changed and measurements repeated until all pairs of points have been mapped. The result of the process is a 6N x 6N matrix, where each element is a frequency dependent function.

The stiffness, impedance, and apparent weight of a system are not directly measurable as a practical matter. They represent the reactive forces or moments required to hold zero motion at all points when the excitation point is given a unit amount of motion. These quantities are derivable from measurements by the relations

$$[K(f)] = [C(f)]^{-1} \quad \text{(a)}$$
$$[Z(f)] = [M(f)]^{-1} \quad \text{(b)} \qquad (21)$$
$$[W(f)] = [I(f)]^{-1} \quad \text{(c)}$$

The primary measurands in most experimental situations are force and acceleration, hence all the quantities can be derived from the accelerance matrix by the relations

$$[C] = -[I]/\omega^2$$
$$[M] = [I]/i\omega \qquad (22)$$

This discussion is directed toward the measurement of accelerance properties, with apparent weight as a feature to be determined from it.

3.1.1. Payload Apparent Weight Determination

The apparent weight of the payload may be experimentally determined on a vibration shaker table by means of procedures developed earlier [2]. Specifically,

$$W_p(f) = \frac{|K(f)|^2 G_{CC}(f) + W_T^2 G_{AA}(f) - 2W_T \, Re[K(f) G_{CA}(f)]}{K(f) G_{CA}(f) - W_T G_{AA}(f)} \qquad (23)$$

where

$K(f)$ = Calibration factor of shaker, pounds/amp

$G_{CC}(f)$ = Spectral density of shaker current, amp^2/Hz

$G_{AA}(f)$ = Spectral density of shaker acceleration, g^2/Hz

$G_{CA}(f)$ = Cross spectrum of shaker current and acceleration, amp-g/Hz

This formulation is based upon the assumption that the shaker table is sufficiently rigid to drive all the payload mounting points into uniform linear motion along the shaker axis, and that the current applied to the shaker coil is directly proportional to the generated electromagnetic force. No rotational or lateral motion of the attachment points is allowed.

3.1.2 Support Structure Apparent Weight Determination

Because the support structure of an aerospace vehicle carrying the payload is generally quite large and cannot easily be tested on a shaker table, alternate procedures to estimate the apparent weight must be employed. These procedures commonly make use of a small shaker or impulse hammer to excite the structure at the individual attachment points, and measurements of the vibration response at these points.

In very special circumstances, where the payload is rather small and the attachment mounting points are close together, a portable shaker with an appropriate mounting adapter may be fastened directly to the support structure and measurements made. If the resulting motion of the attachment points is truly in unison in the direction of the shaker axis, with no lateral motion or rotation, measurements of shaker current and fixture acceleration may be used in Equation (23) to determine the support structure apparent weight.

A general procedure for determining the apparent weight involves the excitation of the support structure at the payload attachment points, and measurement of the resulting vibration response at the excitation point and all other mounting points. Referring to Figure 3, a force or moment is applied at x, and the linear or rotational response is measured at y. The quantities of interest are thus

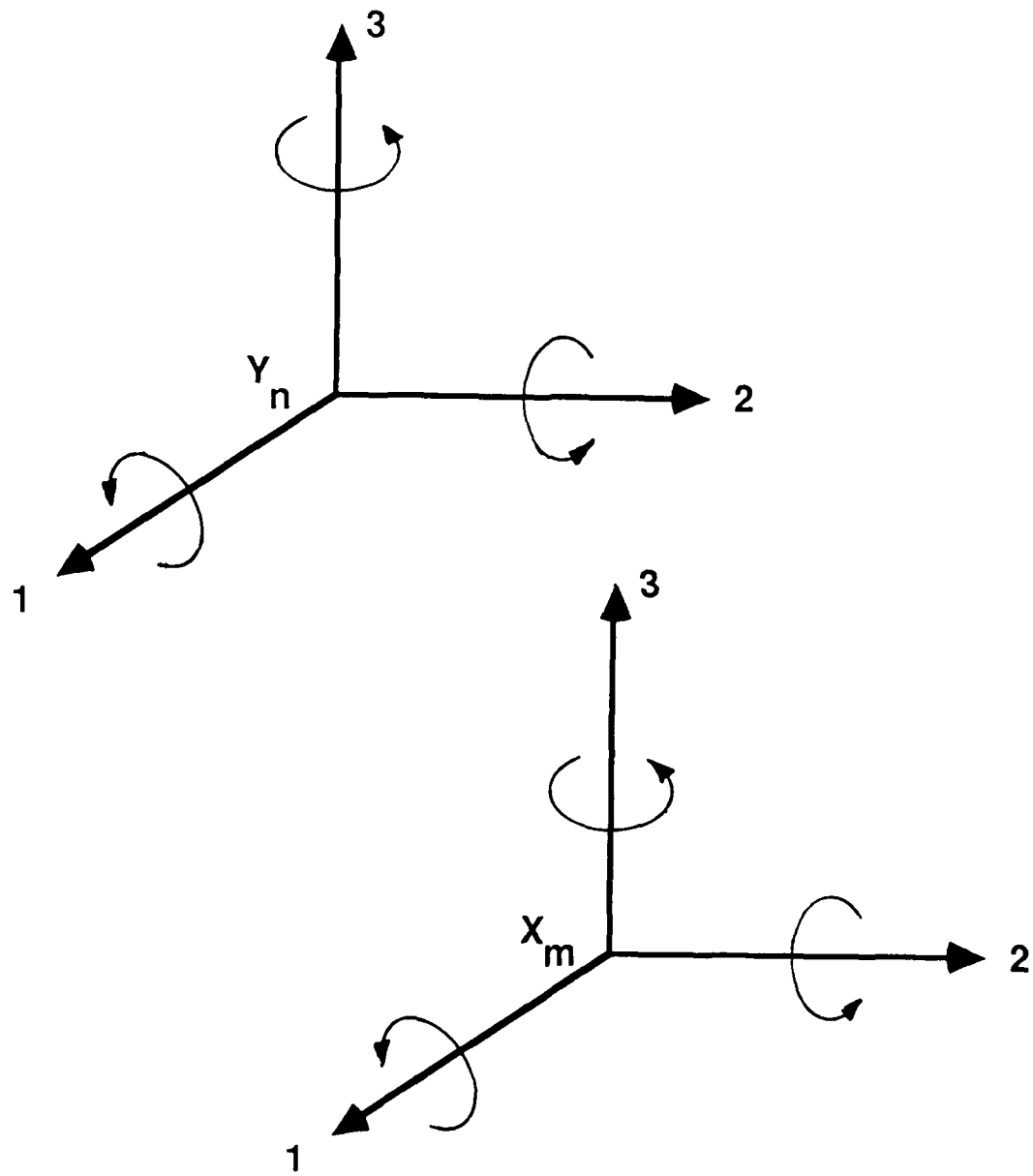

Figure 3. Input and Response Points on Structure.

$F_i(x)$ = Force at x in i direction

$F_j(x)$ = Force at x in j direction

$F_k(x)$ = Force at x in k direction

$M_i(x)$ = Moment at x along i axis

$M_j(x)$ = Moment at x along j axis

$M_k(x)$ = Moment at x along k axis

$A_i(y)$ = Response at y in i direction

$A_j(y)$ = Response at y in j direction

$A_k(y)$ = Response at y in k direction

$\theta_i(y)$ = Rotation at y along i axis

$\theta_j(y)$ = Rotation at y along j axis

$\theta_k(y)$ = Rotation at y along k axis

All the above quantities are, in addition, frequency dependent functions.

Using the above defined quantities, the response of the system to an array of forces and moments at the attachment points is given by

$$\{R\} = [I]\{F\} \tag{24}$$

where {R} is a 6N x 1 column matrix made of 6x1 columns of the form

$$\{R_n\} = \begin{Bmatrix} A_1(y_n) \\ A_2(y_n) \\ A_3(y_n) \\ \theta_1(y_n) \\ \theta_2(y_n) \\ \theta_3(y_n) \end{Bmatrix} \tag{25}$$

The forcing matrix is similarly a 6Nx1 column matrix composed of 6x1 sub-matrices of the form

$$\{F_n\} = \begin{Bmatrix} F_1(y_n) \\ F_2(y_n) \\ F_3(y_n) \\ M_1(y_n) \\ M_2(y_n) \\ M_3(y_n) \end{Bmatrix} \tag{26}$$

The accelerance matrix is a 6Nx6N square matrix composed of 6x6 sub-matrices of the form

$$I_{mn} = \begin{bmatrix} \frac{A_1(y_m)}{F_1(x_n)} & \frac{A_1(y_m)}{F_2(x_n)} & \frac{A_1(y_m)}{F_3(x_n)} & \frac{A_1(y_m)}{M_1(x_n)} & \frac{A_1(y_m)}{M_2(x_n)} & \frac{A_1(y_m)}{M_3(x_n)} \\ \frac{A_2(y_m)}{F_1(x_n)} & \frac{A_2(y_m)}{F_2(x_n)} & \cdots & & & \frac{A_2(y_m)}{M_3(x_n)} \\ \vdots & & & & & \vdots \\ \frac{\theta_3(y_m)}{F_1(x_n)} & \cdots & & & & \frac{\theta_3(y_m)}{M_3(x_n)} \end{bmatrix} \quad (27)$$

The individual terms in the accelerance matrix have the physical meaning of being the response in a given direction at a mounting point to a unit force or moment applied at another mounting point.

It is apparent that a rather comprehensive measurement program is required if all degrees of freedom at each mounting point are considered. A system with four attachment points would call for a 24x24 matrix of frequency dependent functions. Instrumentation, and data analysis errors and variability, can lead to random and/or bias errors in the accelerance terms. Numerical inversion of such a matrix to generate an apparent weight matrix is extremely sensitive to such variations, and is fraught with danger of complete instability or total failure [5].

It is proposed that certain assumptions and approximations be introduced in order to derive a workable and useful procedure to estimate the support structure apparent weight. While these assumptions have not been rigorously checked in a wide range of situations, preliminary results, detailed in Section 3.2, do tend to confirm their validity for the single structural system considered. The first and most significant assumption is that off-axis forces and moments are uncoupled. That is, a force in the i-th direction produces only linear motion in the i-th direction and negligible rotation and motion in the other two directions. The immediate consequence of this assumption is to reduce the accelerance matrix to 6 independent NxN matrices, and allow the equations of motion for the 6 degrees of freedom to be written independently. Thus,

$$\{R_i\} = \begin{Bmatrix} A_i(y_1) \\ A_i(y_2) \\ A_i(y_3) \\ \cdot \\ \cdot \\ A_i(y_n) \end{Bmatrix} = [I_i] \times \begin{Bmatrix} F_i(x_1) \\ F_i(x_2) \\ F_i(x_3) \\ \cdot \\ \cdot \\ F_i(x_3) \end{Bmatrix} \tag{28}$$

where the reduced accelerance matrix is

$$[I_i] = \begin{bmatrix} \frac{A_i(y_1)}{F_i(x_1)} & \frac{A_i(y_1)}{F_i(x_2)} & \frac{A_i(y_1)}{F_i(x_3)} & \cdots & \frac{A_i(y_1)}{F_i(x_n)} \\ \frac{A_i(y_2)}{F_i(x_1)} & \frac{A_i(y_2)}{F_i(x_2)} & \cdots & & \frac{A_i(y_2)}{F_i(x_n)} \\ \cdot & & \cdot & & \cdot \\ \cdot & & & & \cdot \\ \cdot & & \cdot & & \cdot \\ & & & & \\ \frac{A_i(y_n)}{F_i(x_1)} & \cdots & & & \frac{A_i(y_n)}{F_i(x_n)} \end{bmatrix} \tag{29}$$

Vibration testing is performed only along the three orthogonal axes, with no rotation allowed. Considering each axis separately and, in the context of a vibration test on a shaker, the motion to be examined is that where all points move simultaneously with the same amplitude. Thus,

$$\{R_i\} = R_i\{1\} = [I_i]\{F_i\} \tag{30}$$

The total force acting on the mounting points is the sum of elements in the $\{F_i\}$ matrix, that is,

$$\begin{aligned} F_i &= \sum_{n=1}^{N} F_{in} = (1)\{F_i\} \\ &= R_i(1)\,[I_i]^{-1}\,\{1\} \end{aligned} \tag{31}$$

From this, the function representing the apparent weight for rigid body motion in the i-th direction is

$$W_i = F_i/R_i = (1)[I_i]^{-1}\{1\} \tag{32}$$

From the definition of apparent weight in Equation (32), it is seen that the apparent weight of the support structure, when forced to move with uniform motion at the attachment points, is the sum of all the terms in

the apparent weight matrix. A similar result could have been derived by observing that the matrix of forces at the attachment points is

$$\{F_i\} = [W_i]\{1\}R_i \tag{33}$$

and

$$F_i = \sum_{n=1}^{N} F_{in} = (1)[W_i]\{1\}R_i \tag{34}$$

By assuming that motion in the 6 degrees of freedom is uncoupled and independent, the measurement process, and more importantly, the numerical computation of the apparent weight has been greatly reduced.

3.2 Experimental Studies

The expression for apparent weight of a distributed system with multiple mounting points was verified by tests on a steel bar. The test set-up, shown in Figure 4, consisted of a 0.5 in. x 1.25 in. x 29 in. steel bar supported at two points by thin strings. It was excited into lateral vibration at each of the four designated points by a PCB Model B02 impact hammer, and the resulting motion at all four points was measured with a PCB 30303 accelerometer (2 grams). Signals from the force transducer in the hammer and the accelerometer were captured on a Hewlett-Packard 3562A signal analyzer. In the transient mode, the force signal was used to trigger the signal capture. The frequency response function relating the response acceleration to the input force was measured for all pairs of points, with each response function being the average from 10 repeated hits. The analysis was performed over the frequency range 0-800 Hz, with one Hz resolution. A typical frequency response function is shown in Figure 5. This illustrates the modal structure of the undamped bar. The modes are in agreement with calculated frequencies for a free-free beam.

Frequency response functions generated on the HP-3562A were transferred via an IEEE-488 bus to a Compaq 286 PC for additional processing. These data represented a 4 x 4 accelerance matrix. The complex matrix was inverted to obtain an apparent weight matrix. Application of Equation (32) then resulted in the single, frequency dependent apparent weight function shown in Figure 6.

If the bar had been mounted on a shaker table and driven into uniform motion at the four attachment points, it would appear as a rigid mass at low frequencies. In this frequency region the apparent weight is the actual

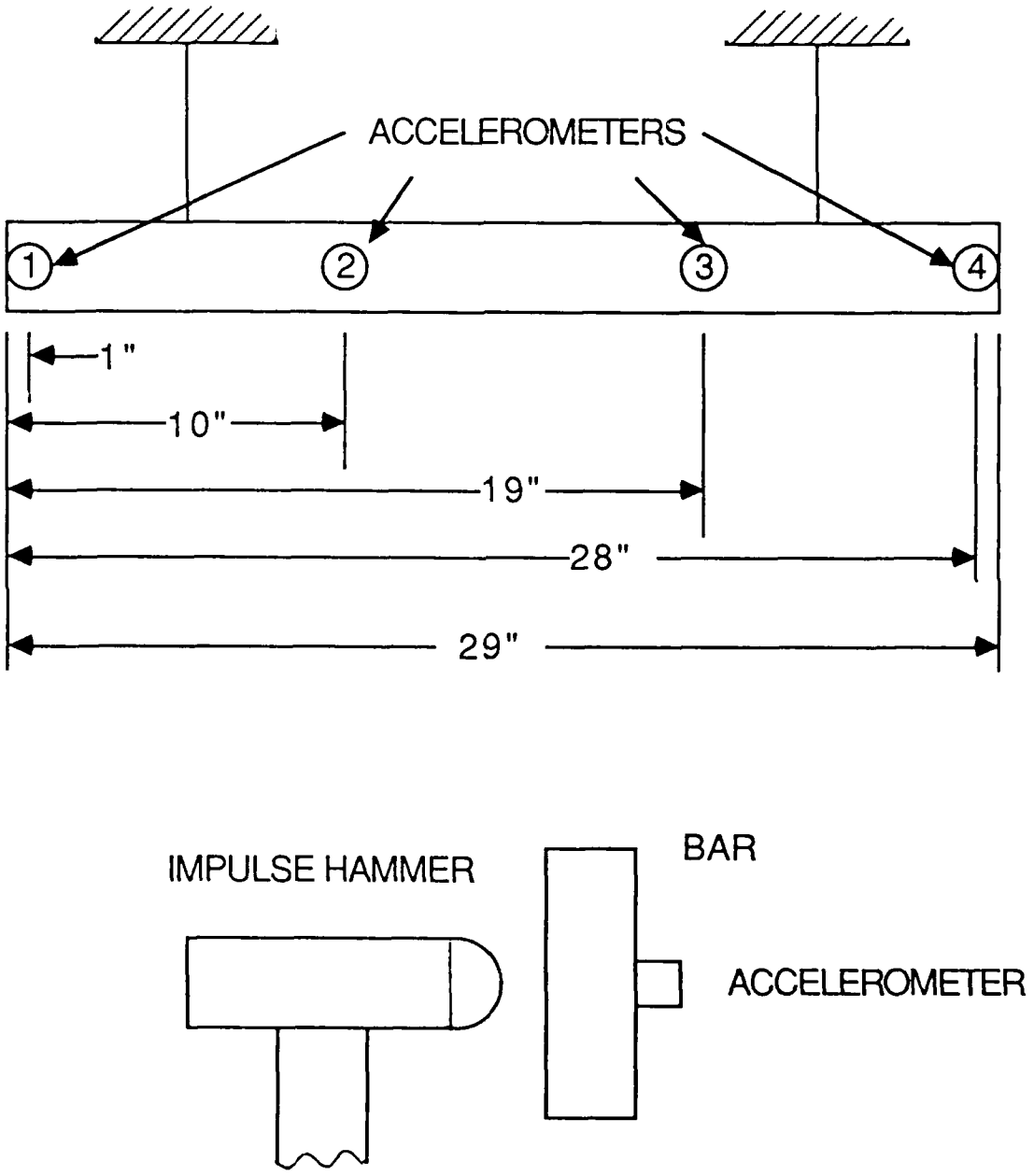

Figure 4. Accelerance Measurements on Bar.

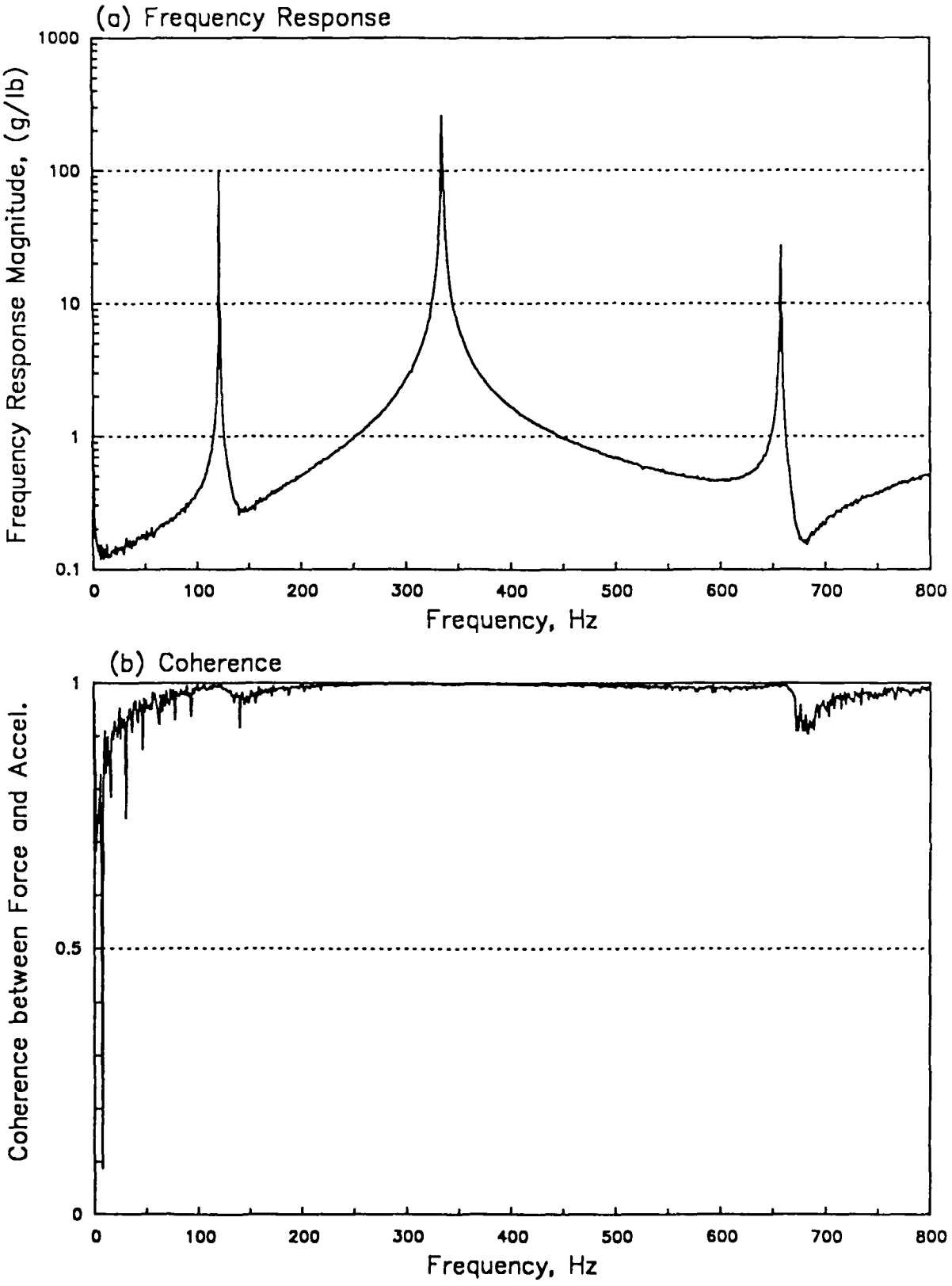

Figure 5. Accelerance at Location 3. Steel Bar (5.22 lb) Accelerance Tests, using Hammer Excitation.

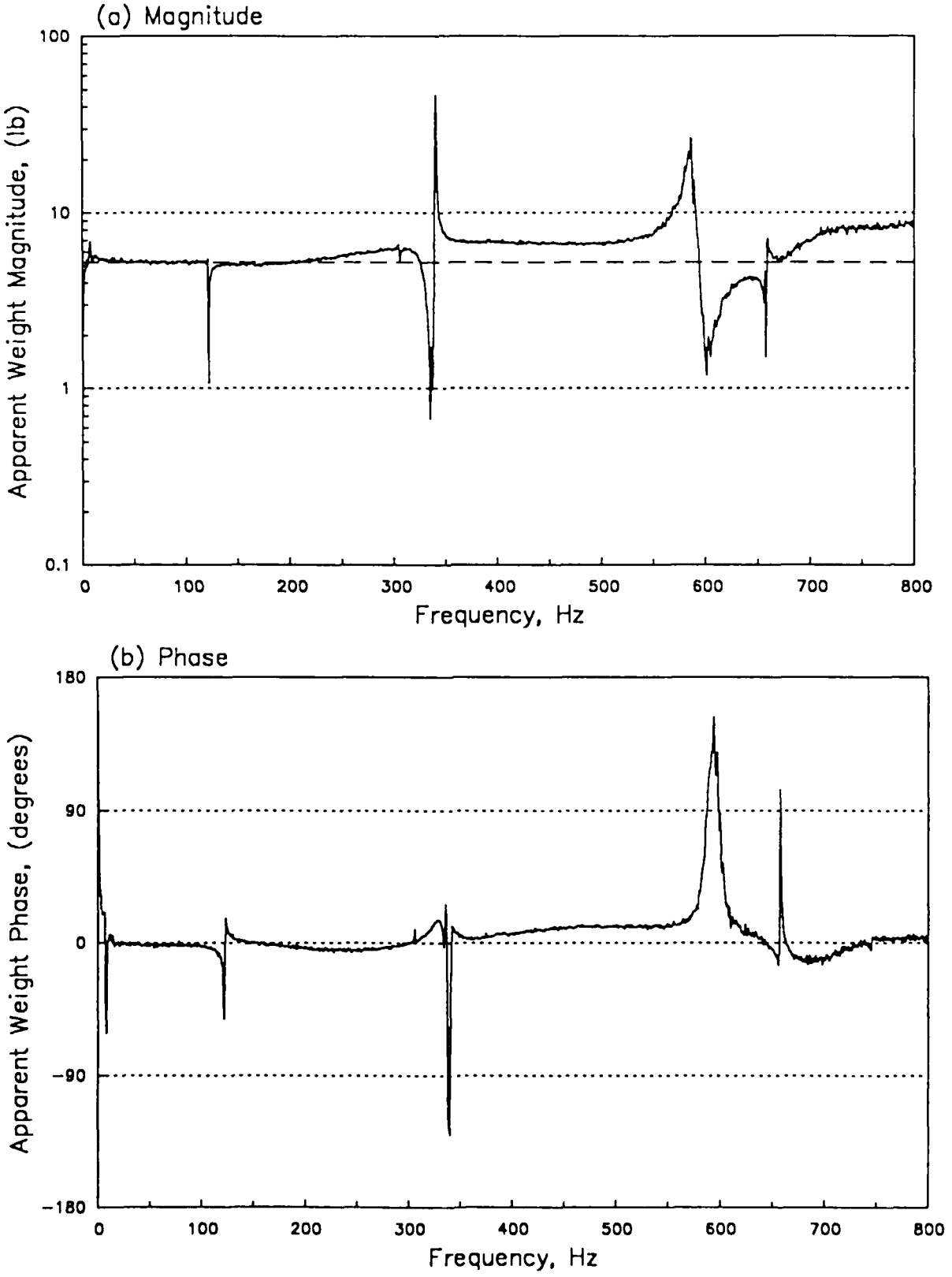

Figure 6. Apparent Total Weight of System. Steel Bar (5.22 lb) Accelerance Tests, using Hammer Excitation.

weight of the bar. The validity of the measurement and analysis procedure set forth in this section is demonstrated by comparison of the apparent weight estimated by Equation (32) with the actual weight (dashed line) in Figure 6. For further comparison, normal mode analysis was used to develop an analytical expression for the apparent weight of the beam. This function, shown in Figure 7, exhibits a behavior resembling the apparent weight developed from the experiment.

The close agreement of the estimated apparent weight with the actual weight indicates the procedure set forth above may be useful and accurate. It must be noted, however, that the calculation of apparent weight from accelerance measurements involves complex matrix manipulations. Small errors of phase and magnitude (systematic or random) have a severe destabilizing effect upon the matrix inversion, leading to erroneous results. Indeed, all known past efforts to calculate a net apparent weight from the full matrix of accelerance measurements on actual structures have been unsuccessful. Hence, the procedure is considered impractical.

3.3 Apparent Weight Approximation Procedures

Based upon the conclusions from Section 3.2, an approximation in the form of a bound on the net mounting point apparent weight of the SSV sidewall structure is developed using only the diagonal terms in the accelerance matrix. To do this, certain assumptions must be made.

In the first case, consider low frequency motion of a system which has bending wavelengths much longer than the spacing between mounting points. A force applied to one point will move all the points in phase, but with possible different amplitudes. When the payload is mounted on the points and constrained to move in the single direction, its motion is controlled primarily by the point with the least accelerance or highest apparent weight. Here, an upper bound for the apparent weight of the support structure would be the maximum of the apparent weights (or inverse of the accelerances) at the attachment points.

At very high frequencies, in the range where the modal density is quite high, vibration of the mounting points will be essentially uncoupled and independent. This would lead to an accelerance matrix with very small off-diagonal terms. The apparent weight matrix resulting from the inversion of this matrix would similarly be nearly diagonal, and the elements approximately the inverse of the corresponding accelerance matrix elements ($W_{ij} = I_{ij}^{-1}$). An approximation for the structure apparent weight would be the sum of apparent weight terms in the apparent weight matrix. A slightly conservative upper bound for the apparent weight of the structure would then be the maximum value of the apparent weights of the mounting points multiplied by the number of mounting points.

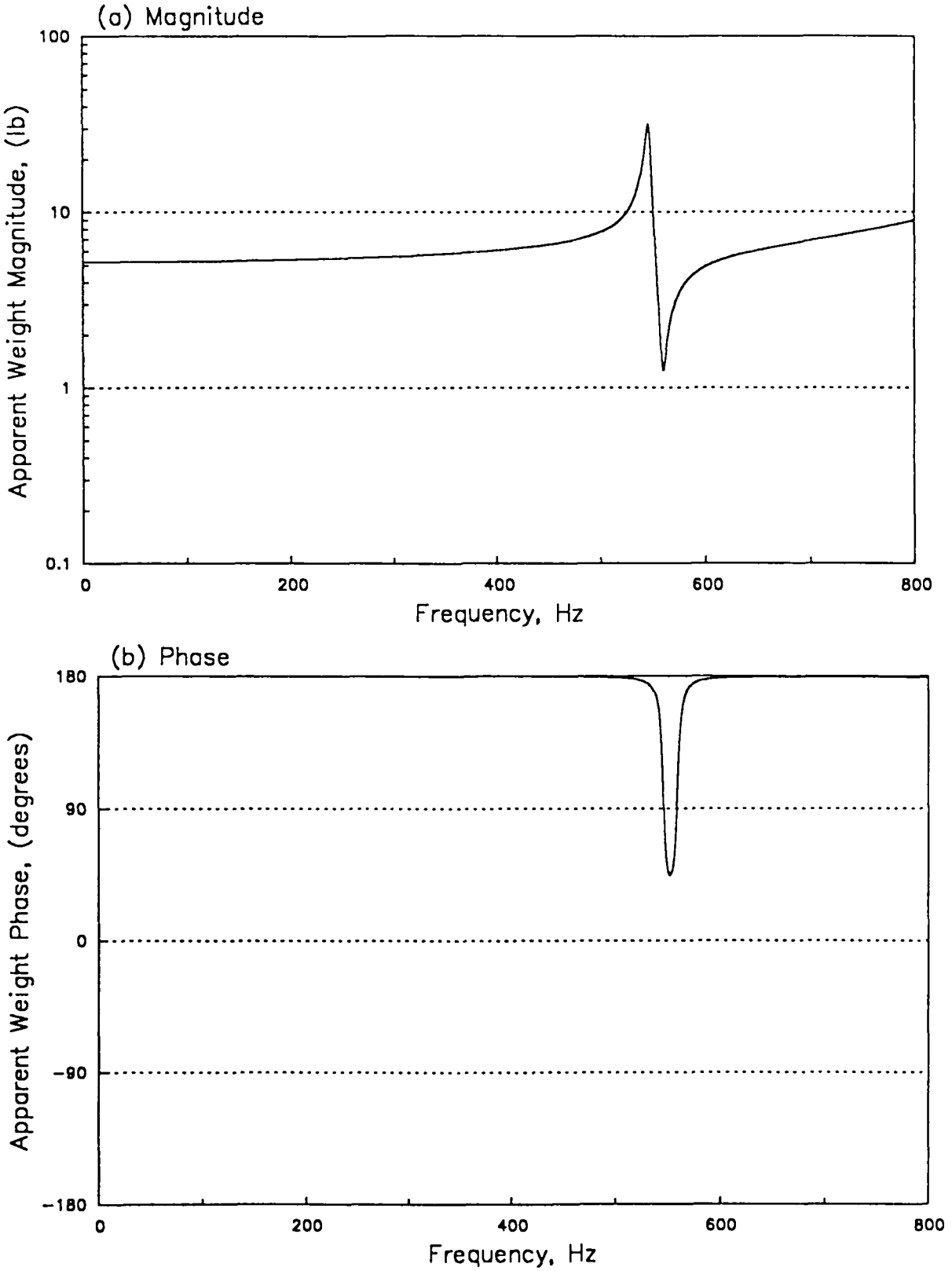

Figure 7. Apparent Total Weight of System. Loss Factor=1%. Steel Bar (5.22 lb) Freely-Supported using 5 Modes with Measured Frequencies.

As an example of this bounding process, the experimental data from the accelerance measurements on the steel bar have been used to generate approximations and upper bounds. These are shown in Figure 8. Because the modal density of the bar is quite low in the frequency range considered, there are several large excursions of the approximation functions. The two bounding values considered are clearly not effective at these frequencies. However, at the higher frequencies above 600 Hz, the bounding values appear to provide reasonable approximations for the net apparent weight. Further experimental investigation of high modal density structures is required to adequately confirm the assumption over a broad frequency range.

3.4 Assessments of OV-101 Accelerance Data

The available apparent weight data for the SSV sidewall were obtained from accelerance measurements made on the first orbiter vehicle (OV-101) at Dulles International Airport in Washington, D.C., by personnel of the NASA Goddard Space Flight Center (GFSC) [2]. The measurements were made as closely as possible to the various attachment points for the Adaptive Payload Carriers (APC) or the Increased Capacity Adaptive Payload Carriers (ICAPC) that interface sidewall mounted payloads to the orbiter structure (both hereafter referred to simply as an APC). An APC attaches to the orbiter sidewall at three locations, which will be denoted as follows (see [2] for detailed descriptions):

L1 - On the 410 longeron providing firm restraint along the x, y, and z axes.

L2 - On a frame (main or stub) providing firm restraint along the z axis, a gapped restraint along the y axis, and no restraint along the x axis.

L3 - On a frame (main or stub) providing a gapped restraint along the y axis, and no restraint along the x and z axes.

Full details of the OV-101 accelerance measurement procedures and general evaluations of the measurements are presented in the Phase I Report [2]. Of concern now are more detailed assessments of the applicability of the data to a determination of the net source apparent weight of the SSV sidewall as seen by an APC/payload along the three orthogonal axes, with special attention to (a) how representative the OV-101 measurements are of the actual APC mounting points, and (b) the possible errors that may be introduced by nonlinear sidewall response characteristics.

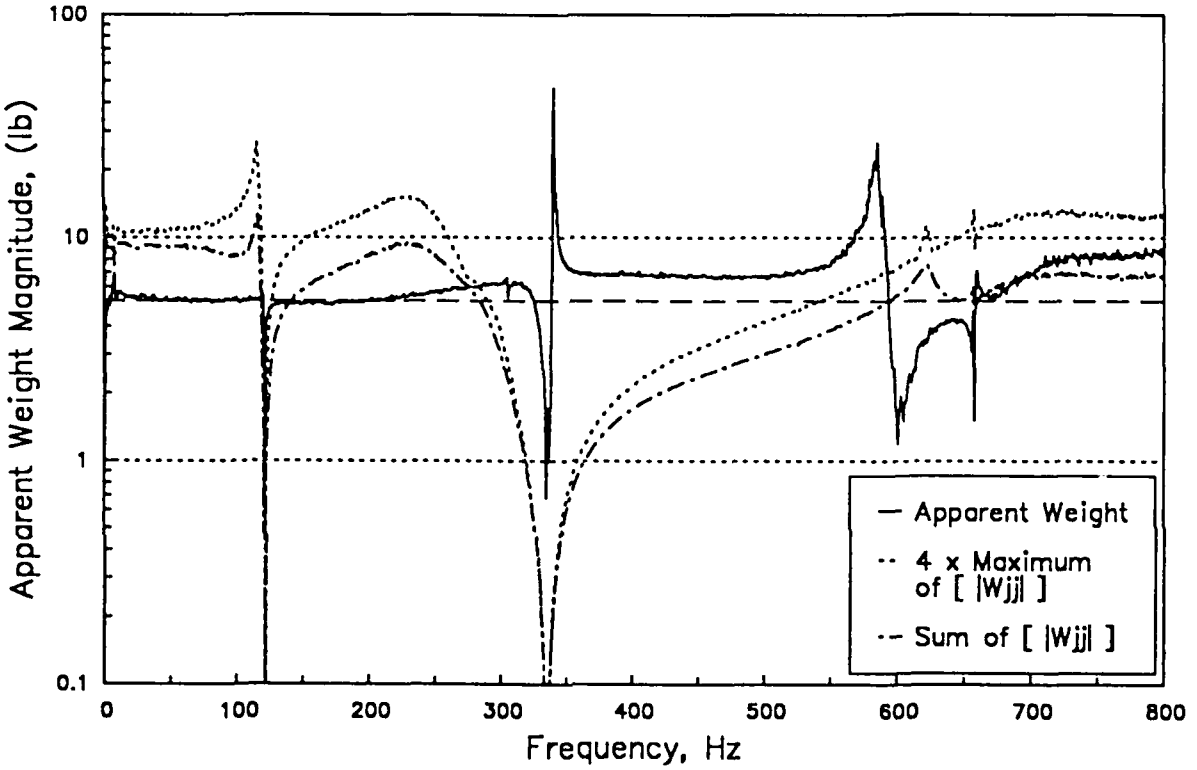

Figure 8. Approximations and Bounds of Apparent Weight for Steel Bar

3.4.1 Representation of APC Mounting Point Locations

Longitudinal (X) Axis Measurements - The only accelerance measurements that could be made along the x axis of the APC attachment points were on the side of the webs for the main and stub frames. After careful review of the resulting data, it has been concluded that these x axis measurements are not adequately representative of the single attachment point that restrains the APC along the x axis, namely, on the 410 longeron (location L1).

Lateral (Y) Axis Measurements - The accelerance data acquired in the y direction are considered fully representative, because all measurements were made at the actual mounting points for APC's. Also, the y axis measurements on the different types of structure (the 410 longeron, various main frames, and various stub frames) produced similar results that allowed the data to be pooled for a single y axis apparent weight function for all attachment points.

Vertical (Z) Axis Measurements - The z axis measurements are also considered fully representative for the L1 locations, because these measurements were made on the 410 longeron immediately above the APC attachment points. However, the L2 locations on either a main frame or a stub frame are about 1 ft below the points where the z axis measurements were made. Nevertheless, due to the high stiffness of the frames along their longitudinal axis, and the relatively short distance of the frame attachment locations from the actual measurement locations, the L1 location data along the z axis are considered acceptably representative of the z axis apparent weight at L2. As for the y axis data, the z axis apparent weight measurements at different positions on the longeron produced similar results that allowed the data to be pooled for a single z axis apparent weight function for all attachment points.

3.4.2 Linearity Considerations

The accelerance data measured on the OV-101 vehicle by GSFC were acquired using a force hammer (a transient input procedure). The force applied for each measurement had a peak value of 50 to 100 lbs, and the coherence function associated with the accelerance measurements over the frequency range from 20 to 200 Hz was typically near unity. This verifies that there are no significant nonlinearities in the orbiter sidewall structural response in this frequency range [6] up to the peak response acceleration level produced by the hammer impacts. These peak response accelerations were not noted during the measurements, but there is little doubt that they were somewhat less than the structural response accelerations that occur during launch. Hence, the high coherence values produced by the accelerance measurements do not conclusively rule out the possibility of significant nonlinear structural response characteristics at the peak launch vibration levels.

To further evaluate possible nonlinearities in the orbiter sidewall structure response at launch vibration levels, the ratio of vibration to acoustic levels during a highly nonstationary period of the SSV launch environment was investigated. If the structural response is linear, this ratio should be nearly constant. The study was performed using vibration and acoustic data from the STS-2 launch [8]. The specific data employed were the vibration measurement made by Accel 389 mounted on the orbiter sidewall structure near the attachment point for the DFI package, and the acoustic measurement made by Mic 220 inside the cargo bay above the DFI package (see [8] for further measurement location details). An internal microphone was selected for the evaluation because it better represents the integrated acoustic loads over the exterior of the orbiter structure than a single exterior measurement. Of course, the internal acoustic measurement might also be influenced by nonlinearities in the SSV cargo bay structure. However, the acoustic levels at the selected measurement location are dominated by acoustic transmission through the cargo bay doors, rather than the sidewall structure where the vibration measurement was made. Although there is no firm proof that the door transmission is linear, it is highly unlikely than it would have nonlinear response properties identical to those of the sidewall structure. The data measured during the lift-off phase are of greatest interest, since they show a dramatic change in level, exceeding a 10 dB change in less than 5 sec.

The ratio of the overall (10-2000 Hz) vibration to acoustic pressure levels computed over contiguous 1 sec intervals during the lift-off of STS-2 are shown in Figure 9 (T+x sec denotes the start of the interval relative to SRB ignition). Data prior to T+3 sec are excluded to eliminate the lift-off transient and other nonhomogeneous effects caused by the SRB ignition. Also shown in Figure 9 are the overall vibration levels during this event, which vary from a high of about 11 g to a low of about 2 g over the event. It is seen in Figure 9 that the ratio of vibration response to acoustic excitation is essentially constant as the vibration response passes through maximum levels.

In conclusion, it is not possible, using available data, to prove the SSV cargo bay sidewall structure has linear response properties over the range of vibration response levels experienced during launch. On the other hand, there is no evidence to indicate that nonlinearities might constitute a significant source of error in the GSFC accelerance measurements made on the OV-101 sidewall. Hence, the OV-101 data are considered to provide an acceptable basis (with the restrictions noted in Section 3.4.1) for the derivation of the SSV sidewall mounting point apparent weights needed to implement the recommended vibration testing procedure.

3.5 Derivation of Net Apparent Weights

The orbiter sidewall mounting point apparent weights determined from the accelerance measurements on OV-101 [2] at the various locations along each of the orthogonal axes were pooled, and an average magnitude and standard deviation of the apparent weight functions were computed. These results for the y and z axis

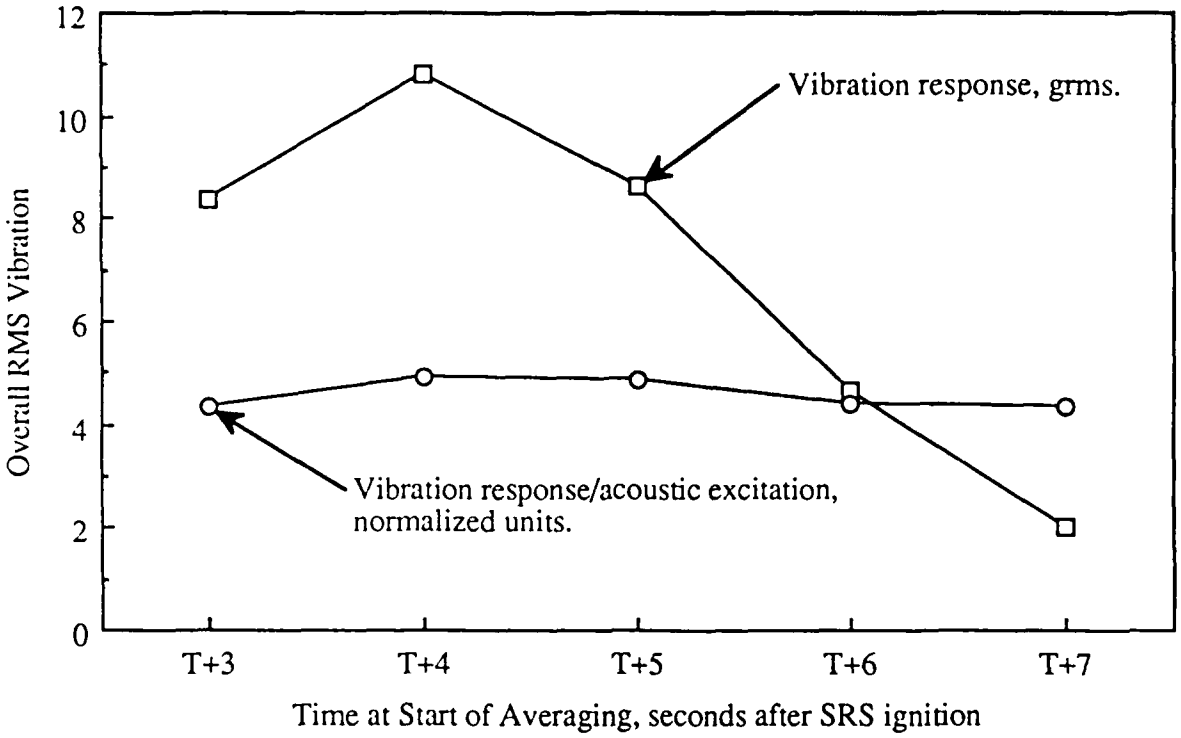

Figure 9. SSV Sidewall Vibration Response During Lift-Off (STS-3).

measurements are detailed in Appendix A (the x axis results are not considered representative, as discussed in Section 3.4). Since an APC attaches to the sidewall structure at three point along the y axis and two points along the z axis, it is necessary to translate the apparent weights for individual points to a net mounting point apparent weight for the APC/payload. At the very low frequencies, where the response of the supporting structure to an applied force at any one point is similar to, and in phase with, the response at all points, the apparent weight at a single location is representative of the net mounting point apparent weight seen by the APC/payload. At the higher frequencies, however, the different mounting points start to appear as independent structural elements, and the net mounting point apparent weight seen by the APC/payload may be approximated reasonably well by the sum of the apparent weights of the individual mounting points (see Section 3.3). To be conservative, this latter situation is assumed to exist for all APC mounting points on the orbiter sidewall at frequencies above 20 Hz.

3.5.1 Lateral (Y) Axis Net Apparent Weight

Since the APC is constrained in the y direction at three locations, an upper bound on the net apparent weight seen by the APC/payload along the y axis was computed by

$$W_{ny}(f) = 3\, W_y(f) + k\, [3\, s^2_y(f)]^{1/2} \qquad (35)$$

where

$W_y(f)$ = Average of apparent weight measurements along the y axis

$s_y(f)$ = Standard deviation of apparent weight measurements along the y axis

k = Tolerance factor for upper bound

To assure a conservative estimate, a tolerance factor of $k = 2$ was used. For the sample size involved in the average and standard deviation calculations ($n = 16$), $k = 2$ corresponds to an approximate upper 90% normal tolerance limit [9]; i.e, the net apparent weights at more than 90% of the APC mounting locations on the orbiter sidewall should be below the value calculated in Equation (35). The calculations using Equation (35) are detailed in Appendix A.

3.5.2 Vertical (Z) Axis Net Apparent Weight

Since the APC is constrained in the z direction at only two locations, an upper bound on the net apparent weight seen by the APC/payload along the z axis was computed by

$$W_{nz}(f) = 2\, W_z(f) + k\, [2\, s^2_z(f)]^{1/2} \qquad (36)$$

where

$W_z(f)$ = Average of apparent weight measurements along the z axis

$s_z(f)$ = Standard deviation of apparent weight measurements along the z axis

k = Tolerance factor for upper bound

As before, to assure a conservative estimate, a tolerance factor of k = 2 was used. For the sample size involved (n = 14), the results again correspond to an approximate upper 90% tolerance interval. The calculations using Equation (36) are detailed in Appendix A.

3.6. Derivation of Blocked Forces

The spectral densities of the blocked force in both the y and z directions were computed using Equation (5), with the net apparent weights estimated by Equations (35) and (36), and the vibration test levels specified in [1]. The results are detailed in Appendix A, and are plotted in Figures 10 and 11. To facilitate simulation procedures and provide a relatively simple analytical description, the "raw" estimates of the blocked force spectral density functions in Figures 10 and 11 were smoothed using a sequence of straight lines on a log magnitude versus a log frequency scale. In the smoothing operation, some peaks in the raw blocked force estimates were blurred out, particularly at the lower frequencies. This was done with the understanding that the computed blocked forces in Figures 10 and 11 already include substantial conservatism from three sources, as follows:

(a) The assumption that the net apparent weight is the sum of the individual apparent weights, which is particularly conservative at the lower frequencies (see Section 3.3).
(b) The use of an approximate 90% upper tolerance limit to define the net apparent weights (see Section 3.5).
(c) The inherent conservatism in the vibration test levels specified in [1].

Hence, the smoothing produced no significant risk of underestimating the force limit applicable to SSV sidewall mounted payloads. The smoothed blocked force spectral density functions are presented in Figures 12 and 13. These plots constitute the upper force limits for the vibration testing along the y and z axes of all Space Shuttle sidewall mounted payloads. There is high confidence that these force limits are conservative.

The remaining issue is to establish an appropriate upper force limit for the vibration testing of SSV sidewall mounted payloads along the x axis. The APC is constrained at only one attachment point in the x direction, namely, on the 410 longeron (L1). As explained earlier in Section 3.4, it was not possible in the OV-101 experiments [2] to measure the apparent weight (accelerance) on the 410 longeron in the x direction. However, from simple geometric considerations, it is clear that the apparent weight of the longeron in the x

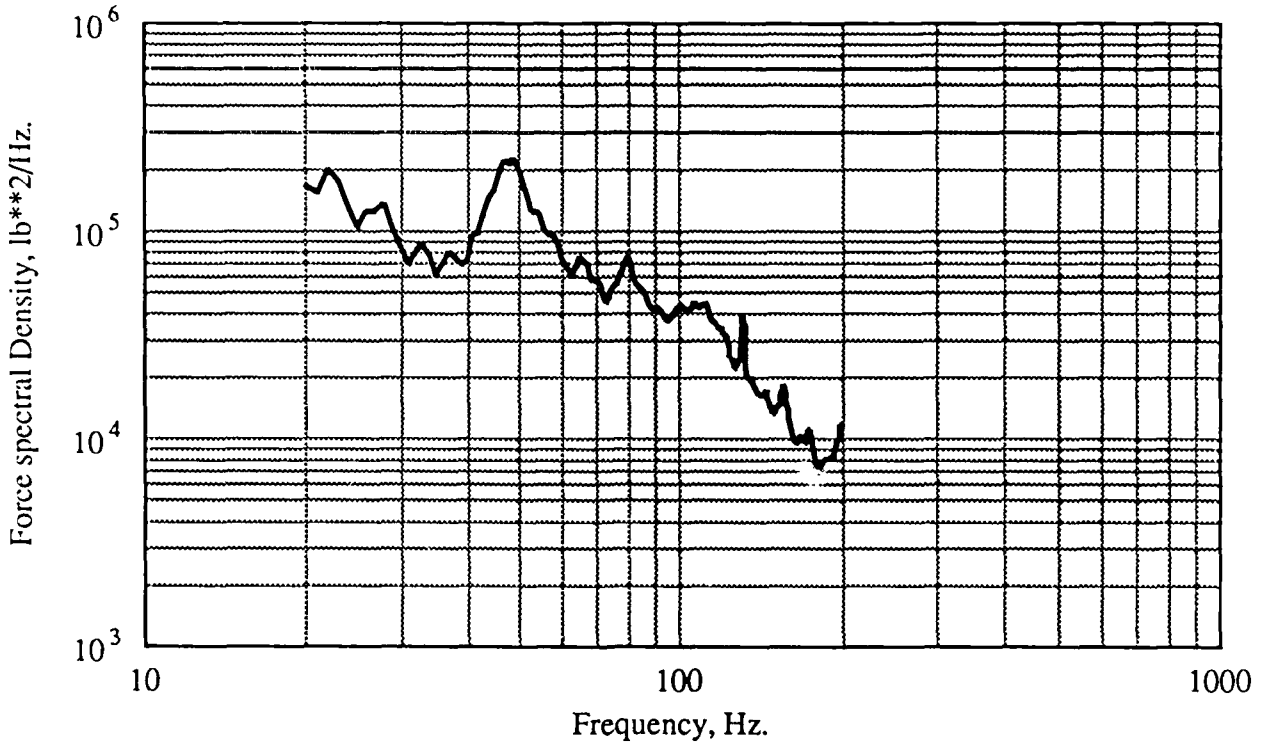

Figure 10. Raw PSD of Estimated Blocked Force for Y Axis.

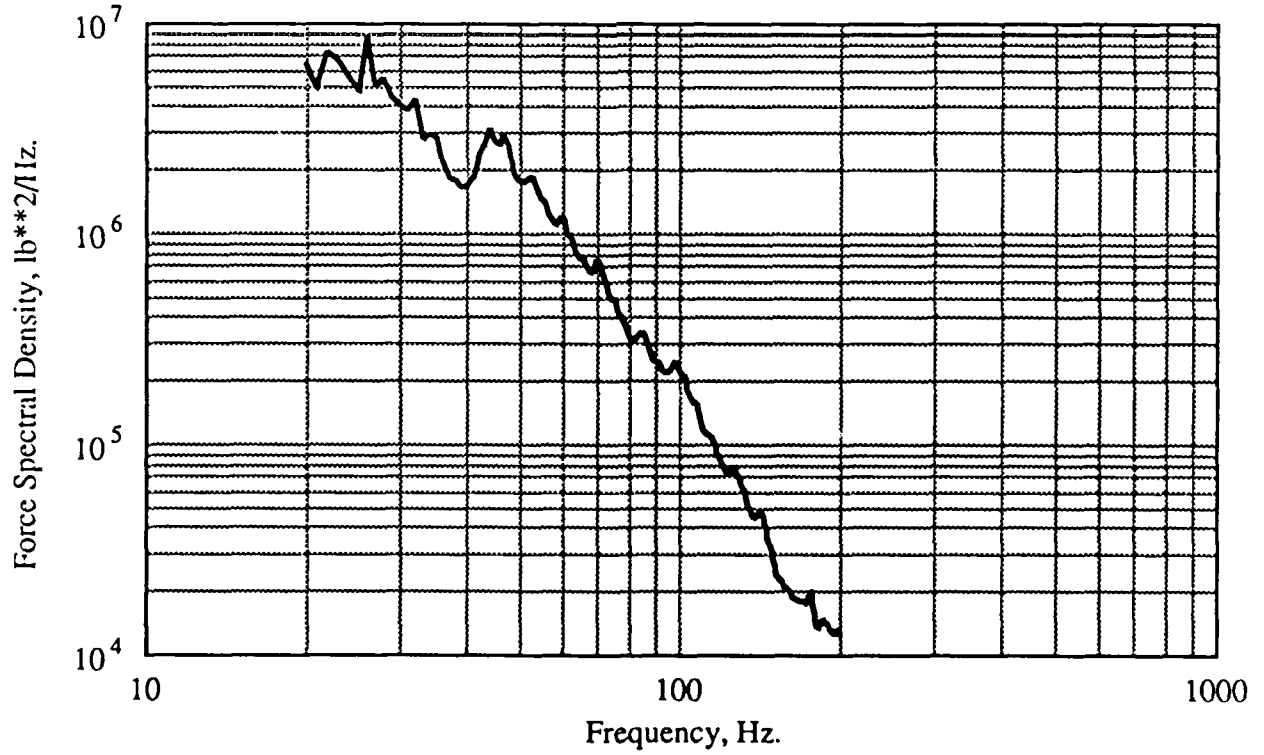

Figure 11. Raw PSD of Estimated Blocked Force for Z Axis.

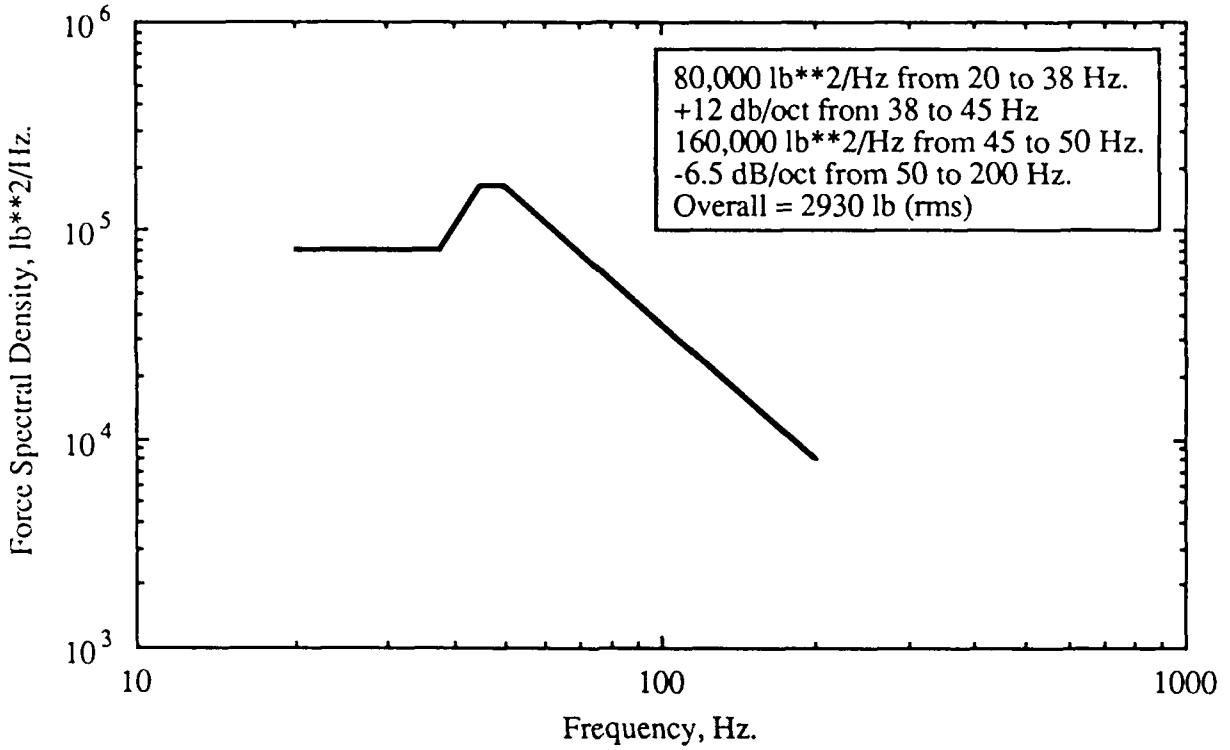

Figure 12. Smoothed PSD for Specified Blocked Force - Y Axis.

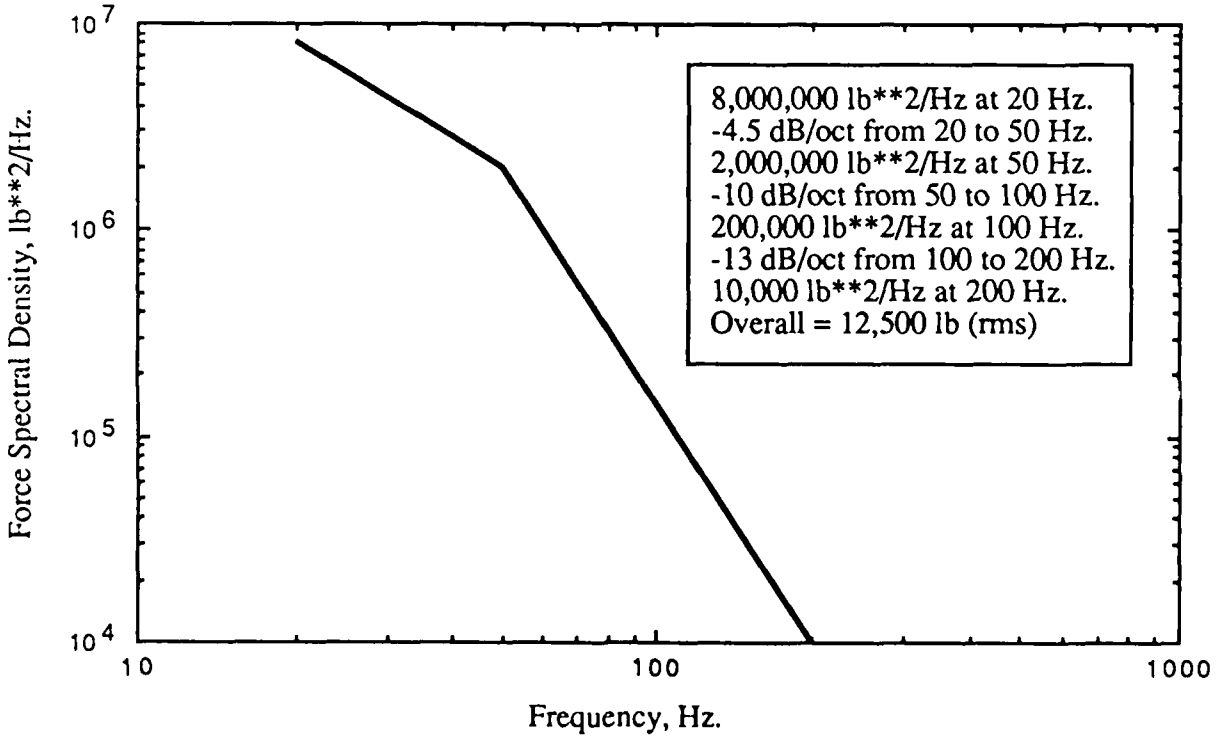

Figure 13. Smoothed PSD for Specified Blocked Force - Z Axis.

direction (along the axis of the longeron) must be substantially higher than in the z direction (normal to the axis of the longeron). Hence, even with one attachment point in the x direction versus two in the z direction, the force limit for an APC/payload along the x axis is probably higher than the force limit computed for the z axis in Figure 13, which is already very high (only a large payload with a very heavy resonant element would cause the input force from a shaker to exceed the force limit along the z axis specified in Figure 13). Due to these uncertainties, the only conservative approach is to assume the x axis force limit is infinite; i.e., vibration tests along the x axis will be performed in th traditional manner using the specified vibration input test level without a force limit.

The above derivations of limit forces for SSV sidewall mounted payloads were relatively straightforward because the modal density of the sidewall structure above 20 Hz is sufficiently high to produce mounting point apparent weight functions that are relatively smooth over frequency; i.e., they do not display sharp peaks and valleys (see [2]). Hence, there is little trouble in determining a smooth net apparent weight function that is consistent with a vibration test specification that is typically smoothed over this same frequency range (see [1]). If the force limit test procedure were applied to payloads that attach to other types of mounting structures, however, situations may arise where the mounting point apparent weight functions at various attachment points display sharp peaks and valleys in the frequency range of interest. This situation would greatly complicate the derivation of a net mounting point apparent weight function. In particular, an envelope procedure, as used for the SSV sidewall data, would not be appropriate because valleys in a mounting point apparent weight function generally correspond to peaks in the vibration response spectrum at that location [11]. Hence, since the specified vibration test spectrum [1] represents a smooth envelope of peak spectral response values, a smooth envelope of apparent weight functions would produce unreasonable conservatism in the resulting limit force function. Possible approaches to this problem are given in Reference 11.

4. EXPERIMENTAL STUDIES

In order to verify the concepts for force limiting which were developed in this project, vibration experiments were performed on a simulated OASIS payload attached to an actual Adaptive Payload Carrier (APC) and shaken along the Y axis. The simulated payload was approximately the same weight as the OASIS, and had two very strong and well defined resonances in the frequency range of interest (20 - 200 Hz). Use of a real APC allowed the introduction of the thermal growth clearance gaps at the APC mounting points and, thus, a simulation of their effect on the payload response during base vibration could be determined.

The tests were carried out at the National Technical Services facility in Los Angeles, CA, using their MB Electronics model C-150 shaker. This shaker is rated to 15,000 pounds peak force. Two test series were performed, one in November 1988 and one in December 1988. The shaker, payload and instrumentations were identical for both tests, and the results are considered to be from a single experimental program.

4.1 Test Set-Up

The simulated OASIS payload is illustrated in Figure 14. It was constructed of a 10 inch deep, steel box frame weighing approximately 130 pounds. Two steel weights, 40 pounds and 50 pounds, were supported in the center of the frame by steel bars acting as springs, allowing vertical motion but preventing rotation. The natural frequencies of the two resonators are calculated to be 119 and 53 Hz respectively. Total weight of the simulator is 246 pounds. It was attached to the APC by 1/4 inch bolts through the normal mounting holes around the periphery of the APC, as shown in Figure 15.

A magnesium head expander was used on the shaker to provide a 30 inch diameter working surface to attach the APC. The configuration is shown in Figure 16. The adjustable feet of the APC were positioned out as far as possible on the head expander. Mounting point 3, was located inside the frame and near the center of the shaker table. The arrangement of the three mounting bolts was not symmetric on any axis.

4.2 Test Instrumentation

Quantities of interest measured and recorded during the test were:

Acceleration of the shaker table, (1)
Electrical current in shaker, (1)
Acceleration of points on the payload frame, (4)
Acceleration of the payload resonators, (2 on second test)

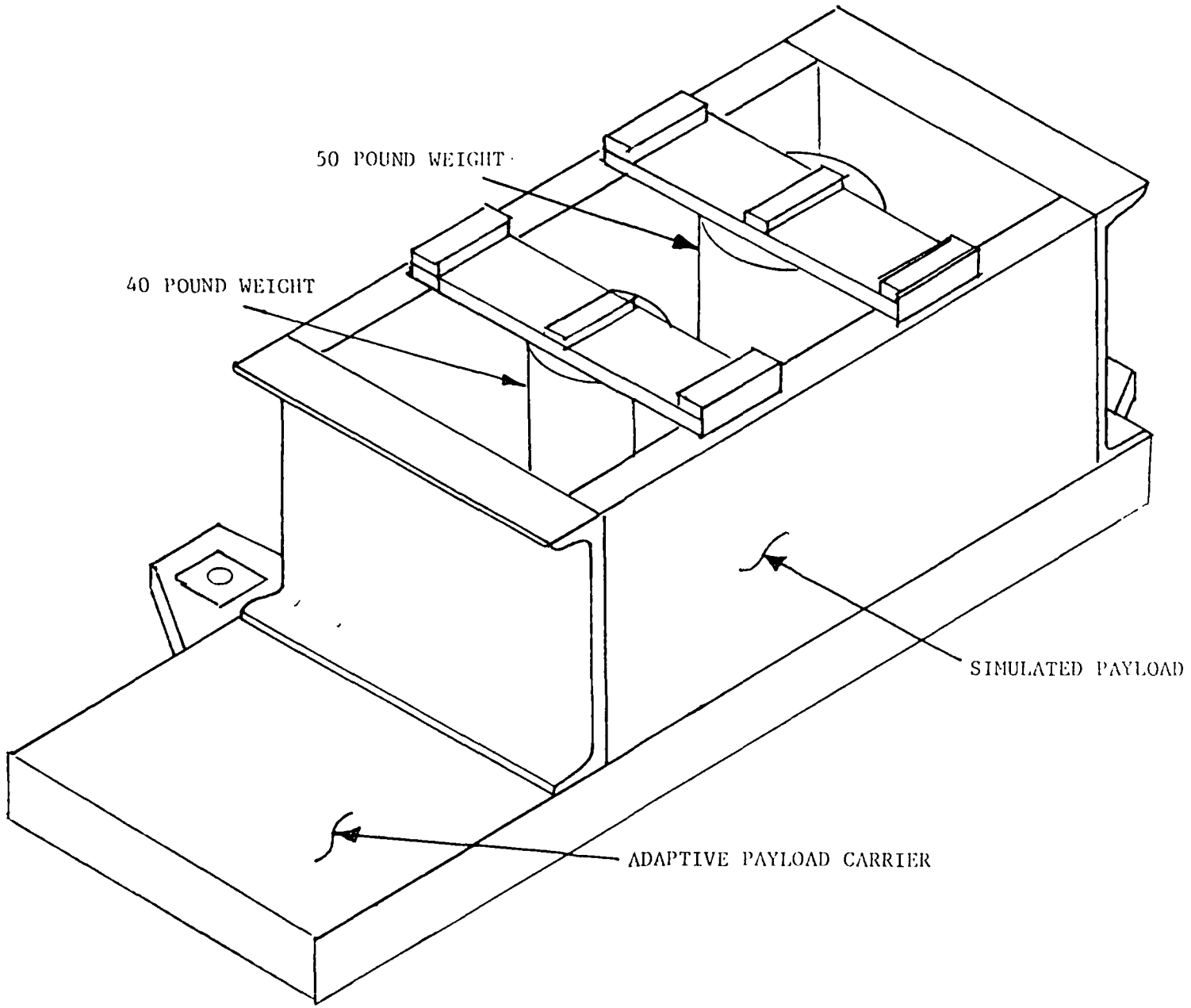

Figure 14. Simulated OASIS Payload on Adaptive Payload Carrier.

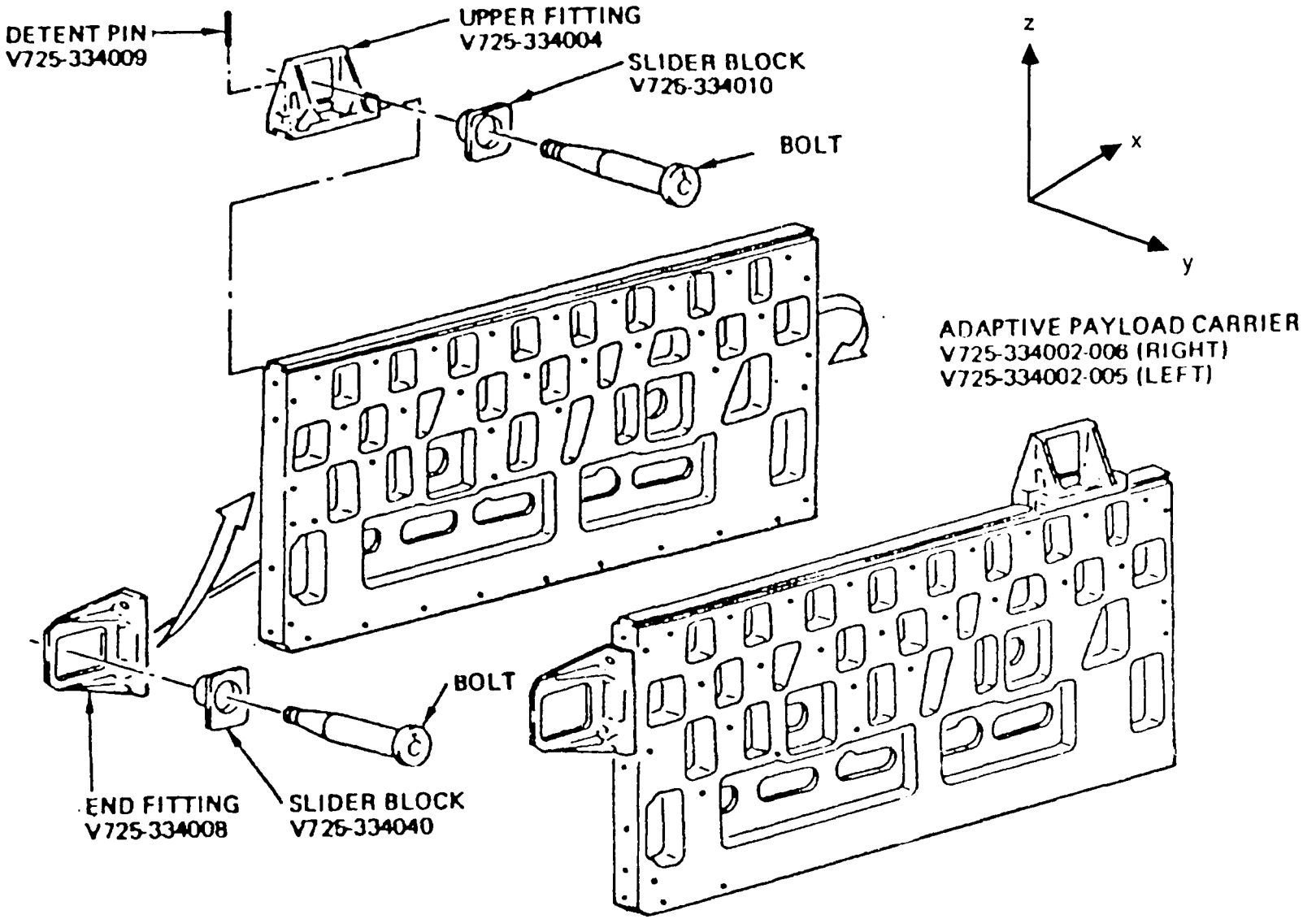

Figure 15. Adaptive Payload Carrier (APC)

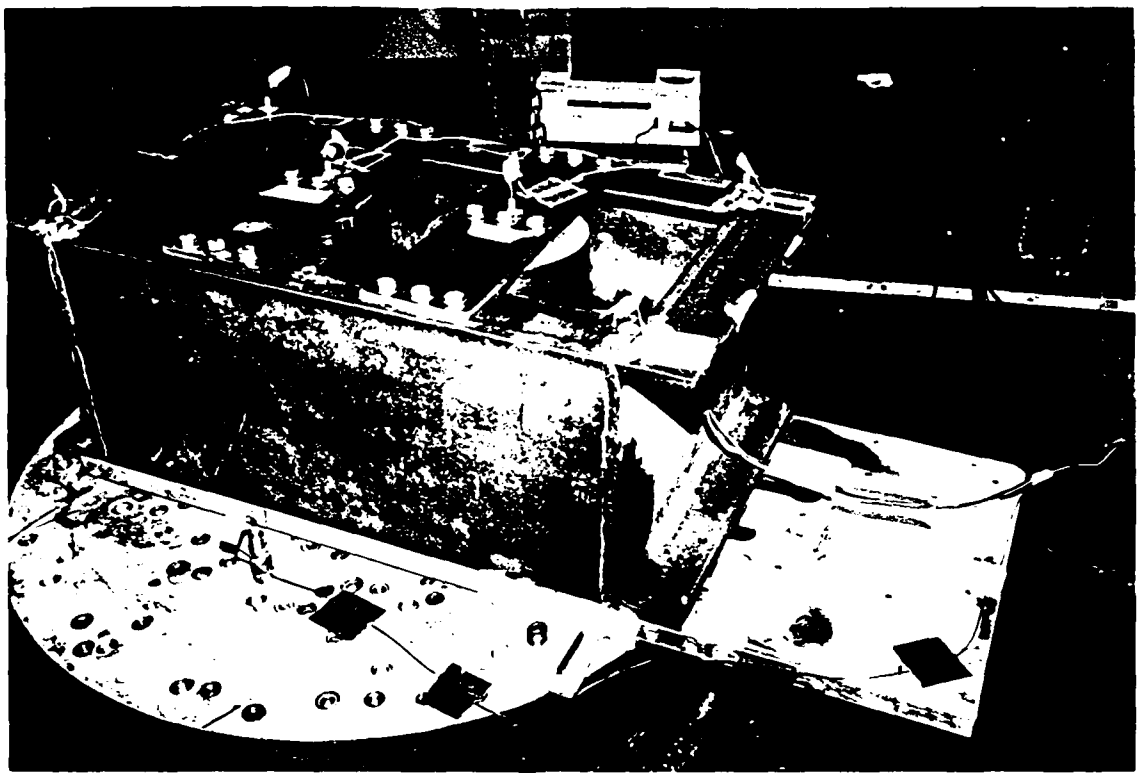

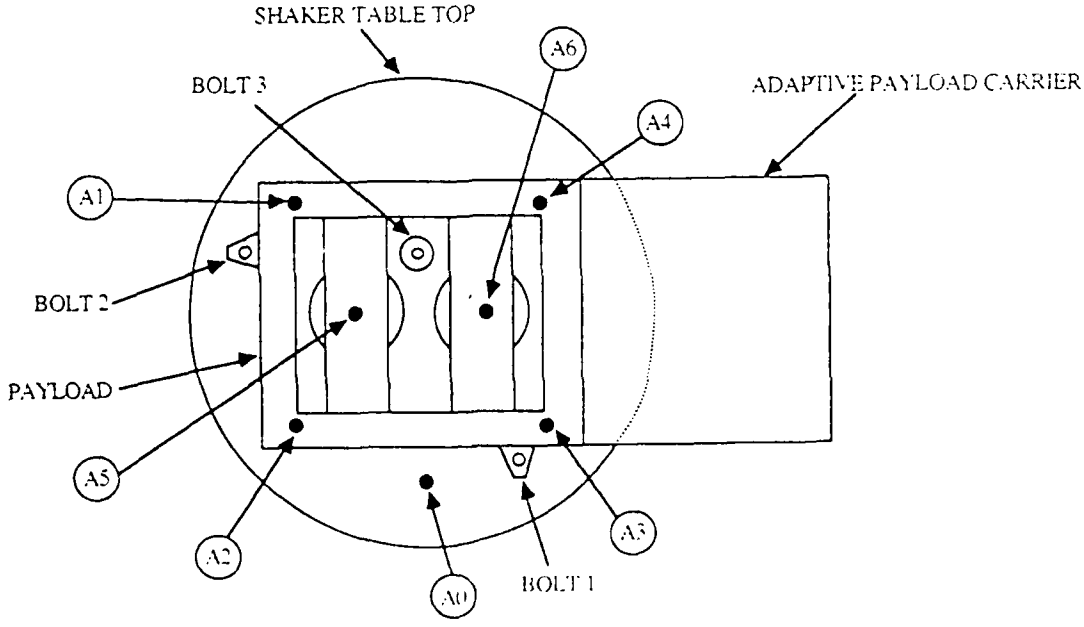

Figure 16. Payload and APC Mounted on Shaker Table.

During testing, signals were observed on an oscilloscope to monitor their quality, and selected signals were analyzed with a 2-channel real time spectrum analyzer. A schematic of the instrumentation and data acquisition system in given in Figure 17.

Accelerometers used in the tests are as follows:

ACCELEROMETER	TYPE	LOCATION
A_0	B & K 4368	Shaker table Reference
A_1	B & K 8303	Top corner of payload
A_2	Endevco 2226C	Top corner of payload
A_3	Endevco 2226C	Top corner of payload
A_4	Endevco 2226C	Top corner of payload
A_5	Endevco 2226C	On 40 pound resonator
A_6	Endevco 2226C	On 50 pound resonator

All accelerometers were furnished by NTS, and were connected to their charge amplifiers. The charge amplifier gain levels were set to give tape recorder input levels of a few hundred millivolts to obtain adequate signal to noise ratio, but less than 1.0 volt peak to avoid distortion. During the test, all accelerometers except A_0 were attached to the payload with a hard adhesive (Krazy Glue), using a thin electrical isolation layer.

A signal related to the shaker current was obtained from the shaker power amplifier by a current transformer and resistor. The signal was adjusted by the resistor to give approximately 1 volt peak signal to the tape recorder at full power. This signal is directly proportional to the shaker current, but no absolute calibration factor (volts/amp) was obtained. By a basic calibration procedure, the relation between this signal and the force delivered by the shaker was determined (lb/volt).

All signals were recorded on a TEAC XR-50 FM tape recorder. Tape speed was set at 9.5 cm/sec., which gives a frequency response range of 0-5000 Hz. Calibration signals of +/- 1.0 volts DC, and 2 volts peak to peak AC were recorded on tape prior to acquiring data. An end to end calibration of the system was performed by mounting all accelerometers on a GENRAD 1557 vibration calibrator and recording the signals on the tape recorder. The measured voltage of the playback signal established the calibration factor (mV/g) for each channel.

The accelerometer on the shaker table, A_0, was used as the reference accelerometer for the NTS shaker equalization system. The computer controlled system performed a spectrum analysis on this signal and

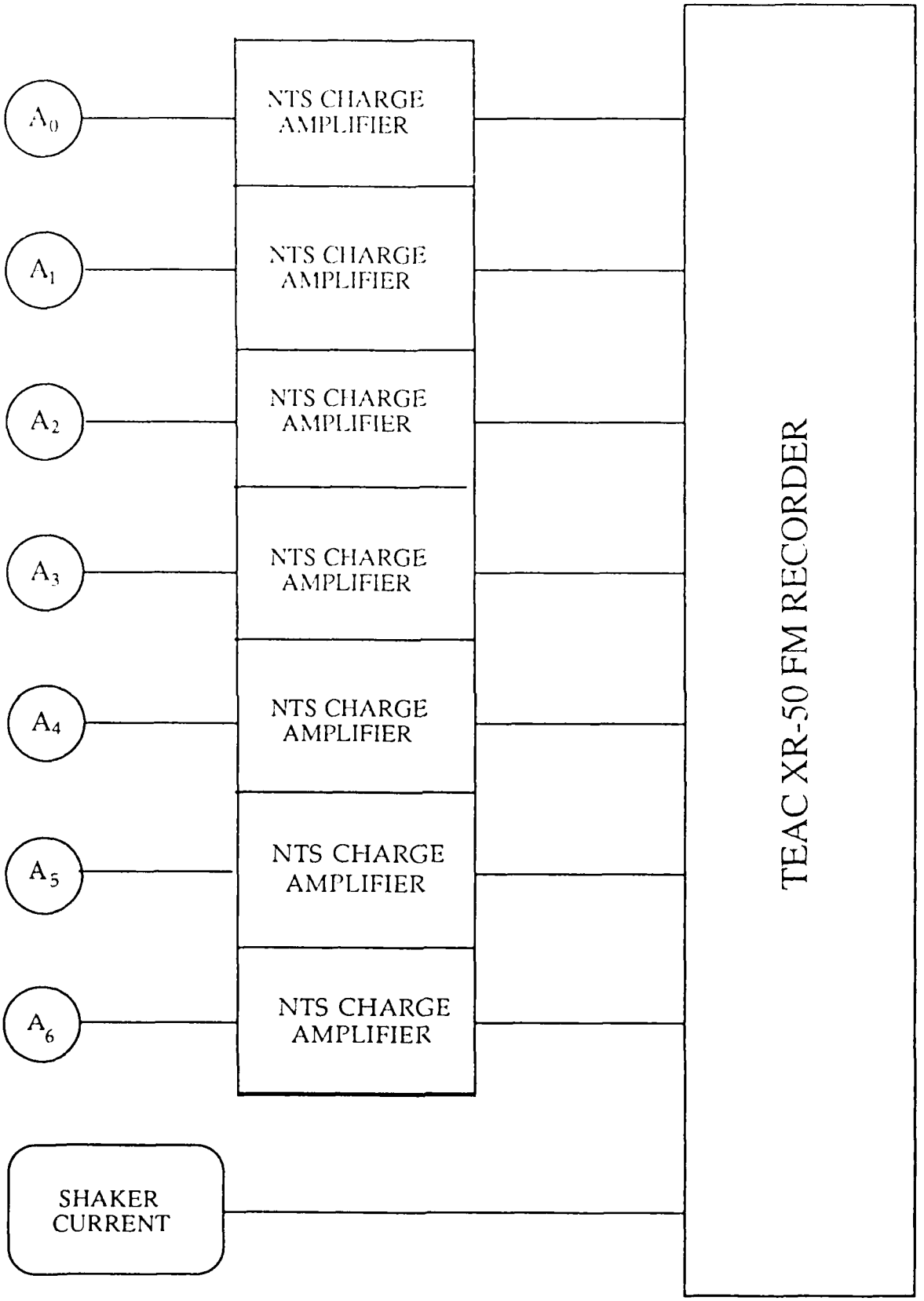

Figure 17. Data Acquisition Systtem.

automatically adjusted the driving current spectrum to maintain the desired spectrum shape and level at the reference accelerometer.

4.3 Shaker Calibration

Previous tests on a smaller MB shaker [2] showed that the current in the shaker was directly proportional to the force produced by it. This behavior was verified on the C-150 shaker by a calibration experiment. A rigid steel weight of 245 pounds was bolted on the shaker expander head and excited with broad band random vibration with the spectrum shape given in Figure 18. The frequency response function relating the table acceleration to the driving current shown in Figure 19 is almost constant with frequency, and very coherent. The sharp dip at 60 Hz is a power line interference artifact.

The shaker armature force calibration factor is given by

$$K(f) = W_T H_{CA}^*(f) \tag{37}$$

where

W_T = Total weight of armature, head expander, and dead weight, lb

$H_{CA}(f)$ = Frequency response function of current and acceleration, g/amp

Using a total weight of 543 pounds, the shaker table calibration factor shown in Figure 20 results. It appears to be very stable with frequency, and have little phase shift. This calibration function was stored on computer disk for later calculations of payload apparent weight and force applied to the payload. Equation (23) was used on the data from this test to calculate the apparent weight of the rigid weight, a procedure to check the consistency of the data acquisition and analysis system. The results, shown in Figure 21, are in near perfect agreement with the true value of 245 pounds, except at the three power line harmonics of 60, 180, and 300 Hz.

4.4 Data Analysis

Spectral analysis of the signals was performed on a Hewlett-Packard 3562A two channel real time spectrum analyzer. This instrument gives an 800-line analysis of autospectra, cross spectra, coherence, frequency response, and phase between selected pairs of channels. During the testing operation, the various channels were briefly analyzed to assure good signal quality and proper operation. The data analysis set-up used in Astron's office for complete post-test analysis is shown in Figure 22. In this analysis, spectral quantities were computed over the frequency range from 0 to 400 Hz, with 0.5 Hz resolution. The Hanning window used for the spectral analyses gave an effective bandwidth of 0.75 Hz. Reduced data in spectral form were transferred

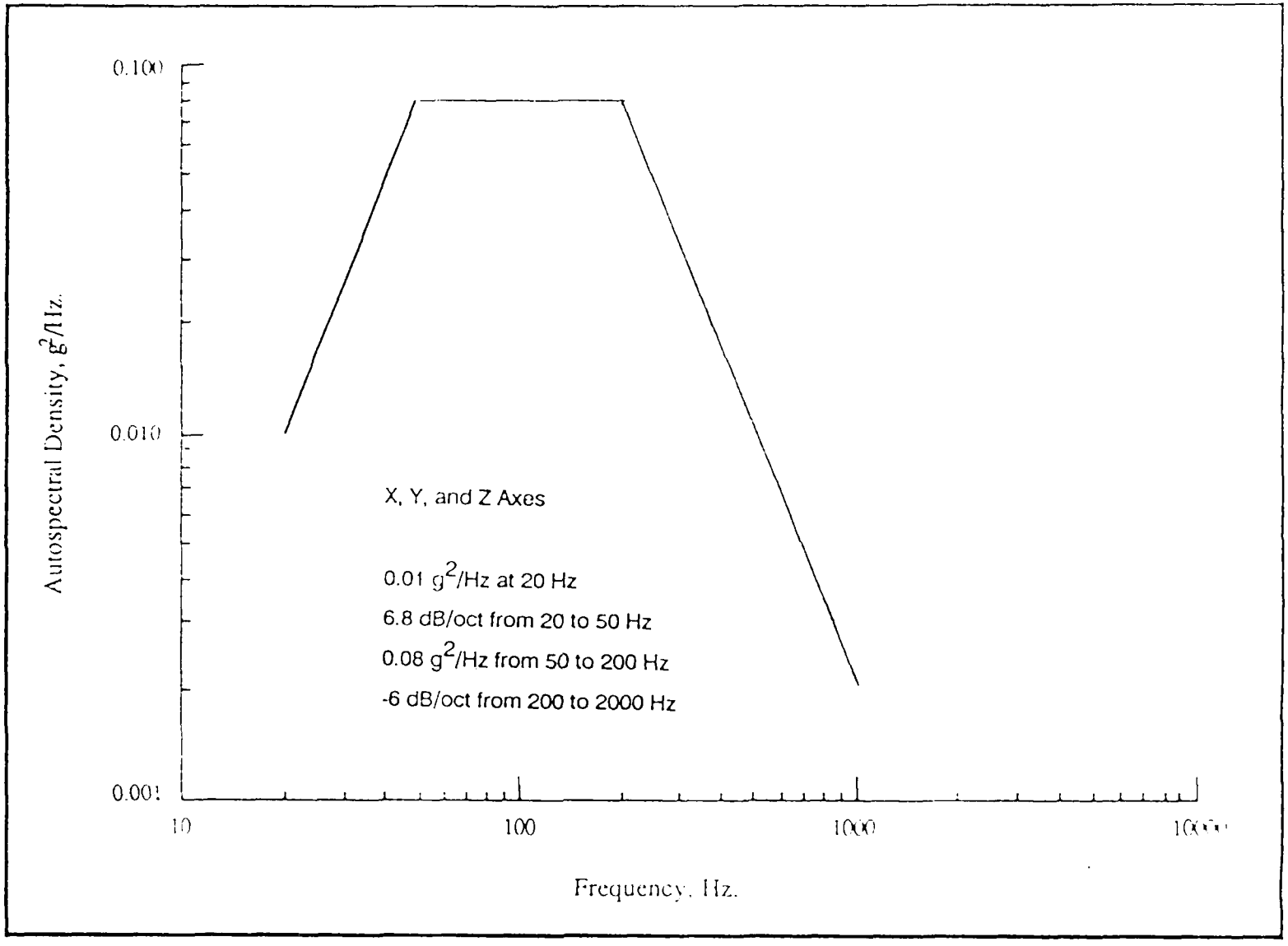

Figure 18. Acceleration Spectrum for Vibration Testing of Simulated Payload.

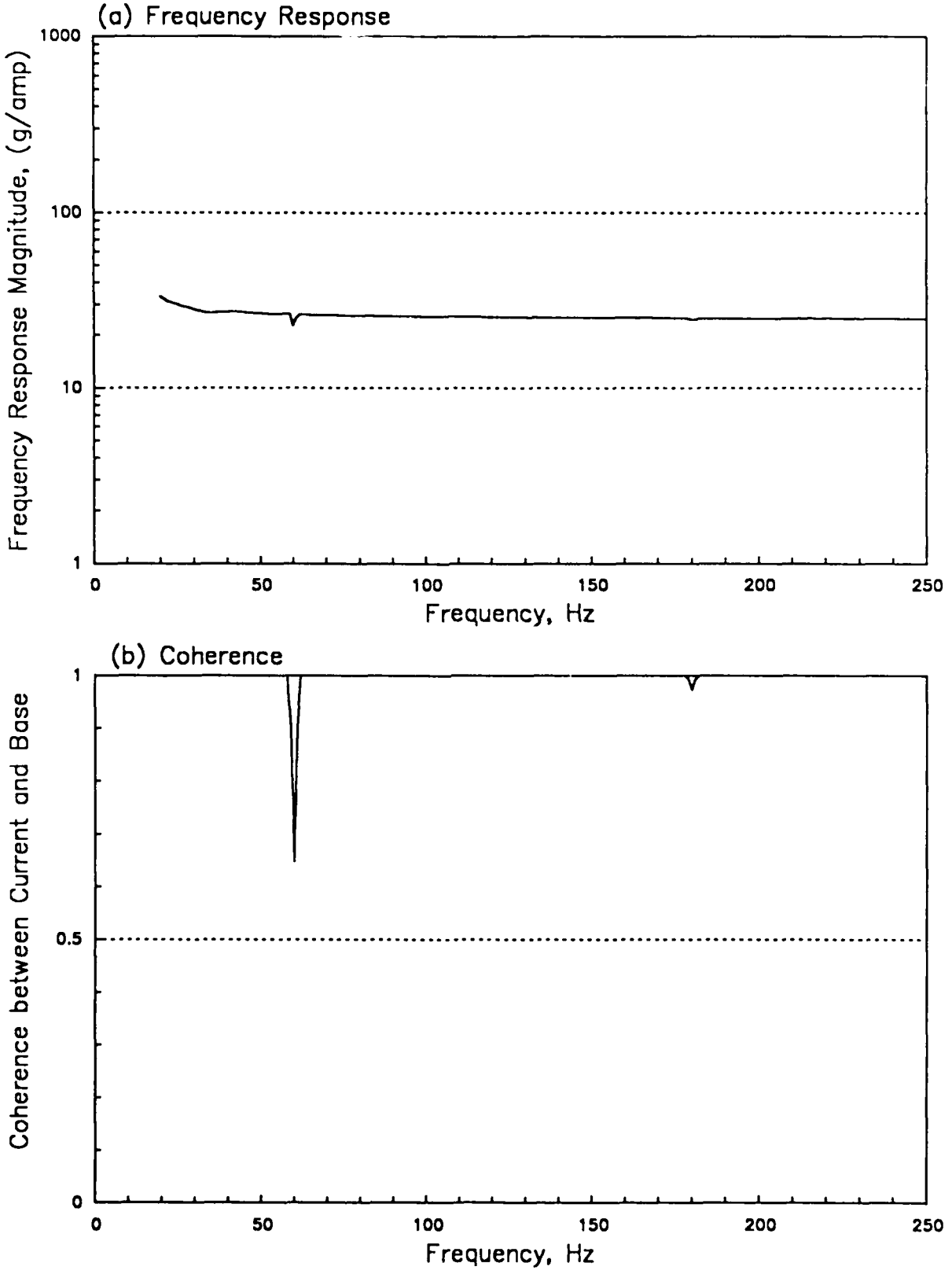

Figure 19. Shaker Current and Table Acceleration, 245 lb Dead Weight.

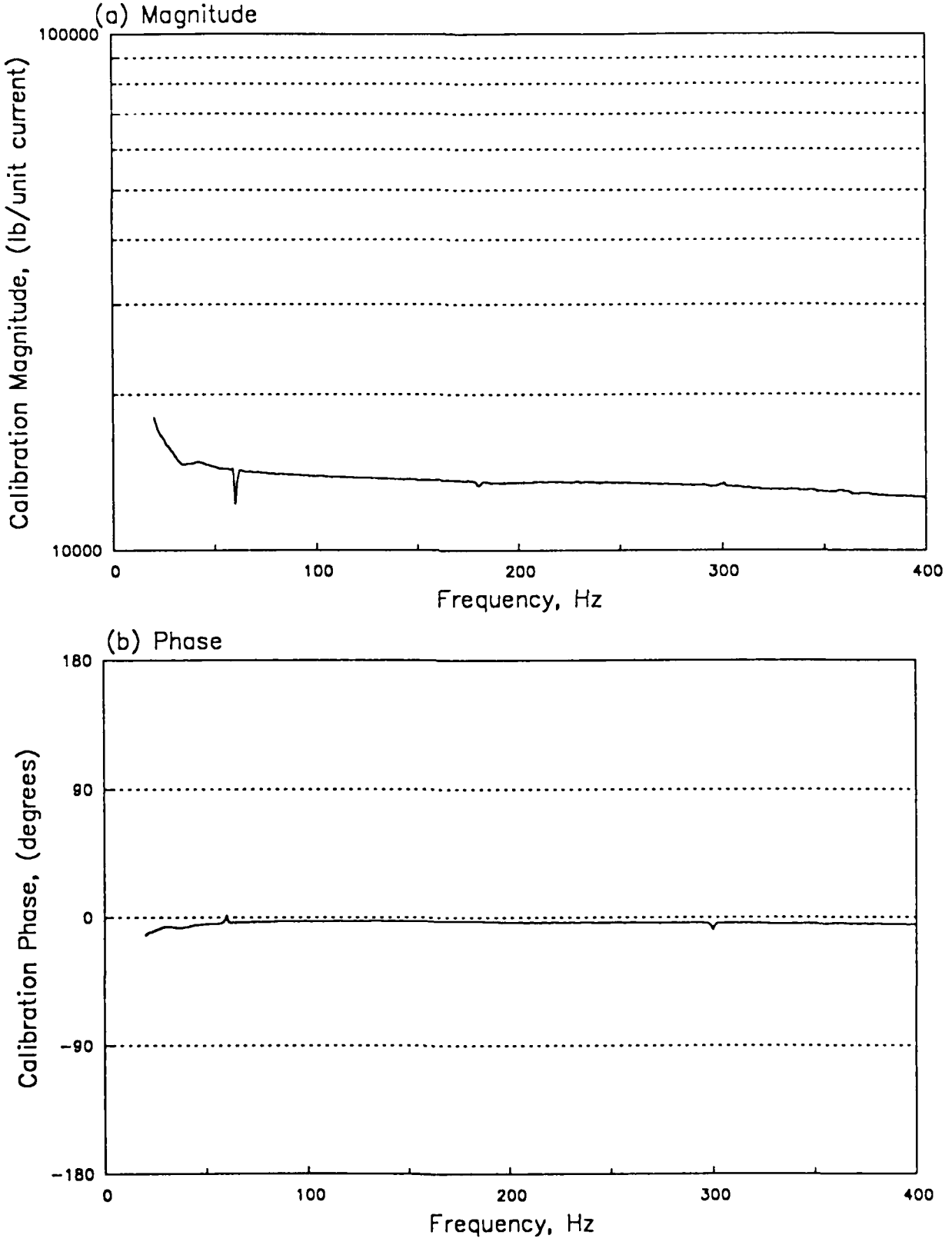

Figure 20. Shaker Table Calibration Factor (lb/unit current).

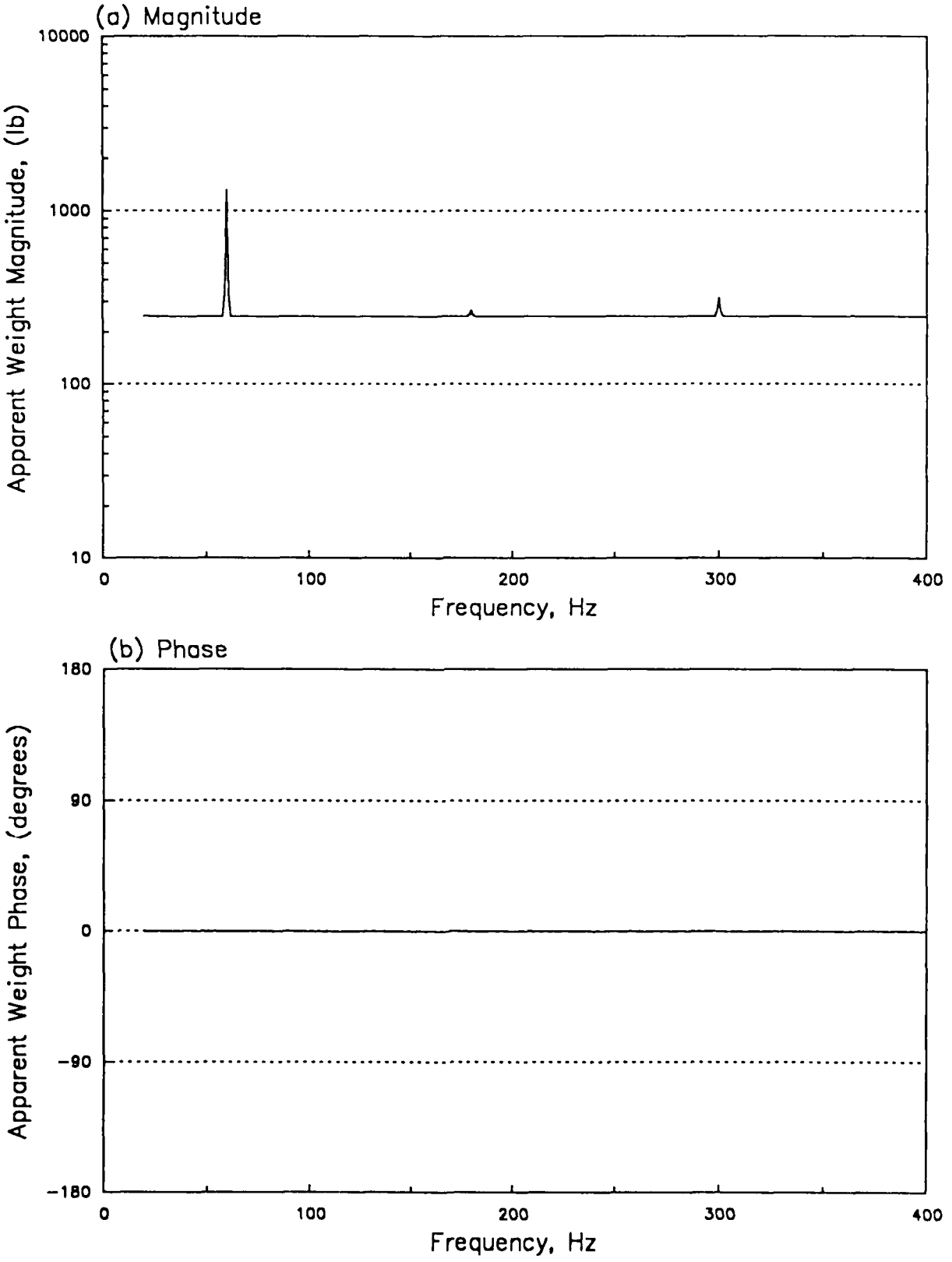

Figure 21. Apparent Total Weight of System on Shaker Table. Dead Weight, 245 lb.

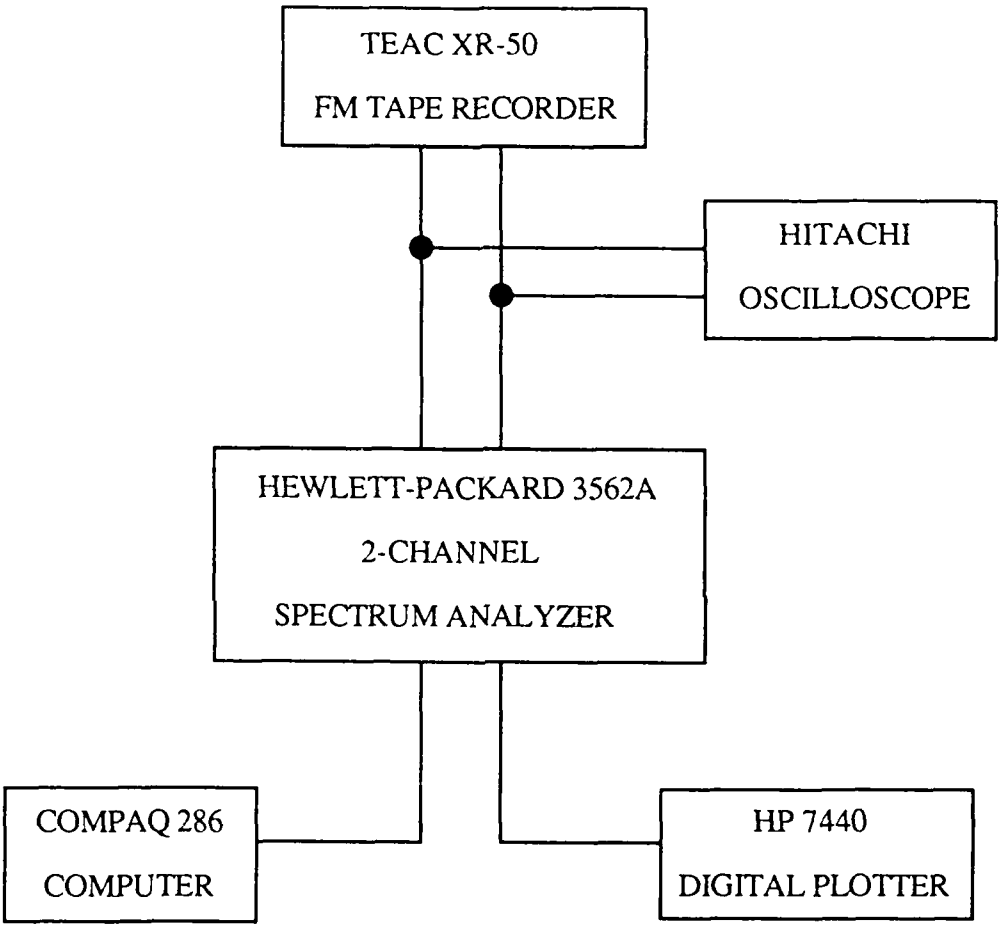

Figure 22. Data Analysis System.

to the Compaq 286 computer via an IEEE-488 bus. This information was also used to send the information to a Hewlett-Packard 7440 digital plotter to generate hard copy. The full frequency range (0-400 Hz) of the data was transferred, but only the range from 20 to 250 Hz was plotted.

Once transferred to the PC, the spectral data were manipulated using the appropriate equations to determine apparent weights and excitation forces.

4.5 Exploratory Tests

After performance of the initial calibration test with a dead weight, four exploratory tests with the simulated payload and APC were performed to determine the dynamic properties of the components. These tests were:

1. Payload only mounted rigidly on shaker,
2. Payload on APC, mounted rigidly on shaker,
3. Payload on APC, 0.005 in. attachment point clearance,
4. Payload on APC, 0.002 in. attachment point clearance.

These tests are described below.

4.5.1 Rigidly Mounted Payload

The payload was clamped rigidly to the shaker table by 3 magnesium bars pulled down with 1/2 inch threaded rods. Vibration excitation was with the spectrum given in Figure 18. Tests were performed and data recorded at vibration levels 12, 9, and 6 dB below the specification level. Tests were not run at the full level because NTS personnel were concerned about possible high force levels damaging their shaker. (It had been overloaded and destroyed twice in the previous month and they were justifiably cautious).

During each test, signals from the accelerometers and current were examined on an oscilloscope for clipping and distortion, and recorded for approximately 90 seconds. Also, a 2 channel spectral analysis was performed on the table acceleration and shaker current signals to determine the frequency response function and coherence between them. High coherence was observed, indicating good signal to noise ratio and linearity.

4.5.2 Payload on APC, Rigid Mount

The payload was attached to the APC by the 1/4 inch bolts around its periphery, and bolted solidly to the shaker head expander top surface at the three mounting locations with 1/2 inch steel bolts. This bolting

arrangement duplicated that of actual service installation in the SSV. It was confirmed by inspection with feeler gages that there were no gaps under the mounting points, and the APC was pulled down tightly against the shaker table.

As with the payload alone, tests were performed at 12, 9, and 6 dB below the specification level. Accelerometer and current signals were observed on an oscilloscope for distortion or clipping, and 90 seconds of data were recorded at each vibration level. Frequency response and coherence calculations between the shaker current and shaker table acceleration were performed during the test, and it was determined that there was good signal to noise ratio and linearity. It was observed that the large portion of the APC which extended beyond the edge of the shaker table appeared to add more dynamic effects to the behavior of the system, but produced no great changes in the payload resonant frequencies.

4.5.3 Payload on APC, 0.005 inch gap

Mounting points 2 and 3 were shimmed to achieve a static clearance of 0.005 inch. There was a slight "springiness" to the APC, and the APC and shaker table top were not exactly plane. Thus the true clearance or rattle space could potentially be slightly larger than 0.005 inch. Mounting point 1 remained tightly fastened.

Tests were performed at the vibration levels of 12, 9, and 6 dB below the vibration specification, with signals observed and data recorded for 90 seconds at each level. Even at the lowest level there was a very noticeable rattle. At the high levels it was very strong; so strong, in fact, that there was metal deformation and wearing at the points of contact between the shaker table top and the bottom of the APC.

Examination of the spectra of signals during the tests showed that the strengths of the resonances were greatly reduced, as was the coherence between the shaker table acceleration and the driving current.

4.5.4 Payload on APC, 0.002 inch gap

Shims at mounting points 2 and 3 were changed to produce a gap of 0.002 inch. Again, because of the springiness of the APC and the lack of flatness of the APC and shaker table top, the effective gap could be slightly larger.

Tests were run at 12, 9, and 6 dB below the vibration specification of Figure 18. At each level the signals were examined for clipping and distortion as they were being recorded. The looseness of the mounting caused a very definite rattle to be observed. However, it was not quite as strong as that seen with the 0.005 inch gap.

4.6. Results of Exploratory Tests

Frequency response functions between the shaker current and table reference accelerometer are quite affected by the presence of a payload having strong resonances. This is demonstrated in Figures 23 and 24 for the case of the simulated OASIS payload bolted rigidly to the shaker table. These functions, taken at vibration levels 6 and 12 dB below the specification level clearly show the effects of the two resonant masses. The two minima, at 67 and 110 Hz, indicate that a large current or shaker force is applied to the load, but there is little resulting motion of the payload. Such action is related to a very high apparent weight. The maxima at 72 and 119 Hz show that little shaker force is required to achieve considerable motion at these frequencies.

This behavior is better expressed as the apparent weight function, shown in Figure 25. The high apparent weight at 67 and 110 Hz of about 4000 pounds corresponds to the minima in the accelerometer/current frequency response function. At these frequencies the resonators act as dynamic vibration absorbers, having large vibrations while the payload frame is relatively motionless.

The simulated payload, consisting of two weights on springs and a rigid frame, has distinct dynamic properties which should be noted and correlated with actual payloads. Each weight may be considered as an independent 50 pound mass connected by a spring to a 200 pound frame. When driven by a force on the frame, there is a frequency where the weight moves with a large amplitude while the frame undergoes very small motion. The ratio of force to input motion is very high, hence giving a large value of apparent weight. At a slightly higher frequency the situation reverses and the weight almost stands still while the frame has large motion. In this case the reactive force of the vibrating mass is exactly in phase with the input force and results in large frame motion for reduced input force. This condition is clearly identifiable as the point of minimum apparent weight. Because the static natural frequencies of the simulated payload resonators are widely separated, there is negligible interaction and the behavior of both is clearly seen. In view of these observations, the behavior of the payload apparent weight shown in Figure 25 becomes more understandable. Measurements of the motion of the resonator weight, presented later in this section, confirm this explanation.

Comparison of the frequency response and apparent weight functions at the two different input levels shows them to be practically identical, and both with very high coherency. These facts are excellent indicators of linearity in the shaker system and in the dynamic structure of the simulated payload.

An illustration of the force applied to the rigidly mounted payload is given in Figure 26. As expected, there are very high force input levels at 67 and 110 Hz. Part (b) of this figure gives a breakdown of the components in Equation 2 for the calculated applied force. It shows that the shaker current autospectrum term is the major contributor to the calculation of total force at the peak value, and that the table acceleration

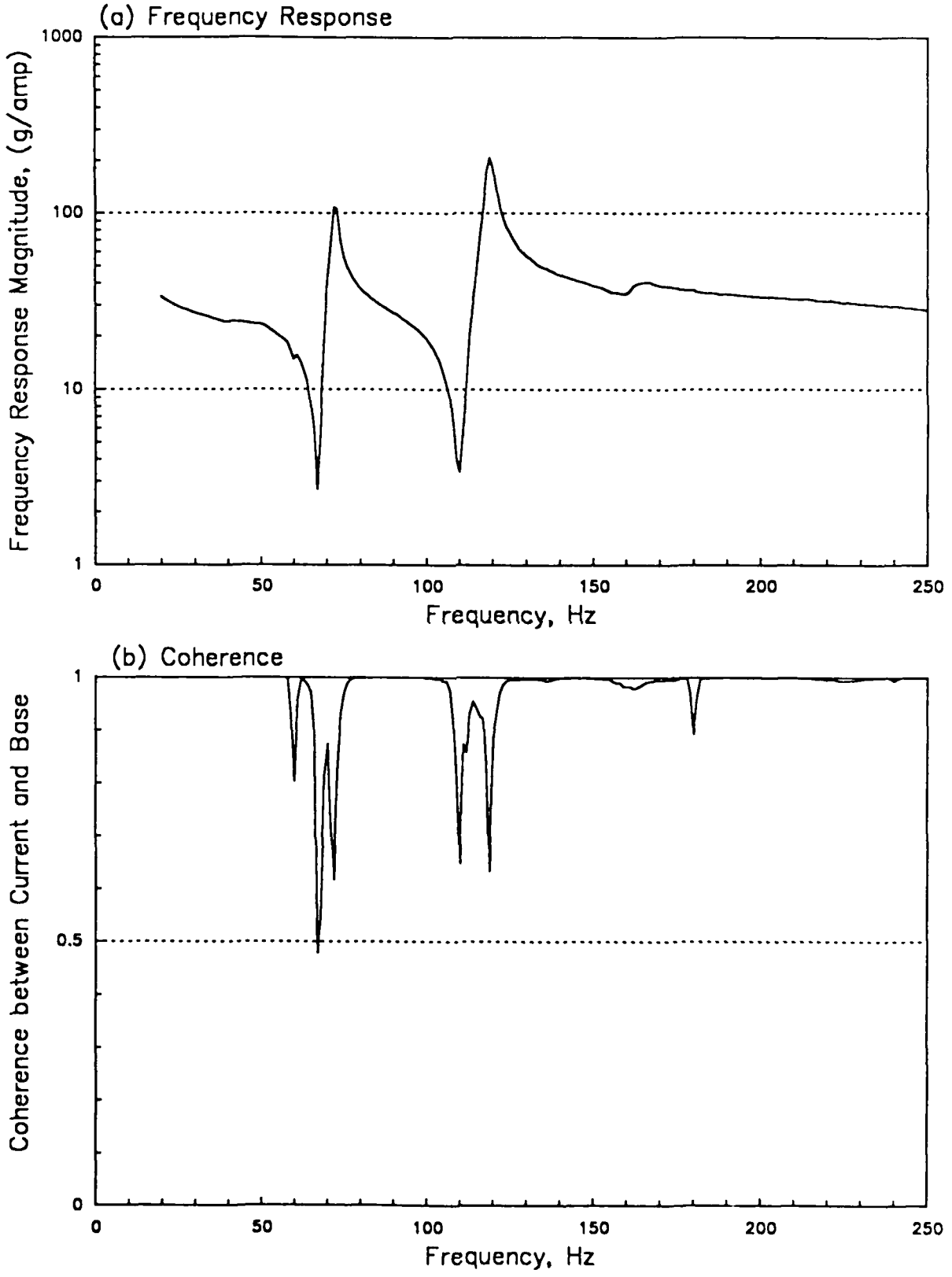

Figure 23. Shaker Current and Table Acceleration, Payload Rigid Mount, 6 dB below Vibration Specification.

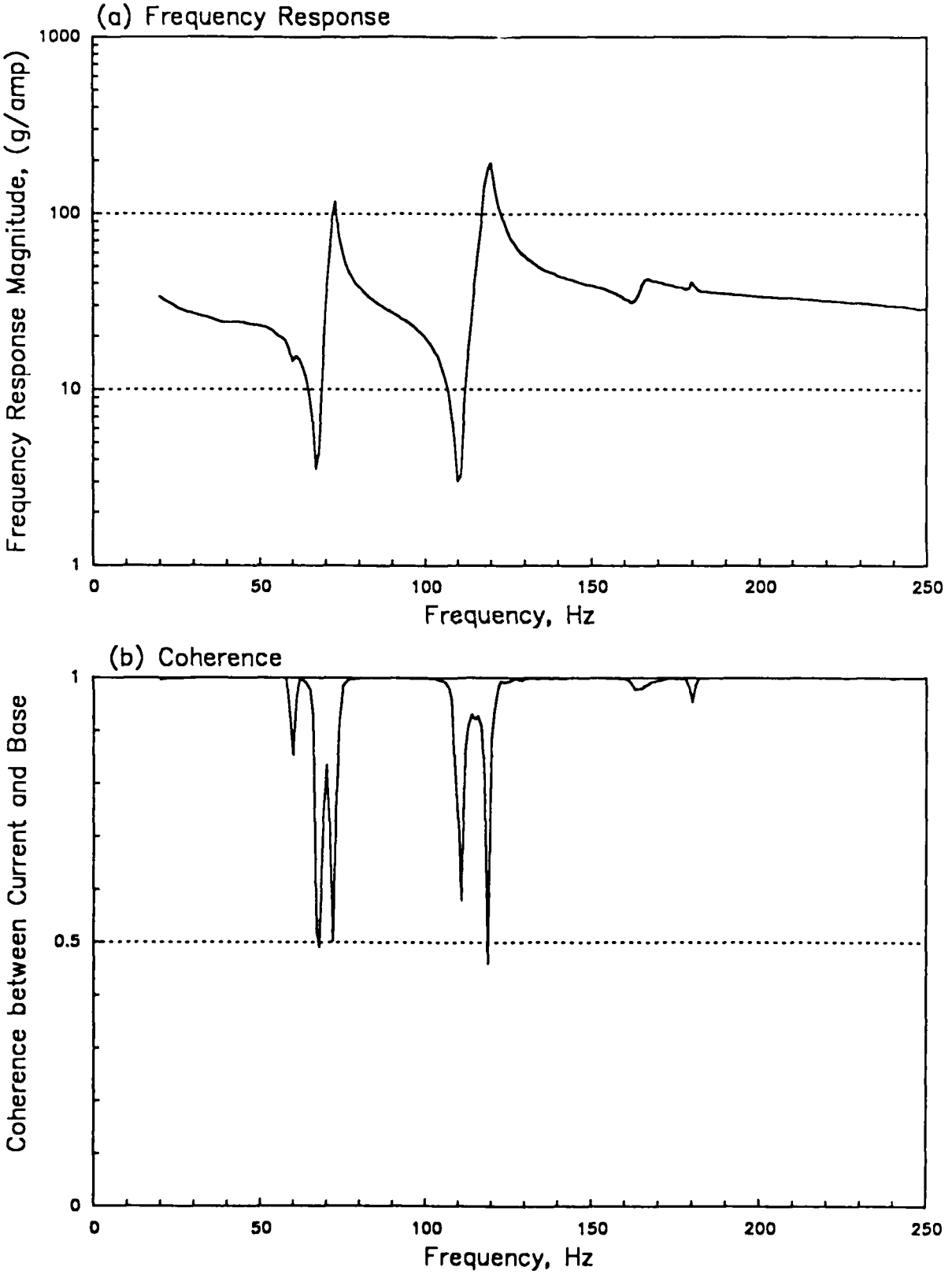

Figure 24. Shaker Current and Table Acceleration, Payload Rigid Mount, 12 dB below Vibration Specification.

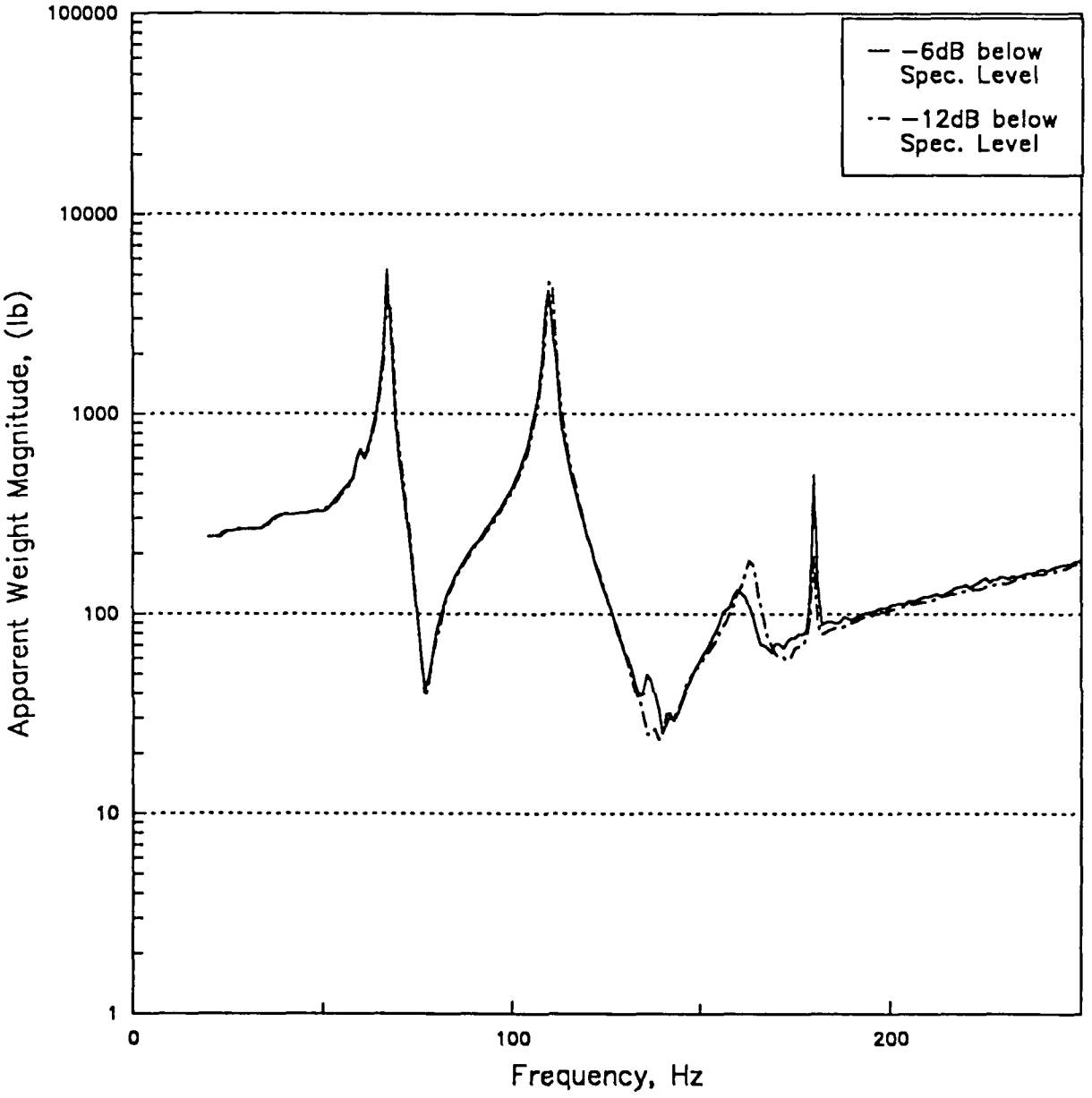

Figure 25. Apparent Total Weight of Payload Rigid Mount.

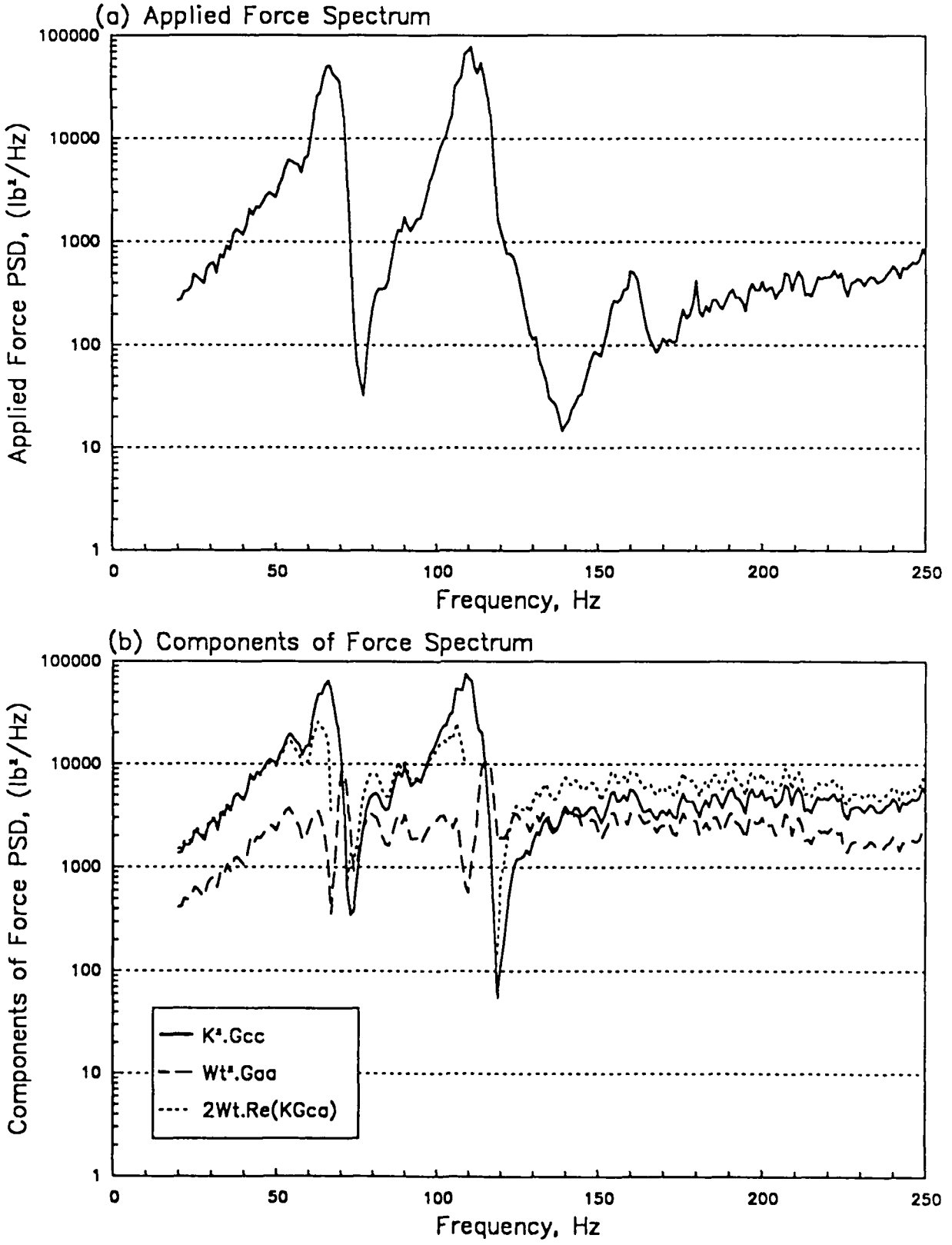

Figure 26. Applied Force Spectrum, Payload Rigid Mount, 6 dB below Vibration Specification.

autospectrum term is relatively insignificant over most of the frequency range. This observation is of considerable significance in considerations of a force limiting procedure.

Mounting the simulated payload on the APC and fastening it rigidly to the shaker table changes the vibration and force characteristics of the system to some degree. Figure 27 shows that the APC does not make a great difference in the frequency response function of table acceleration to shaker current at the payload resonances, but does add some unique features at higher frequencies. This effect is more evident in the applied force spectrum shown in Figure 28. Comparison of this figure with Figure 26 indicates that the large overhang of the APC over the shaker table, and the unsymmetrical stiffness due to its hold-down bolt arrangement causes several higher modes to appear.

Introduction of the 0.005 in. thermal growth allowance gaps at two of the APC/shaker attachment bolts causes a drastic change in the system response. In Figure 29 the large variations (+/- 15 dB) in frequency response functions between shaker table acceleration and driving current normally associated with a rigidly mounted payload or APC have been greatly reduced to less than +/- 8 dB. Above 100 Hz the response is very flat with frequency. This is associated with a reduction of coherence, indicating non-linear behavior (not surprising, considering the rattle). A similar change in the applied force spectrum may be seen in Figure 30. The peak in spectral density of applied force has been reduced from about 45,000 lb^2/Hz at 68 Hz (see Figure 28) to about 20,000 lb^2/Hz at 50 Hz, and there are no significant high frequency peaks.

The implications of the mounting bolt gap are made more clear in the apparent weights shown in Figures 31-33. Here, the results of different mounting configurations are compared on the same graph. Allowing the APC to rattle at the mounting bolts reduces the peak magnitude of the calculated apparent weight of the payload, and makes it a smoother and more uniform function of frequency. This is true for all three levels of vibration (12, 9, and 6 dB below the specification spectrum of Figure 18).

A different view of the process is obtained by using the test data to estimate the force that would be applied to the payload had the full scale shaker table acceleration spectrum been maintained. Figures 34-36 show that, in each case, the presence of the gaps causes the applied force spectrum to be sharply reduced near 110 Hz, but slightly increased in the region above 200 Hz.

The blocked force, or the maximum force which could have been applied to a payload mounted on the SSV sidewall, has been calculated from Equation 5 using the experimental data from the OV-101 tests. This force spectrum is shown in Figure 12. A simplified version of this spectrum has been used as the provisional specification line in Figures 34-36. It is seen that the rigidly mounted payload, or the payload on an APC with no thermal clearance gaps, would require significant force limiting at the two frequency bands near the

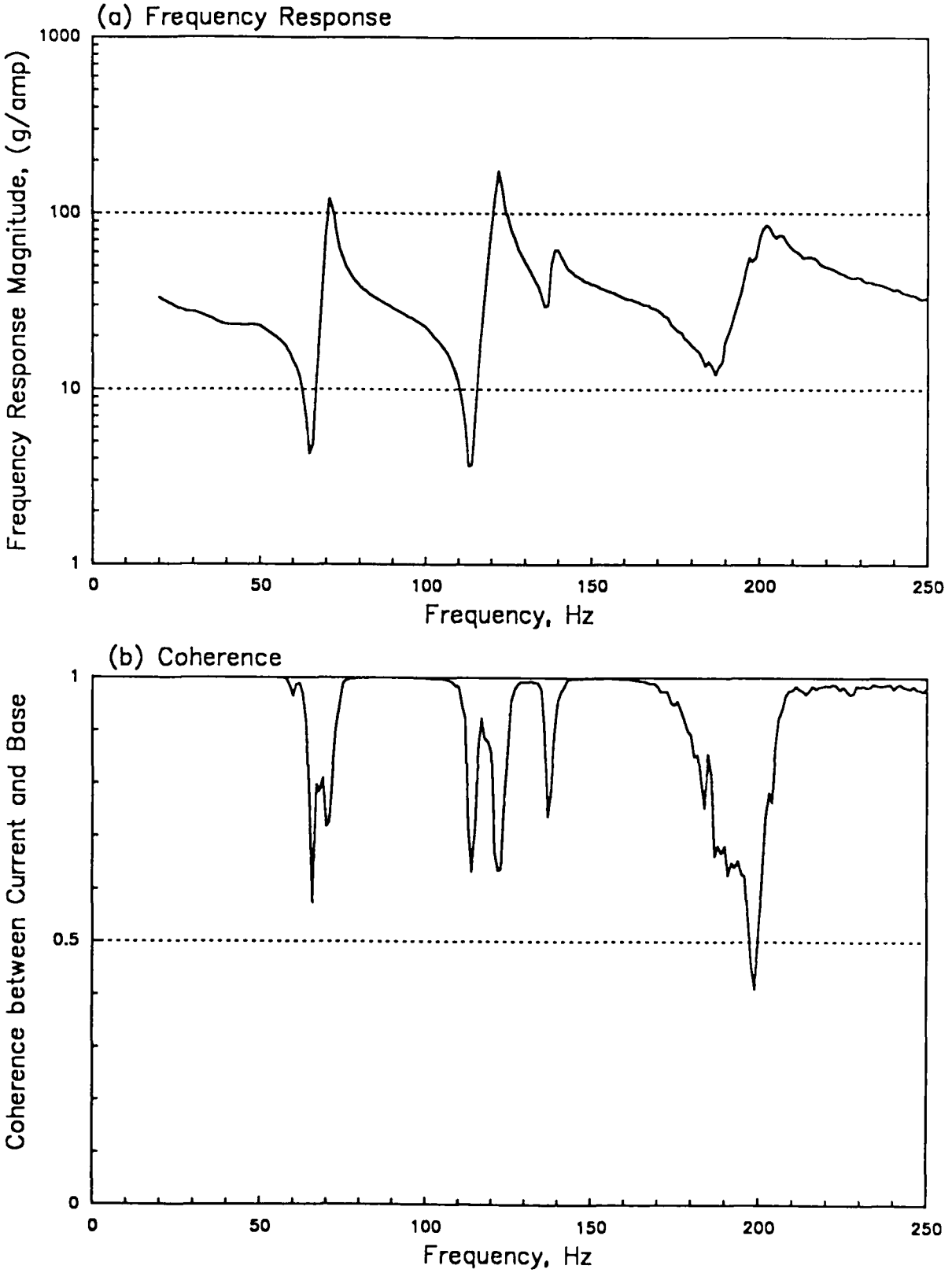

Figure 27. Shaker Current and Table Acceleration, Payload Rigid Mount on APC, 6 dB below Vibration Specification.

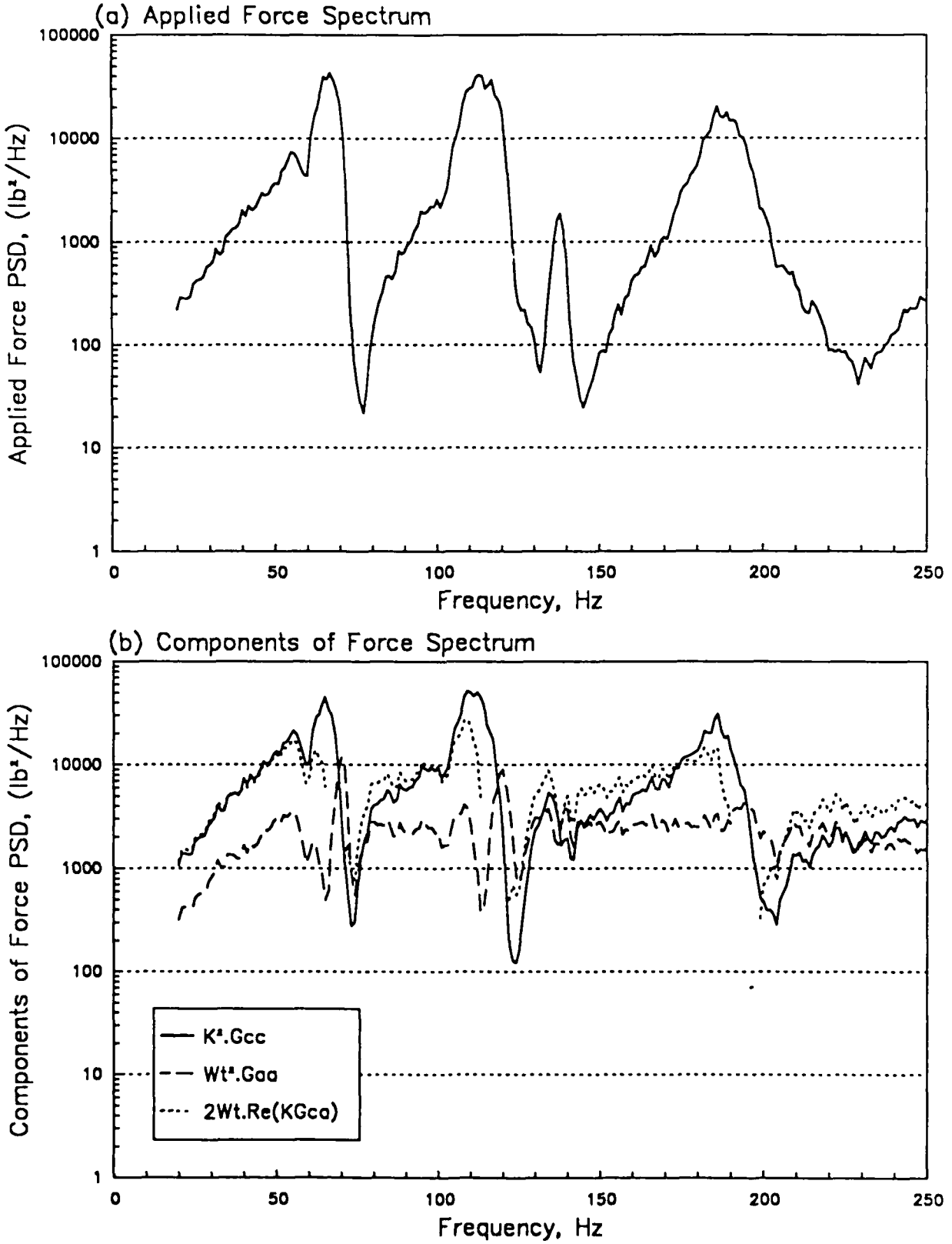

Figure 28. Applied Force Spectrum, Payload Rigid Mount on APC, 6 dB below Vibration Specification.

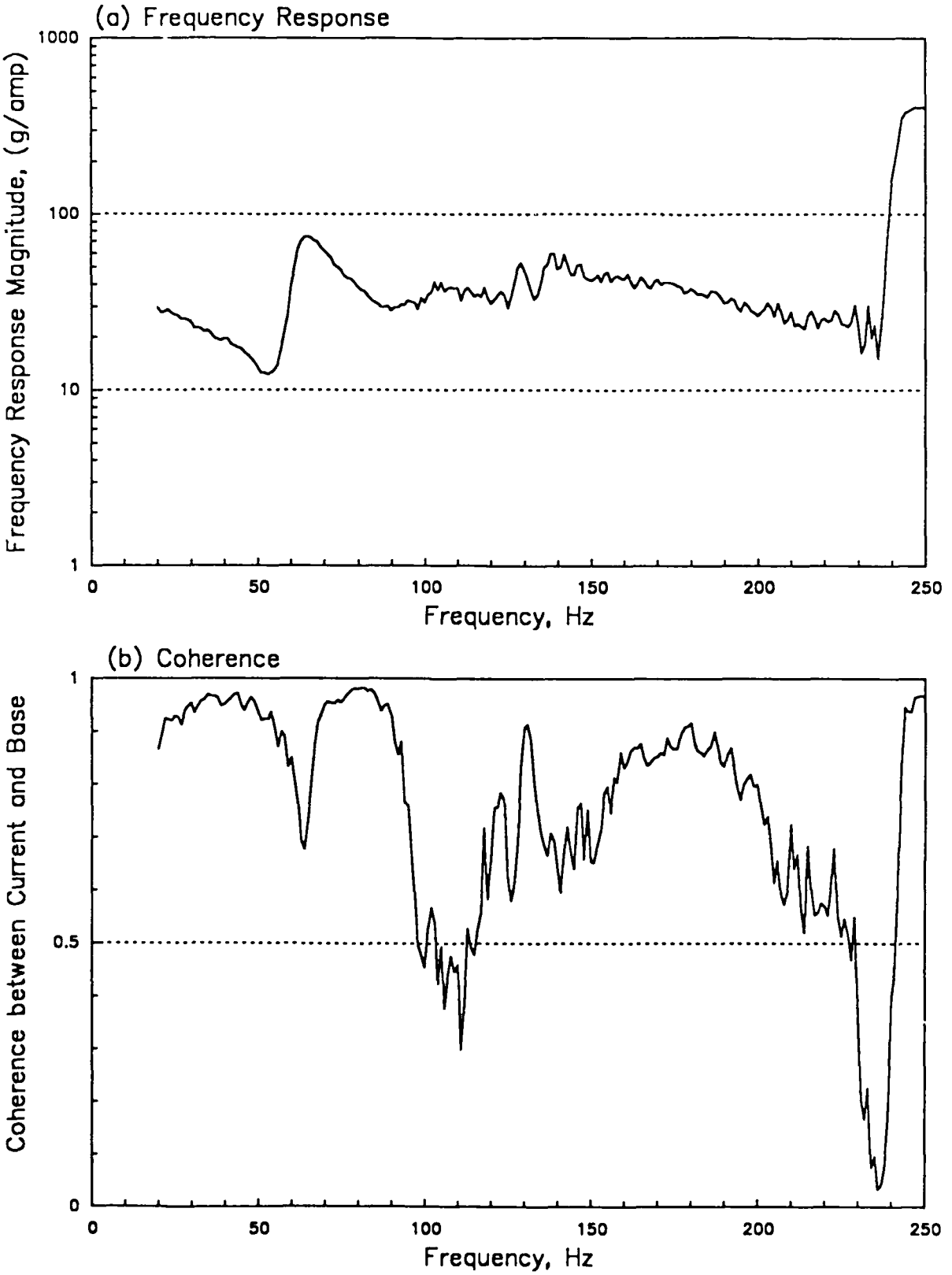

Figure 29. Shaker Current and Table Acceleration, Payload on APC with 0.005" Gap, 6 dB below Vibration Specification.

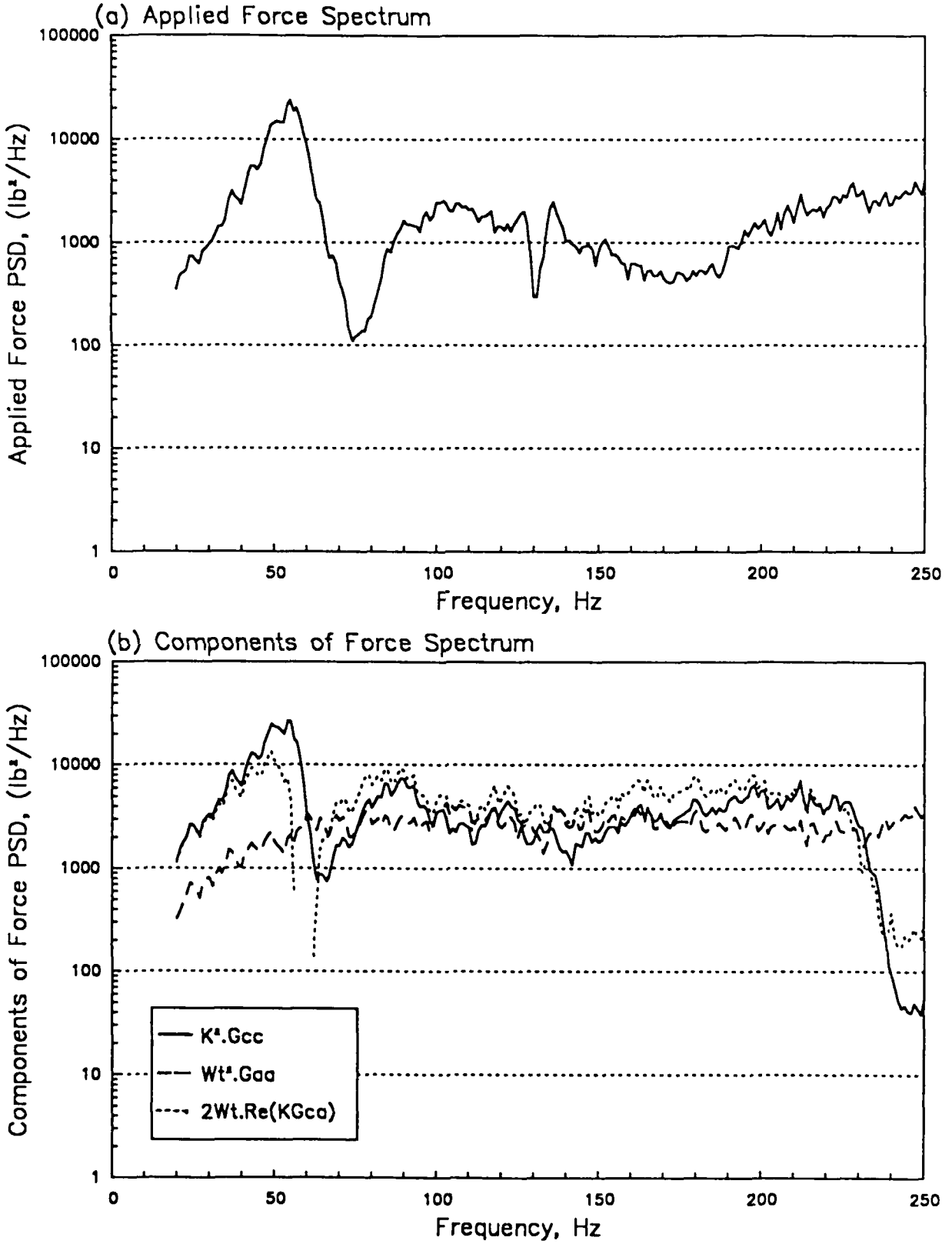

Figure 30. Applied Force Spectrum, Payload on APC with 0.005" Gap, 6 dB below Vibration Specification.

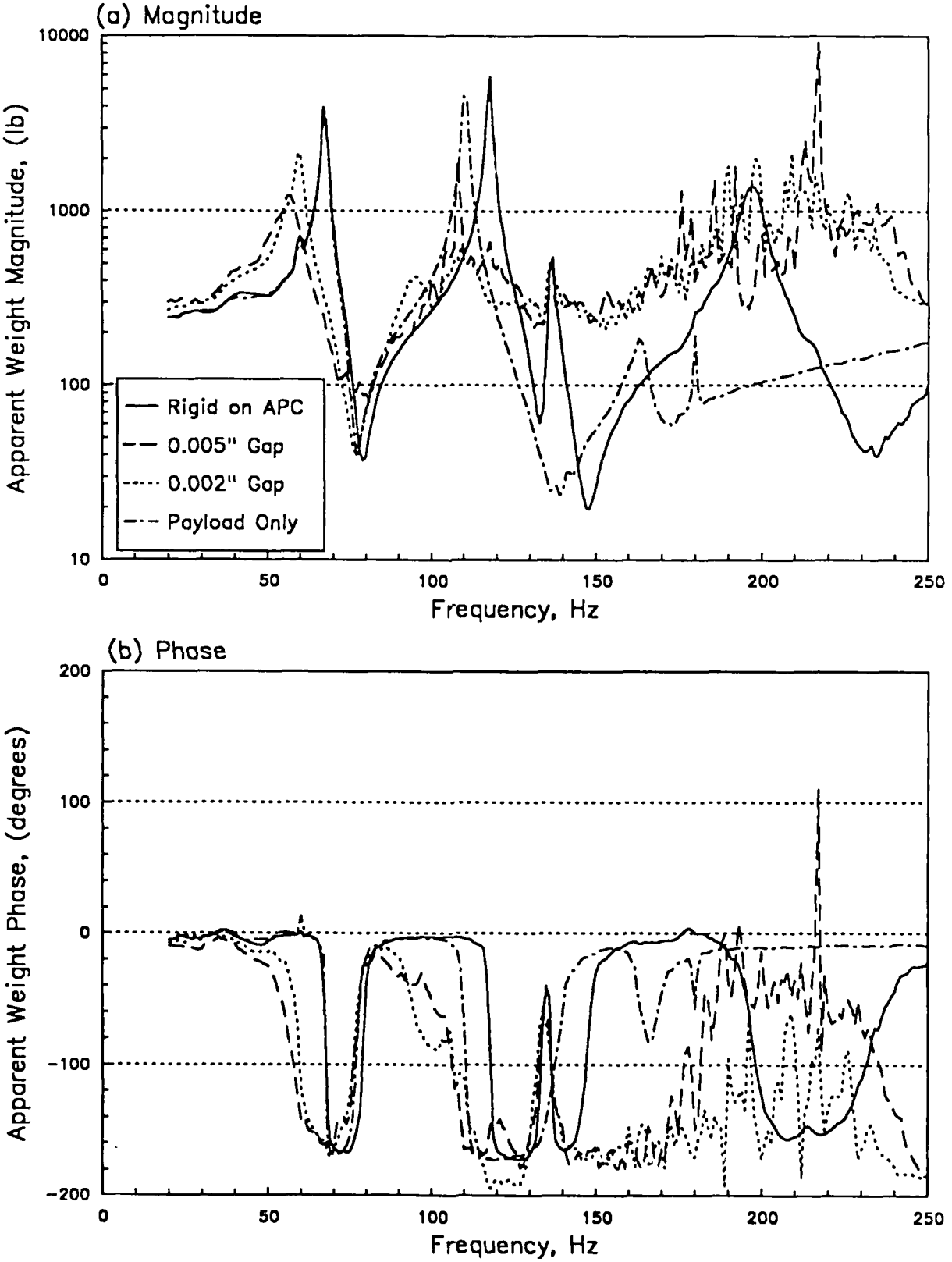

Figure 31. Apparent Total Weight of Payload, 12 dB below Specification Level.

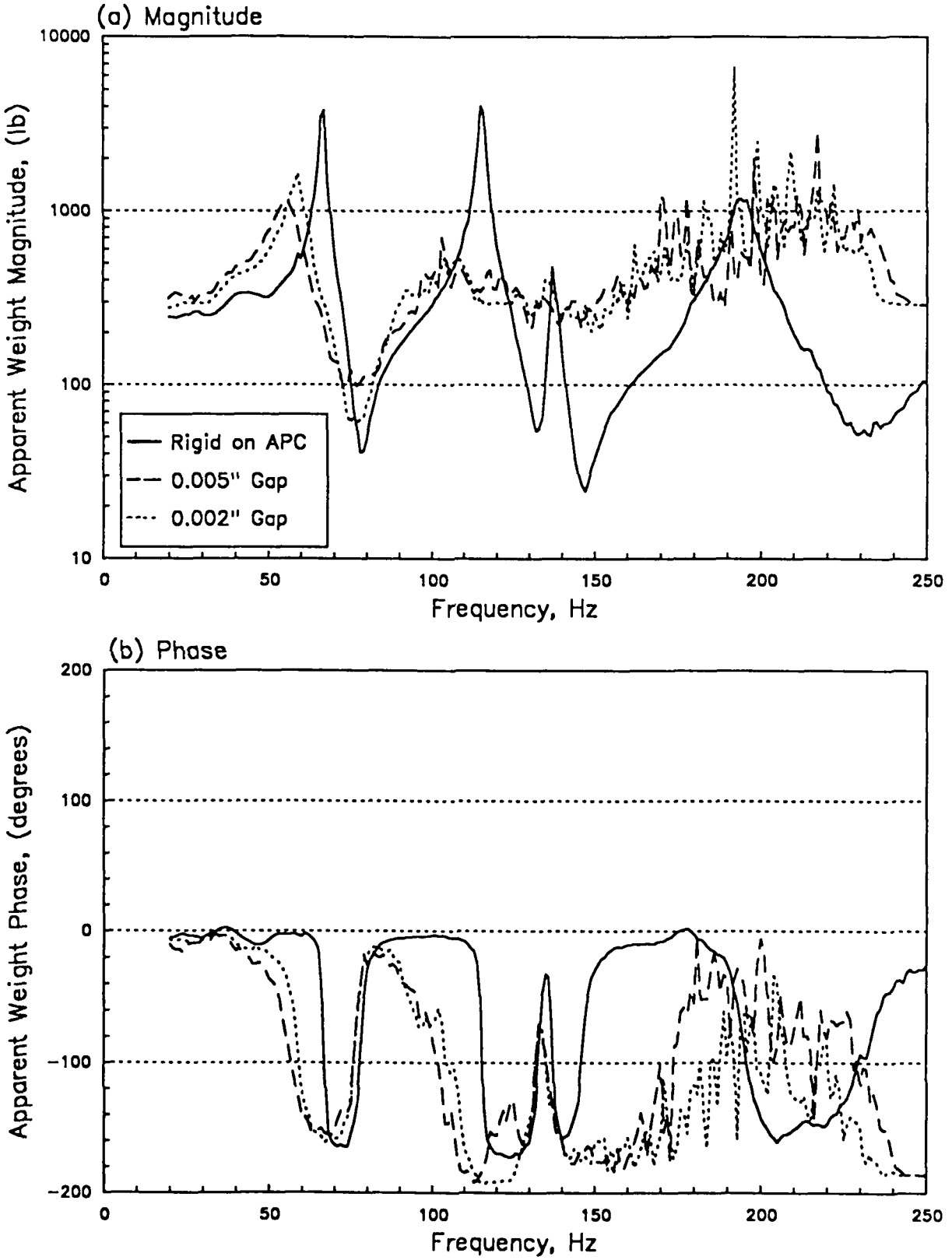

Figure 32. Apparent Total Weight of Payload, 9 dB below Specification Level.

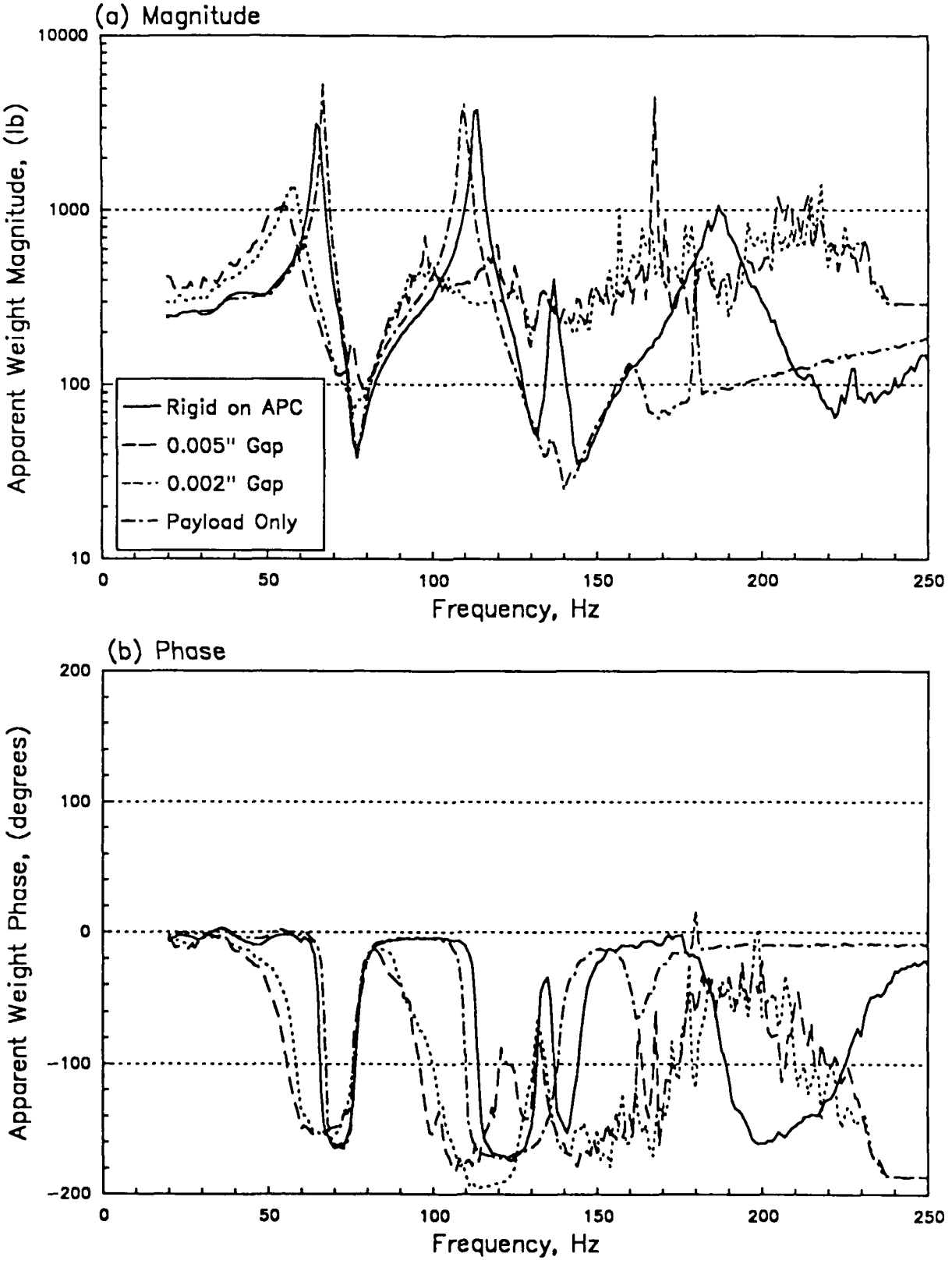

Figure 33. Apparent Total Weight of Payload, 6 dB below Specification Level.

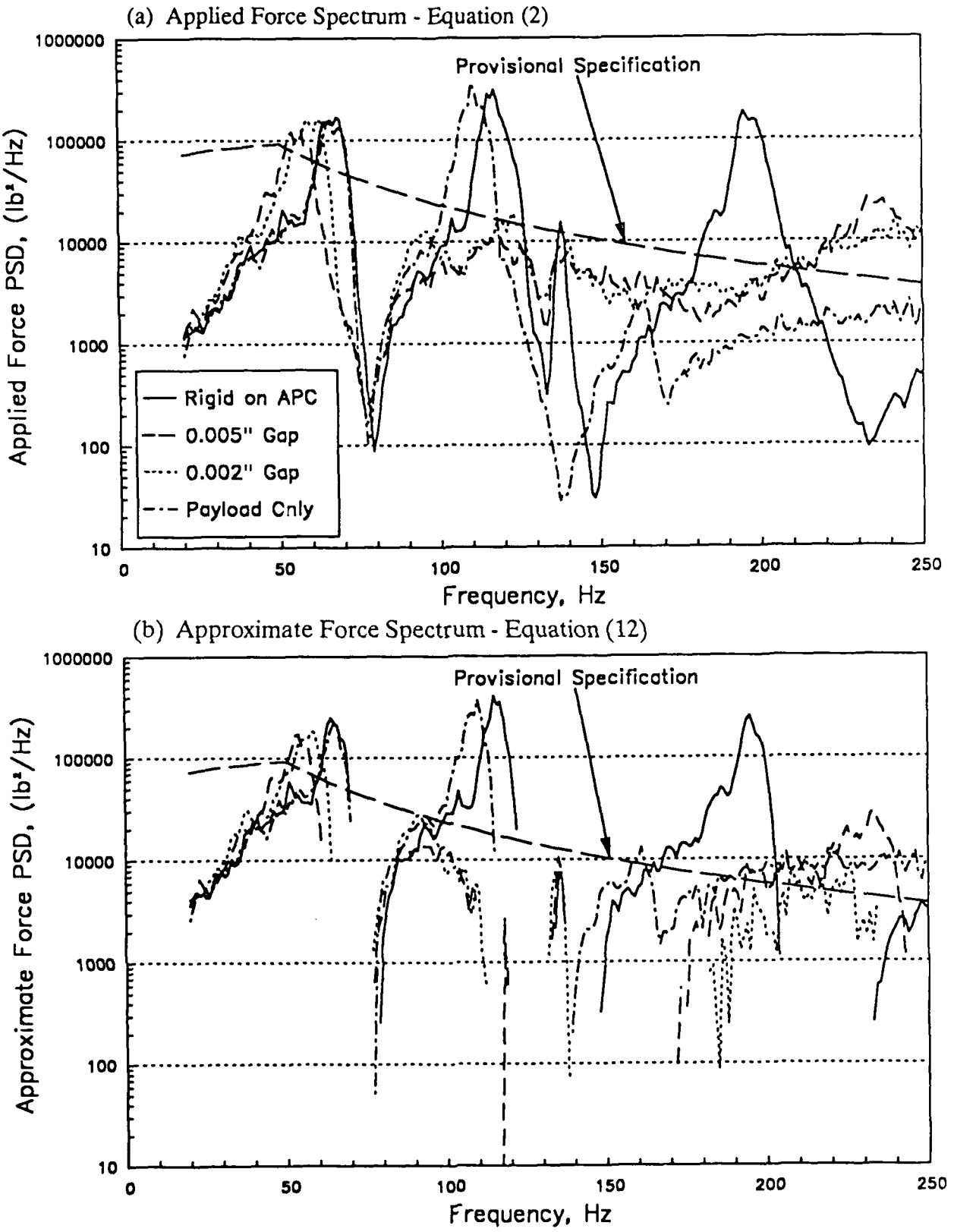

Figure 34. Applied and Approximate Force Spectrum, 12 dB below Vibration Specification.

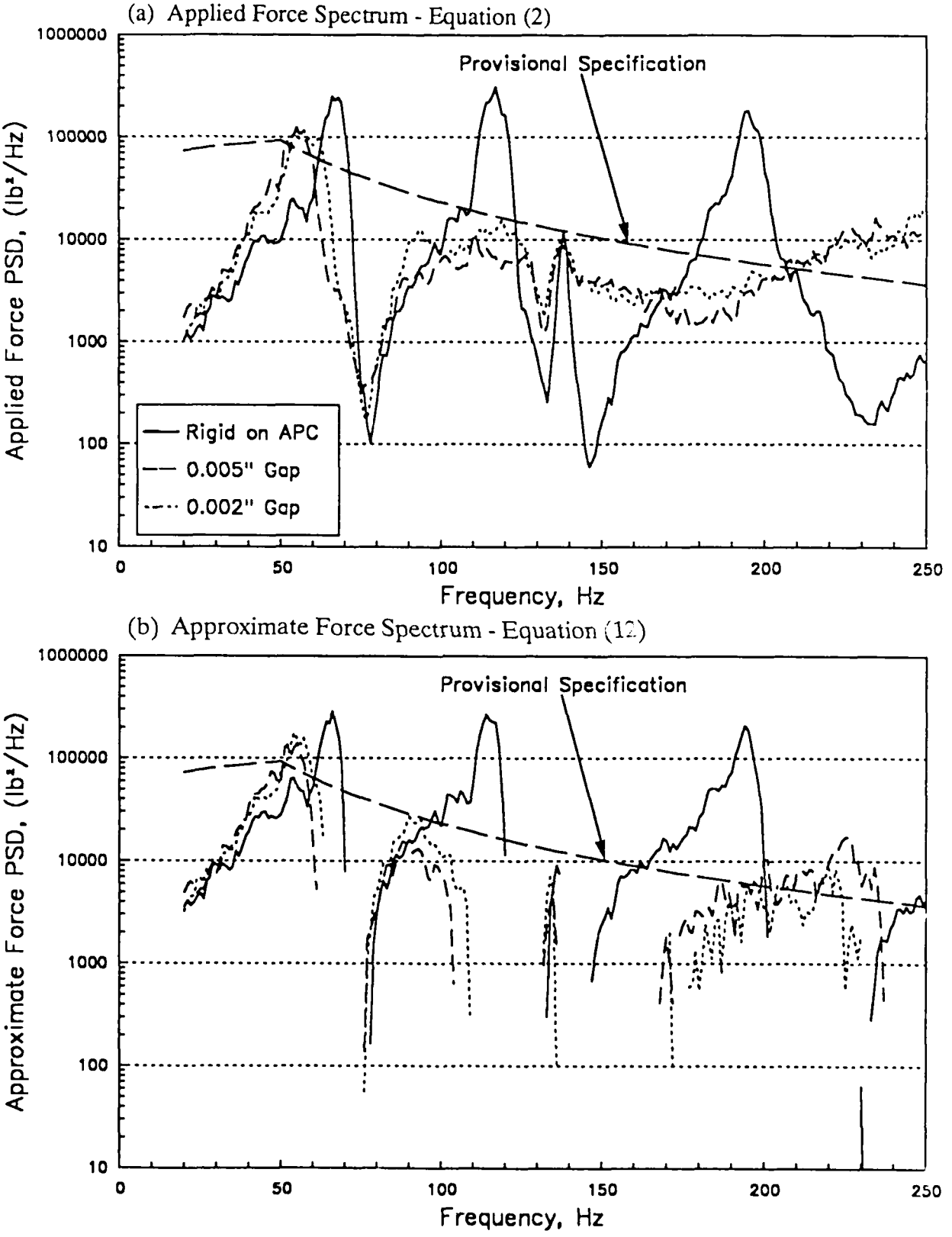

Figure 35. Applied and Approximate Force Spectrum, 9 dB below Vibration Specification.

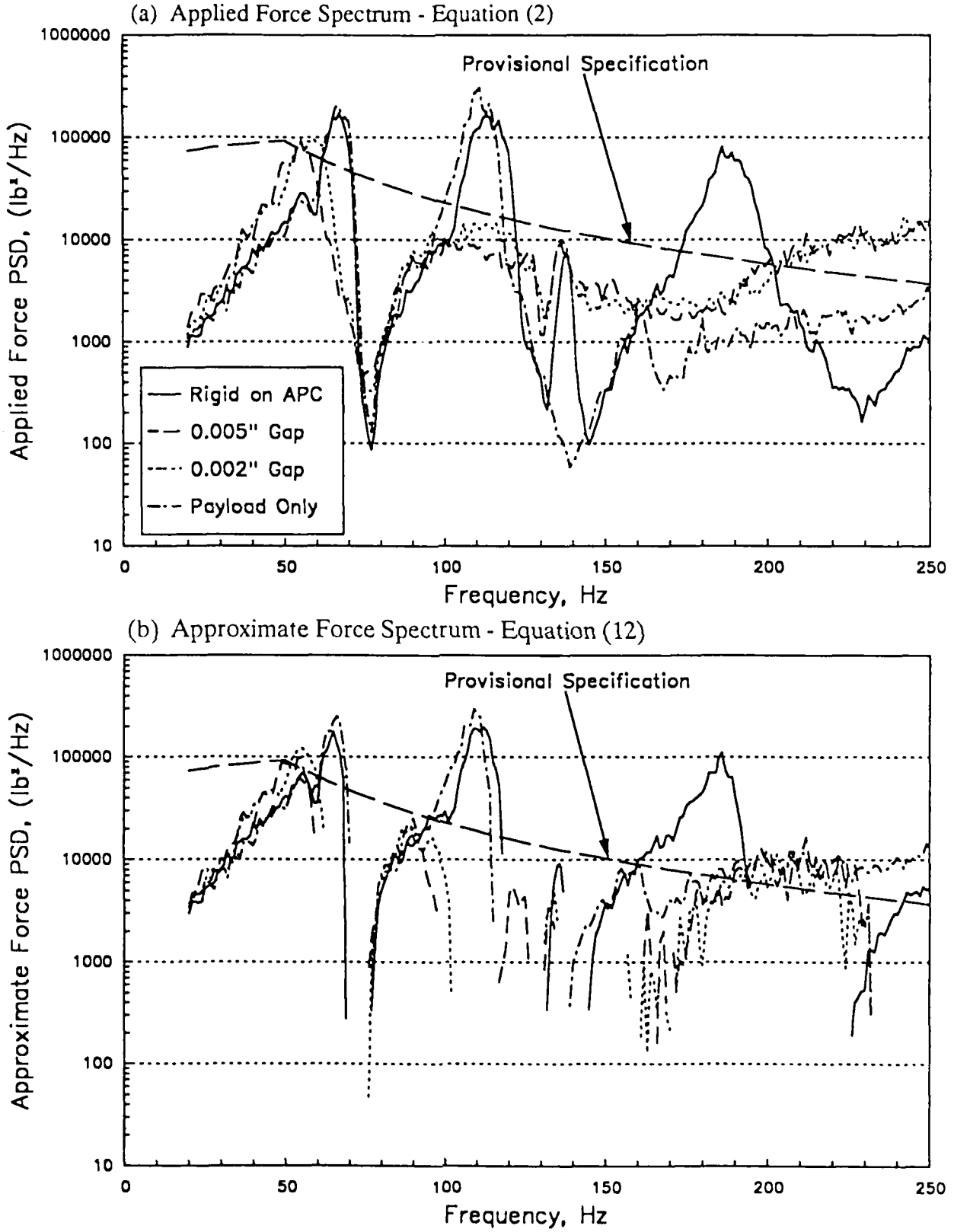

Figure 36. Applied and Approximate Force Spectrum, 6 dB below Vibration Specification.

payload resonances to comply with the force limit specification. The looseness at the mounting point appears to cause the resonant behavior to appear as a very highly damped system with much less peak force transmitted into the payload.

The force transmitted into the payload may be reduced by decreasing the shaker current at the appropriate frequencies. This force limiting is achieved by lowering the current spectrum and shaker table acceleration by an amount proportional to the difference between the actual transmitted force and the specification limit, as seen in Figures 34-36.

The severe payload rattle during vibration testing caused by the gaps at the mounting points induces extraneous and rather incoherent noise in all the transducer signals. As a result, there is a loss of coherency between the driving shaker current and the force applied to the payload. The shaker reference accelerometer senses not only the direct motion caused by the current in the armature coil, but also the ringing and local vibration of the armature structure caused by the payload hitting and rebounding during the rattling process. Consequently, the equalization system works to control the shaker motion with a signal contaminated by noise. While the system is sufficiently robust to control this non-linear process and maintain any desired acceleration spectrum at the shaker table, there is concern that the transmitted force estimate based upon the shaker current and acceleration will not be an accurate estimate of the true force applied to the payload. Without force sensing transducers at the mounting points, there is no other procedure available to estimate force.

The effect of the clearance gap on the equalization can be seen in Figure 37. These curves give the shaker current spectra for a constant acceleration spectrum at the reference accelerometer on the shaker table. It is seen that the current spectra for rigidly mounted payloads, on or off an APC, are quite similar. Adding a clearance gap changes the current spectrum considerably. It is very obvious that the rattling in the gap has a strong influence upon the equalization. The slight change in frequency of the second resonance of the APC mounted payload was caused by inadvertently reversing the configuration of the payload with respect to the APC in the second test. Even though the peripheral mounting bolt pattern allows the payload to be reversed, the 40 and 50 pound weights cause asymmetric static and dynamic payload characteristics. This occurrence serves to emphasize the importance of the APC-payload coupling at higher frequencies.

Response of the two resonators is also affected by the mounting clearance gap. With a rigidly mounted system, on or off the APC, the frequency response between the resonator accelerometers (A_5 and A_6) and the shaker table (A_0) is well defined and has high coherence. Figures 38 and 39 show that the resonator motion is very large relative to the shaker table motion at precisely those frequencies of high apparent weight and large input force (Figures 31-36). Figure 40 shows a drastic change in the frequency response function when the gap

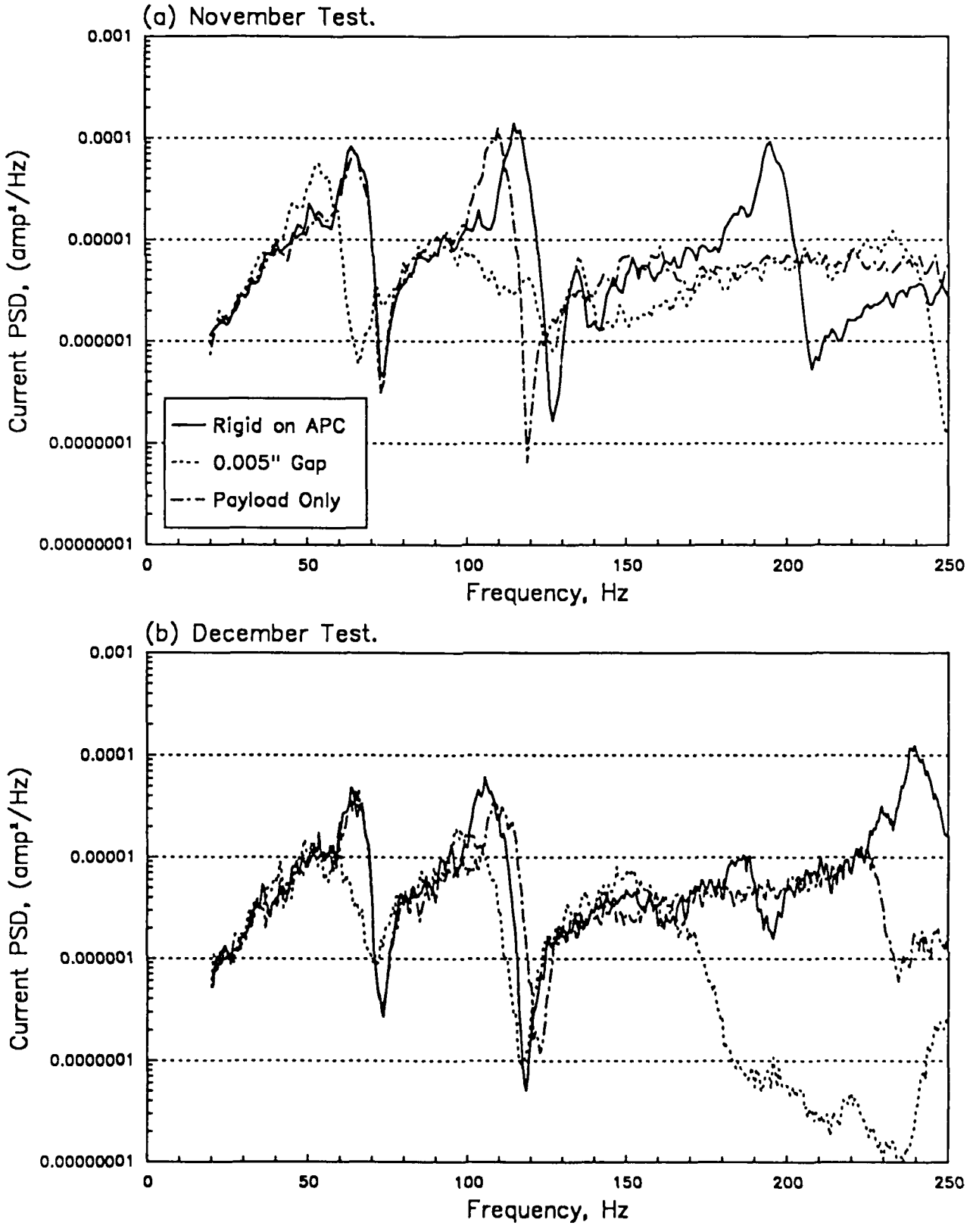

Figure 37. Shaker Current PSD, 12 dB below Vibration Specification.

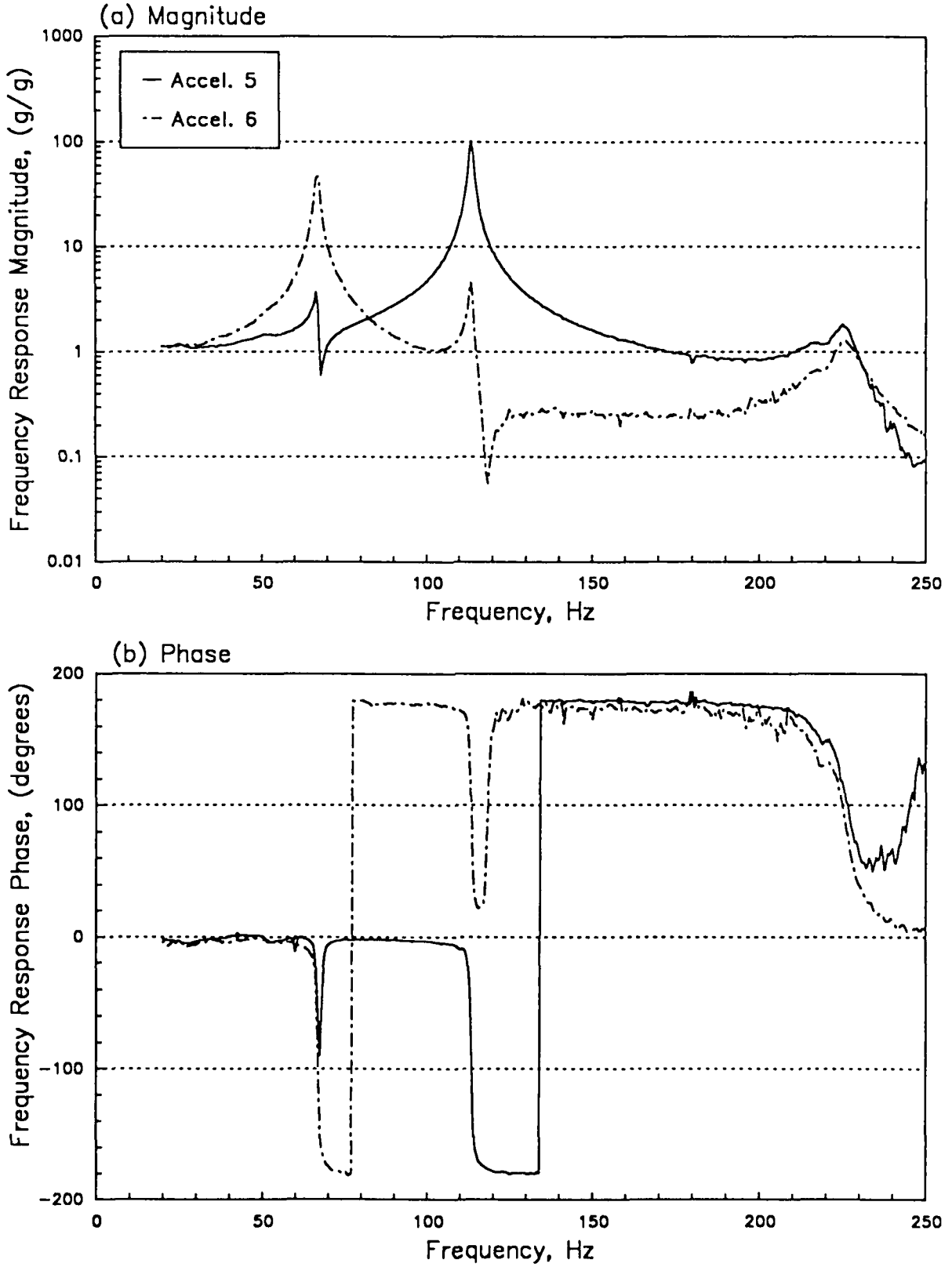

Figure 38. Payload Masses and Table Accelerations, Payload Rigid Mount, 12 dB below Vibration Specification.

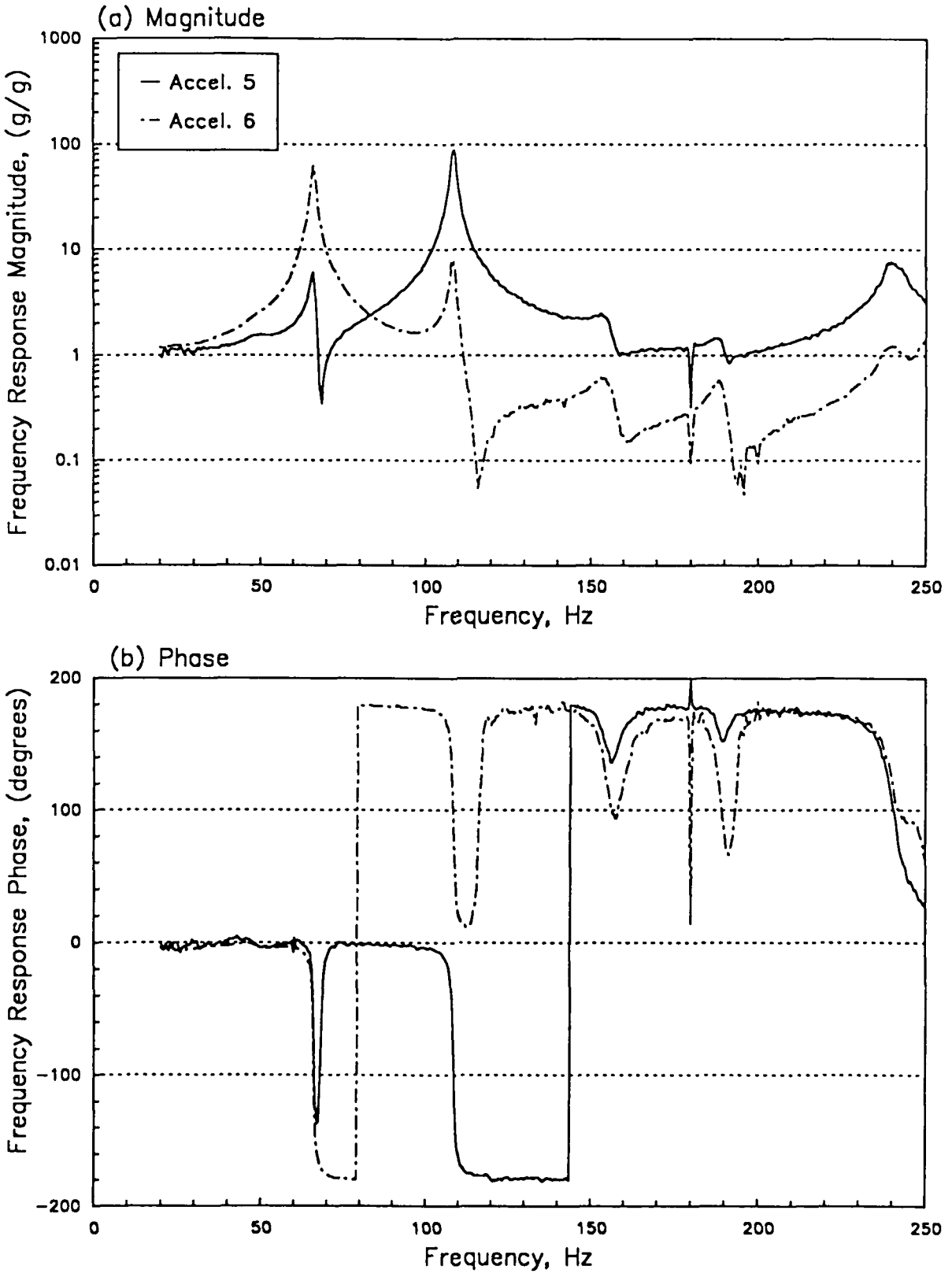

Figure 39. Payload Masses and Table Accelerations, Payload Rigid Mount on APC, 12 dB below Vibration Specification.

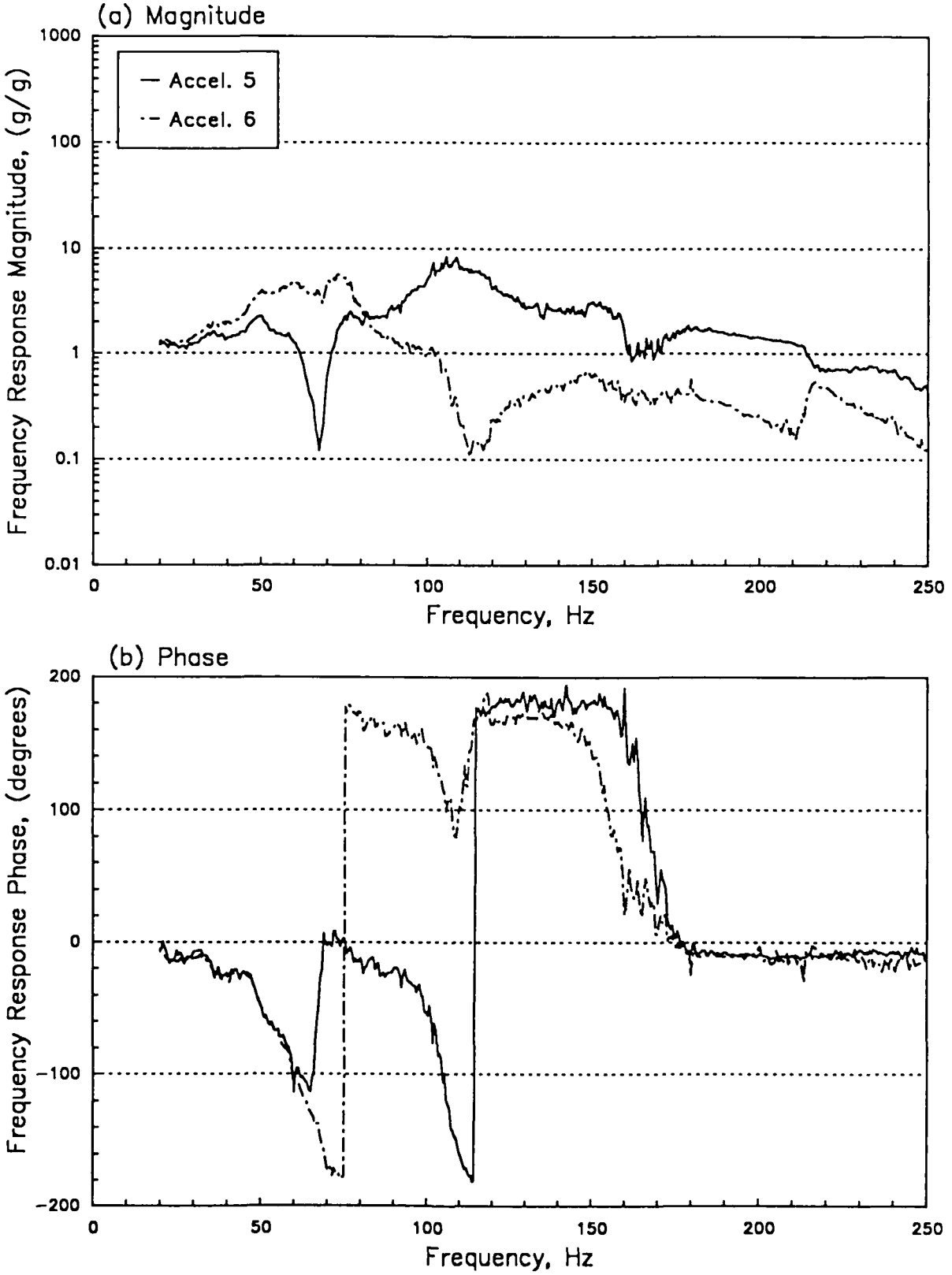

Figure 40. Payload Masses and Table Accelerations, Payload on APC with 0.005" Gap, 12 dB below Vibration Specification.

is introduced, with behavior that is very different from a lightly damped resonator. These features are summarized in Figure 41.

The reduction of resonant component response relative to the shaker table due to mounting clearance gaps has an important implication in the vibration of real payloads. In actual service, there will be less resonant behavior of the payload components, with consequent reduction in peak acceleration and loads at the component resonant frequencies. There will, however, be increased energy in higher frequency regions because the repeated impacts of the rattle produce more high frequency energy. In the test environment the payload may be tested by two alternate procedures, with different results. In one case, the payload may be mounted with the clearance gaps and the shaker equalized to a predetermined spectrum, for example as in Figure 18. Here, the response of the resonant components in the payload will be less than if the payload were hard mounted. A second procedure is to set up the payload rigidly on the shaker, and equalize the vibration to the desired level. The payload mounting is then shimmed appropriately to obtain the desired clearance, and then driven with the same shaker current as for the rigidly mounted case. This too will result in component response levels less than with a rigidly mounted payload.

4.7 Application of Force Limit Procedure

The behavior of the payload and APC was confirmed by an independent series of tests using the same apparatus and instrumentation described in Sections 4.1-4.4. In addition to testing the system for repeatability, the excitation was modified by the process described in Section 2. While the various frequency response functions between shaker current, reference acceleration, payload response, and component response were very similar for both tests, as were the applied force and apparent weight functions, there were notable differences in the corresponding functions for the gapped mounting. These are best illustrated in Figures 42-44. Such differences only serve to emphasize the point that testing with a thermal clearance gap at the APC mounting points is not a very controlled situation. It would be difficult and time consuming to set up a test configuration that would be a meaningful representation of the real environment, and one that would allow for the proper degree of confidence in its repeatability to be established.

The force limit procedure was implemented by establishing a spectrum of limiting shaker current based upon Equation 15. This current spectrum was calculated for the appropriate values of acceleration spectrum, SSV sidewall apparent weight, and shaker armature weight to yield the curves shown in Figure 45. These curves do not represent the true value of Y axis limiting forces given in Figure 12, but are simplified versions suitable for the demonstration experiment. The current of Figure 45 corresponds to the provisional specification force curves given in Figures 34-36.

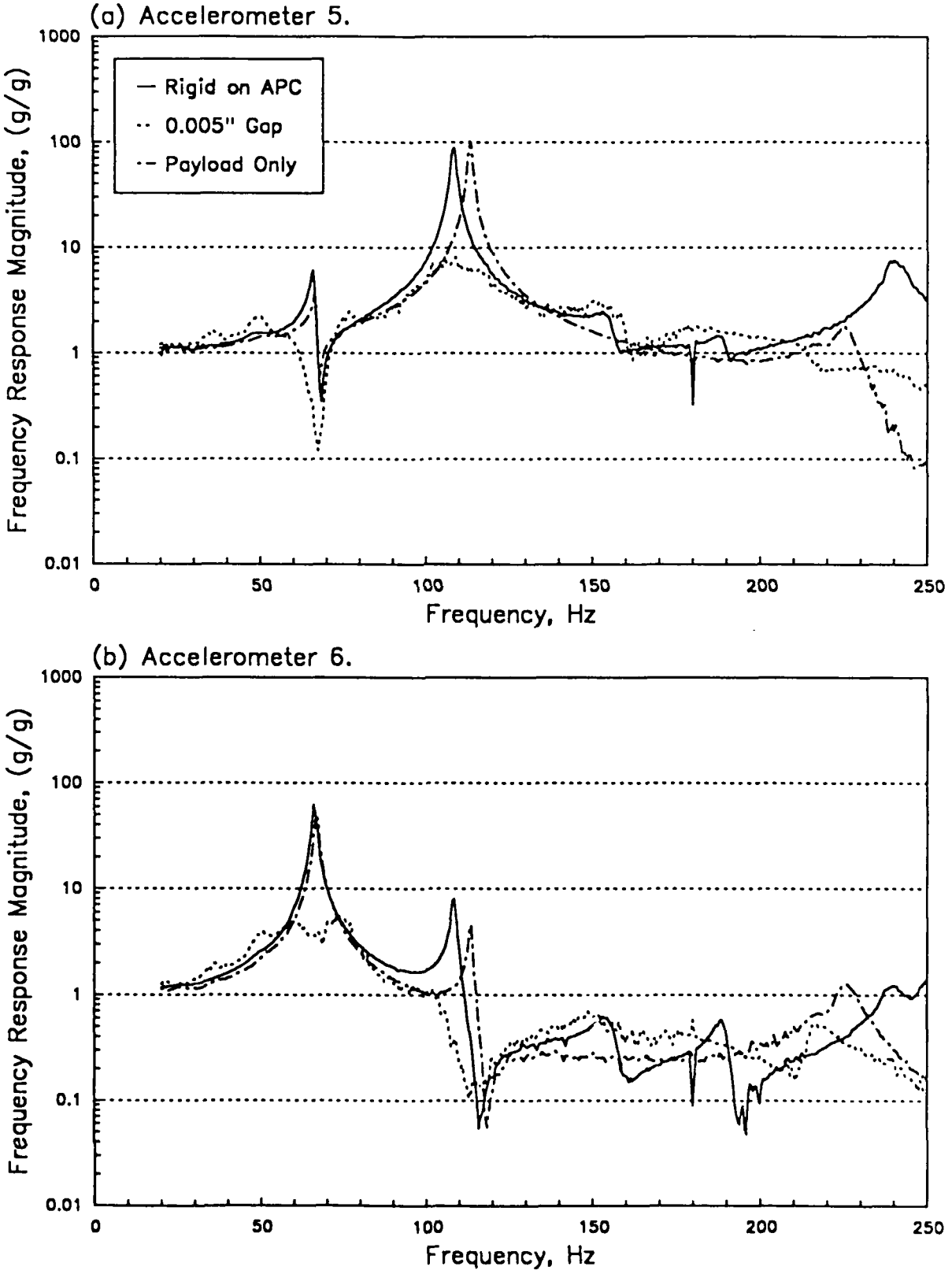

Figure 41. Payload Masses and Table Accelerations, 12 dB below Vibration Specification.

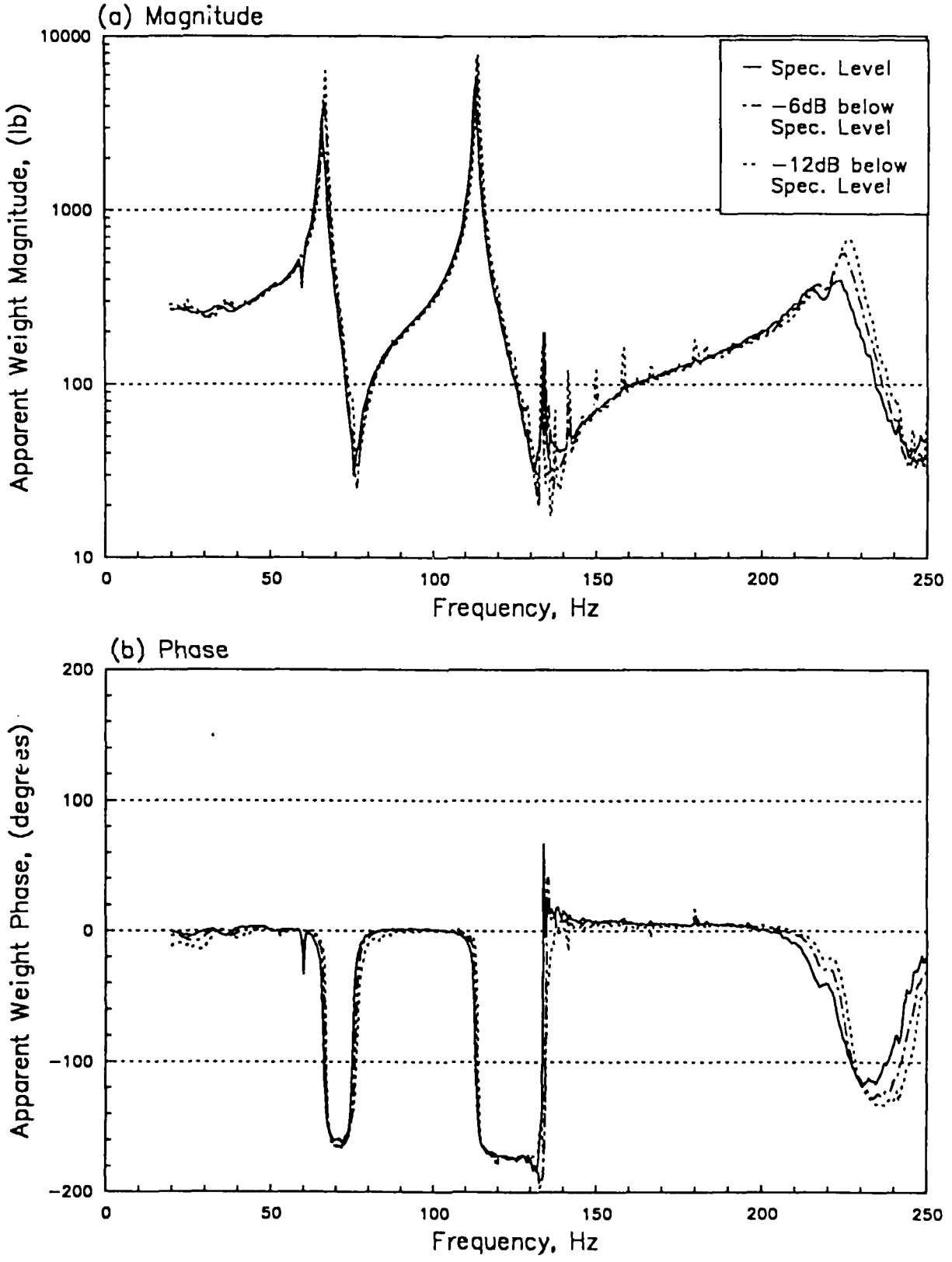

Figure 42. Apparent Total Weight, Payload Rigid Mount, Modified Spectrum.

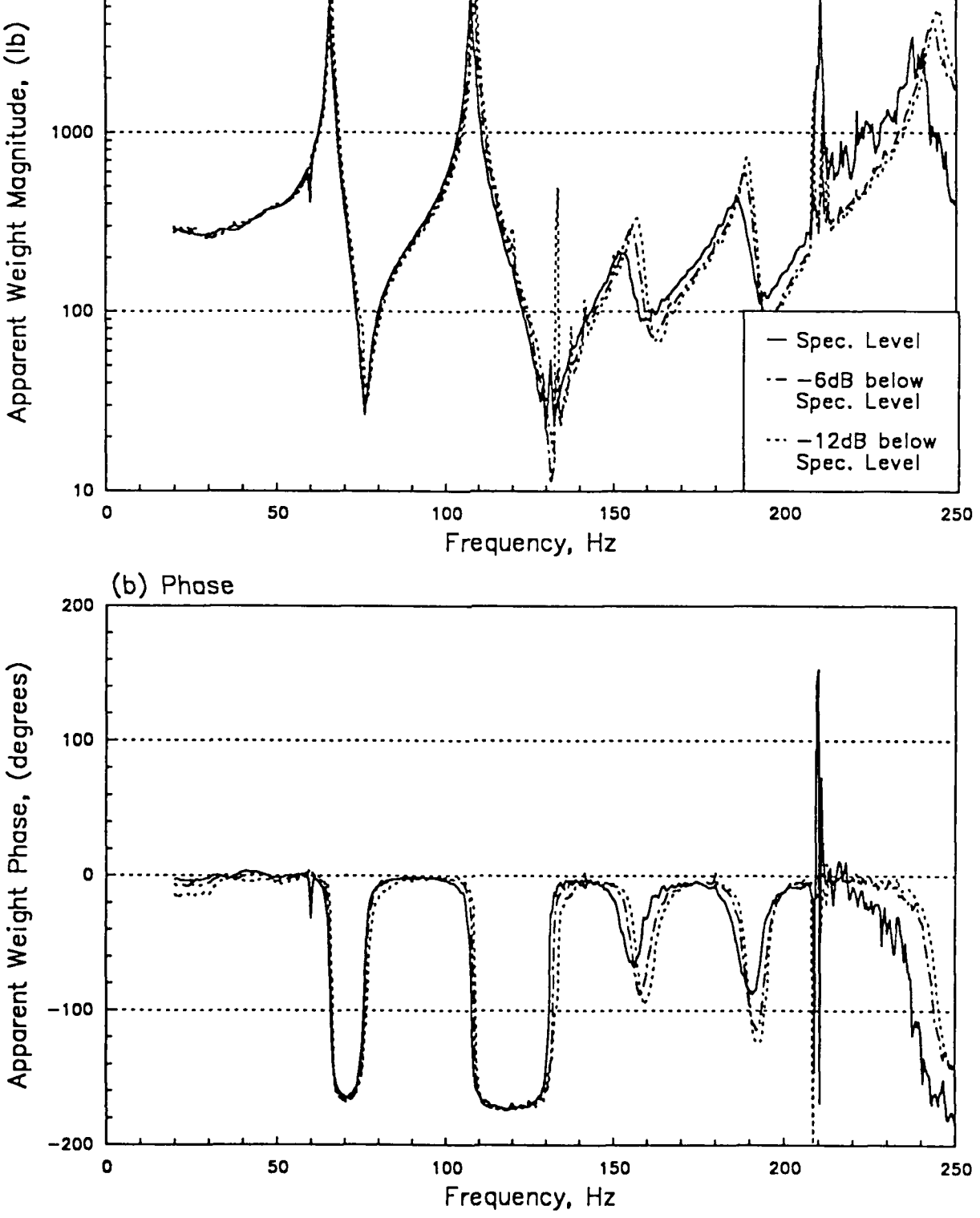

Figure 43. Apparent Total Weight, Payload Rigid Mount on APC, Modified Spectrum.

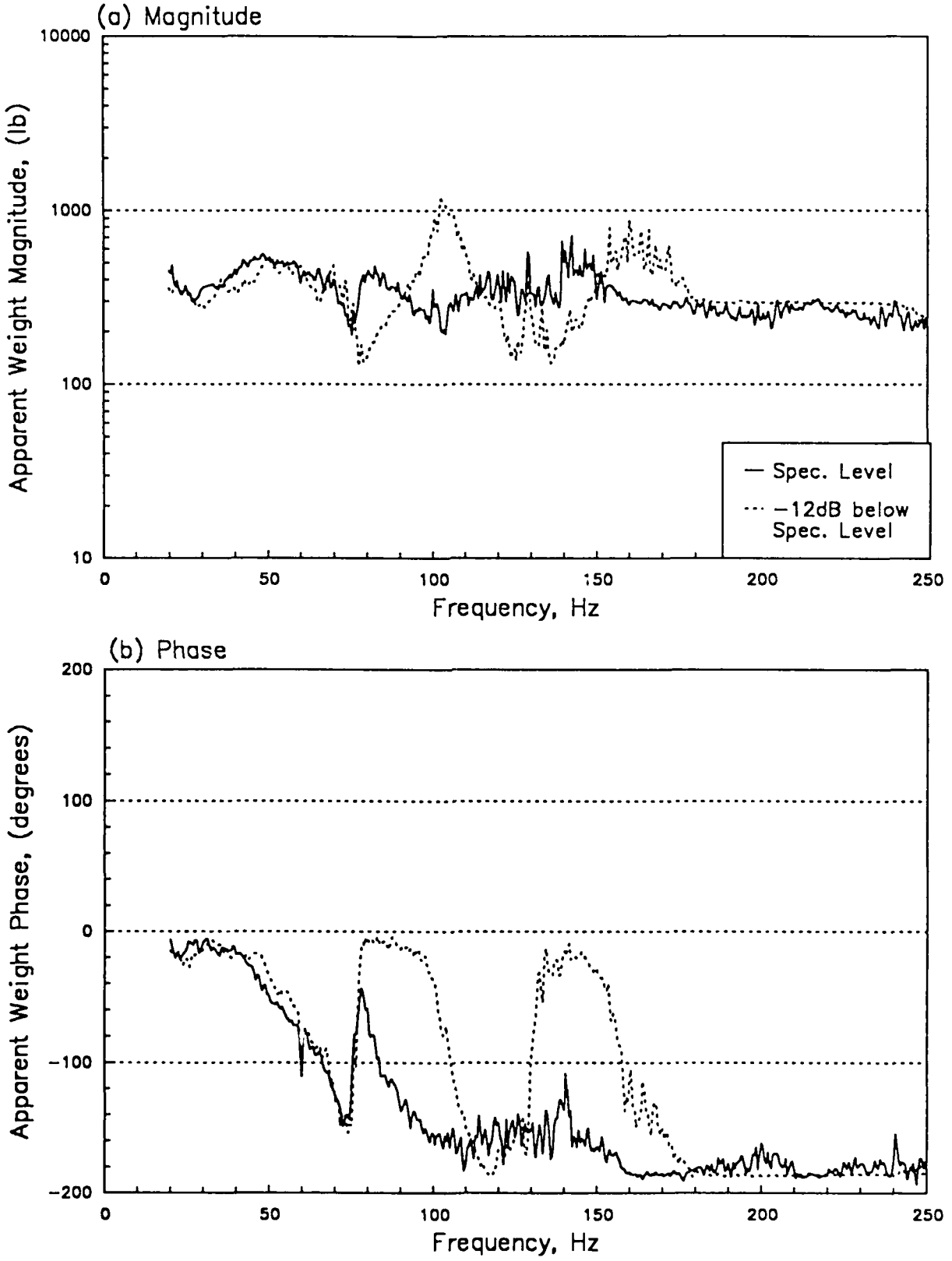

Figure 44. Apparent Total Weight, Payload on APC with 0.005" Gap, Modified Spectrum.

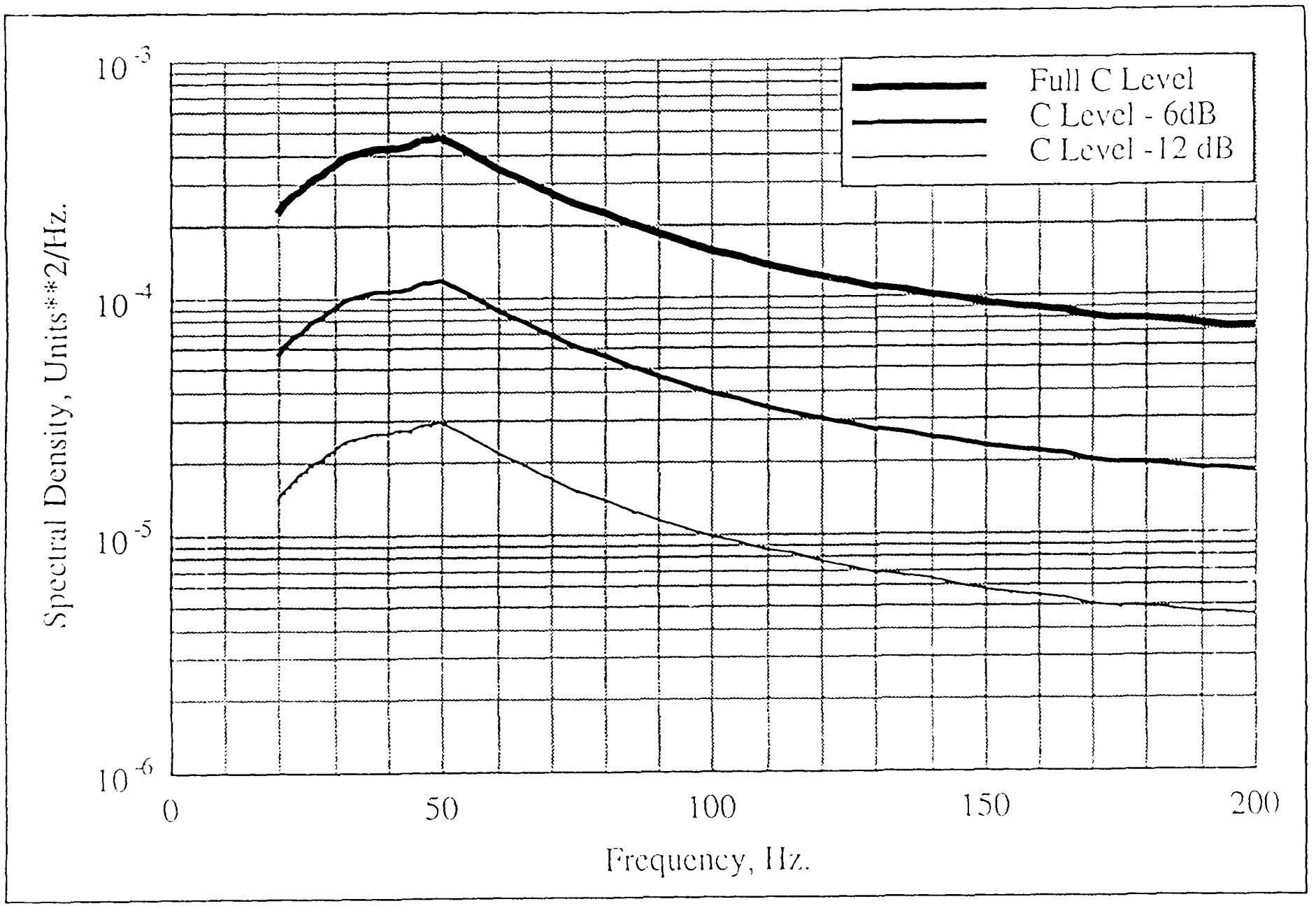

Figure 45. Y Axis Current Limit for Space Shuttle Sidewall Mounted Payloads / Components.

For each set-up, a preliminary vibration test was performed with a table acceleration spectrum 12 dB below that of Figure 18. During this trial run, a spectral analysis of the shaker current was performed with the HP 3562A analyzer, and results compared to the lower curve of Figure 45. From this comparison, it was possible to estimate the amount and location of force limiting to be performed. This force limiting was done manually with the shaker control system computer, and the test repeated (again at 12 dB below the full spectrum level). The procedure required three modifications to satisfy the current spectrum for the payload alone, one modification for the payload on the APC, and no modifications for the payload on the APC with a 0.005 inch gap. Time limitations for the tests dictated that the force limiting be applied only in the frequency regions near the large apparent weight (around 60 and 110 Hz); no attempt was made to establish complete force limiting above 200 Hz.

The applied force spectrum, calculated by the exact method of Equation (2) and the approximation

$$G_{FF}(f) \approx |K(f)|^2 G_{CC}(f) - W_S^2 G_{AA}(f) \tag{38}$$

are presented in Figures 46-48. It is evident that the system with no gaps is linear and scalable over the 12 dB range. Also quite noticeable is the significant change in the applied force spectrum over this range for the gapped case. The actual applied force calculated by Equation (2) or (38) depends upon linearity and high coherency between the shaker acceleration and current; a condition satisfied by the rigidly mounted payload, but not with the loosely mounted payload.

The linearity of the rigidly mounted payload system is further demonstrated by observing the frequency response function between the component weight motion and the shaker current. Figures 49 and 50 show that the magnitude of these frequency response functions are relatively insensitive to excitation level. However, this is only weakly true for the 0.005 inch gap configuration, as seen in Figure 51. A slightly different view of this behavior is shown in Figures 52 and 53. It may be noted that the component response of the gap mounted payload is more closely related to the shaker current than to the shaker table acceleration (Figure 41).

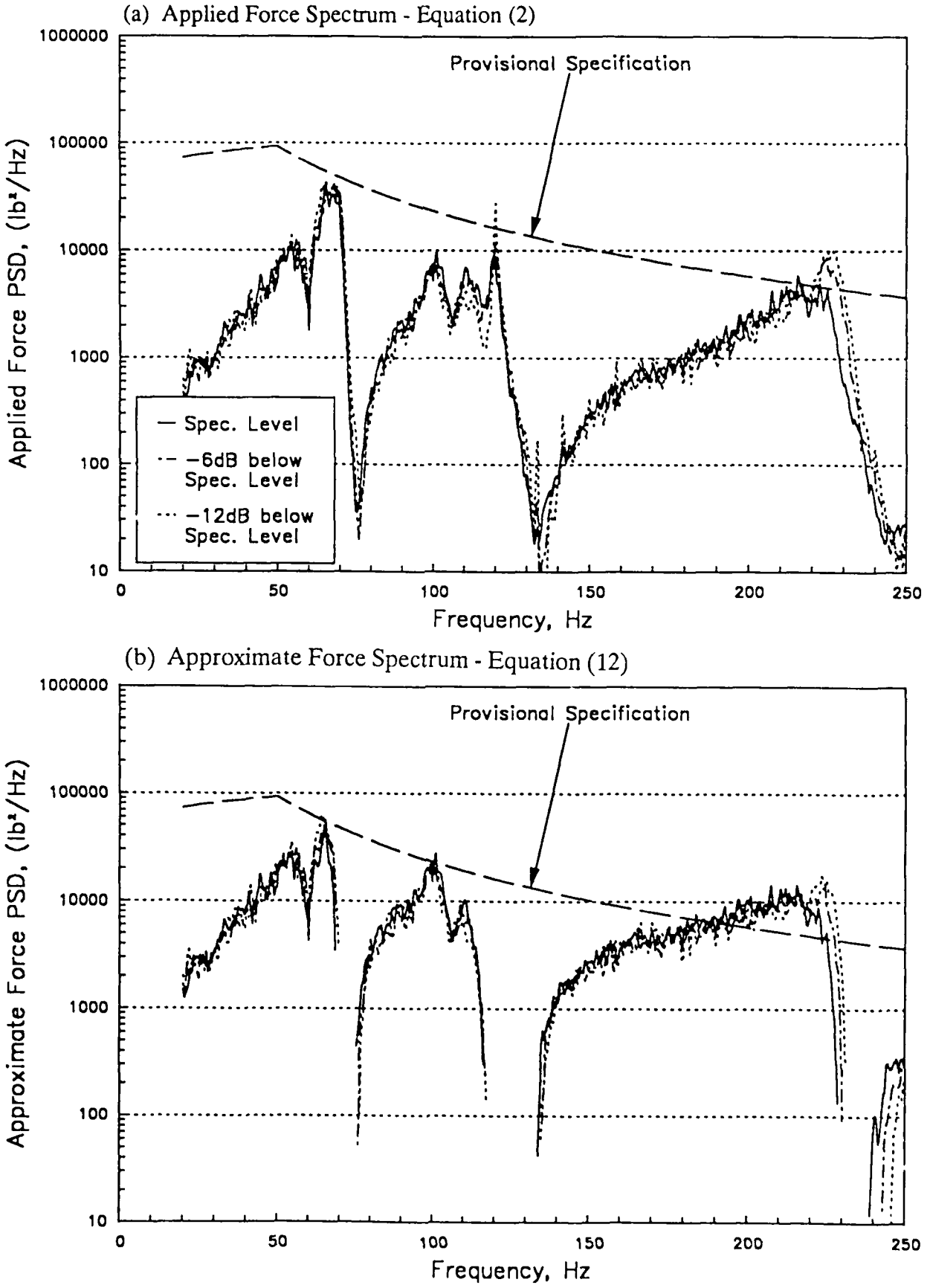

Figure 46. Applied and Approximate Force Spectrum, Payload Rigid Mount, Normalized to Vibration Acceleration Specification of Figure 18.

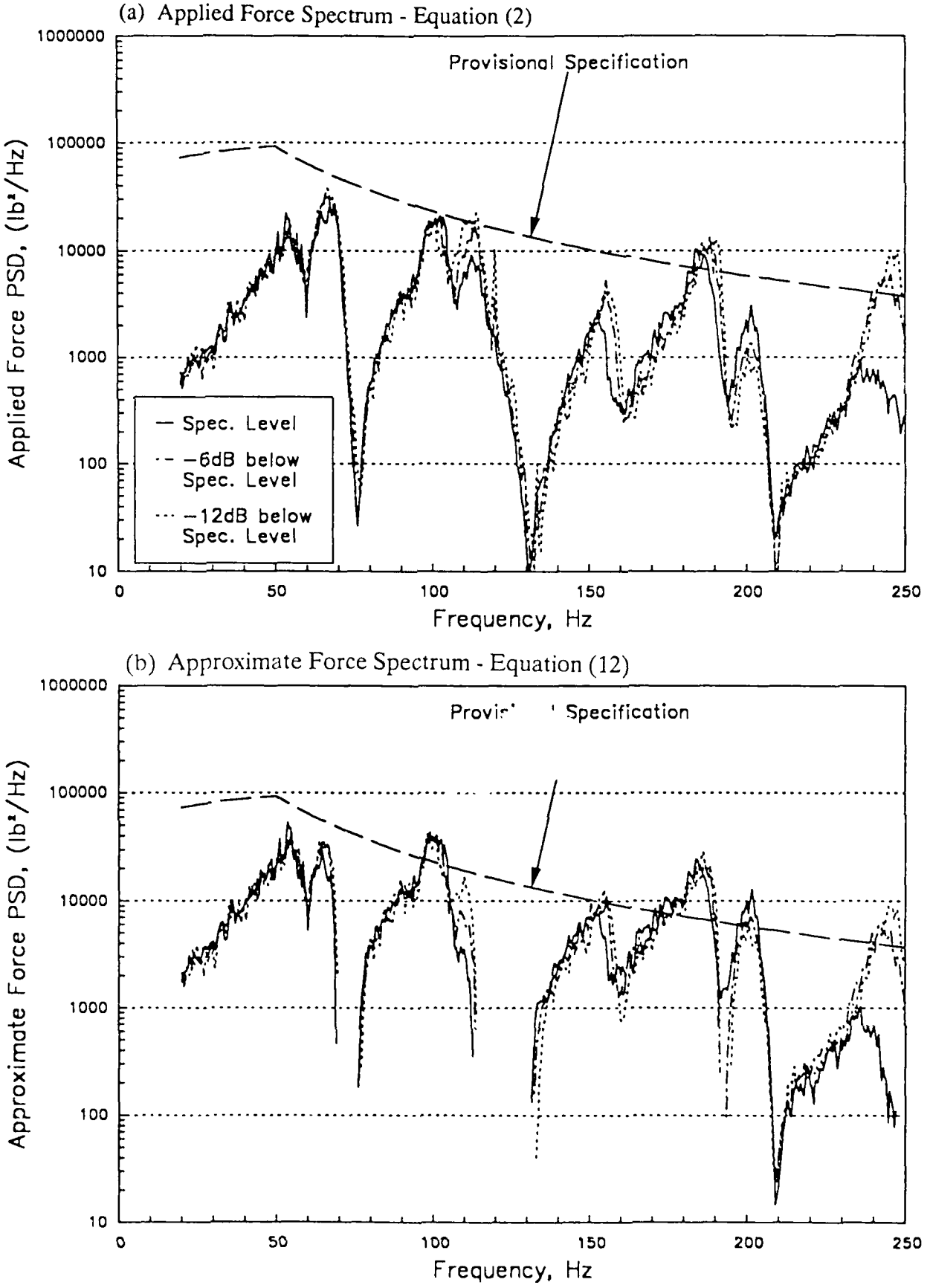

Figure 47. Applied and Approximate Force Spectrum, Payload Rigid Mount on APC, Normalized to Vibration Acceleration Specification of Figure 18.

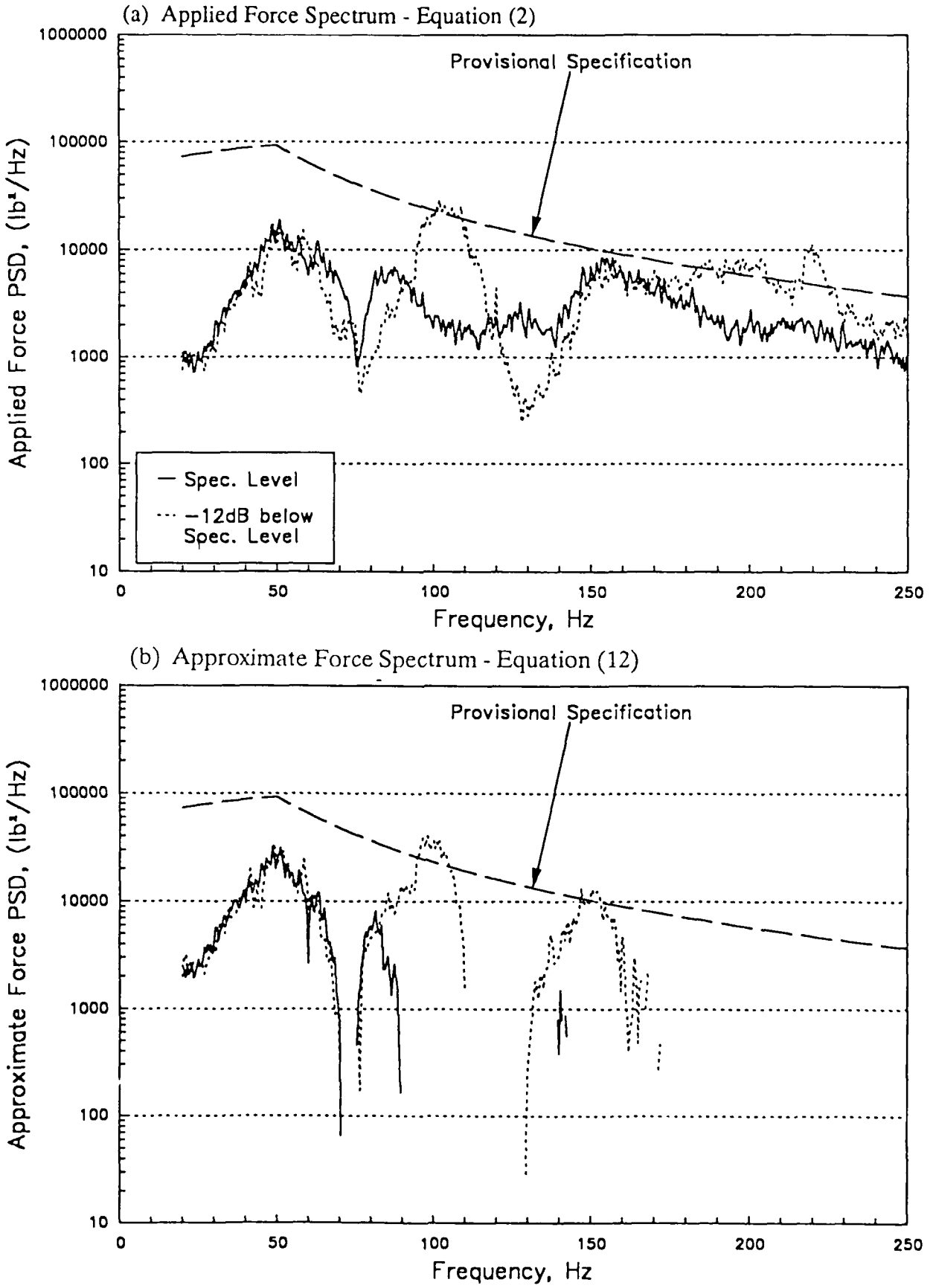

Figure 48. Applied and Approximate Force Spectrum, Payload on APC with 0.005" Gap, Normalized to Vibration Acceleration Specification of Figure 18.

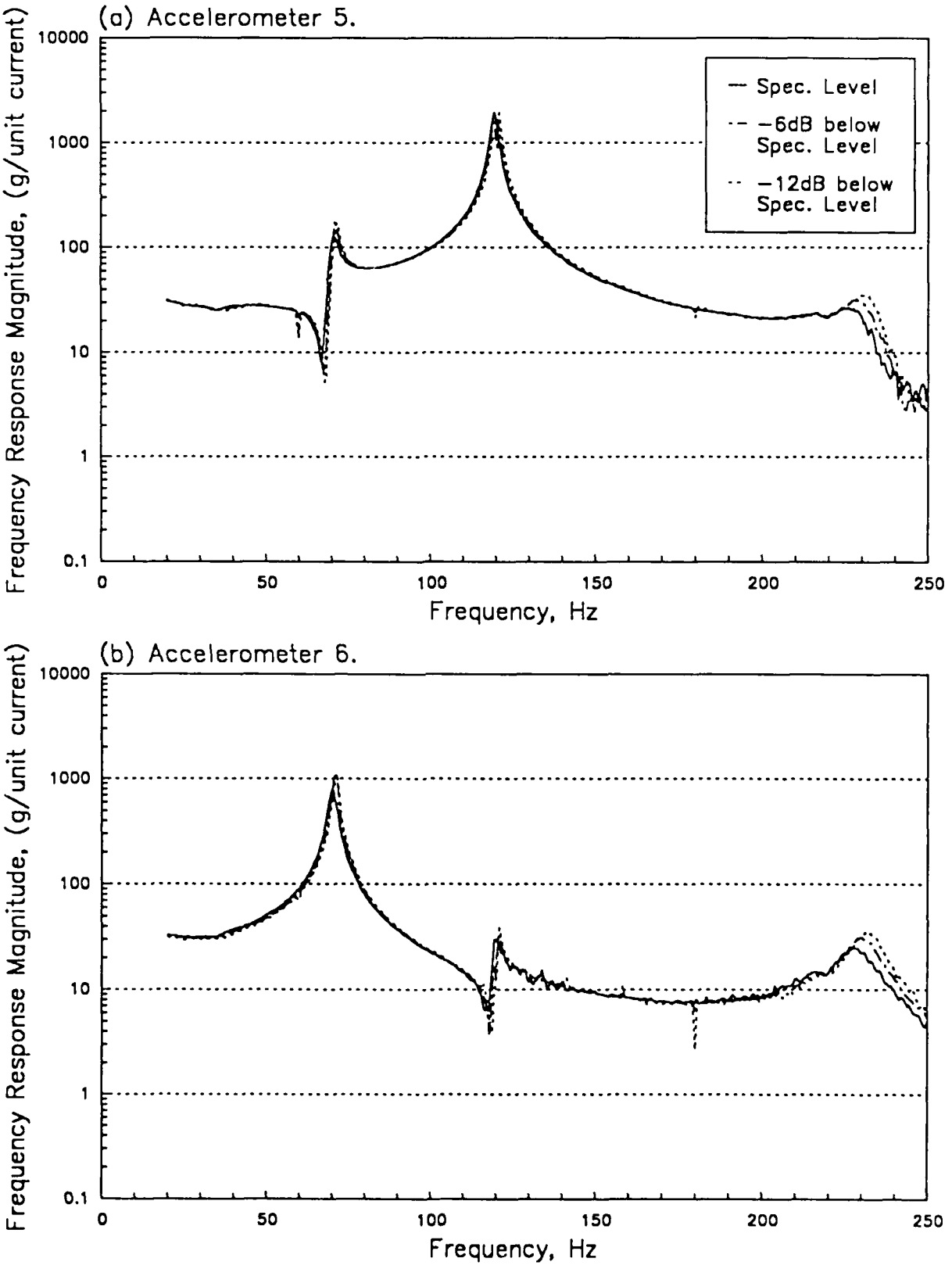

Figure 49. Shaker Current and Payload Mass Acceleration, Payload Rigid Mount, Modified Spectrum.

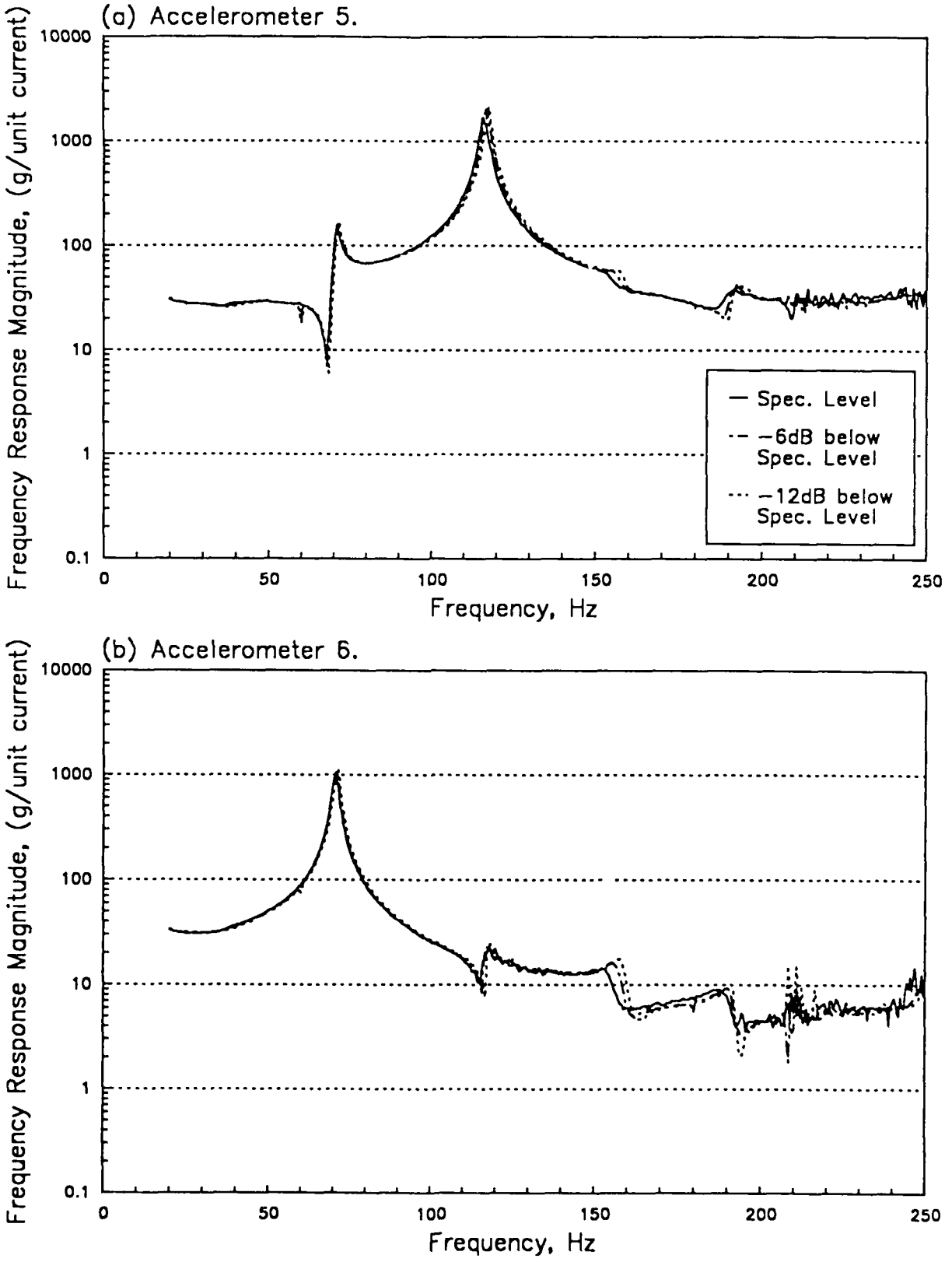

Figure 50. Shaker Current and Payload Mass Acceleration, Payload Rigid Mount on APC, Modified Spectrum.

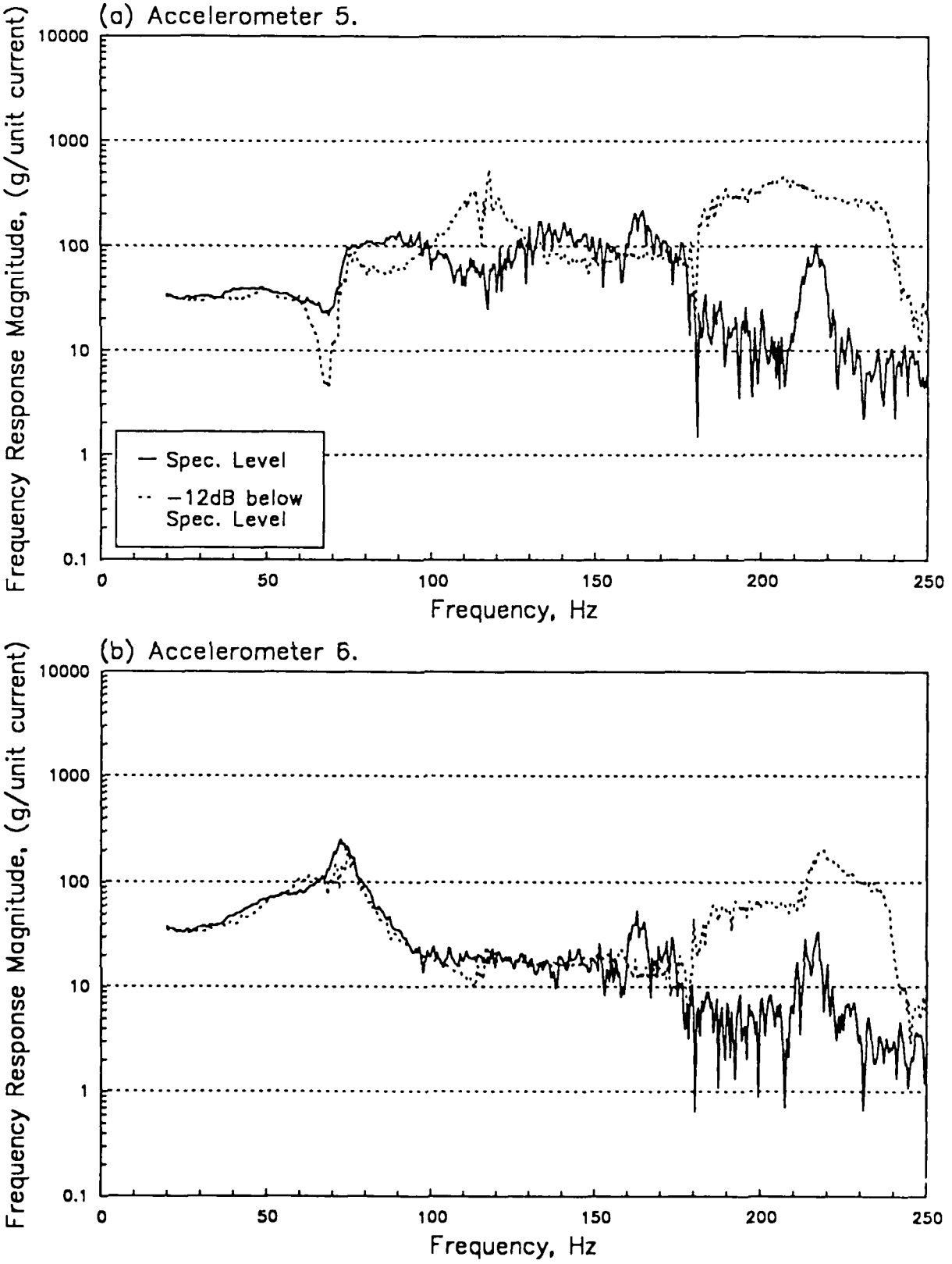

Figure 51. Shaker Current and Payload Mass Acceleration, Payload on APC with 0.005" Gap, Original Spectrum.

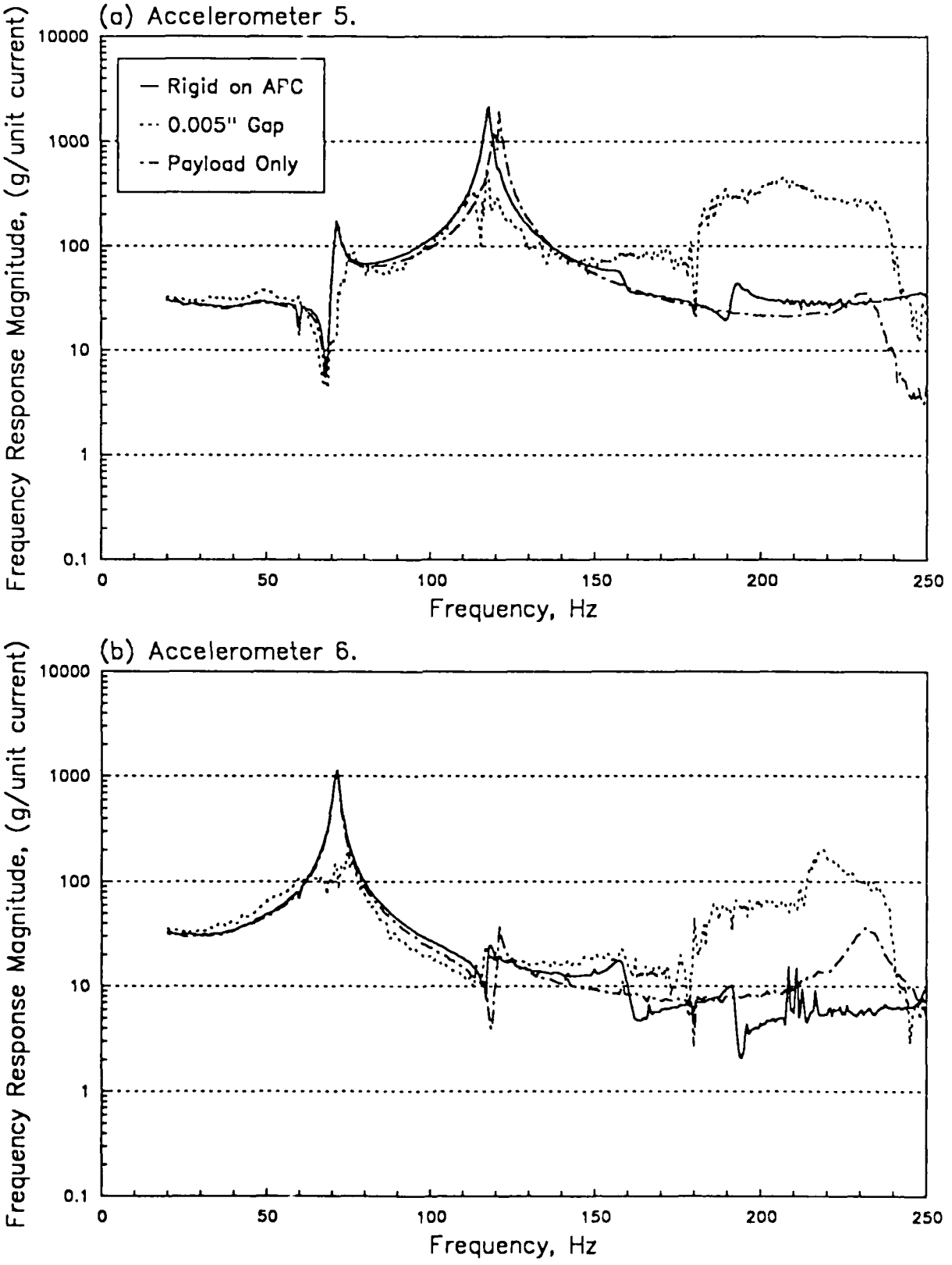

Figure 52. Shaker Current and Payload Mass Acceleration, 12 dB below Vibration Specification.

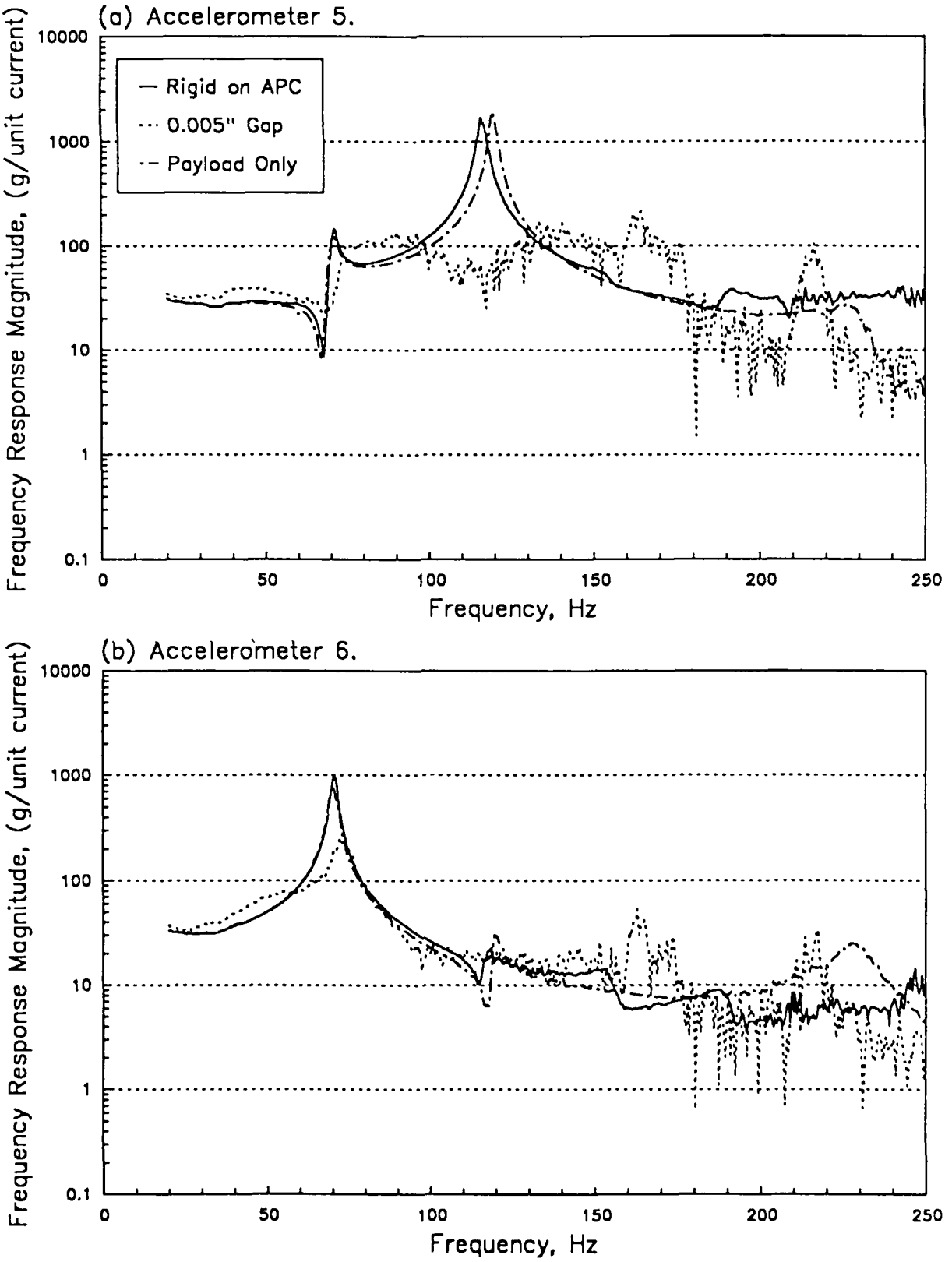

Figure 53. Shaker Current and Payload Mass Acceleration, at Full Modified Vibration Specification.

5. CONCLUSIONS AND RECOMMENDATIONS

The conclusions drawn from the Phase II study to develop improved vibration testing procedures for SSV sidewall mounted payloads may be summarized as follows:

1. Validity of basic procedure - The basic blocked force limiting vibration test procedure recommended in the Phase I study for payloads mounted on the SSV cargo bay sidewall has been verified as effective and practical. Specifically, severe over-testing will be avoided if the vibration tests of sidewall mounted payloads are performed using a dual control (acceleration and force) of the shaker input, where the specified input acceleration spectral density to the payload is limited so that the input force to the payload does not exceed the blocked force that can be delivered to the payload in service by the sidewall structure.

2. Validity of orbiter sidewall accelerance data - Based upon empirical evaluations of SSV launch vibration and acoustic data, as well as the coherence functions associated with the OV-101 sidewall accelerance measurements obtained during the Phase I study, it is concluded that the available accelerance data are adequate to confidently define a conservative blocked force for the SSV cargo bay sidewall structure in the y (lateral) and z (vertical) directions. However, the available data are not considered adequate to confidently define a conservative blocked force in the x (longitudinal) direction. Hence, no force limiting in the vibration testing along the x axis of SSV cargo bay sidewall mounted payloads is recommended at this time.

3. Validity of shaker current/force relationship - It has been verified that, for conventional electrodynamic shakers with wire-wound armatures, the armature current has an essentially perfect linear relationship with the interface force delivered from the shaker table to a firmly attached payload. It follows that the shaker current can be used as an accurate measure of the net interface force delivered to a payload by the shaker during the vibration test.

4. Shaker table attachment of the payload - Extensive laboratory vibration tests on a simulated OASIS payload indicate that SSV cargo bay sidewall mounted payloads (with or without an APC as part of the payload) should be firmly attached to the shaker table for vibration testing, even though the payloads are attached to the sidewall structure in service with controlled gaps between the APC and the sidewall to allow thermal growth. The inclusion of the gaps in a vibration test would undoubtedly provide a more accurate simulation of the payload/ component vibration environment. However, the laboratory tests revealed a significant influence of the gap produced "rattling" between the shaker table and the payload APC on both the table acceleration and armature current signals needed to equalize and control the vibration test. Of course, this test control problem could be circumvented by (a) setting up a proper equalization with the gaps shimmed closed so that the payload is firmly attached to the shaker table, (b) tape recording the power amplifier output

current to the armature for this condition, and (c) removing the shims and performing the vibration test using the tape recorded power amplifier current as the armature input. However, it is not believed the increase in test fidelity provided by the above approach justifies the increased complexity of the testing procedure.

5. Implementation of test procedure - The formulation of a shaker equalizer system that would allow real-time dual control (acceleration and force) of a vibration test has been detailed, and is believed to provide the best alternative to the single control (acceleration only) vibration testing procedures in current use. Although present shaker equalizers are not designed to provide such dual control at this time, it could be achieved in the near future by relatively minor modifications to present equalizer systems. In the meantime, a quasi-real-time control procedure that is suitable for present shaker equalizer systems has been formulated, experimentally demonstrated, and found to be acceptably accurate and practical for immediate use.

Based upon the above conclusions, a detailed vibration test specification for SSV cargo bay sidewall mounted payloads has been prepared. The recommended test specification is included as an attachment to this Phase II report.

Although the test procedure detailed in the attachment is considered adequate for immediate applications, there are three deficiencies in the procedure that should receive further attention, as follows:

(a) As noted in Conclusion 2 above, the procedure does not define a limit force for the x axis vibration because representative measurements of the accelerance at the APC mounting points on the orbiter sidewall structure could not be obtained along this axis (see Section 3.4).

(b) The derivation of the net limit forces for the y and z axes were based upon conservative assumptions necessitated by a lack of cross-accelerance measurements for the orbiter sidewall structure (see Section 3.5).

(c) As noted in Conclusion 4 above, the procedure does not fully account for the nonlinear effects introduced by the thermal clearance gaps in the attachment of the APC to the SSV cargo bay sidewall (see Section 4.6).

It is believed that the accuracy of the test procedure could be enhanced if these deficiencies were resolved. It is further believed that a proper resolution of deficiencies (a) and (b) could be achieved by computer simulation studies using the finite element model (FEM) for the orbiter sidewall structure developed for the Jet Propulsion Laboratory (JPL) by Astron Research and Engineering [10]. Hence, it is recommended that an additional study effort be considered to enhance the accuracy of the net mounting point apparent weights and

the resulting limit forces for the SSV cargo bay sidewall through computer simulations using the JPL FEM for the orbiter sidewall structure. It is further recommended that additional studies be performed to consider possible modifications to the test procedure to account for the nonlinear effects on the payload vibration environment caused by the APC thermal gaps.

References

1. "Definition of SSV Structure-Borne Vibration Environment For DoD Payloads", SD-CF-0206, U.S. Air Force Space Division, Los Angeles, CA, 12 January 1987.

2. "Vibration Test Procedures For Orbiter Sidewall-Mounted Payloads: Phase I Final Report", Report No. 7114-01, Astron Research and Engineering, Santa Monica, CA, March 1988.

3. Bendat, J. S., and Piersol, A. G., RANDOM DATA: Analysis and Measurement Procedures, 2nd edition, pp. 34-36, Wiley, New York, 1986.

4. Hixson, E. L., "Mechanical Impedance", Shock and Vibration Handbook, 2nd edition (Eds: C. M. Harris and C. E. Crede), p. 10-15, McGraw-Hill, New York, 1976.

5. Ewins, D.J., and Sainsbury, M.G., "Mobility Measurements for the Vibration Analysis of Connected Structures", Shock and Vibration Bulletin, 42, Pt 1, pp 105-122, 1972.

6. Bendat, J. S., and Piersol, A. G., Engineering Applications of Correlation and Spectral Analysis, pp. 83-85, Wiley, New York, 1986.

7. White, A. F., Jr., et al, "Payload Bay Acoustic and Vibration Data from STS-3 Flight", DATE Report 004, Goddard Space Flight Center, Greenbelt, MD, January 1982.

8. White, A. F., Jr., et al, "Payload Bay Acoustic and Vibration Data from STS-2 Flight", DATE Report 003, Goddard Space Flight Center, Greenbelt, MD, June 1981.

9. Bowker, A. H., and Lieberman, G. J., Engineering Statistics, pp. 230-231, Prentice-Hall, Englewood Cliffs, NJ, 1959.

10. Hipol, P.J., "Finite Element Model of the Space Shuttle Cargo Bay," Report No. 7128-1, Astron Research and Engineering, Santa Monica, CA, January 1988.

11. Hunter, N.F., and Otts, J.V., "The Measurement of Mechanical Impedance and Its Use in Vibration Testing," Shock and Vibration Bulletin, No. 42, Part 1, pp. 55-69, January 1972.

APPENDIX A

OV-101 APPARENT WEIGHT DATA AND BLOCKED FORCE CALCULATIONS

TABLE A1. OV-101 APPARENT WEIGHT DATA AND BLOCKED FORCE CALCULATIONS.

Frequency Hz	Y Axis Apparent Weight Magnitude lb/g	Std Dev. lb/g	Y Net lb/g	Z Axis Apparent Weight Magnitude lb/g	Std Dev. lb/g	Z Net lb/g	Specification Y,Z Accel g2/Hz	Blocked Force Y lb.	Z lb.
20	867	427	4081	8543	2886	25249	0.010	166531	6375040
21	786	383	3684	6990	2368	20678	0.011	151638	4776445
22	872	391	3970	7533	3228	24196	0.012	195690	7268661
23	798	329	3532	6860	2920	21979	0.014	171294	6634378
24	684	267	2976	6541	2167	19211	0.015	134007	5582780
25	556	235	2482	5456	2052	16716	0.017	102205	4637105
26	598	237	2616	5793	3615	21811	0.018	124134	8629650
27	555	241	2500	4589	2381	15912	0.020	123560	5004189
28	668	141	2491	4557	2408	15925	0.022	133187	5443290
29	555	126	2103	4296	1857	13844	0.023	102751	4455054
30	451	136	1823	3579	1936	12634	0.025	83452	4006799
31	397	115	1590	3448	1785	11945	0.027	68365	3858394
32	414	109	1620	3680	1710	12197	0.029	76301	4323452
33	434	104	1664	2935	1263	9442	0.031	86261	2778718
34	394	89	1488	2868	1305	9427	0.033	73893	2963978
35	335	88	1309	2813	1156	8896	0.036	61017	2818726
36	319	115	1354	2384	993	7575	0.038	69593	2179169
37	314	132	1400	2104	866	6659	0.040	79152	1791?92
38	298	124	1322	2050	821	6422	0.043	75025	1770327
39	289	103	1226	1977	717	5982	0.046	68452	1629400
40	301	91	1218	1921	710	5849	0.048	71612	1650095
41	326	110	1359	1954	746	6017	0.051	94235	1846988
42	319	113	1349	2127	830	6602	0.054	98002	2348806
43	343	119	1441	2148	897	6834	0.057	118003	2654475
44	370	125	1540	2243	959	7197	0.060	142041	3102004
45	363	142	1581	2083	822	6492	0.063	157554	2655515
46	366	175	1705	2022	803	6315	0.066	192657	2641564
47	380	179	1758	1996	899	6535	0.070	215018	2970437
48	384	159	1702	1808	824	5947	0.073	211407	2580741
49	394	151	1704	1553	668	4994	0.077	222007	1906776
50	364	144	1588	1407	664	4692	0.080	201975	1761770
51	332	126	1430	1372	680	4668	0.080	163488	1742929
52	319	102	1311	1449	654	4749	0.080	137514	1804181
53	312	90	1246	1527	628	4830	0.080	124121	1866070
54	321	78	1234	1466	582	4578	0.080	121770	1676338
55	324	70	1214	1388	539	4300	0.080	117936	1479170
56	293	68	1117	1313	546	4170	0.080	99781	1391326
57	271	79	1088	1238	517	3938	0.080	94760	1240458
58	266	87	1098	1207	477	3764	0.080	96366	1133250
59	252	80	1034	1196	462	3699	0.080	85471	1094785
60	237	72	963	1239	495	3877	0.080	74149	1202278
61	235	67	936	1206	499	3823	0.080	70112	1168943
62	231	60	900	1116	461	3537	0.080	64771	1000850
63	221	60	872	1067	437	3370	0.080	60786	908717
64	222	73	920	1011	406	3171	0.080	67753	804229
65	237	73	966	985	387	3065	0.080	74635	751359
66	231	74	947	992	394	3099	0.080	71785	768089
67	217	80	927	949	377	2965	0.080	68789	703259
68	202	71	853	928	349	2844	0.080	58270	647091
69	200	70	840	931	356	2870	0.080	56452	659029
70	206	71	863	957	398	3038	0.080	59628	738250
71	211	53	819	972	380	3018	0.080	53650	728530
72	210	42	775	926	360	2870	0.080	48088	659167
73	205	40	754	865	325	2651	0.080	45459	562042
74	209	44	777	817	306	2499	0.080	48275	499446
75	219	45	814	796	311	2471	0.080	52999	488622
76	224	48	838	793	316	2480	0.080	56149	492091
77	231	50	868	750	292	2326	0.080	60227	432978
78	236	56	901	725	283	2250	0.080	64887	404999
79	236	67	937	686	263	2115	0.080	70288	357884

TABLE A1. (Continued)

Frequency Hz	Y Axis Apparent Weight Magnitude lb/g	Std Dev. lb/g	Y Net lb/g	Z Axis Apparent Weight Magnitude lb/g	Std Dev. lb/g	Z Net lb/g	Specification Y,Z Accel g2/Hz	Blocked Force Y lb.	Z lb.
80	240	72	969	657	252	2025	0.080	75149	328034
81	231	70	935	636	244	1962	0.080	69926	307821
82	213	68	872	629	249	1962	0.080	60804	307954
83	200	69	838	640	255	2001	0.080	56205	320170
84	193	70	820	653	257	2034	0.080	53754	330969
85	193	67	811	655	268	2067	0.080	52599	341801
86	195	61	798	642	263	2028	0.080	50898	328967
87	194	54	771	623	245	1940	0.080	47541	300942
88	190	49	741	604	232	1864	0.080	43885	278008
89	187	47	724	580	224	1793	0.080	41923	257084
90	188	44	715	565	223	1760	0.080	40942	247810
91	193	43	729	559	226	1756	0.080	42488	246746
92	192	41	717	552	224	1736	0.080	41170	241207
93	188	41	706	531	215	1668	0.080	39826	222657
94	183	40	688	523	213	1650	0.080	37834	217902
95	180	41	680	523	214	1651	0.080	37016	218055
96	179	44	691	519	218	1654	0.080	38196	218919
97	177	49	701	522	222	1673	0.080	39291	223783
98	181	50	716	539	230	1726	0.080	41022	238438
99	182	52	725	544	235	1751	0.080	42007	245411
100	179	56	730	526	225	1688	0.080	42676	227870
101	179	58	739	512	219	1644	0.080	43740	216102
102	175	57	724	505	218	1629	0.080	41950	212168
103	173	57	716	494	205	1569	0.080	40967	197060
104	175	57	722	475	194	1499	0.080	41658	179652
105	178	56	729	459	186	1444	0.080	42481	166904
106	183	58	748	449	182	1414	0.080	44790	159975
107	182	58	747	439	180	1386	0.080	44687	153669
108	178	57	731	432	183	1383	0.080	42776	152964
109	175	59	729	416	180	1342	0.080	42488	144052
110	176	60	736	395	170	1273	0.080	43346	129594
111	176	62	741	378	160	1209	0.080	43873	116879
112	174	67	755	371	158	1189	0.080	45554	113061
113	168	65	732	367	152	1162	0.080	42830	108002
114	160	60	687	372	149	1167	0.080	37779	108877
115	159	58	678	375	147	1167	0.080	36786	108903
116	161	56	677	370	139	1133	0.080	36720	102753
117	160	53	663	360	138	1108	0.080	35213	98197
118	157	50	645	345	134	1070	0.080	33286	91513
119	155	54	654	330	135	1041	0.080	34257	86698
120	152	52	636	318	133	1014	0.080	32378	82241
121	149	53	630	312	128	984	0.080	31726	77464
122	145	53	619	309	124	967	0.080	30646	74731
123	140	48	585	309	119	955	0.080	27401	73010
124	136	41	551	313	118	959	0.080	24260	73504
125	135	41	548	320	121	983	0.080	24018	77273
126	131	39	528	320	123	986	0.080	22279	77852
127	130	38	521	321	121	983	0.080	21743	77252
128	131	42	537	317	116	961	0.080	23103	73815
129	131	46	551	312	113	943	0.080	24271	71190
130	126	50	553	308	111	925	0.080	24435	68970
131	130	90	701	299	107	900	0.080	39288	64748
132	122	81	645	290	104	873	0.080	33322	61036
133	111	53	516	287	103	865	0.080	21285	59848
134	108	48	491	279	96	830	0.080	19313	55094
135	108	51	499	265	92	792	0.080	19933	50149
136	105	53	499	259	92	777	0.080	19932	48336
137	100	50	474	255	89	763	0.080	17981	46612
138	98	49	463	251	87	748	0.080	17162	44795
139	96	49	459	252	89	756	0.080	16825	45697

TABLE A1. (Continued)

Frequency Hz	Y Axis Apparent Weight Magnitude lb/g	Std Dev. lb/g	Y Net lb/g	Z Axis Apparent Weight Magnitude lb/g	Std Dev. lb/g	Z Net lb/g	Specification Y,Z Accel g2/Hz	Blocked Force Y lb.	Z lb.
140	93	49	450	255	91	769	0.080	16207	47274
141	92	49	447	256	91	769	0.080	15970	47314
142	91	51	448	258	91	773	0.080	16041	47820
143	90	50	445	255	89	763	0.080	15830	46626
144	91	51	450	249	87	744	0.080	16181	44262
145	94	51	458	244	85	726	0.080	16792	42196
146	95	46	447	236	80	697	0.080	15950	38905
147	93	42	423	227	76	670	0.080	14286	35920
148	92	39	410	219	71	638	0.080	13446	32583
149	92	38	406	210	68	613	0.080	13183	30024
150	92	39	409	203	67	594	0.080	13389	28244
151	93	41	418	197	63	573	0.080	13998	26226
152	94	41	425	192	60	555	0.080	14424	24612
153	95	42	429	187	58	539	0.080	14711	23230
154	97	45	447	186	56	530	0.080	16000	22512
155	100	48	464	185	56	528	0.080	17261	22317
156	100	50	474	182	57	523	0.080	17965	21900
157	97	48	457	178	57	518	0.080	16708	21454
158	91	45	430	175	57	512	0.080	14774	20994
159	88	42	408	173	58	510	0.080	13309	20821
160	85	39	390	172	58	508	0.080	12158	20644
161	81	36	369	171	57	505	0.080	10865	20410
162	76	35	351	169	58	502	0.080	9833	20130
163	75	35	347	164	57	488	0.080	9644	19036
164	76	33	341	161	55	478	0.080	9292	18267
165	76	35	348	163	55	482	0.080	9666	18563
166	75	36	351	162	55	478	0.080	9846	18300
167	74	38	355	160	55	474	0.080	10095	17963
168	75	39	358	160	55	475	0.080	10269	18070
169	76	38	359	159	55	475	0.080	10337	18077
170	75	36	350	158	56	475	0.080	9777	18065
171	74	35	342	157	56	472	0.080	9337	17813
172	75	36	350	155	56	468	0.080	9819	17559
173	79	39	372	156	57	474	0.080	11069	17941
174	79	39	370	158	58	480	0.080	10980	18450
175	77	37	361	158	61	488	0.080	10399	19069
176	76	37	356	158	66	501	0.080	10145	20062
177	74	33	337	154	66	493	0.080	9078	19480
178	71	29	314	147	62	468	0.080	7875	17535
179	68	26	296	141	56	439	0.080	7007	15447
180	67	26	291	136	51	418	0.080	6784	13962
181	67	27	294	133	51	409	0.080	6928	13405
182	67	28	298	131	51	407	0.080	7098	13270
183	68	29	303	131	53	411	0.080	7330	13519
184	69	30	311	132	56	421	0.080	7726	14149
185	70	30	314	132	56	424	0.080	7890	14375
186	70	30	316	135	56	429	0.080	7971	14738
187	70	31	317	134	56	427	0.080	8054	14573
188	69	31	315	132	56	424	0.080	7941	14408
189	68	31	312	132	56	424	0.080	7782	14389
190	69	32	316	132	55	418	0.080	8013	13948
191	70	32	319	130	53	409	0.080	8135	13371
192	69	31	316	128	51	400	0.080	7966	12827
193	69	31	314	129	50	400	0.080	7887	12797
194	70	32	322	128	50	399	0.080	8301	12739
195	72	36	342	129	50	399	0.080	9330	12727
196	75	38	355	130	49	399	0.080	10099	12708
197	75	37	353	131	49	399	0.080	9962	12751
198	76	39	363	132	51	406	0.080	10545	13215
199	79	42	380	131	50	402	0.080	11556	12941
200	80	41	380	129	49	397	0.080	11541	12611

APPENDIX B

SUPPLEMENTARY NTS TEST DATA AND CALCULATIONS

FREQUENCY RESPONSE FUNCTIONS
APPARENT WEIGHT
APPLIED FORCE
COHERENCE

Payload Only (No APC).
Frequency Response of Accelerometers relative to the Shaker Base.
Original Spectrum −12dB below Specification Level.

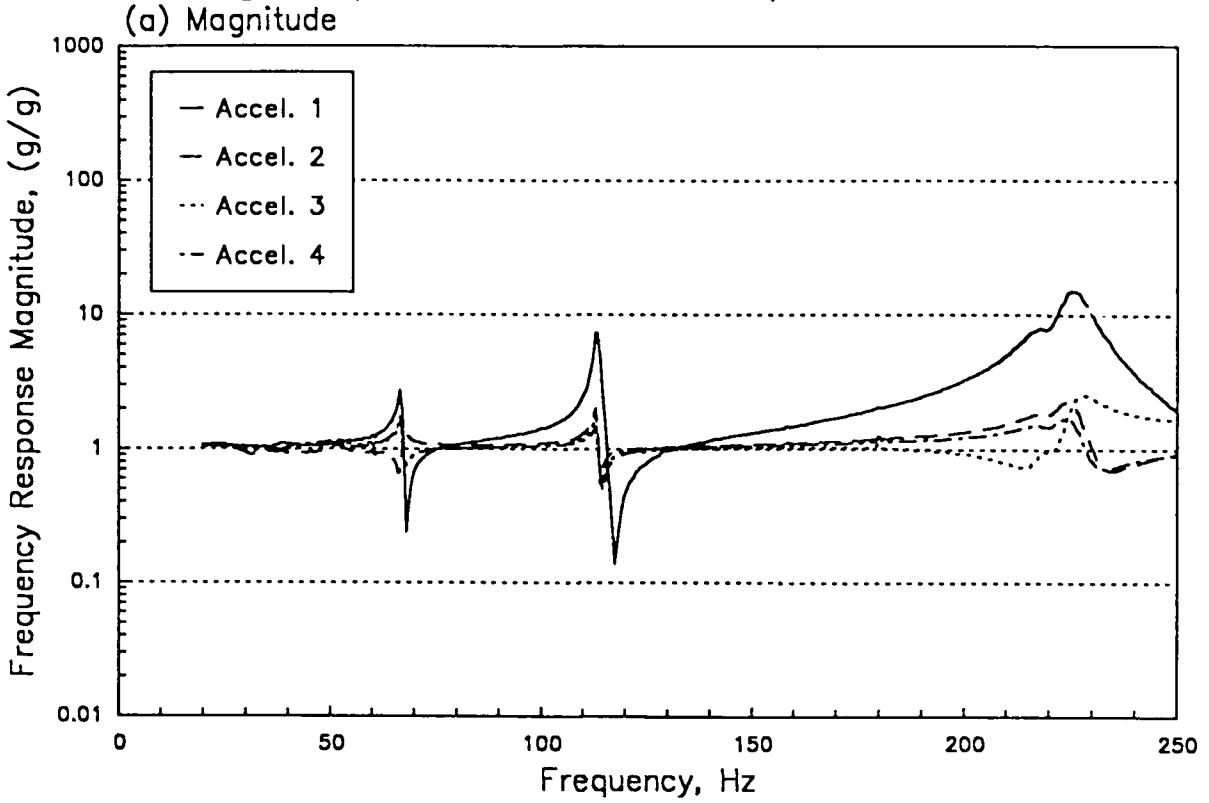

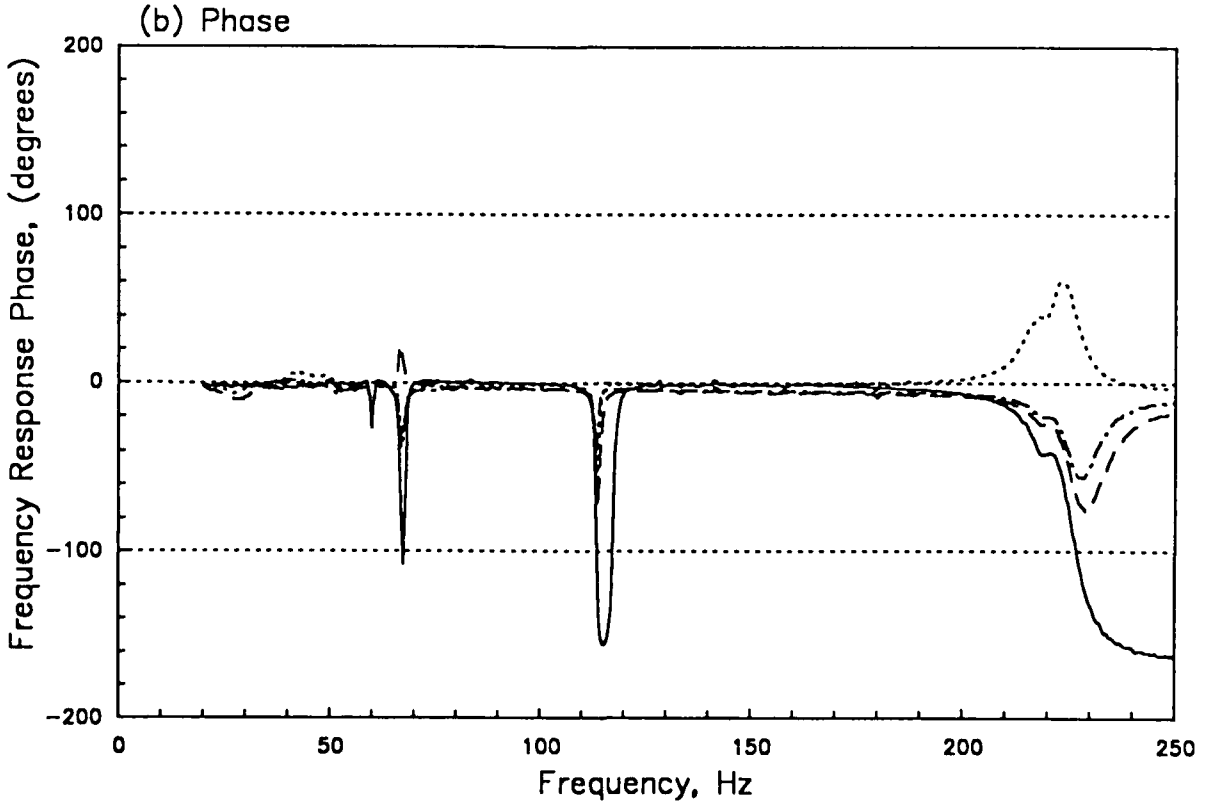

Payload Only (No APC).
Frequency Response of Accelerometers relative to the Shaker Base.
Modified Spectrum (3) −12dB below Specification Level.

(a) Magnitude

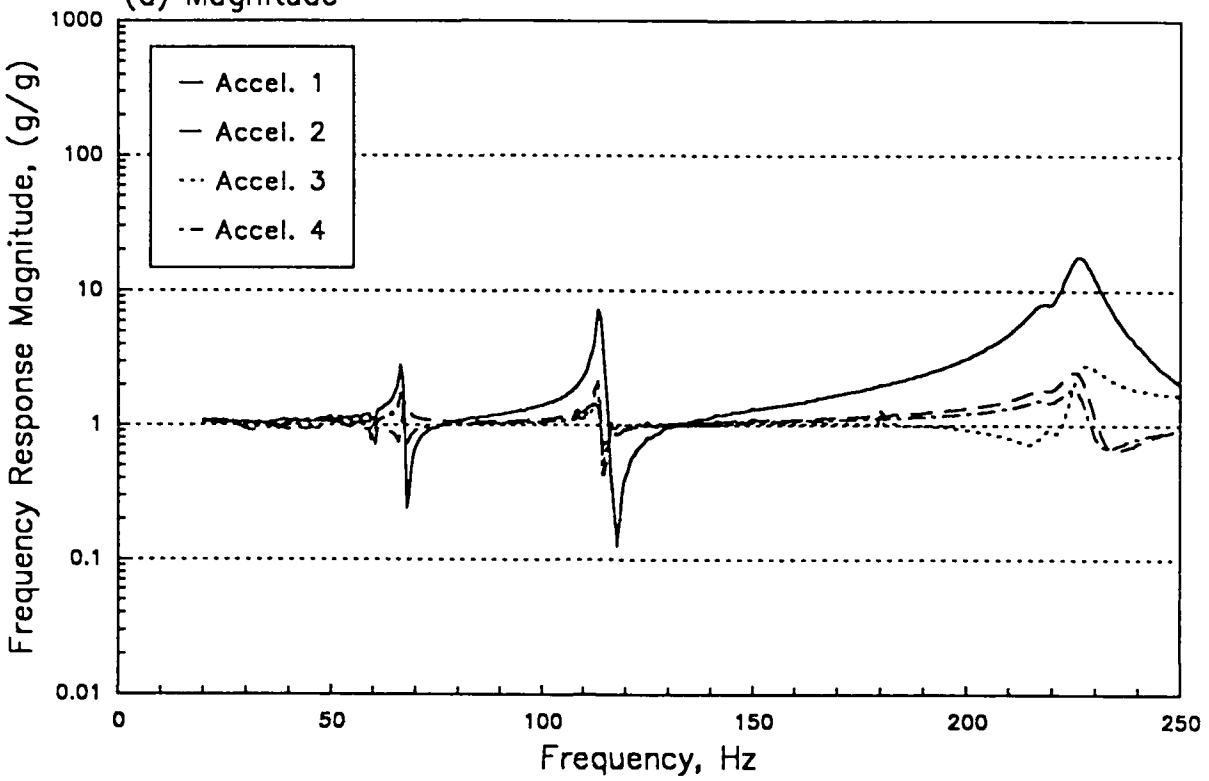

(b) Phase

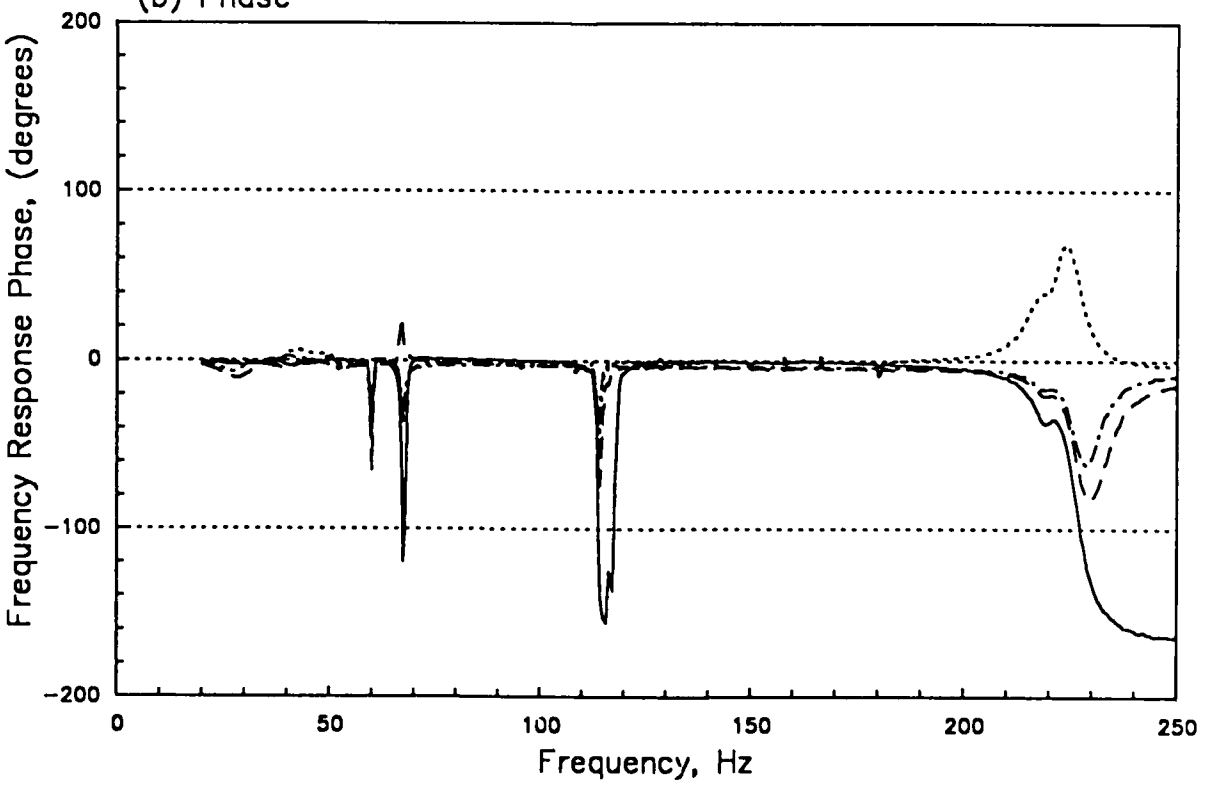

Payload Only (No APC).
Frequency Response of Accelerometers relative to the Shaker Base.
Modified Spectrum (3) −6dB below Specification Level.

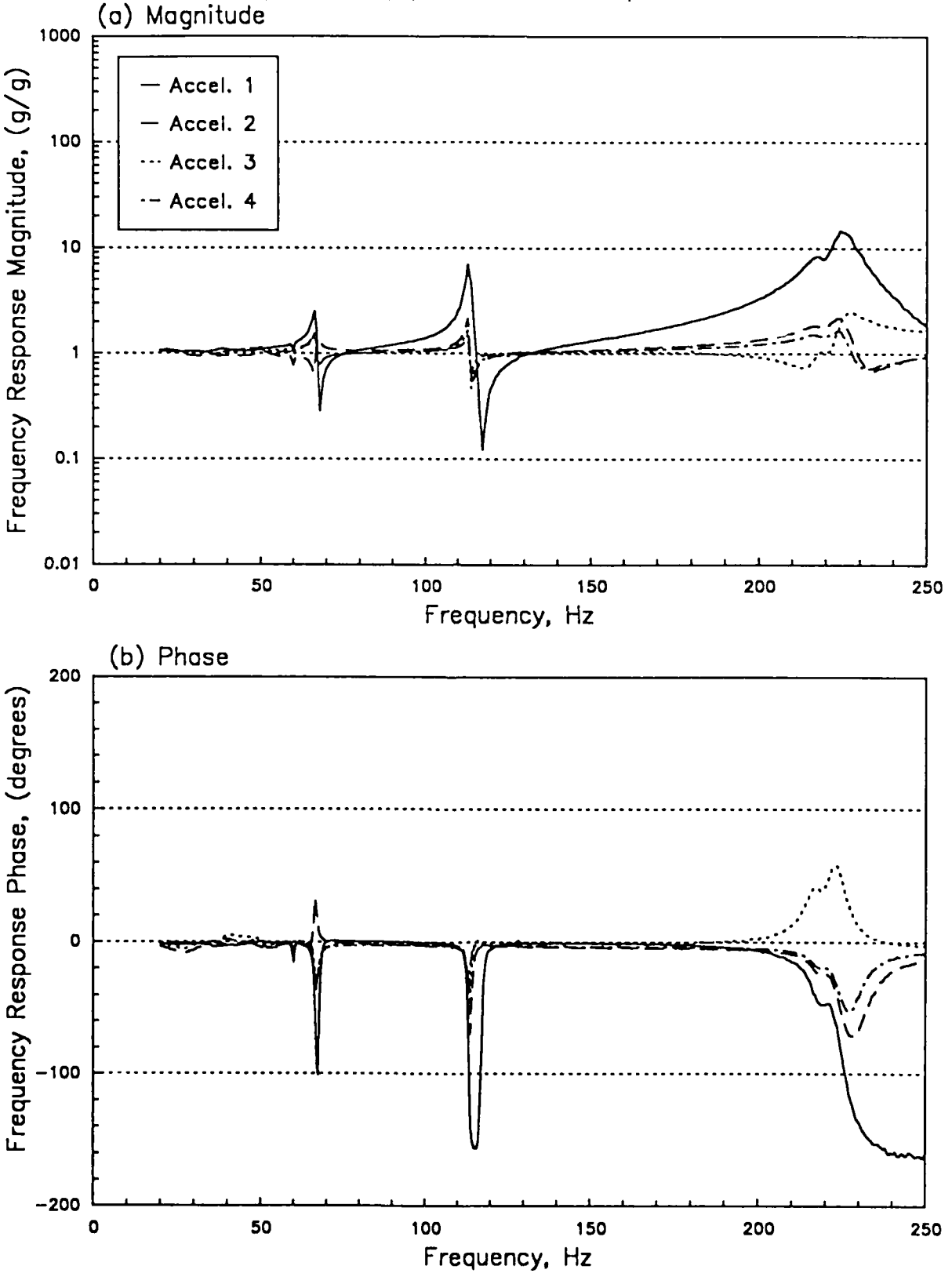

Payload Only (No APC).
Frequency Response of Accelerometers relative to the Shaker Base.
Modified Spectrum (3) at Specification Level.

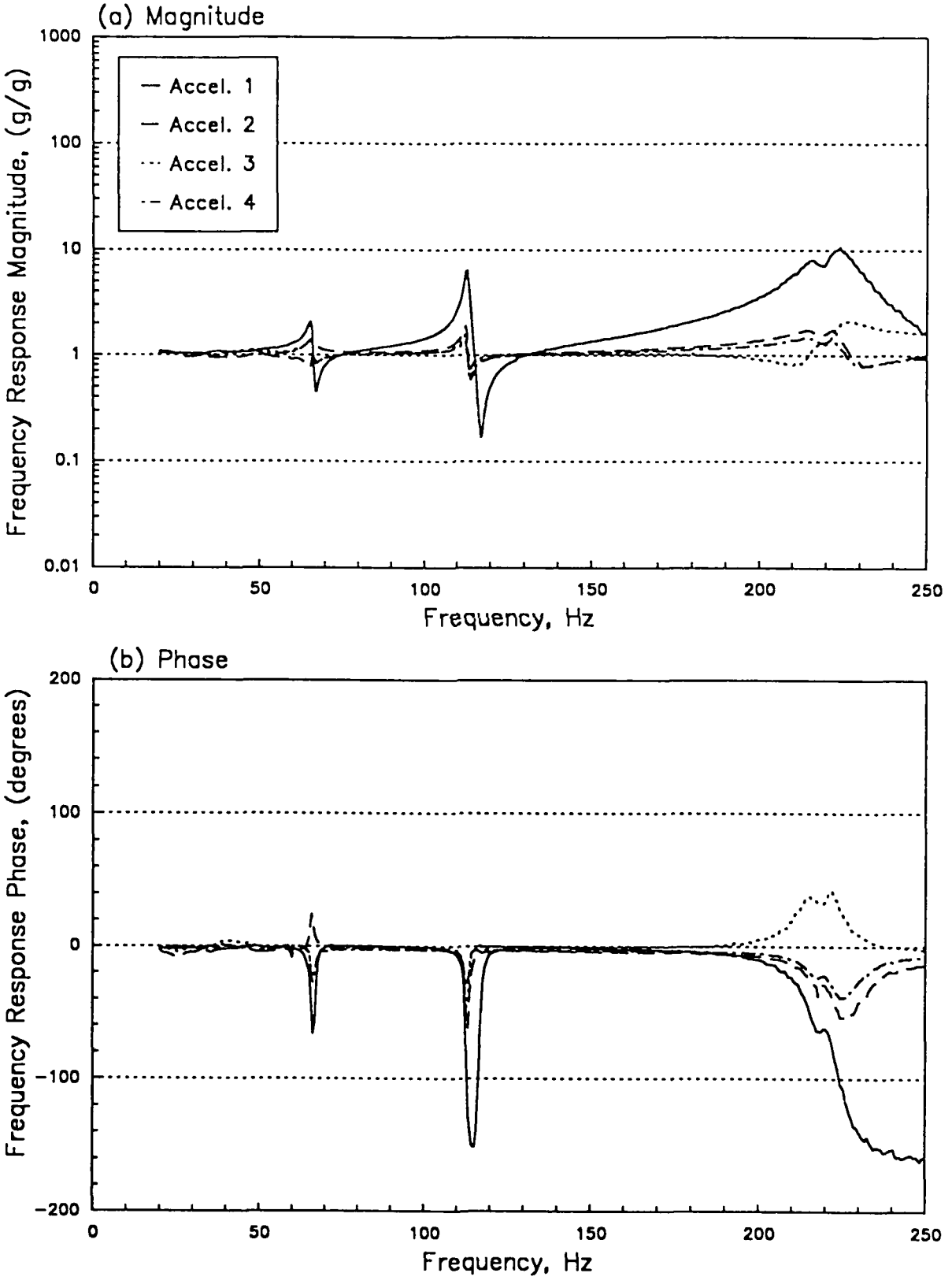

Rigid Payload on APC.
Frequency Response of Accelerometers relative to the Shaker Base.
Original Spectrum −12dB below Specification Level.

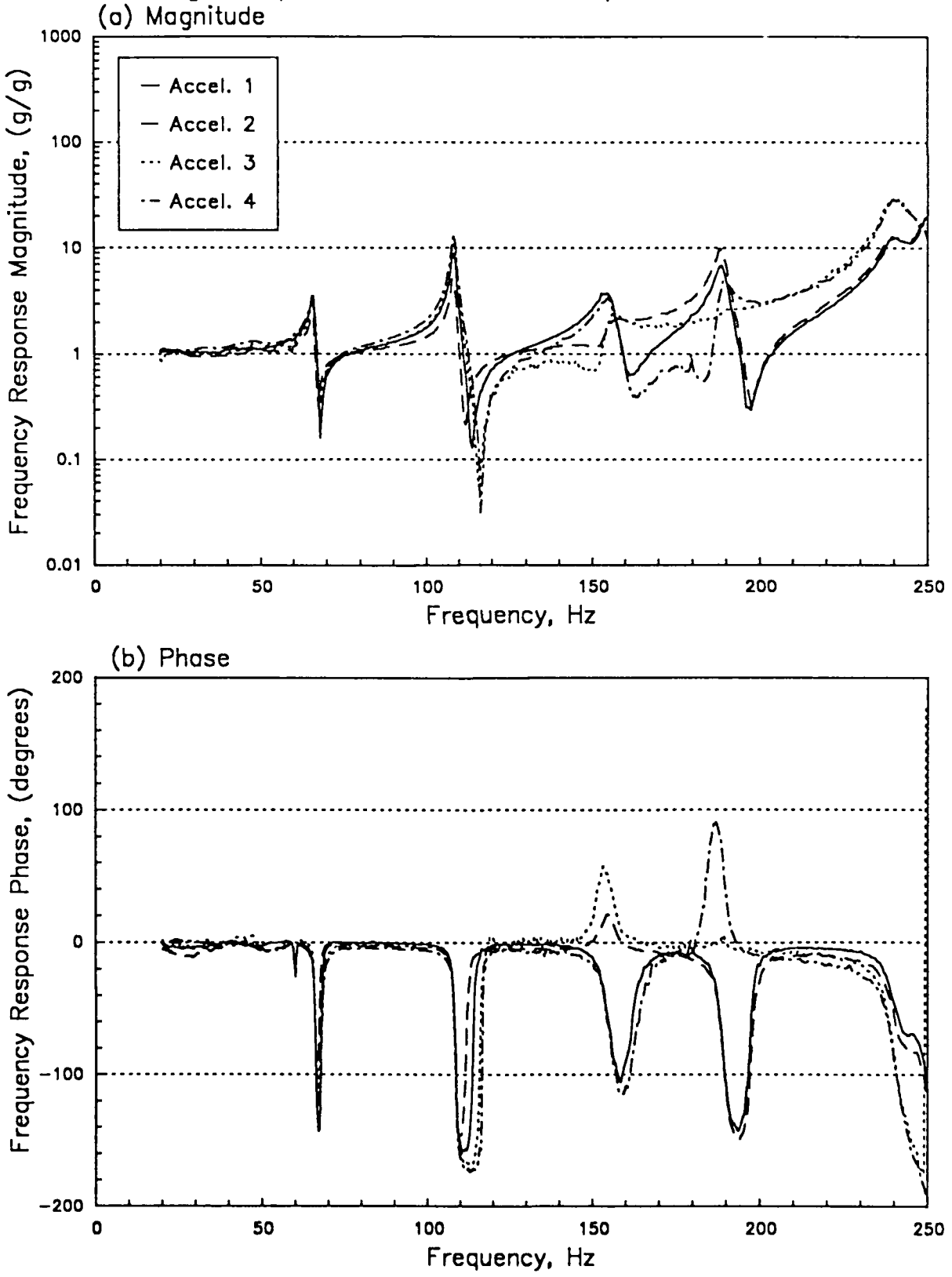

Rigid Payload on APC.
Frequency Response of Accelerometers relative to the Shaker Base.
Modified Spectrum (1) −12dB below Specification Level.

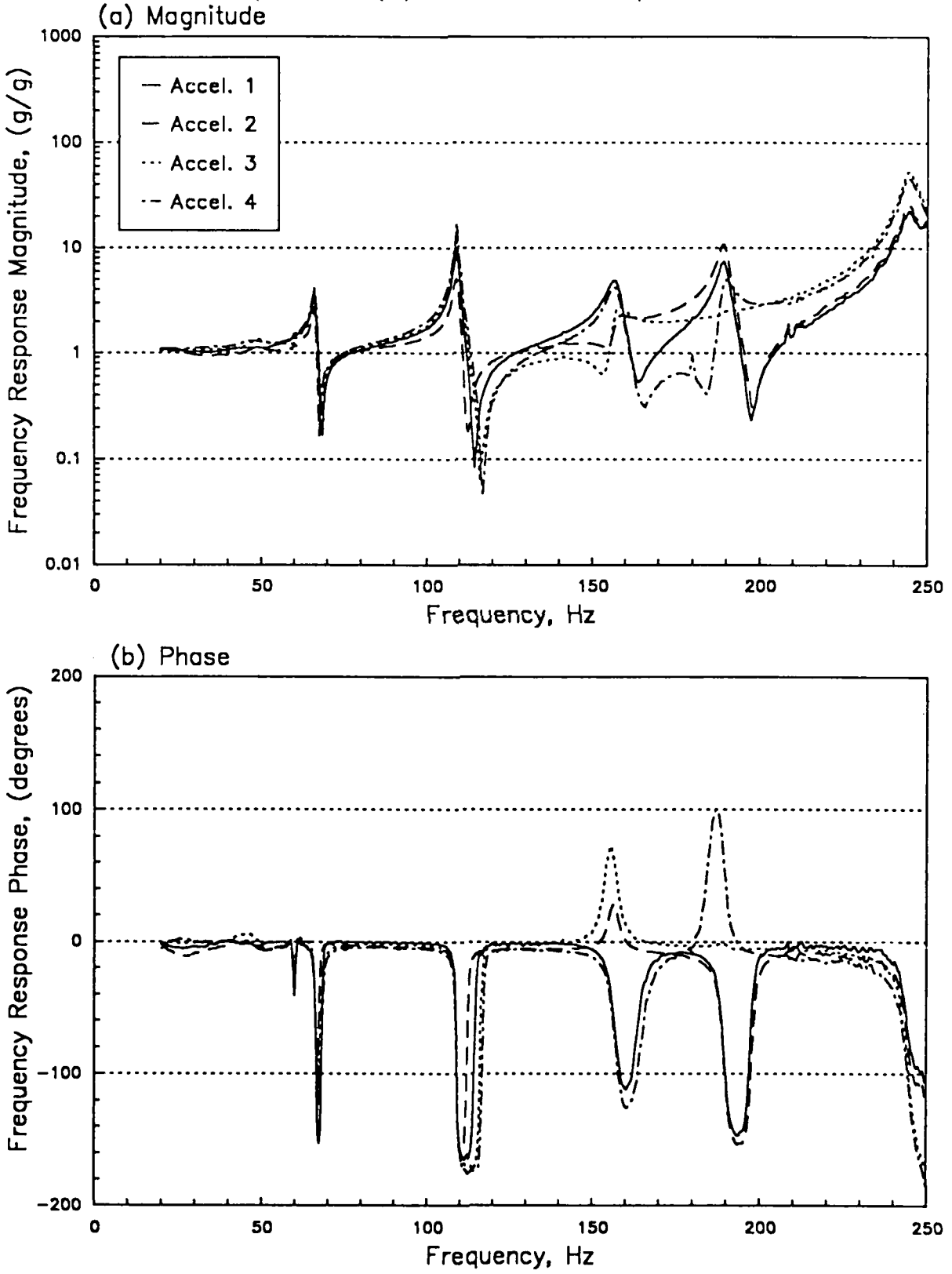

Rigid Payload on APC.
Frequency Response of Accelerometers relative to the Shaker Base.
Modified Spectrum (1) −6dB below Specification Level.

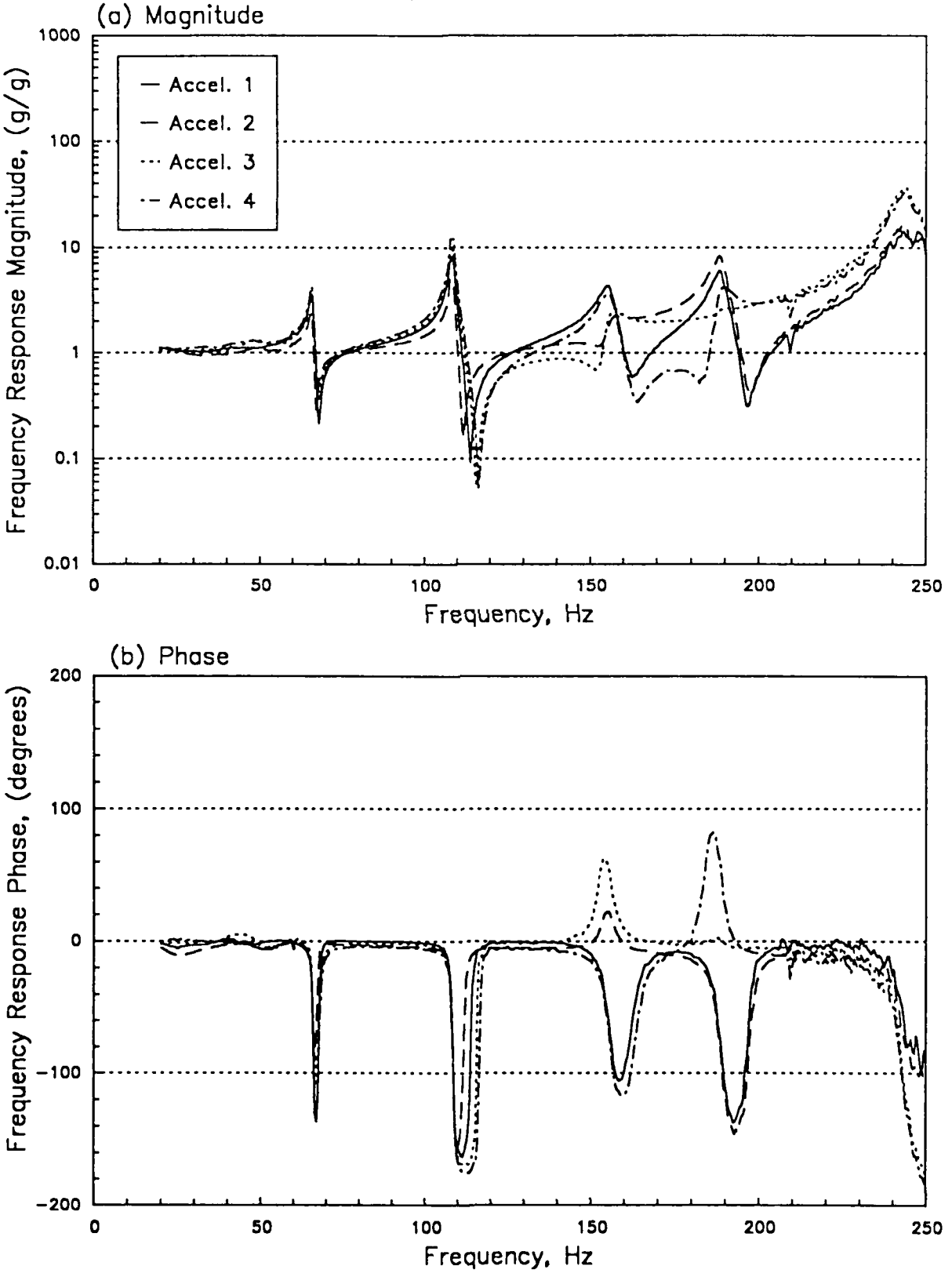

Rigid Payload on APC.
Frequency Response of Accelerometers relative to the Shaker Base.
Modified Spectrum (1) at Specification Level.

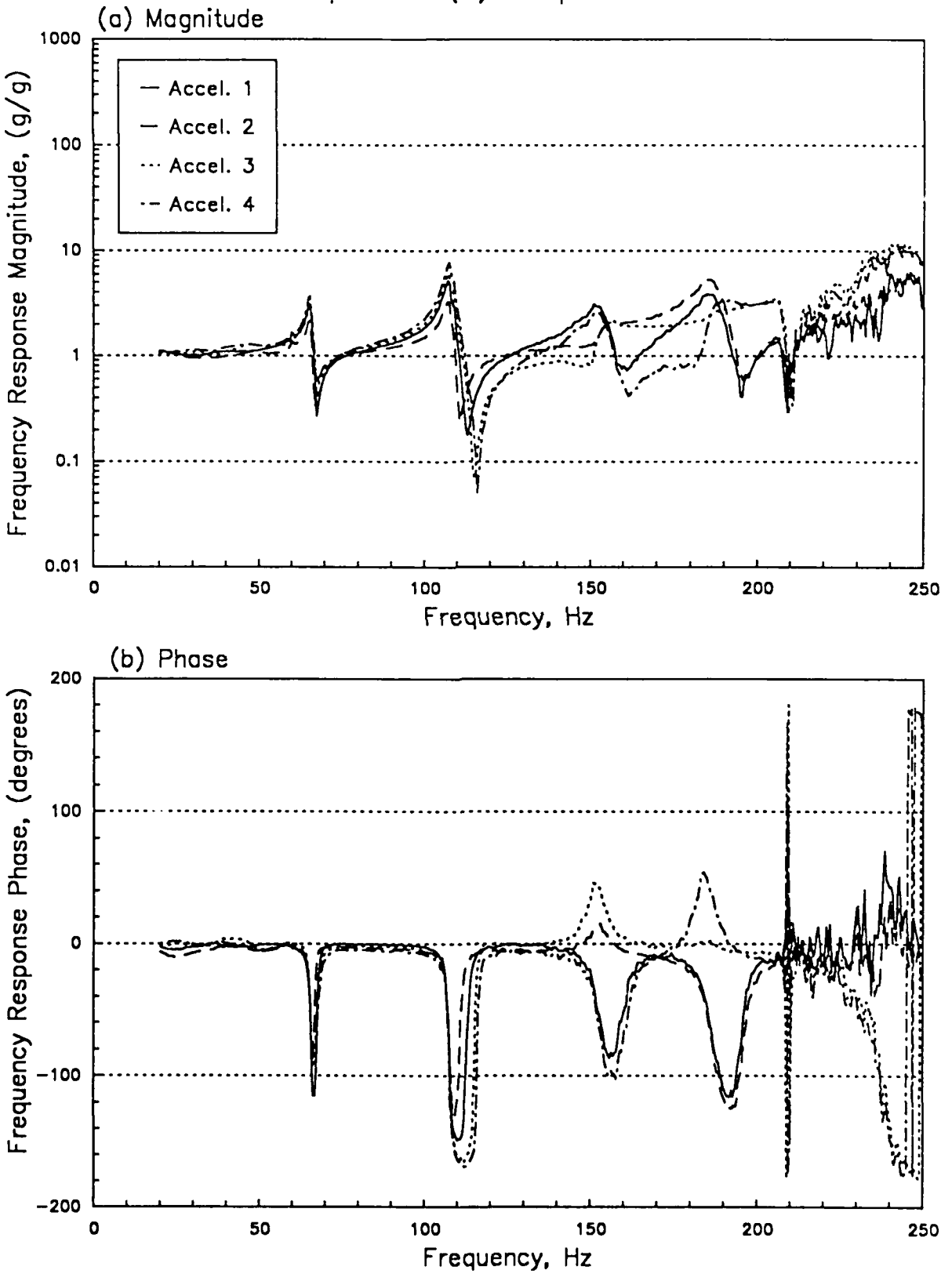

Payload on APC with 0.005" Gap.
Frequency Response of Accelerometers relative to the Shaker Base.
Original Spectrum −12dB below Specification Level.

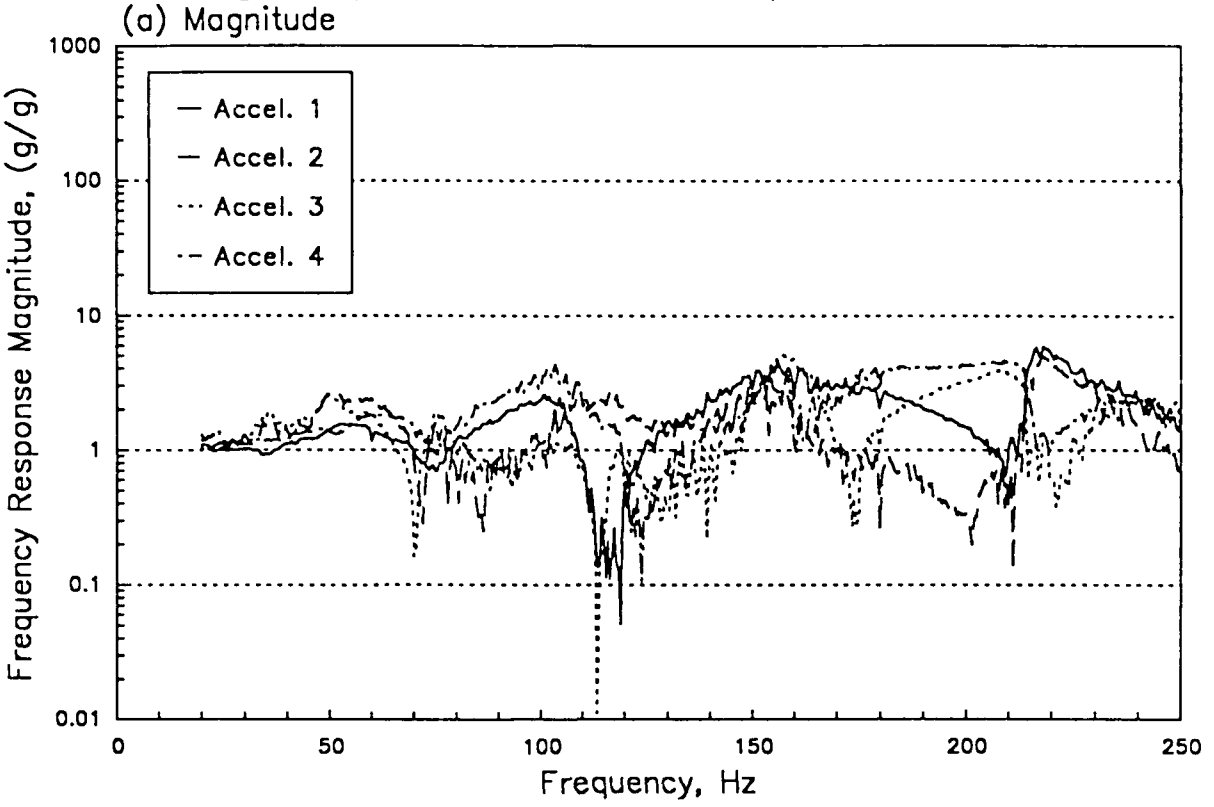

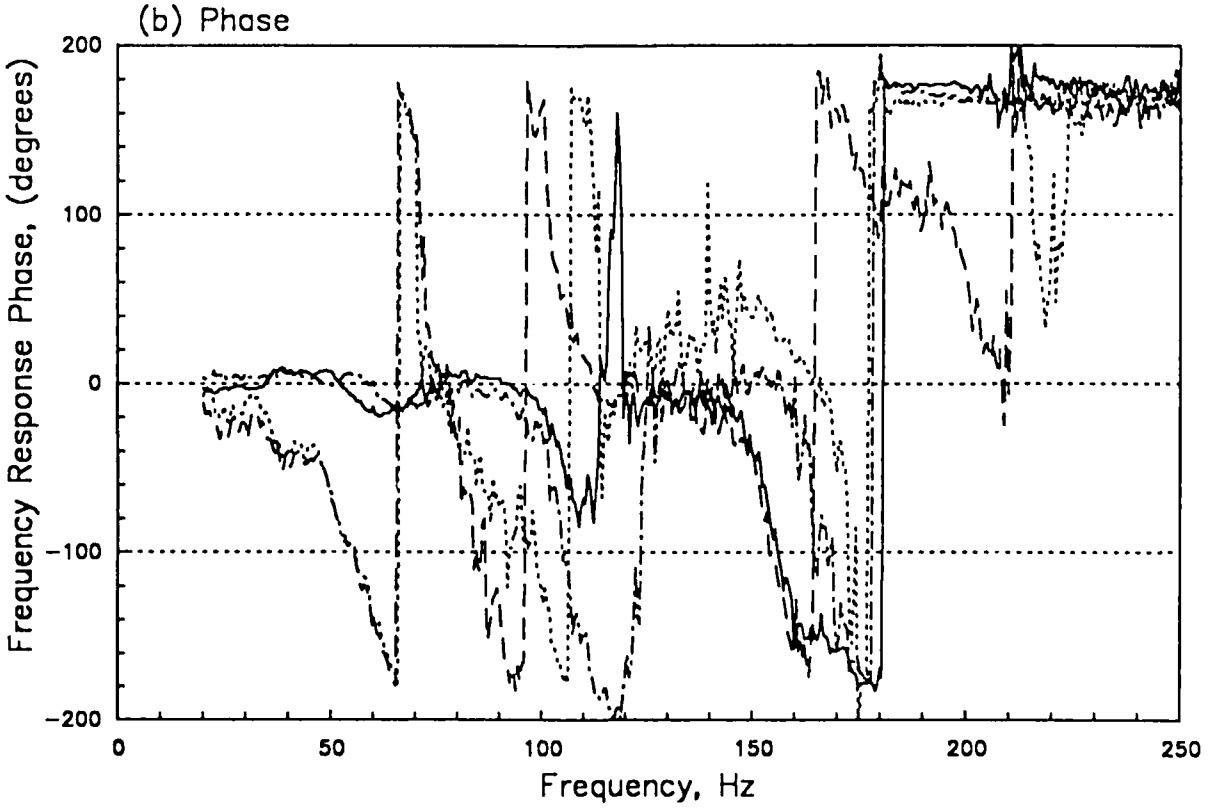

Payload on APC with 0.005" Gap.
Frequency Response of Accelerometers relative to the Shaker Base.
Original Spectrum at Specification Level.

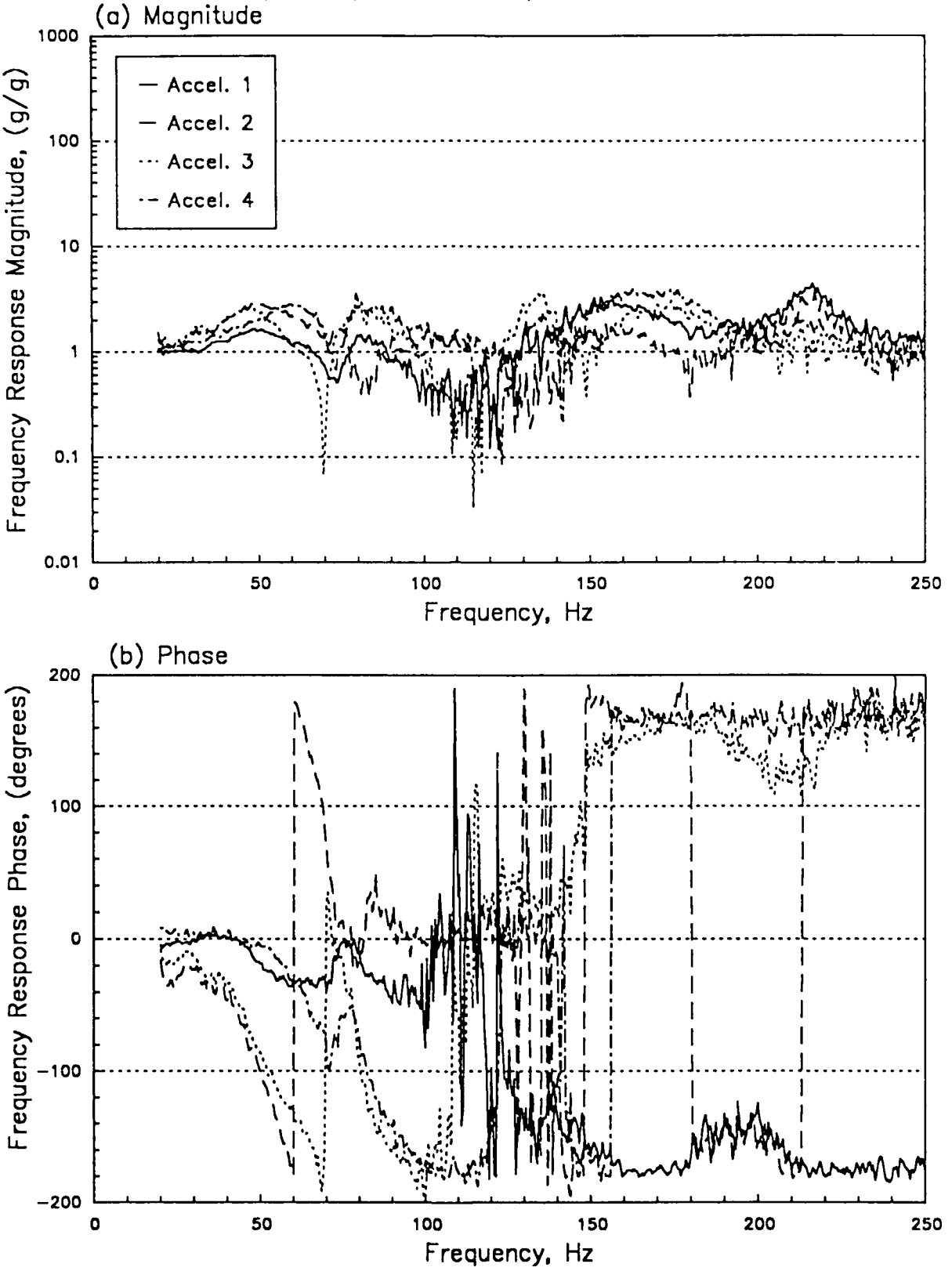

Payload Only (No APC).
Frequency Response of Accelerometers relative to the Shaker Base.
Modified Spectrum (3) at Specification Level.

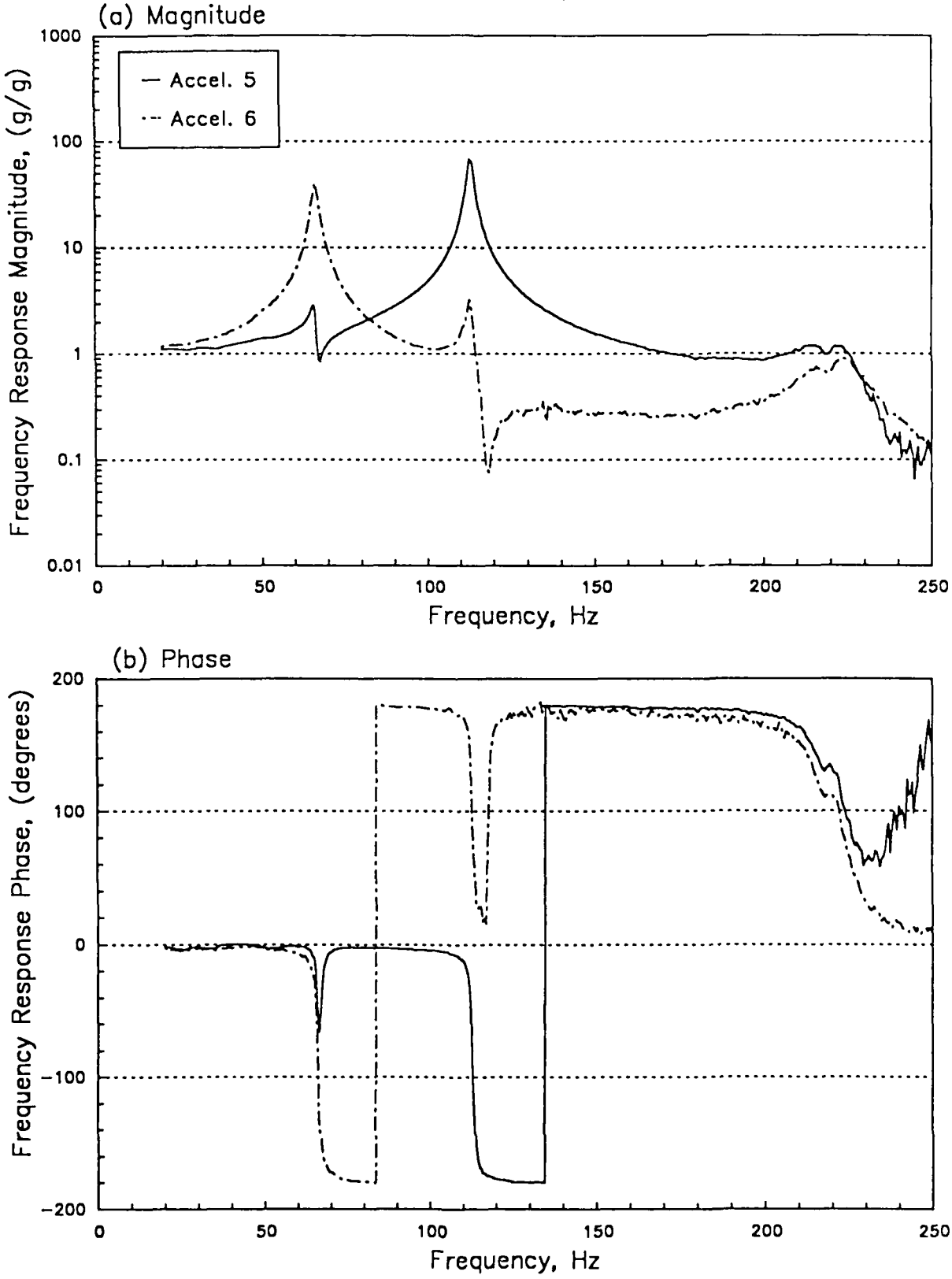

Rigid Payload on APC.
Frequency Response of Accelerometers relative to the Shaker Base.
Modified Spectrum (1) at Specification Level.

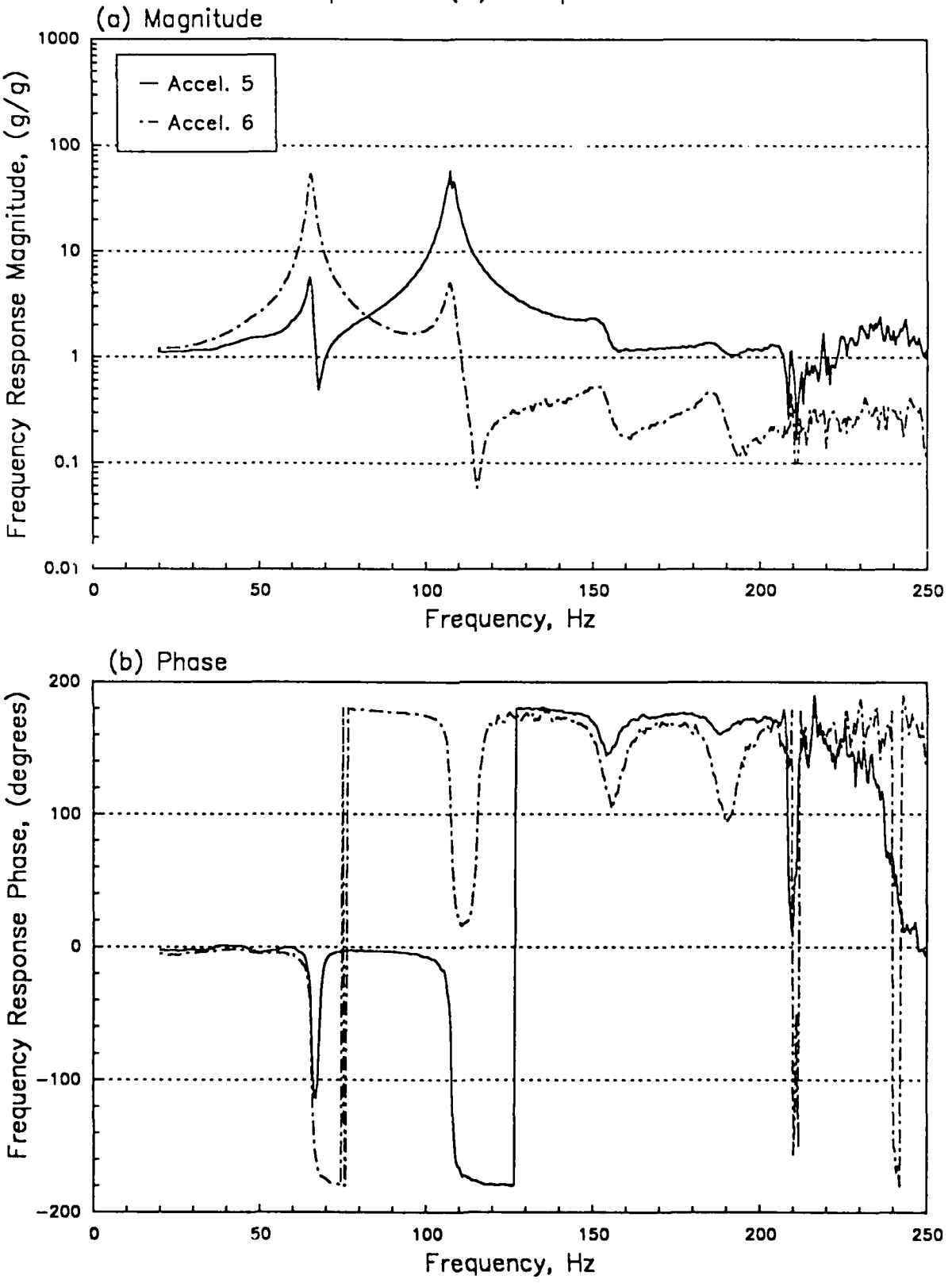

Payload on APC with 0.005" Gap.
Frequency Response of Accelerometers relative to the Shaker Base.
Original Spectrum at Specification Level.

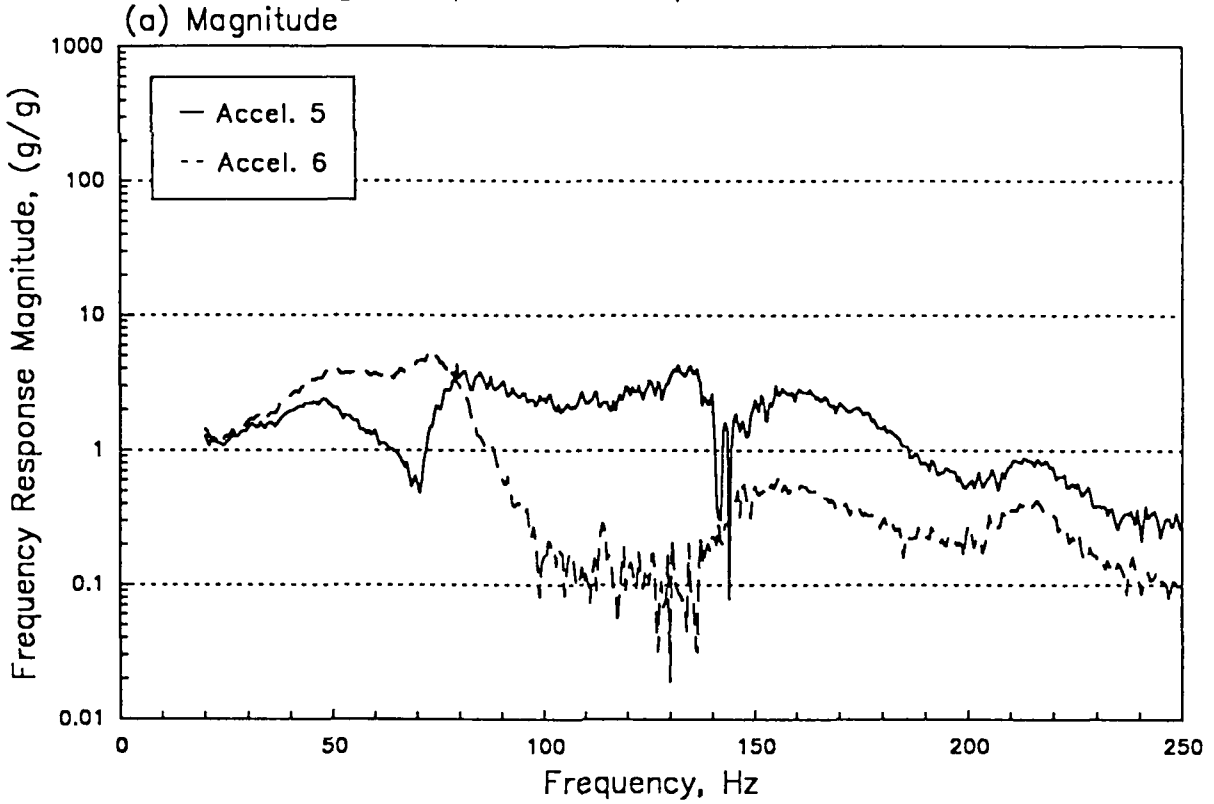

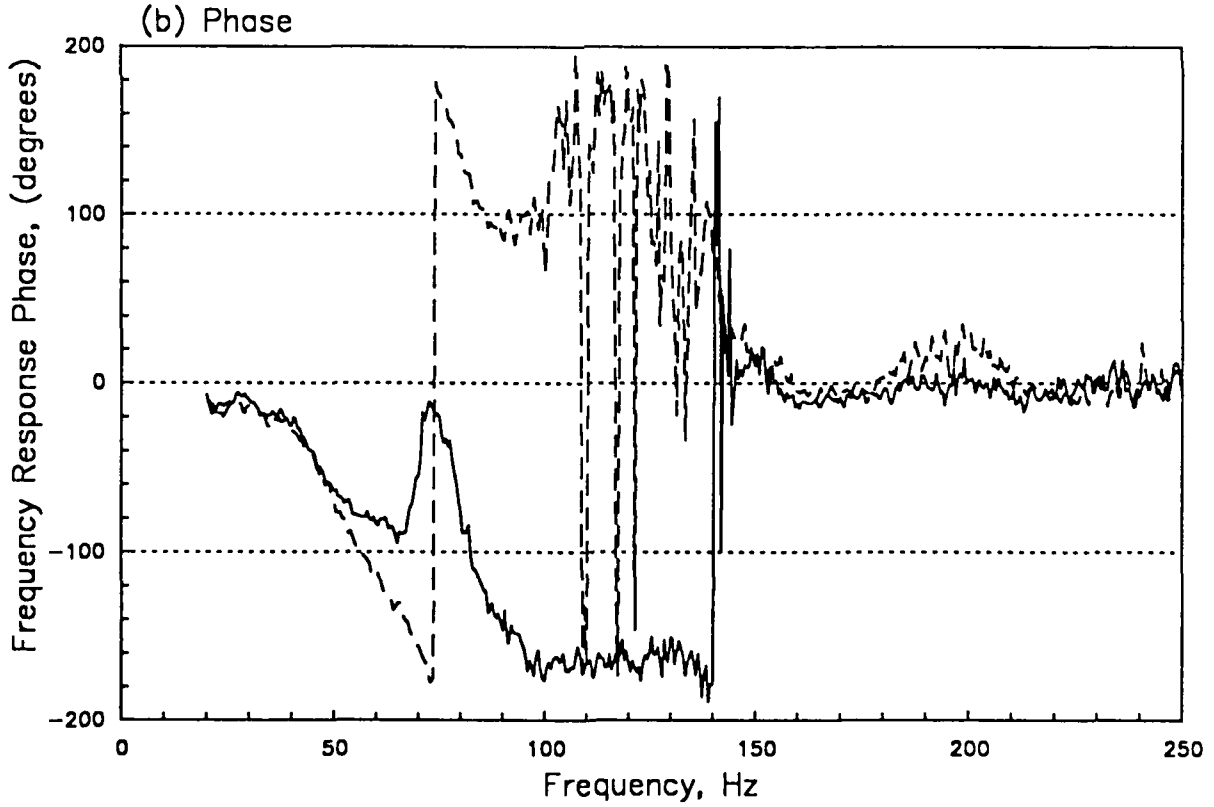

Payload Only (No APC).
Frequency Response of Accelerometers relative to the Shaker Base.
Original Spectrum −12dB below Specification Level.

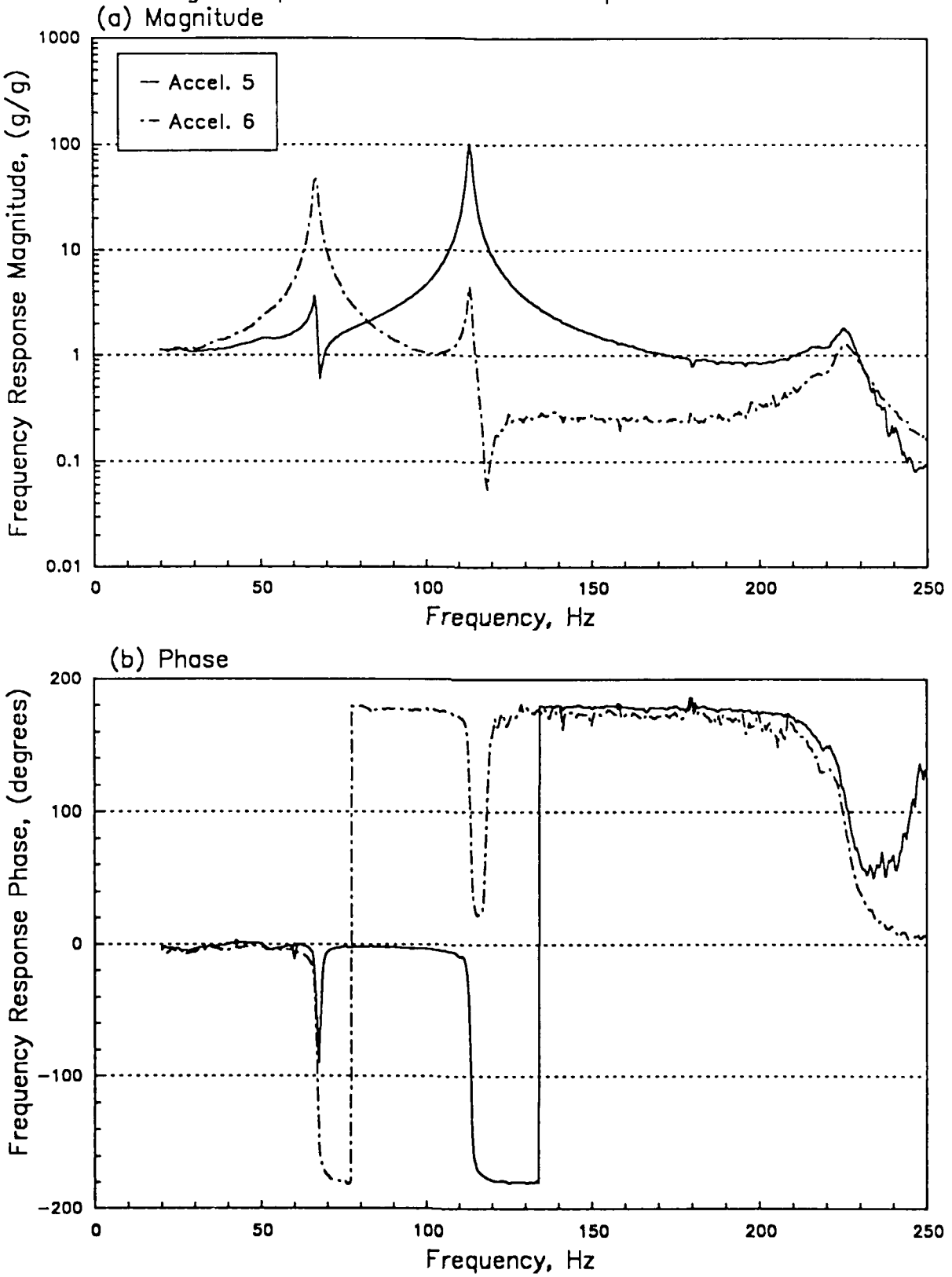

Payload Only (No APC).
Frequency Response of Accelerometers relative to the Shaker Base.
Modified Spectrum (3) −12dB below Specification Level.

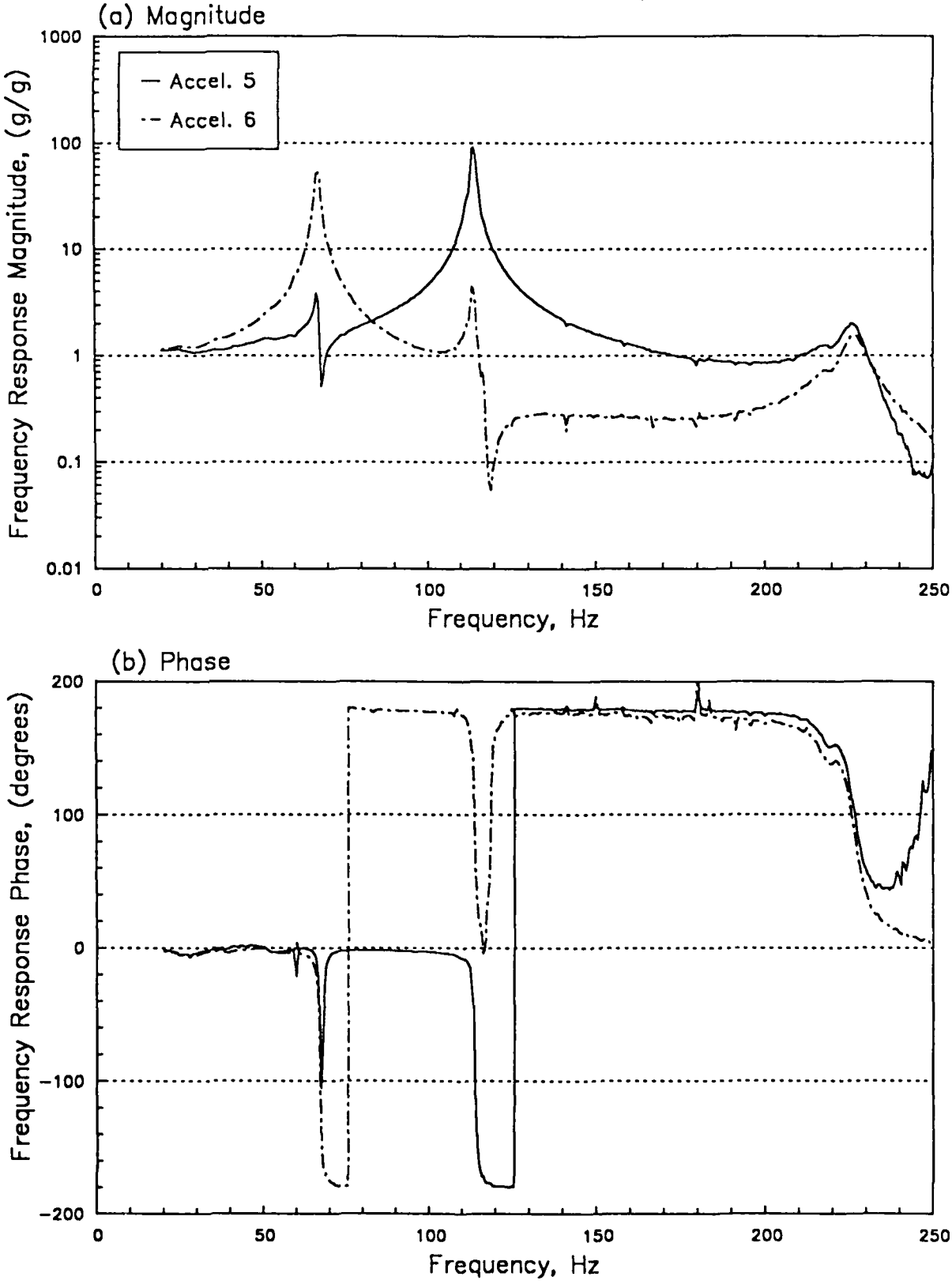

Payload Only (No APC).
Frequency Response of Accelerometers relative to the Shaker Base.
Modified Spectrum (3) −6dB below Specification Level.

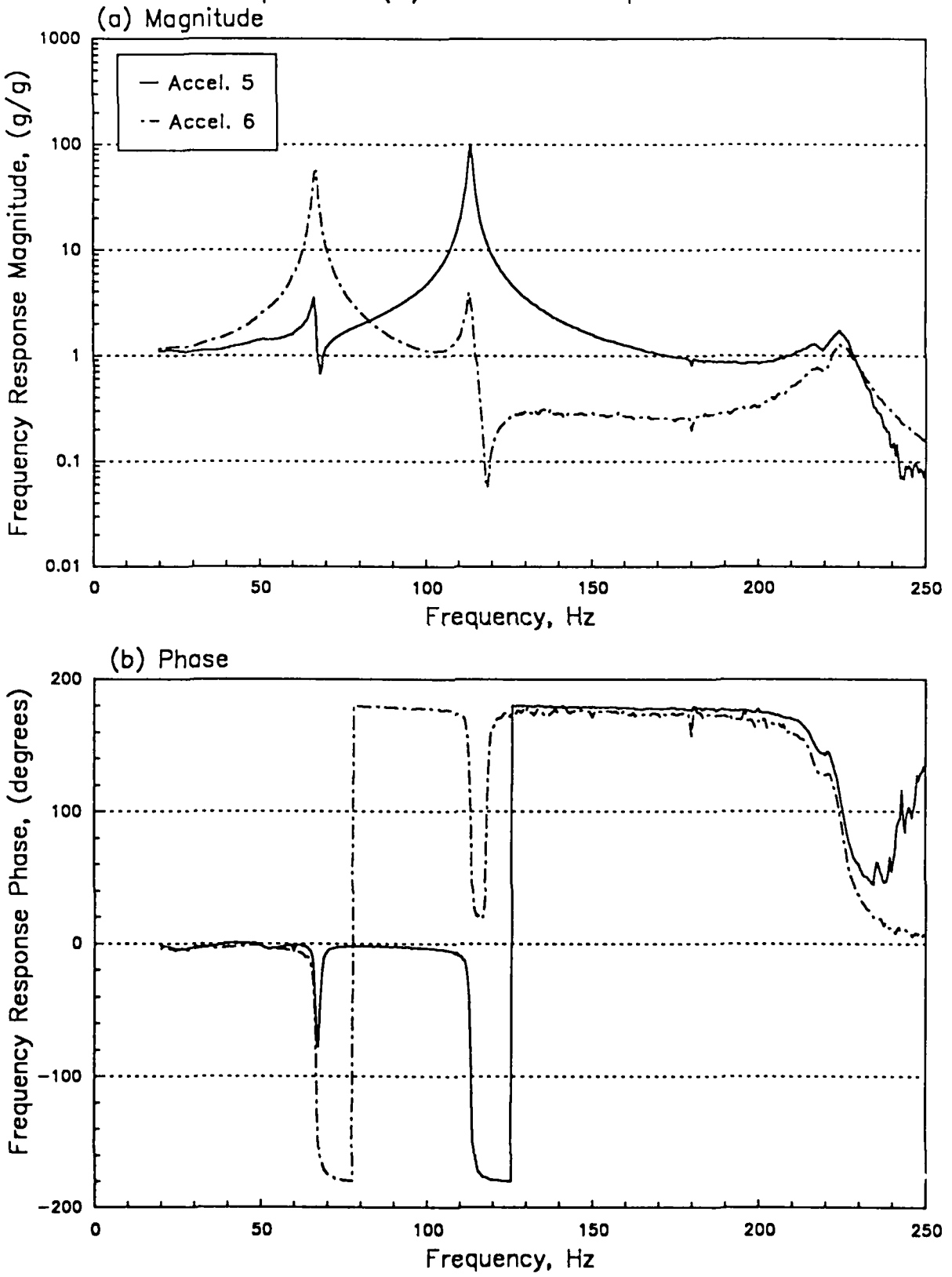

Rigid Payload on APC.
Frequency Response of Accelerometers relative to the Shaker Base.
Original Spectrum −12dB below Specification Level.

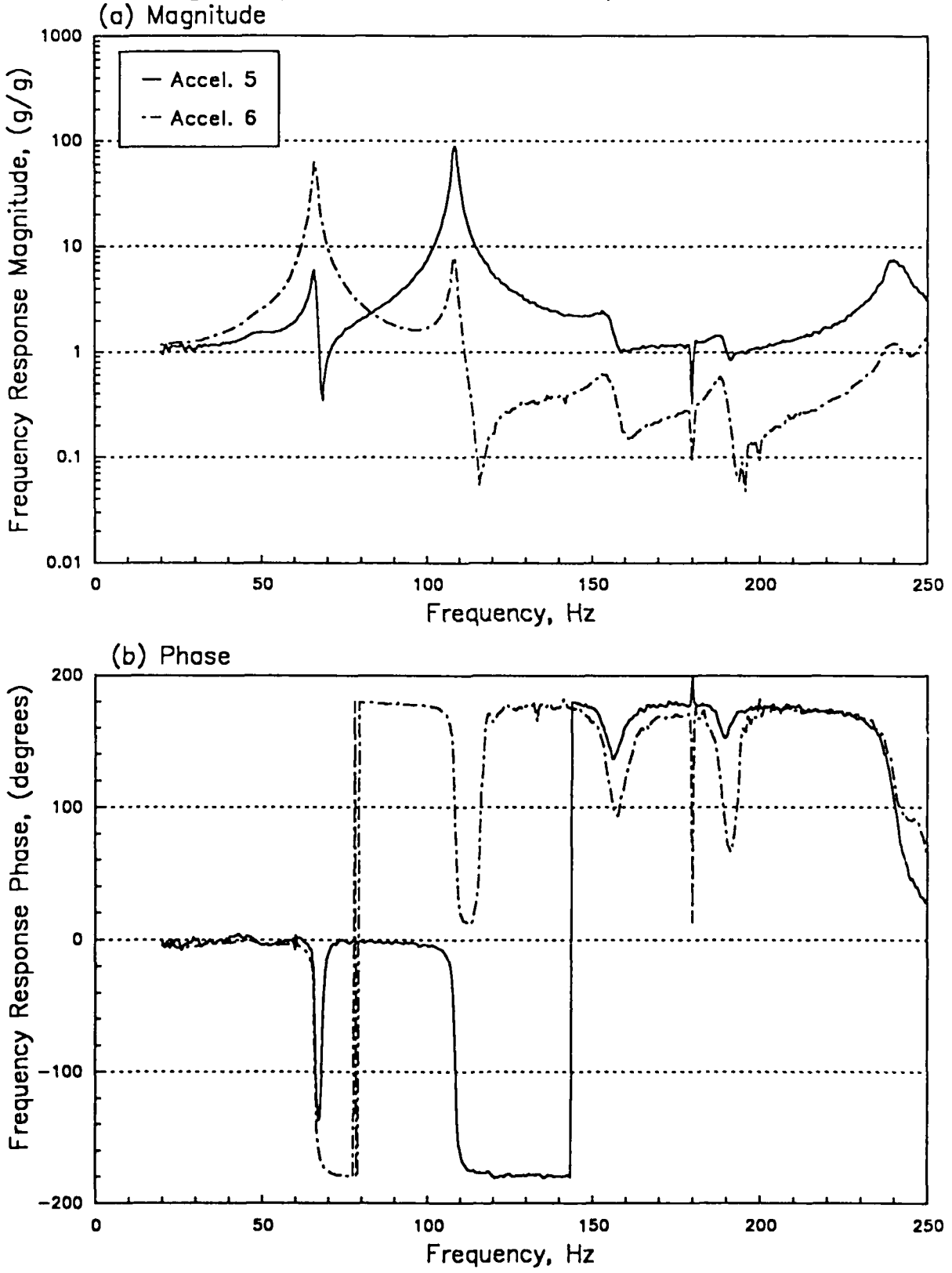

Rigid Payload on APC.
Frequency Response of Accelerometers relative to the Shaker Base.
Modified Spectrum (1) −12dB below Specification Level.

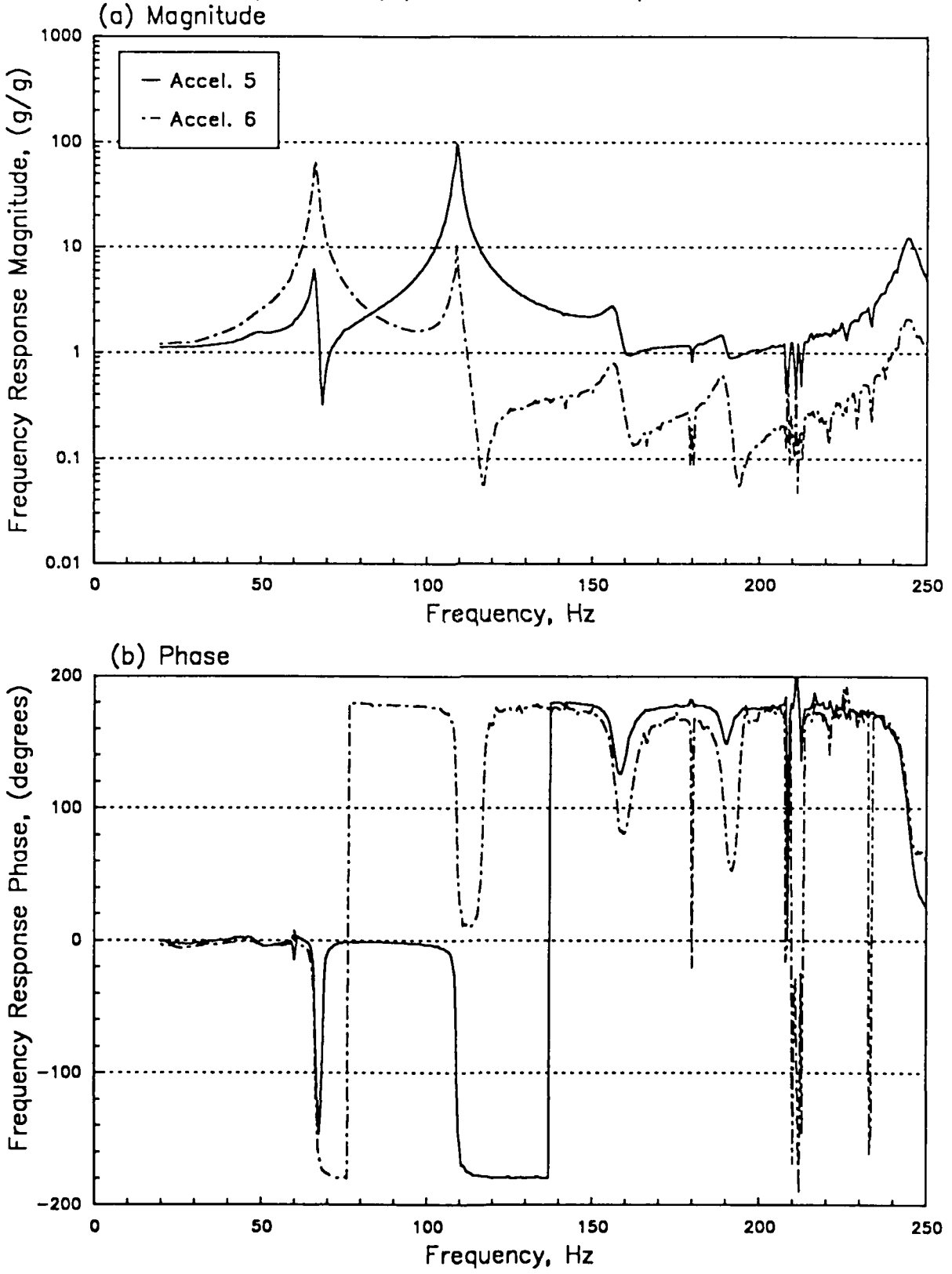

Rigid Payload on APC.
Frequency Response of Accelerometers relative to the Shaker Base.
Modified Spectrum (1) −6dB below Specification Level.

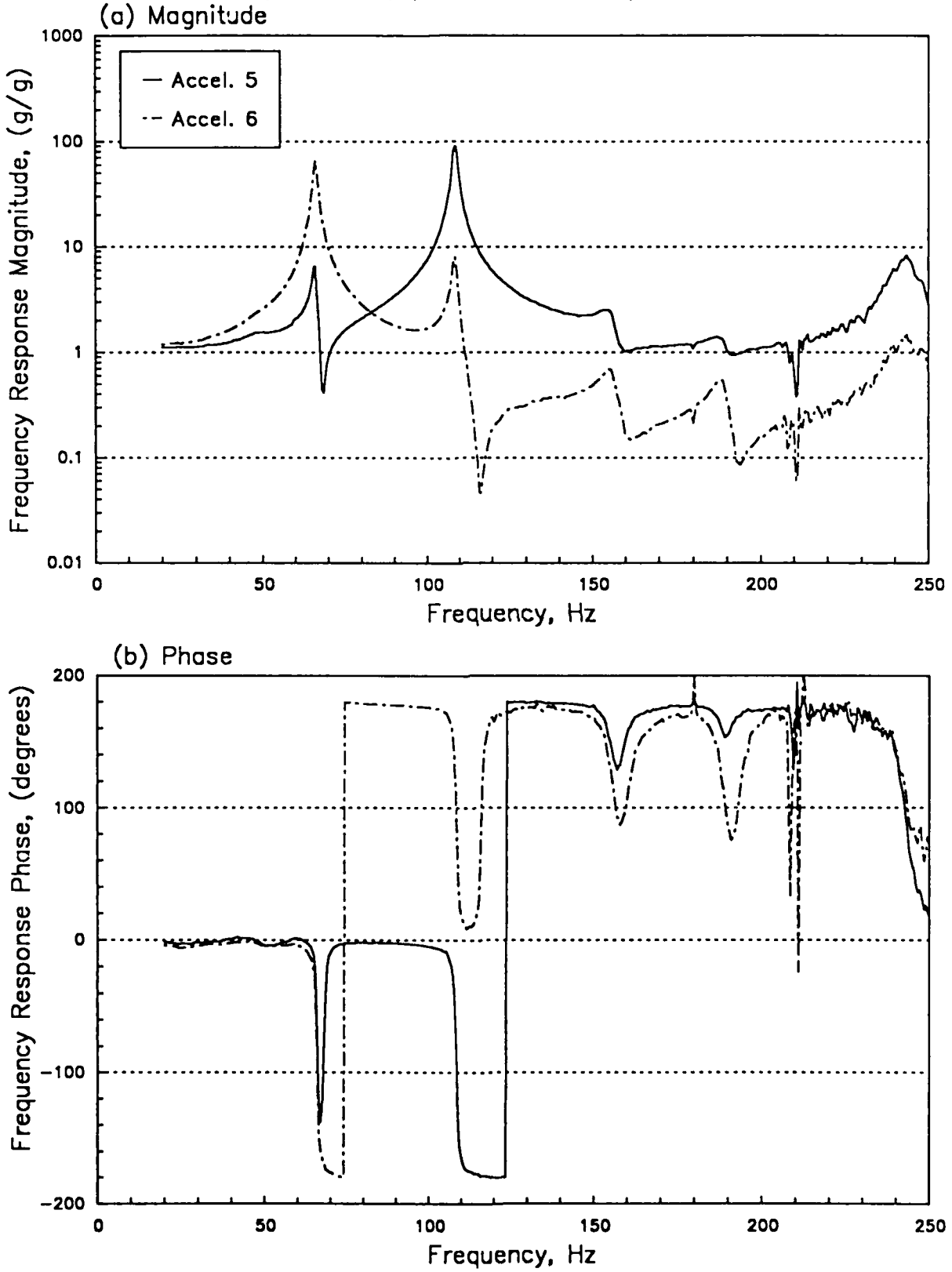

Payload on APC with 0.005" Gap.
Frequency Response of Accelerometers relative to the Shaker Base.
Original Spectrum −12dB below Specification Level.

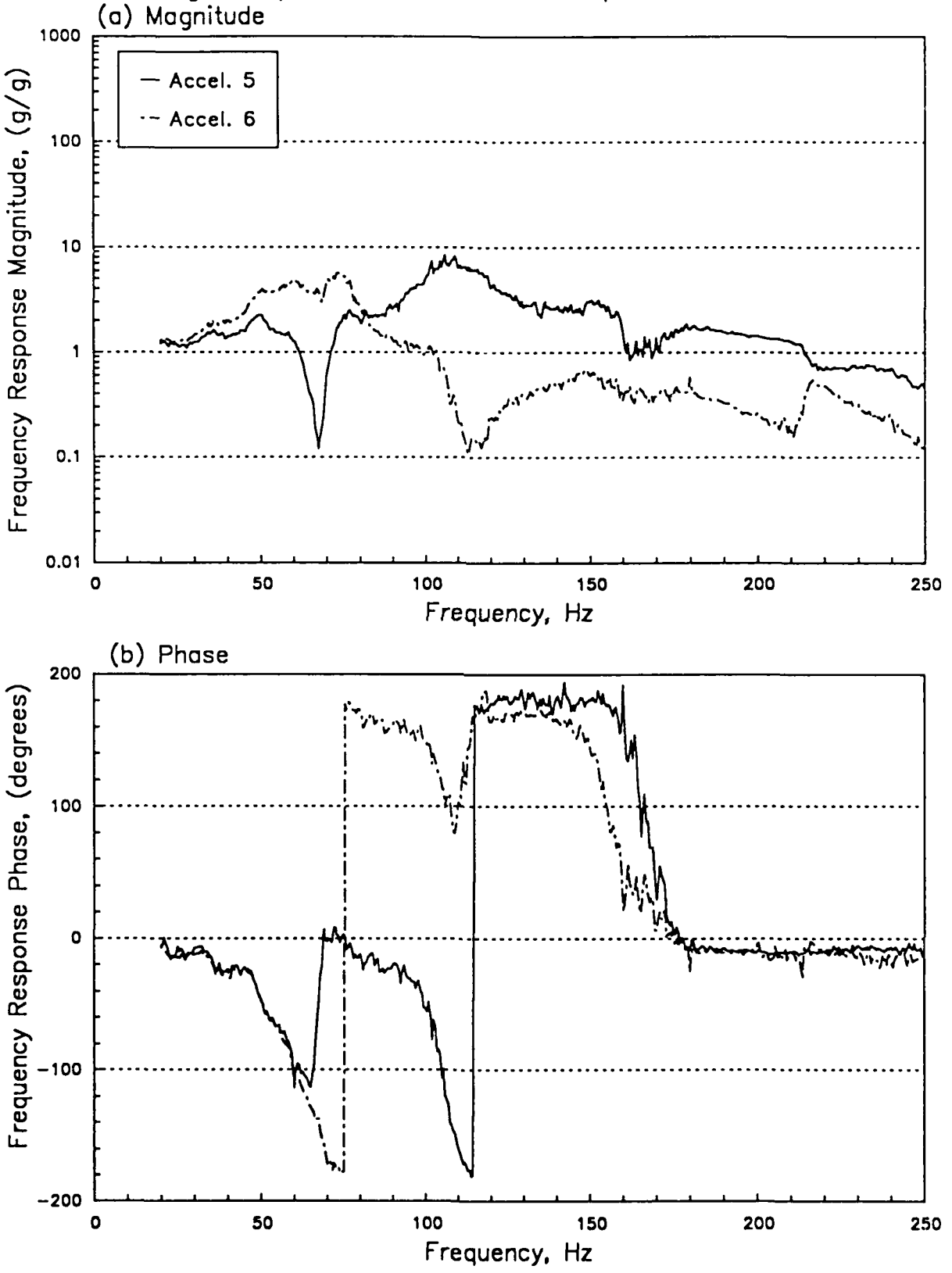

Frequency Response of Accelerometers relative to the Shaker Current.
Spectrum at Specification Level.

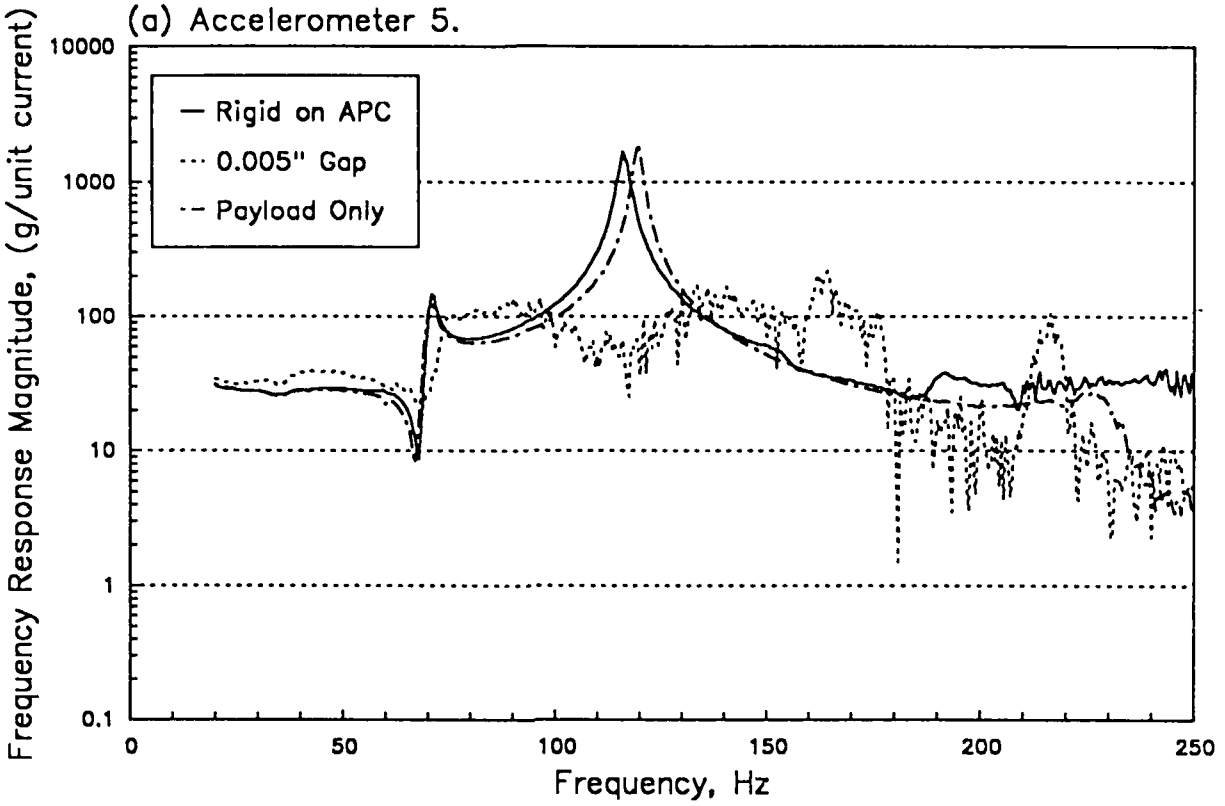

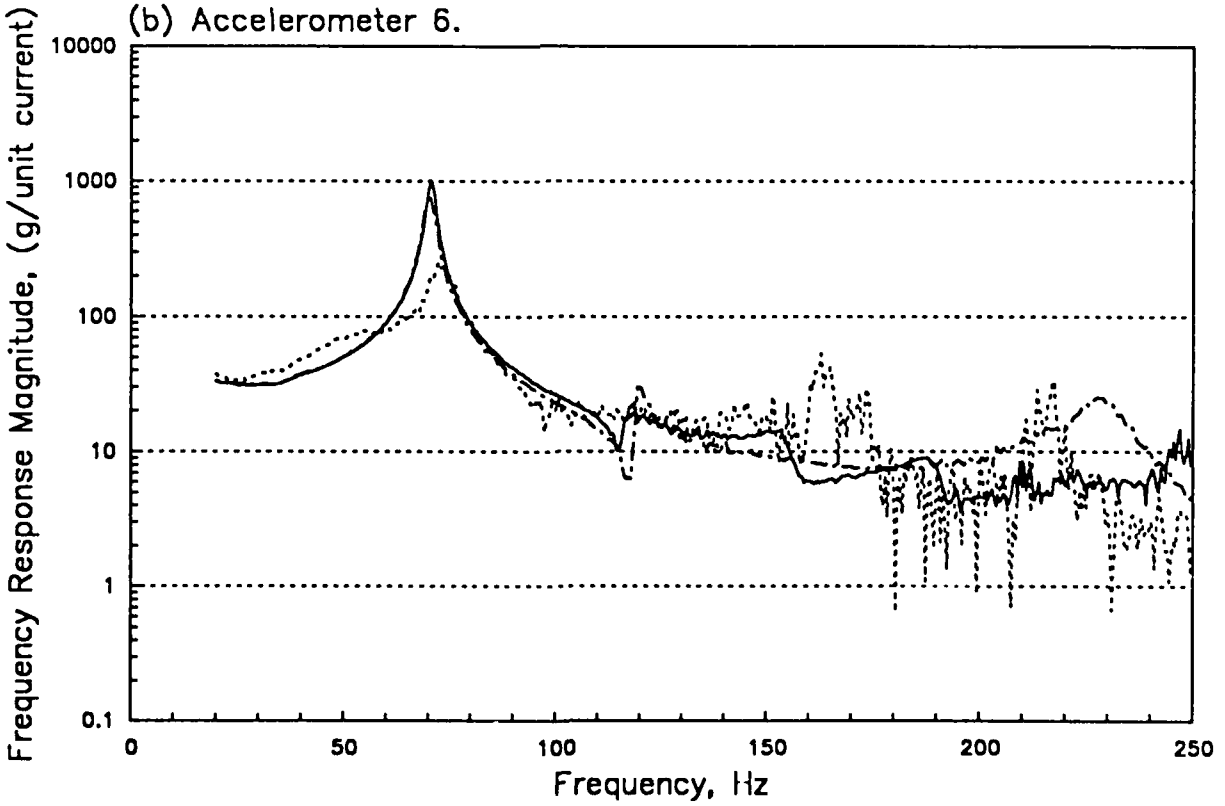

Apparent Total Weight of Payload Only (No APC).
Vibration Level −12dB below Specification.

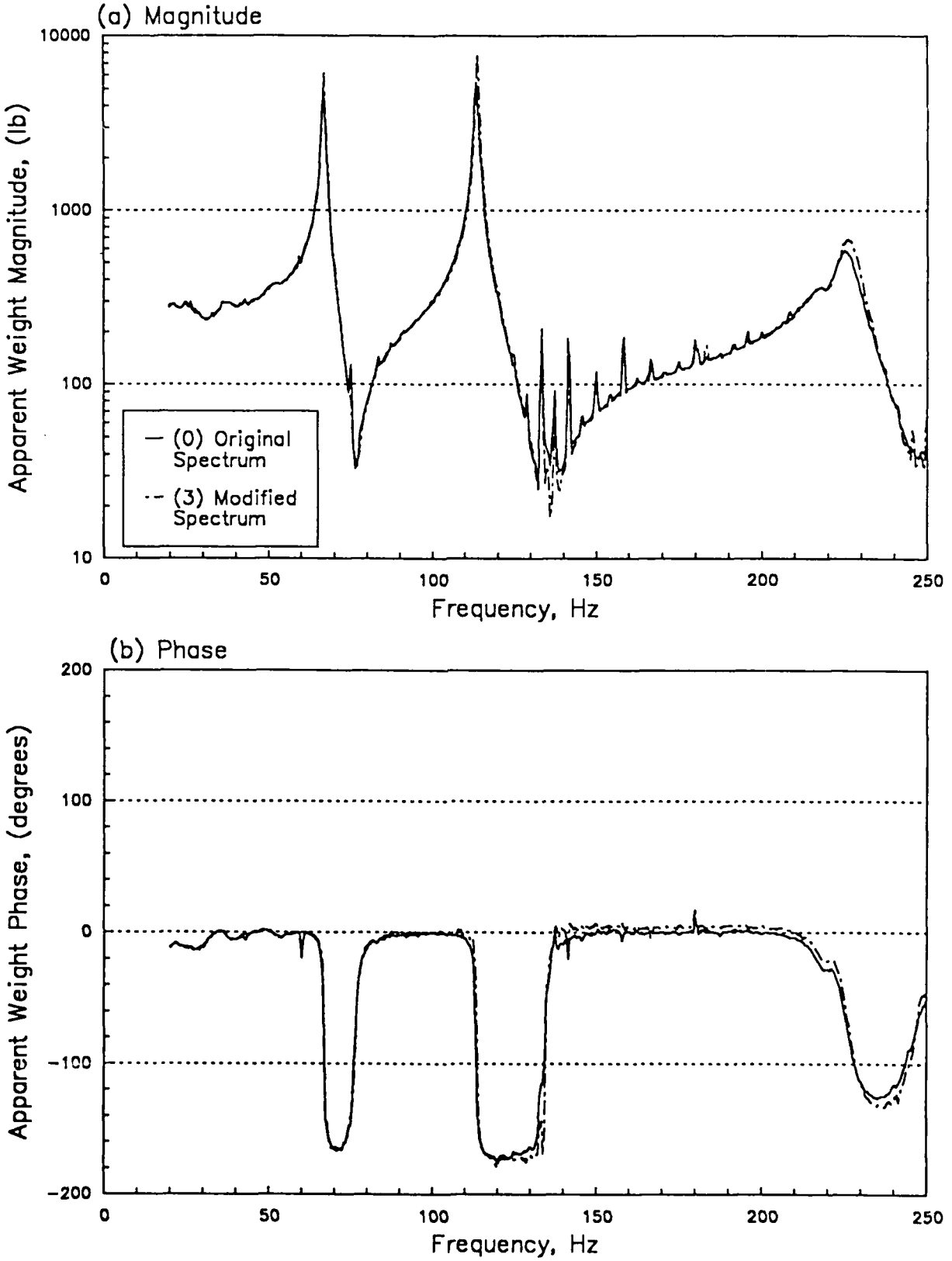

Apparent Total Weight of Rigid Payload on APC.
Vibration Level −12dB below Specification.

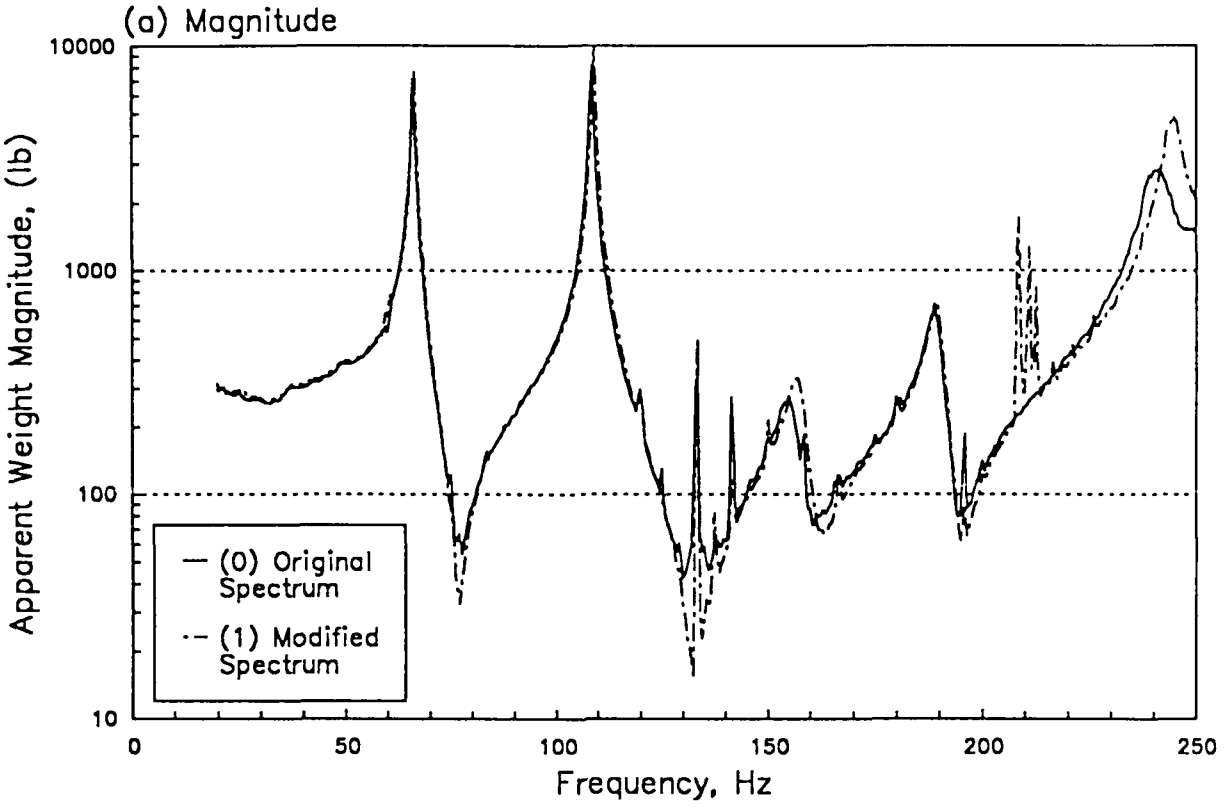

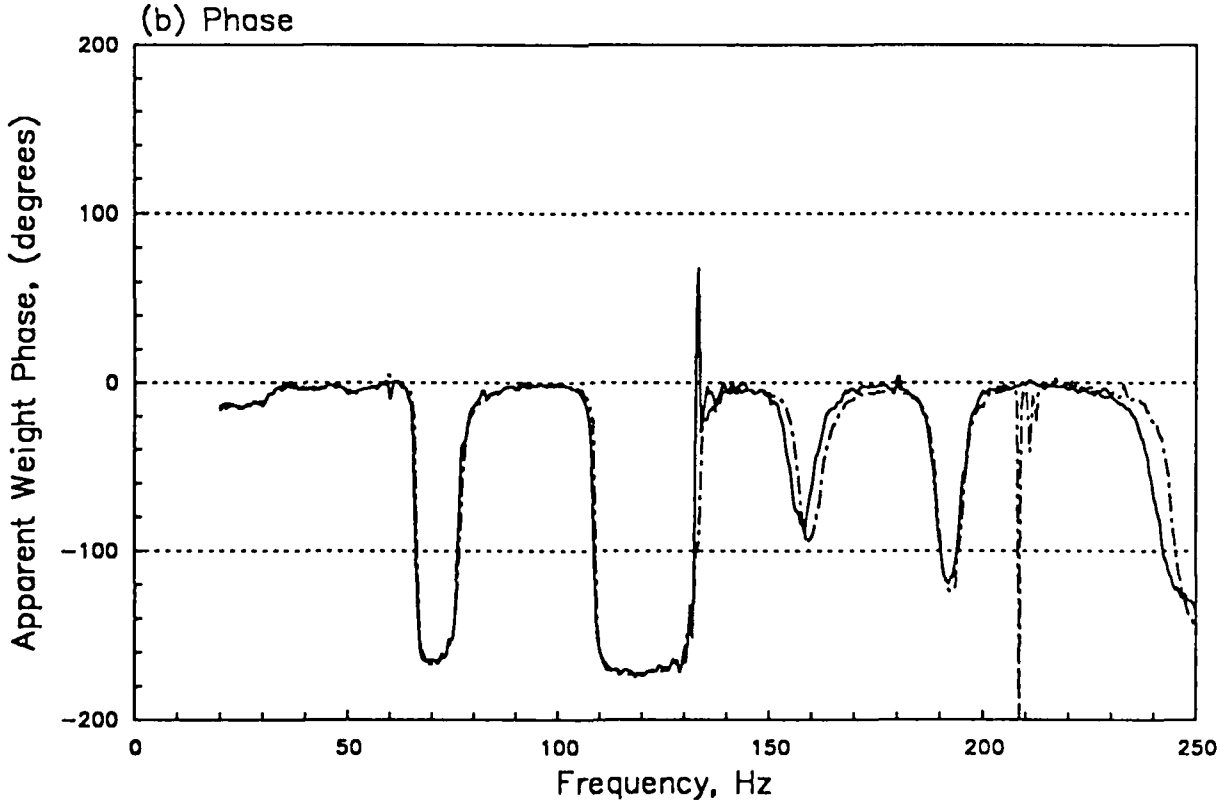

Payload Only (No APC).
Force Spectrum Normalized to Specification Level.
Measurements at −12dB below Specification.

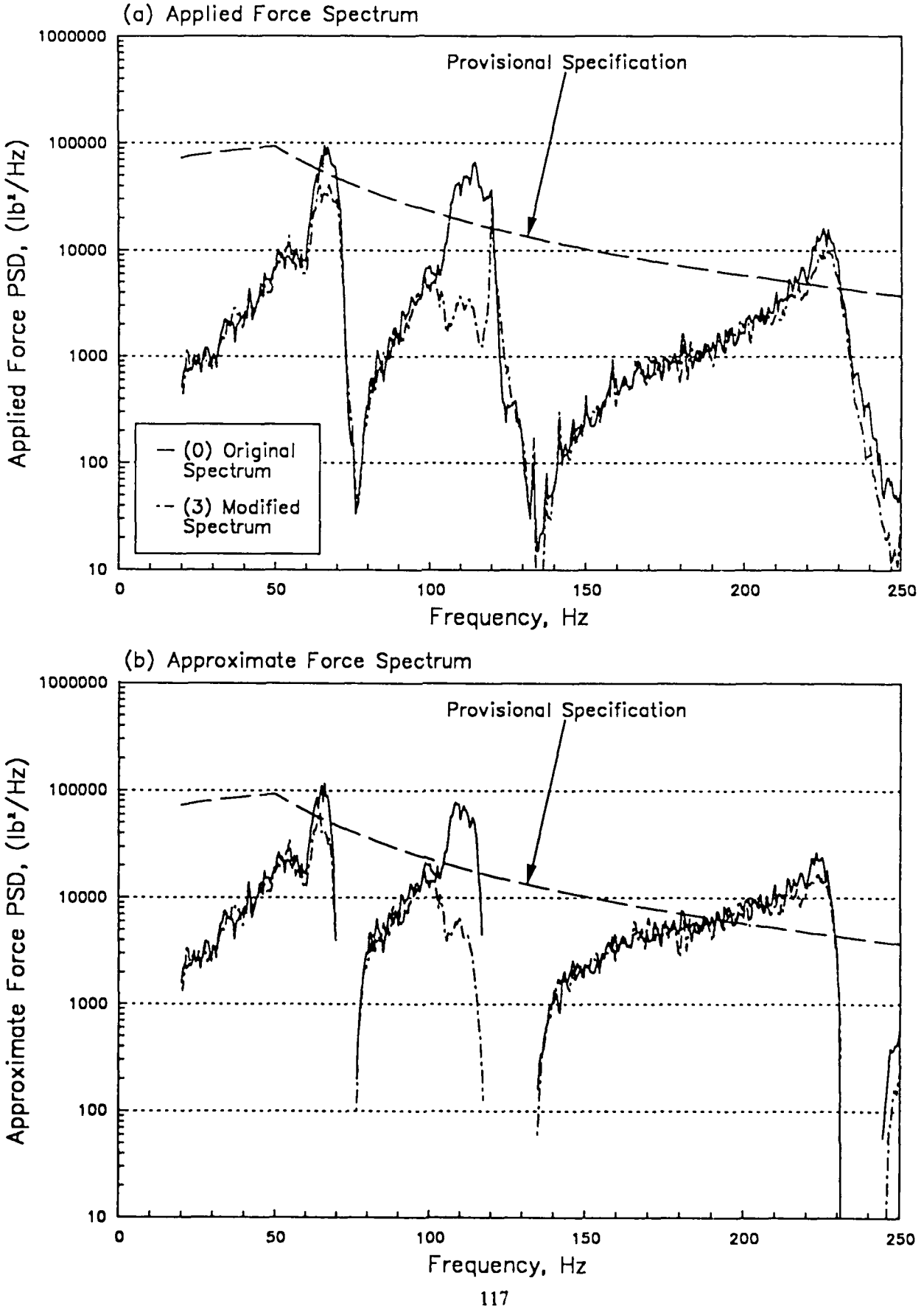

Rigid Payload on APC.
Force Spectrum Normalized to Specification Level.
Measurements at −12dB below Specification.

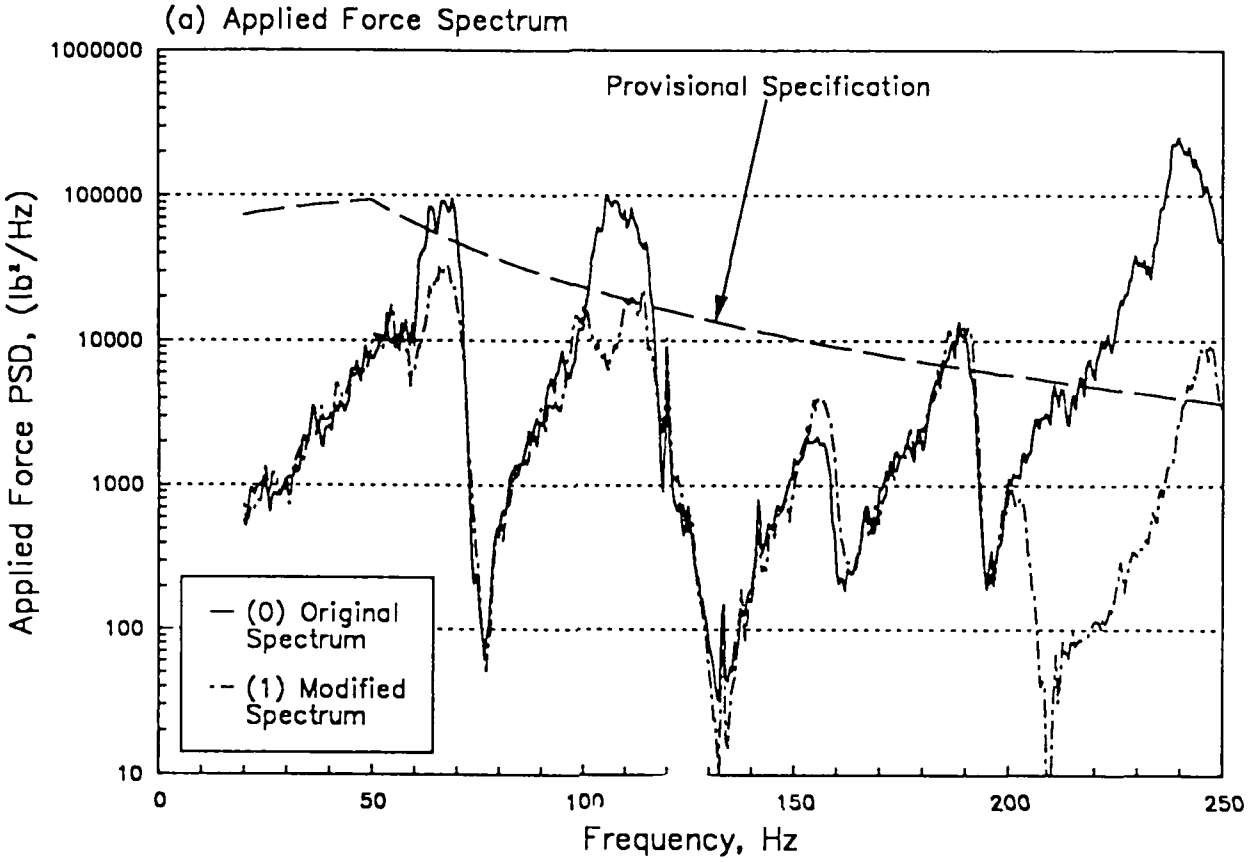

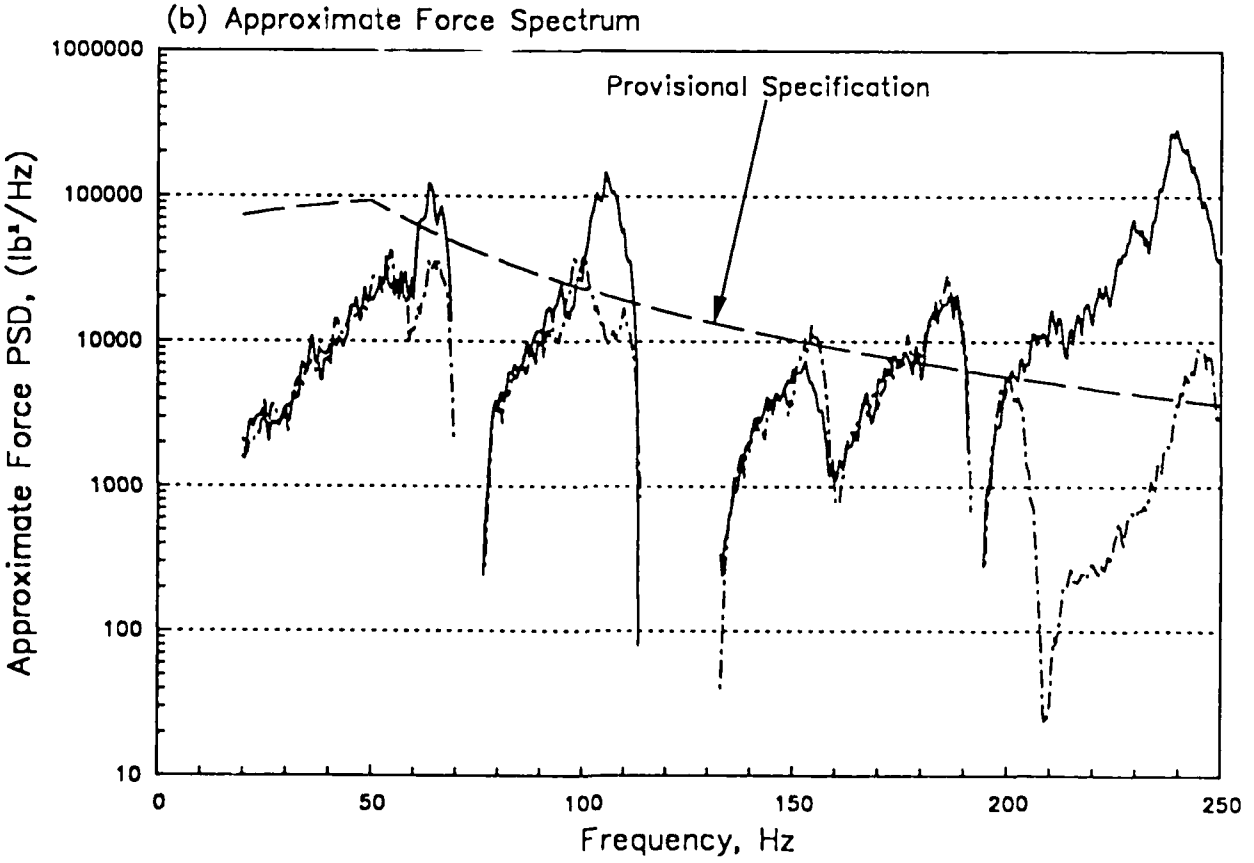

Force/Base Acceleration Cross Spectrum for Payload Only (No APC).
Original Spectrum −12dB below Specification Level.

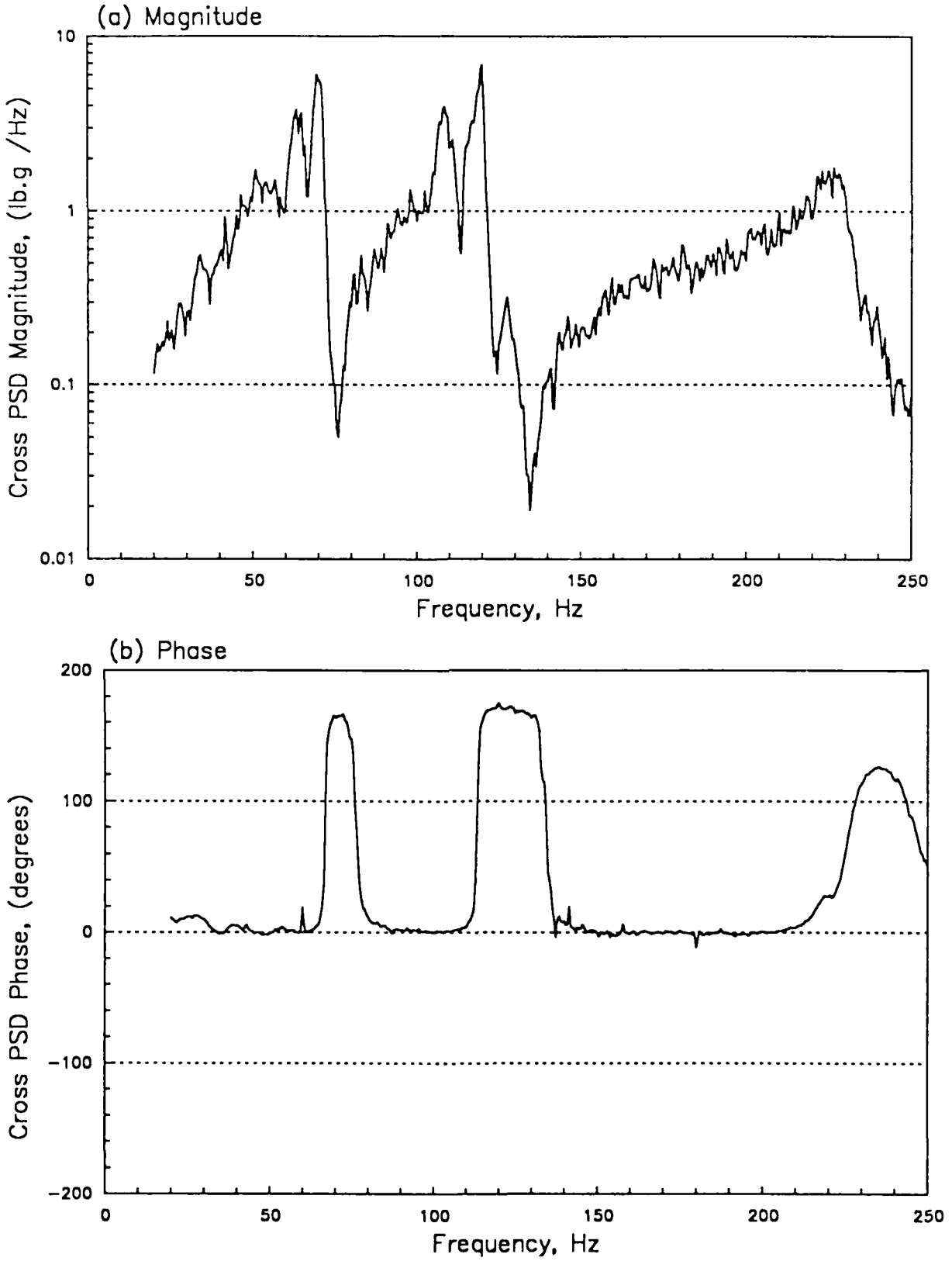

Payload Only (No APC).
Original Spectrum −12dB below Specification Level.

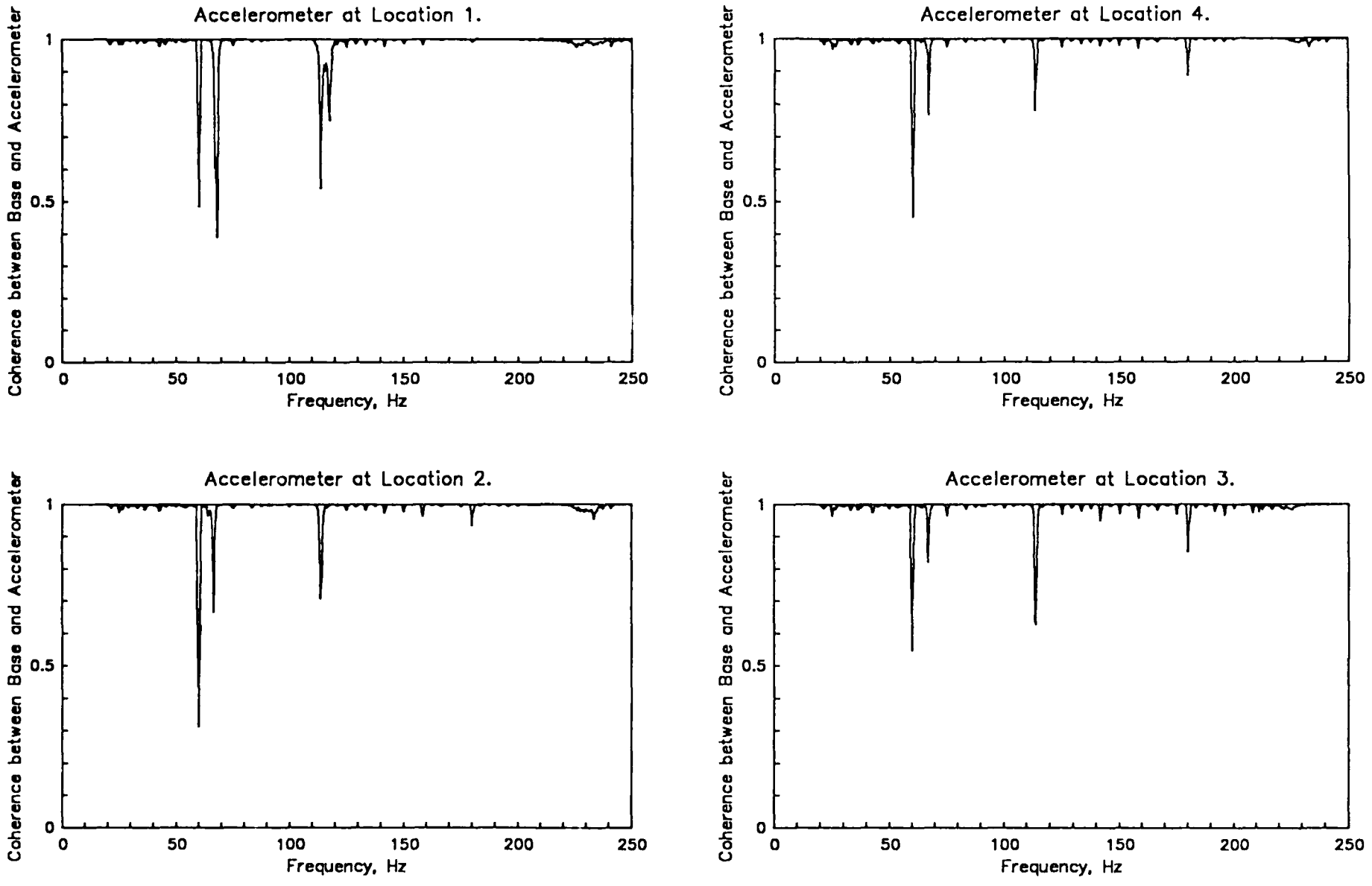

COHERENCE BETWEEN SHAKER BASE AND ACCELEROMETERS 1−4.

Payload Only (No APC).
Modified Spectrum (3) −12dB below Specification Level.

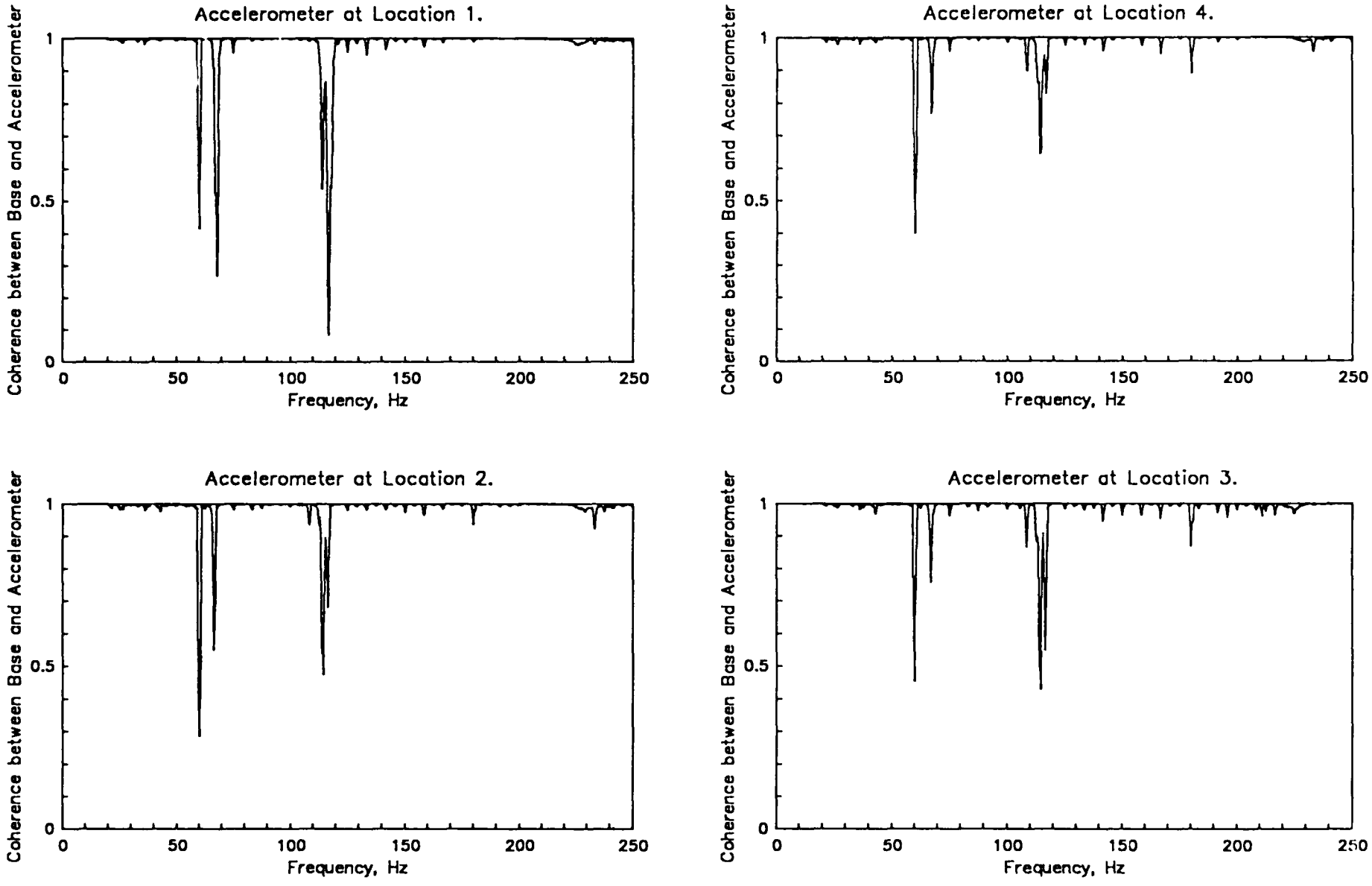

COHERENCE BETWEEN SHAKER BASE AND ACCELEROMETERS 1−4.

Payload Only (No APC).
Modified Spectrum (3) −6dB below Specification Level.

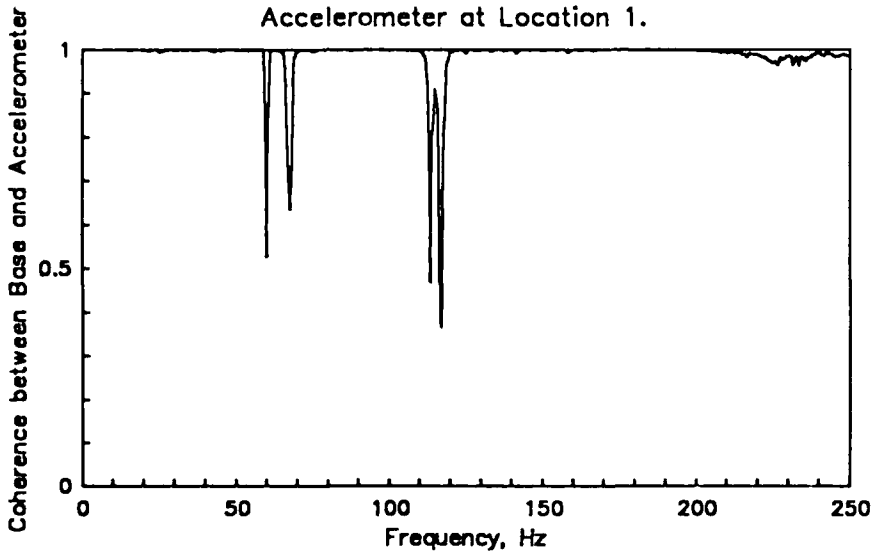

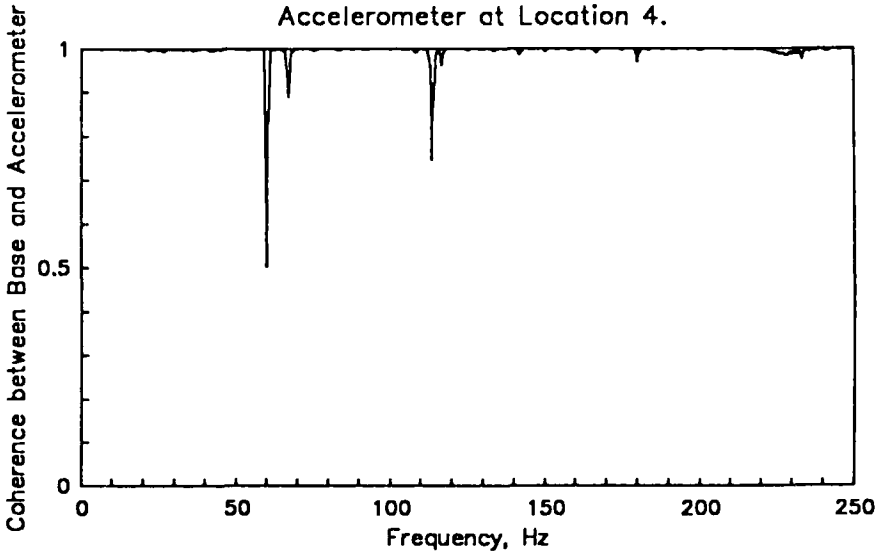

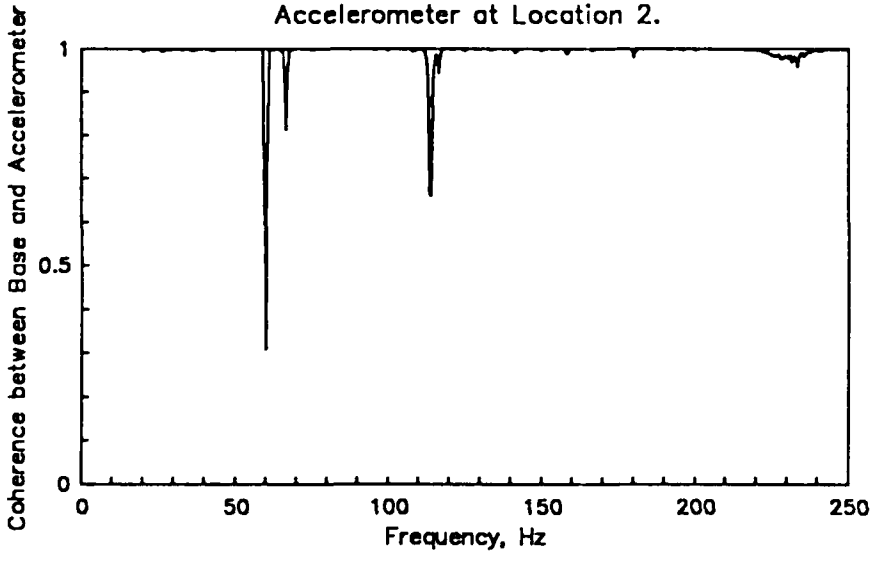

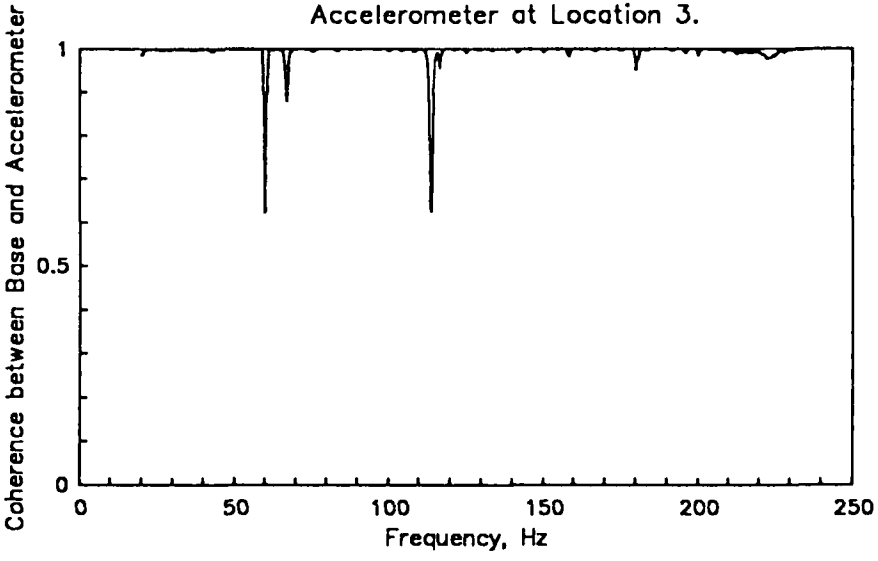

COHERENCE BETWEEN SHAKER BASE AND ACCELEROMETERS 1−4.

8/14/98

Payload Only (No APC).
Modified Spectrum (3) at Specification Level.

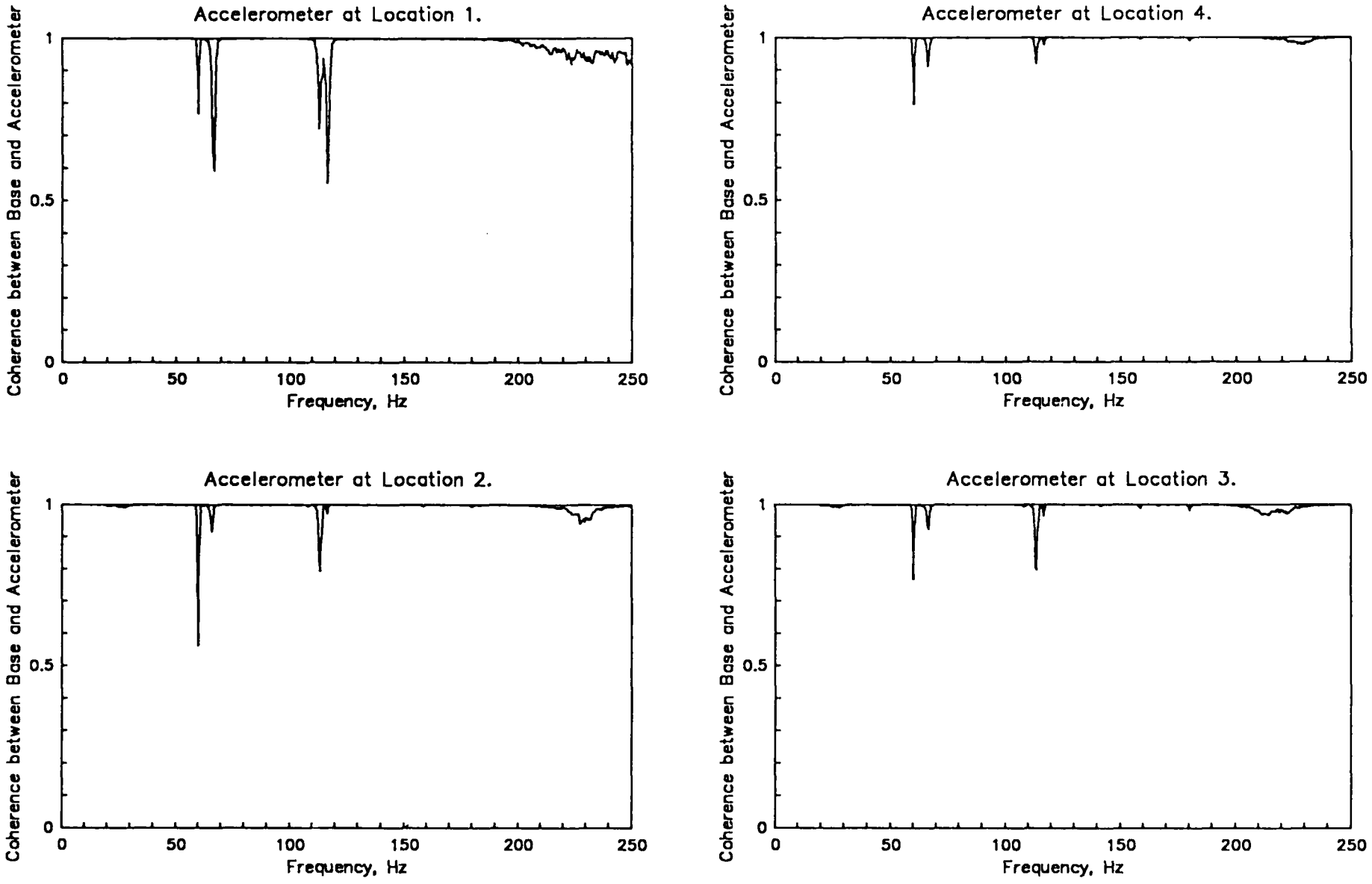

COHERENCE BETWEEN SHAKER BASE AND ACCELEROMETERS 1–4.

8/12/82

Rigid Payload on APC.
Original Spectrum −12dB below Specification Level.

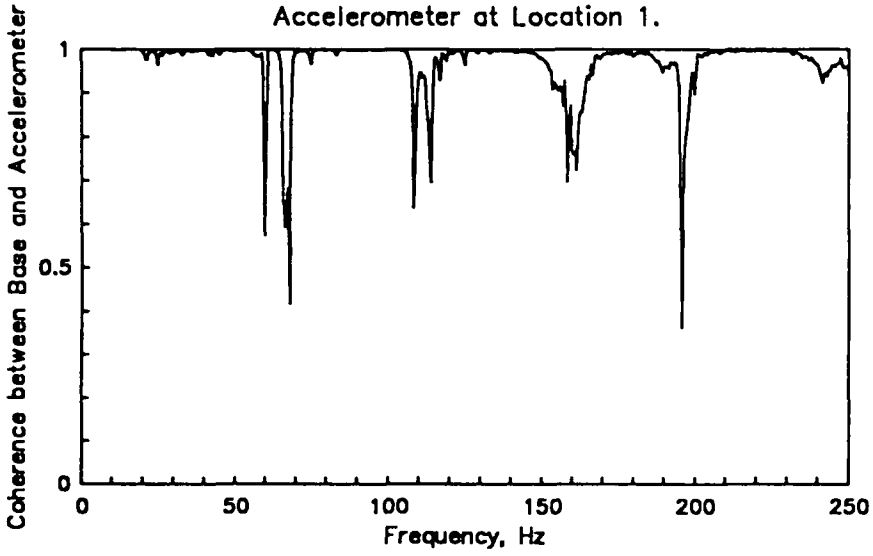

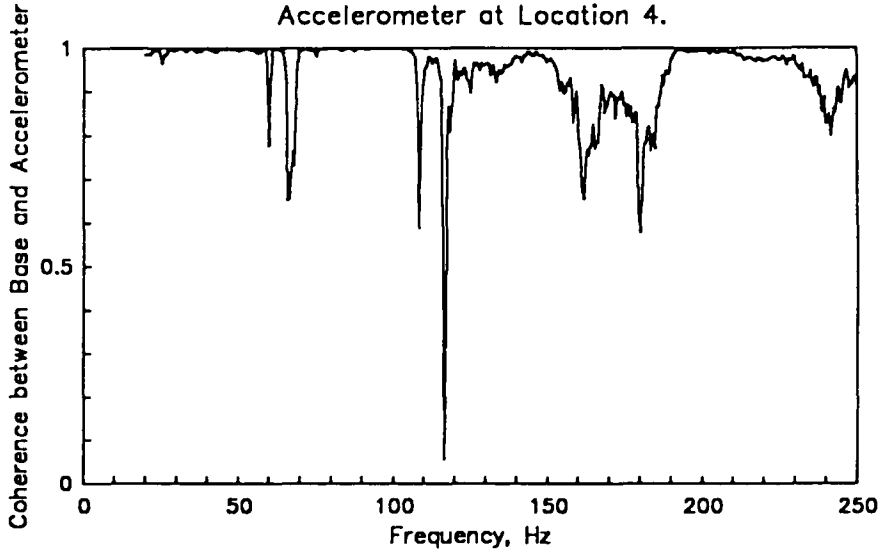

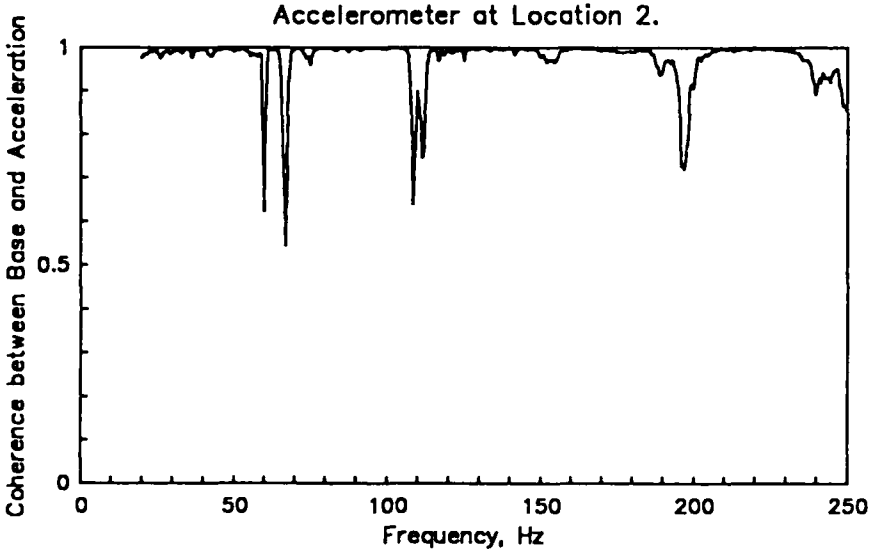

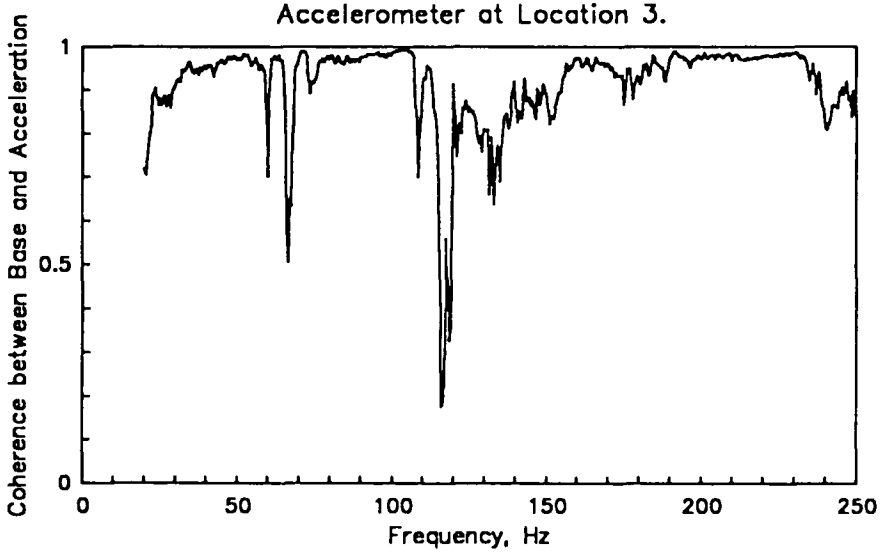

COHERENCE BETWEEN SHAKER BASE AND ACCELEROMETERS 1−4.

8/12/88

Rigid Payload on APC.
Modified Spectrum (1) −12dB below Specification Level.

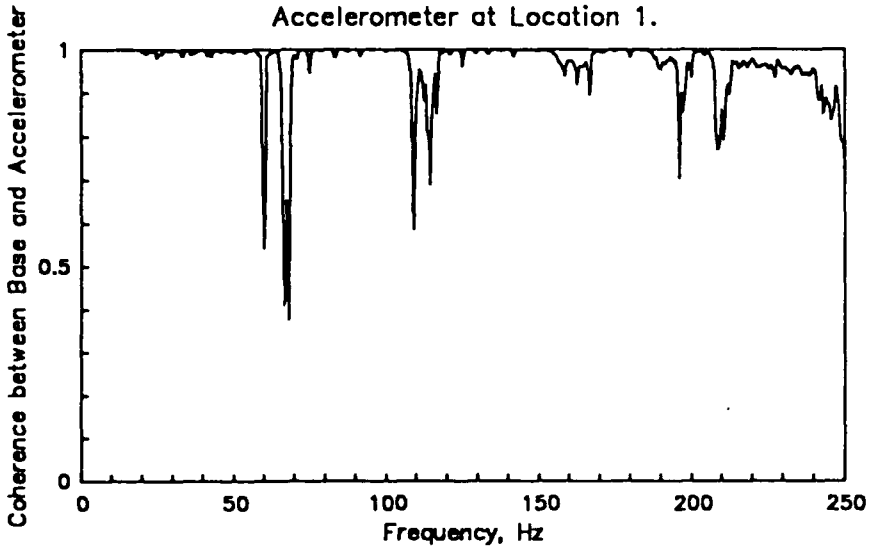

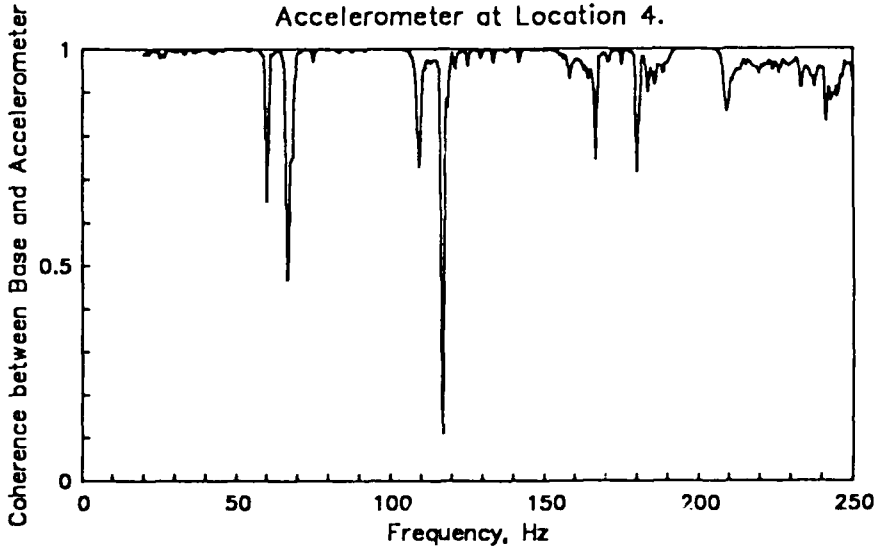

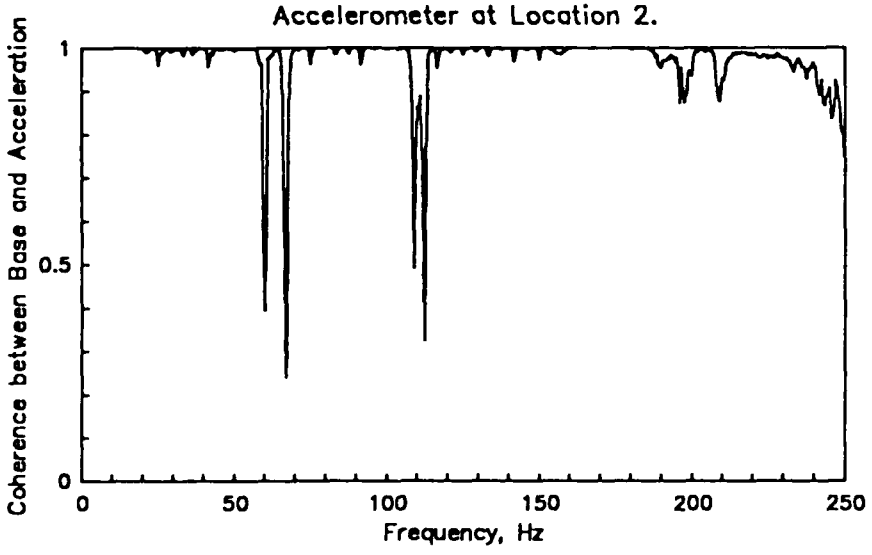

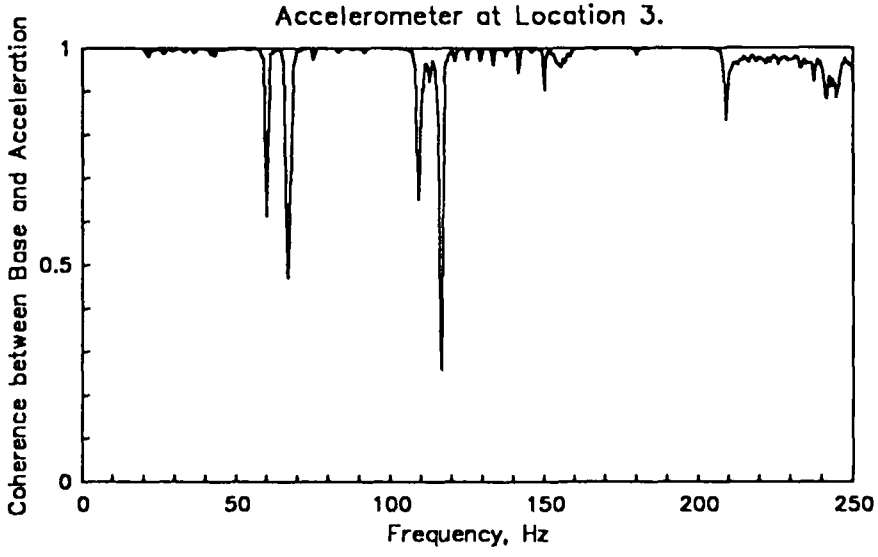

COHERENCE BETWEEN SHAKER BASE AND ACCELEROMETERS 1−4.

8/12/88

Rigid Payload on APC
Modified Spectrum (1) −6dB below Specification Level.

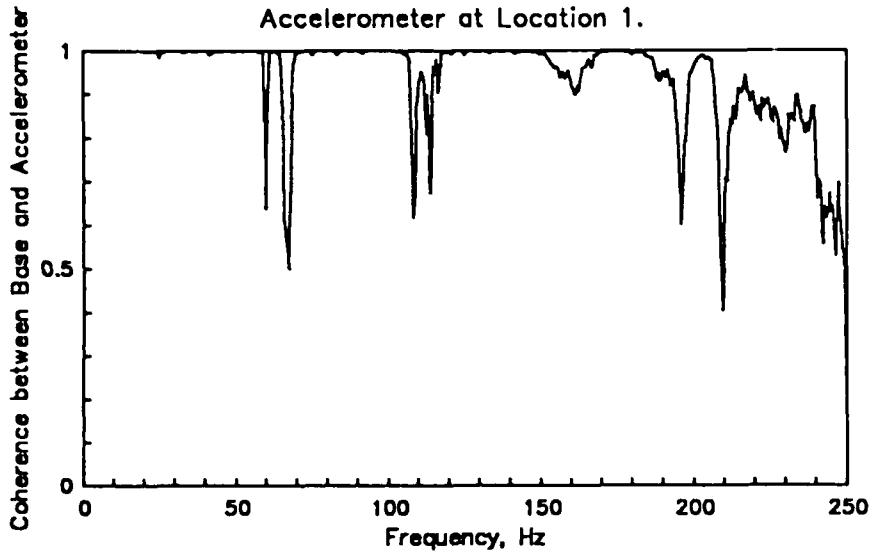

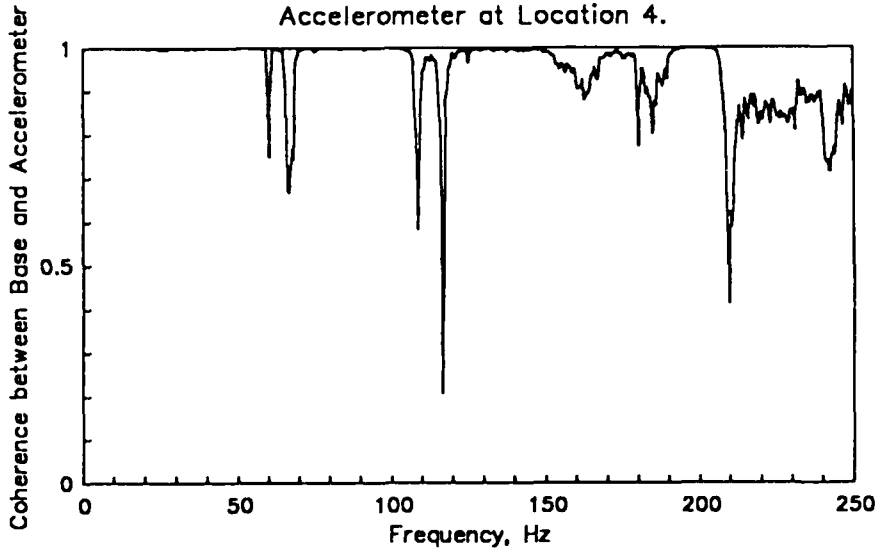

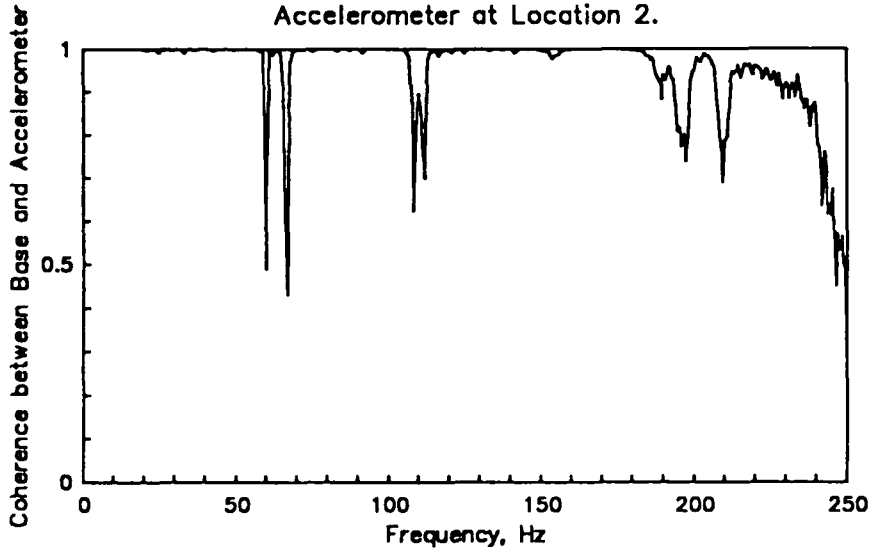

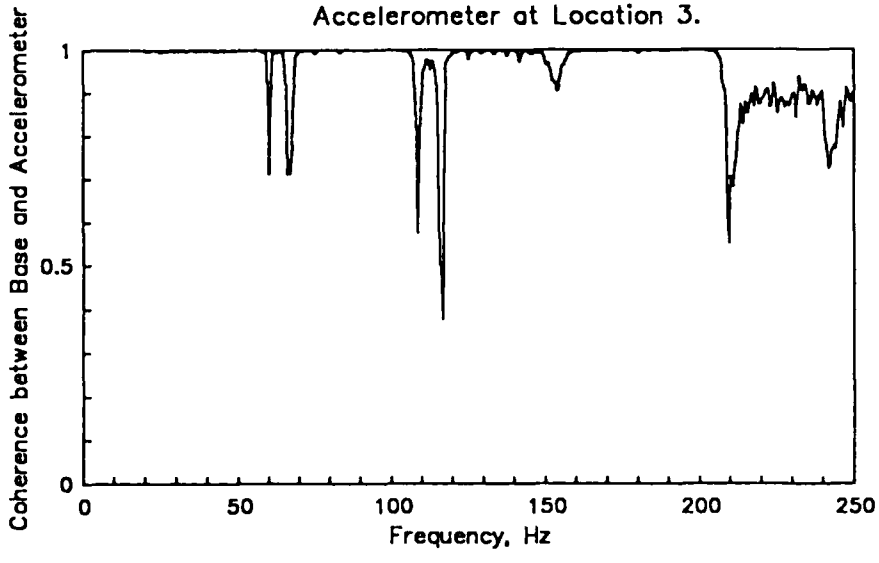

COHERENCE BETWEEN SHAKER BASE AND ACCELEROMETERS 1−4.

8/12/88

Rigid Payload on APC
Modified Spectrum (1) at Specification Level.

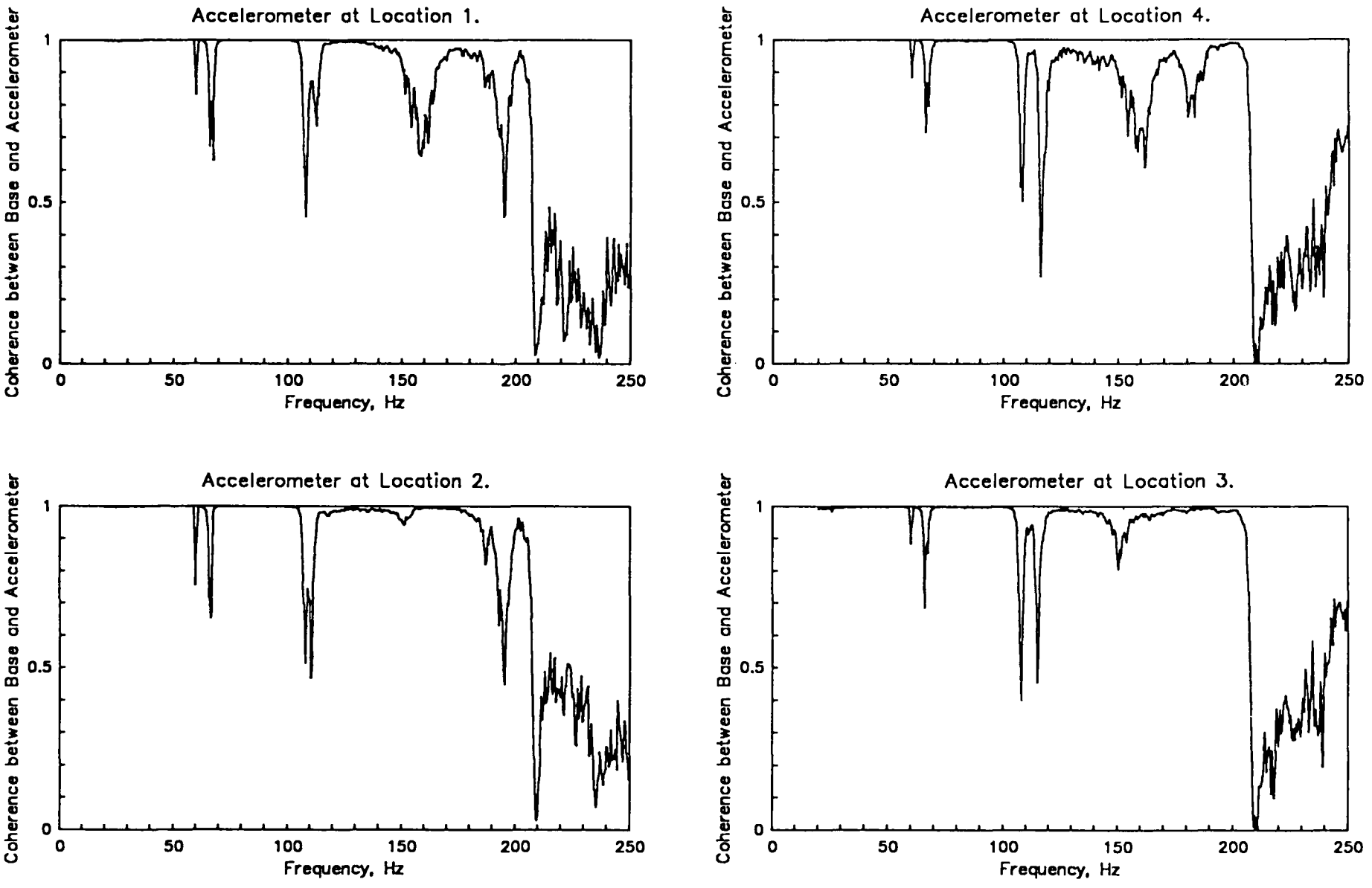

COHERENCE BETWEEN SHAKER BASE AND ACCELEROMETERS 1–4.

8/12/88

Payload on APC with 0.005" Gap.
Original Spectrum −12dB below Specification Level.

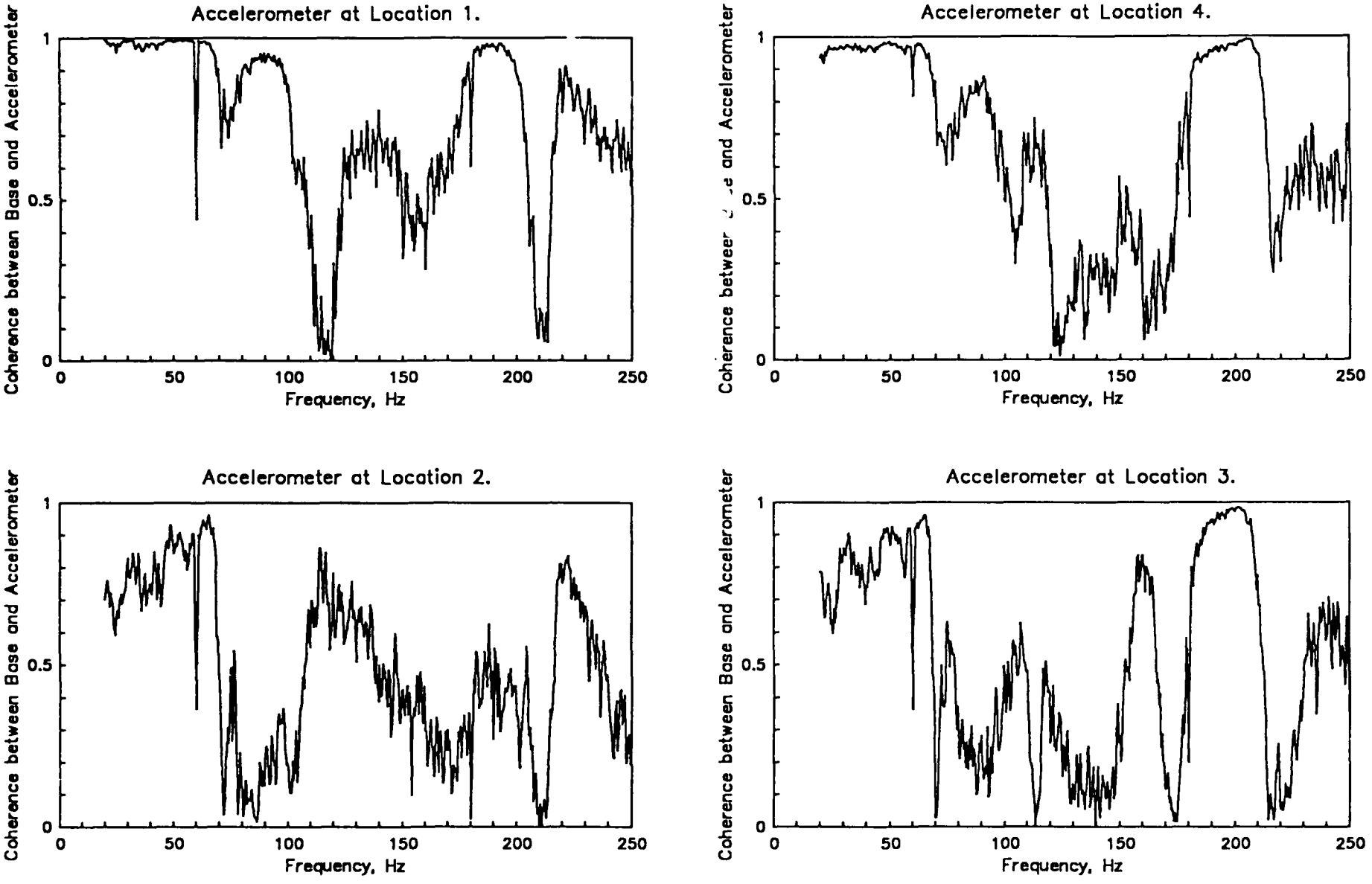

COHERENCE BETWEEN SHAKER BASE AND ACCELEROMETERS 1−4.

8/12/88

Payload on APC with 0.005" Gap.
Original Spectrum at Specification Level.

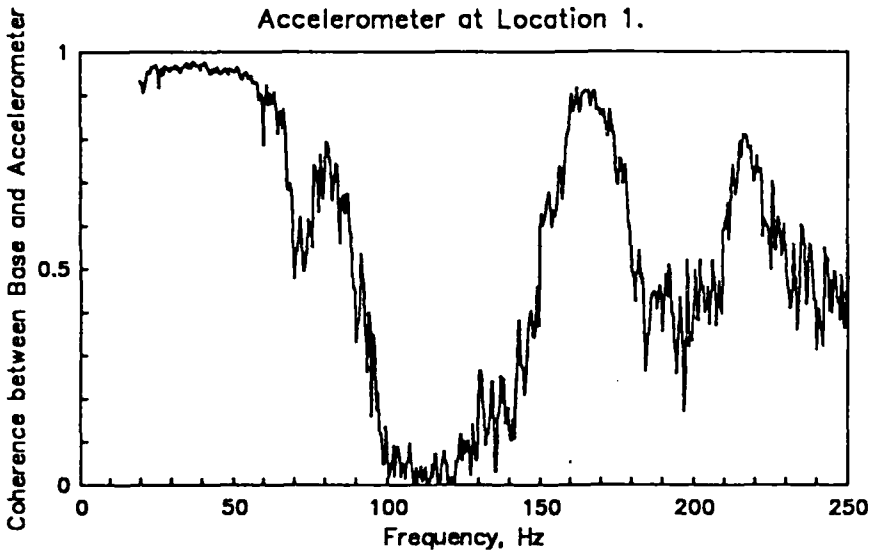

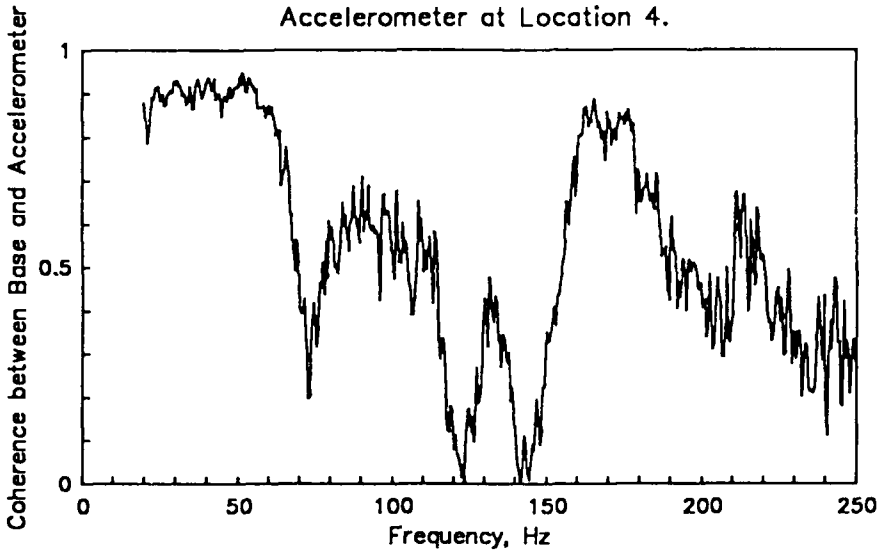

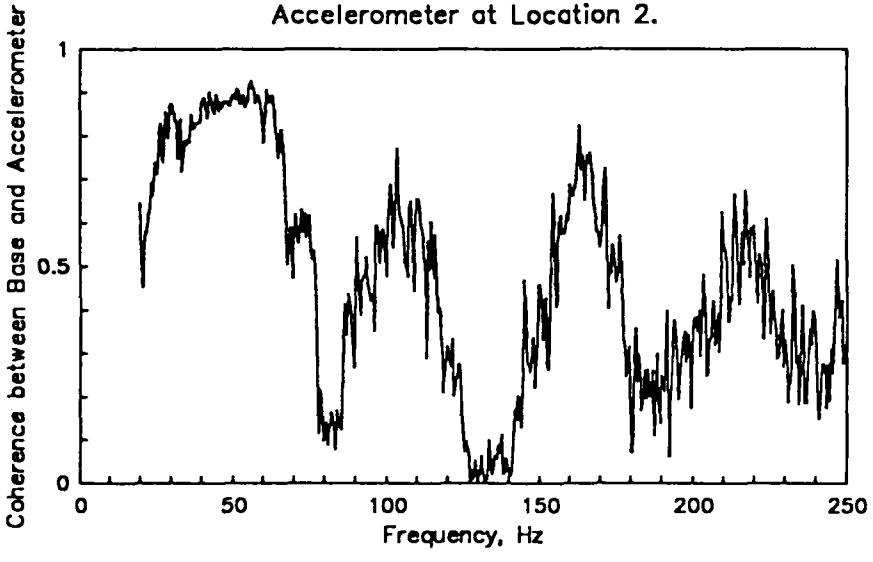

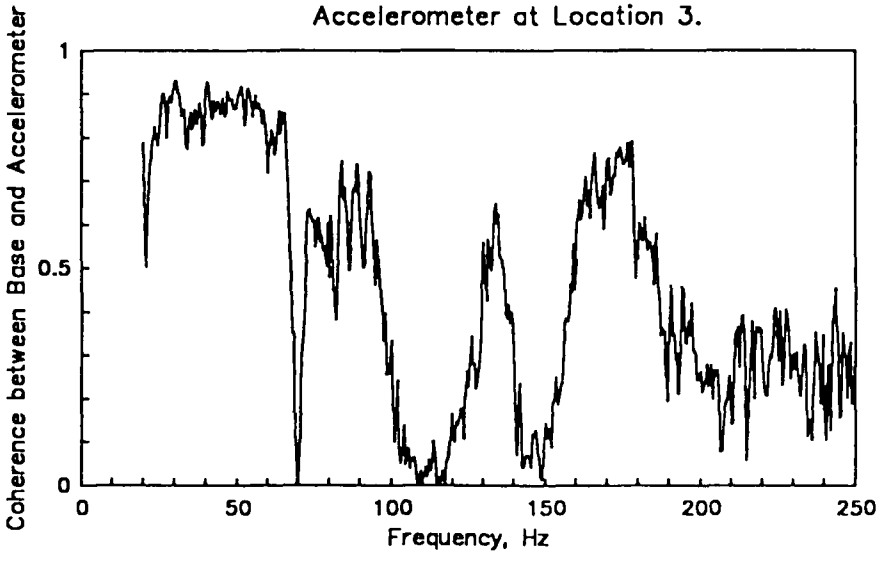

COHERENCE BETWEEN SHAKER BASE AND ACCELEROMETERS 1–4.

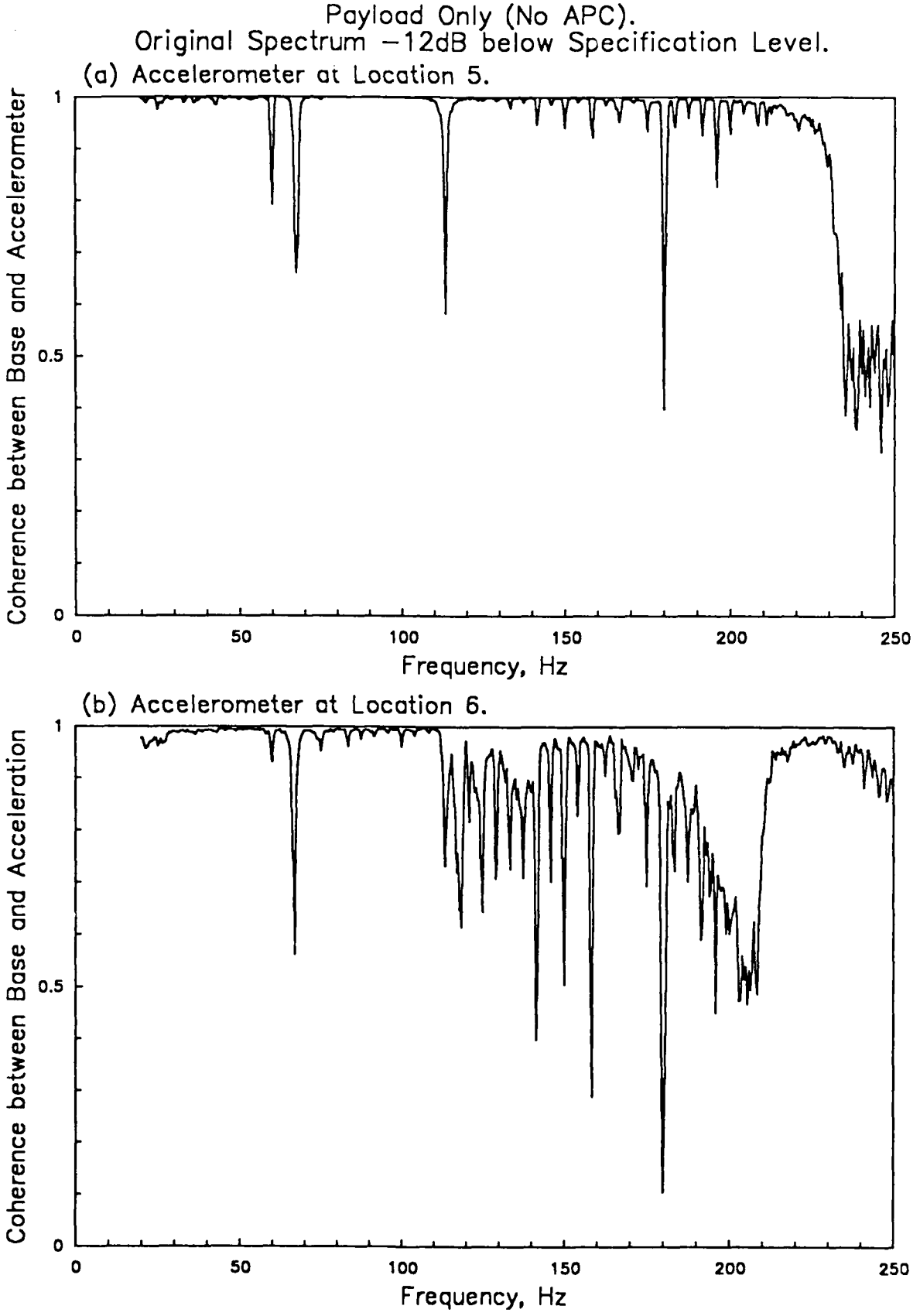

COHERENCE BETWEEN SHAKER BASE AND ACCELEROMETERS 5 AND 6.

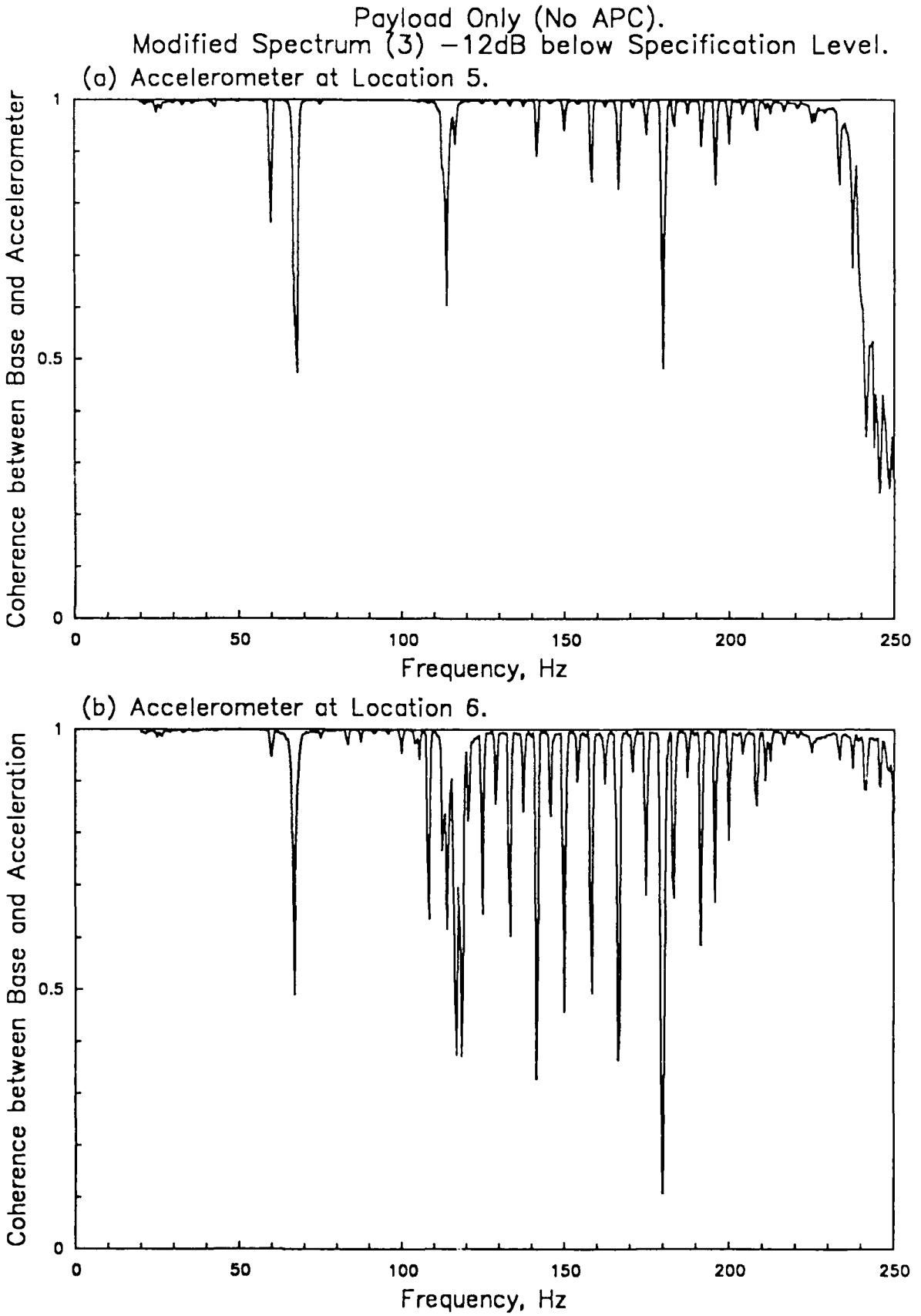

COHERENCE BETWEEN SHAKER BASE AND ACCELEROMETERS 5 AND 6.

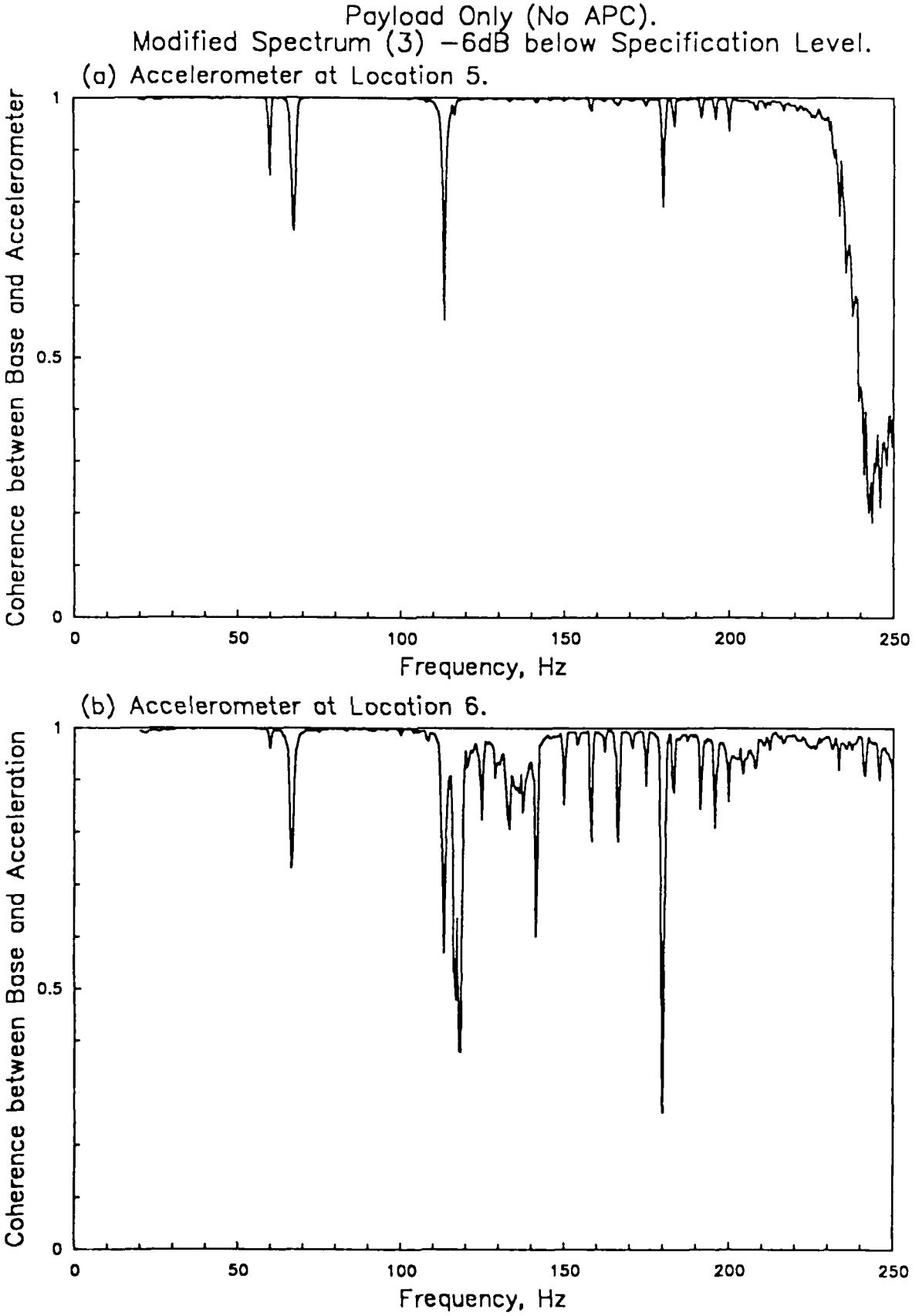

COHERENCE BETWEEN SHAKER BASE AND ACCELEROMETERS 5 AND 6.

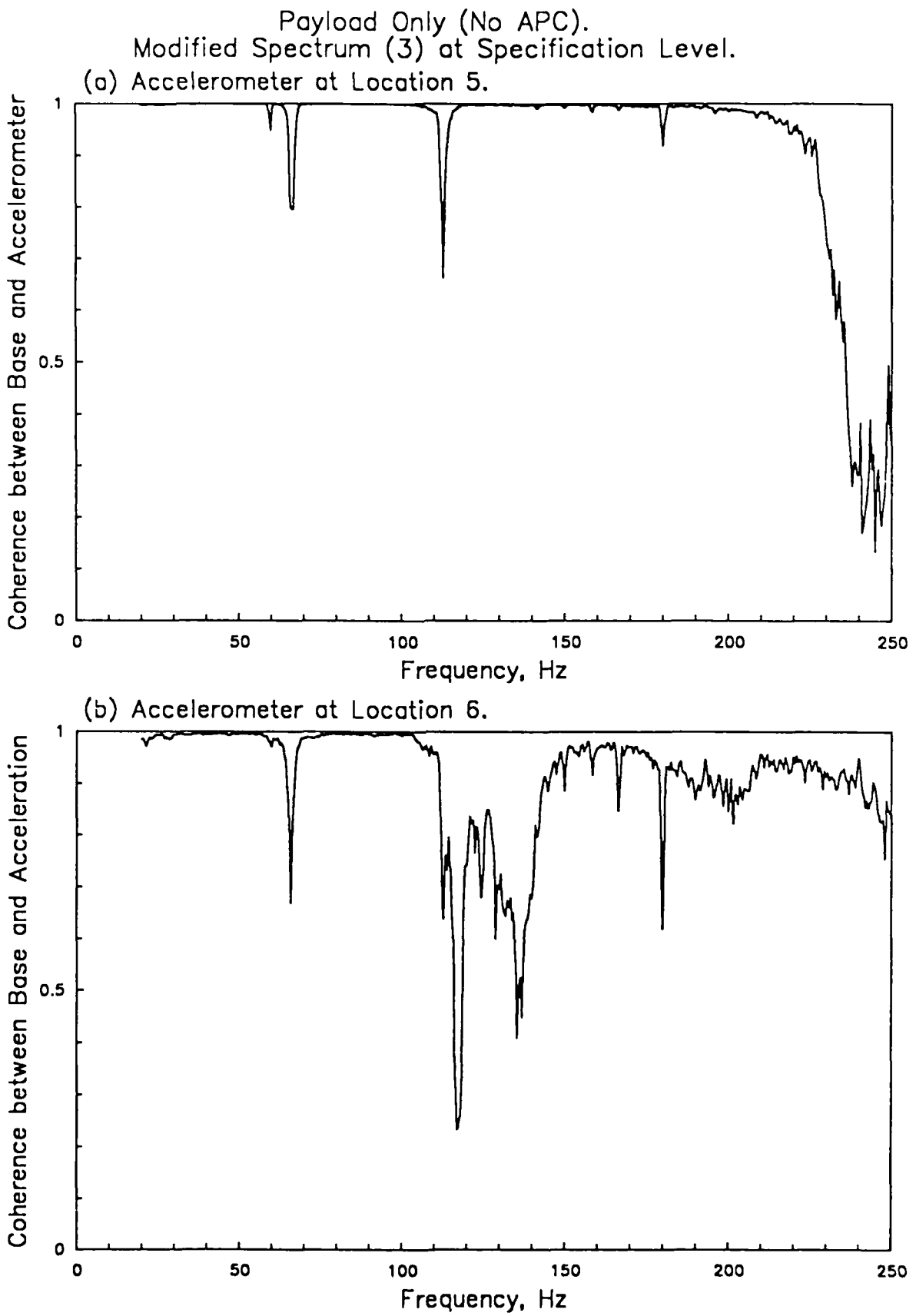

COHERENCE BETWEEN SHAKER BASE AND ACCELEROMETERS 5 AND 6.

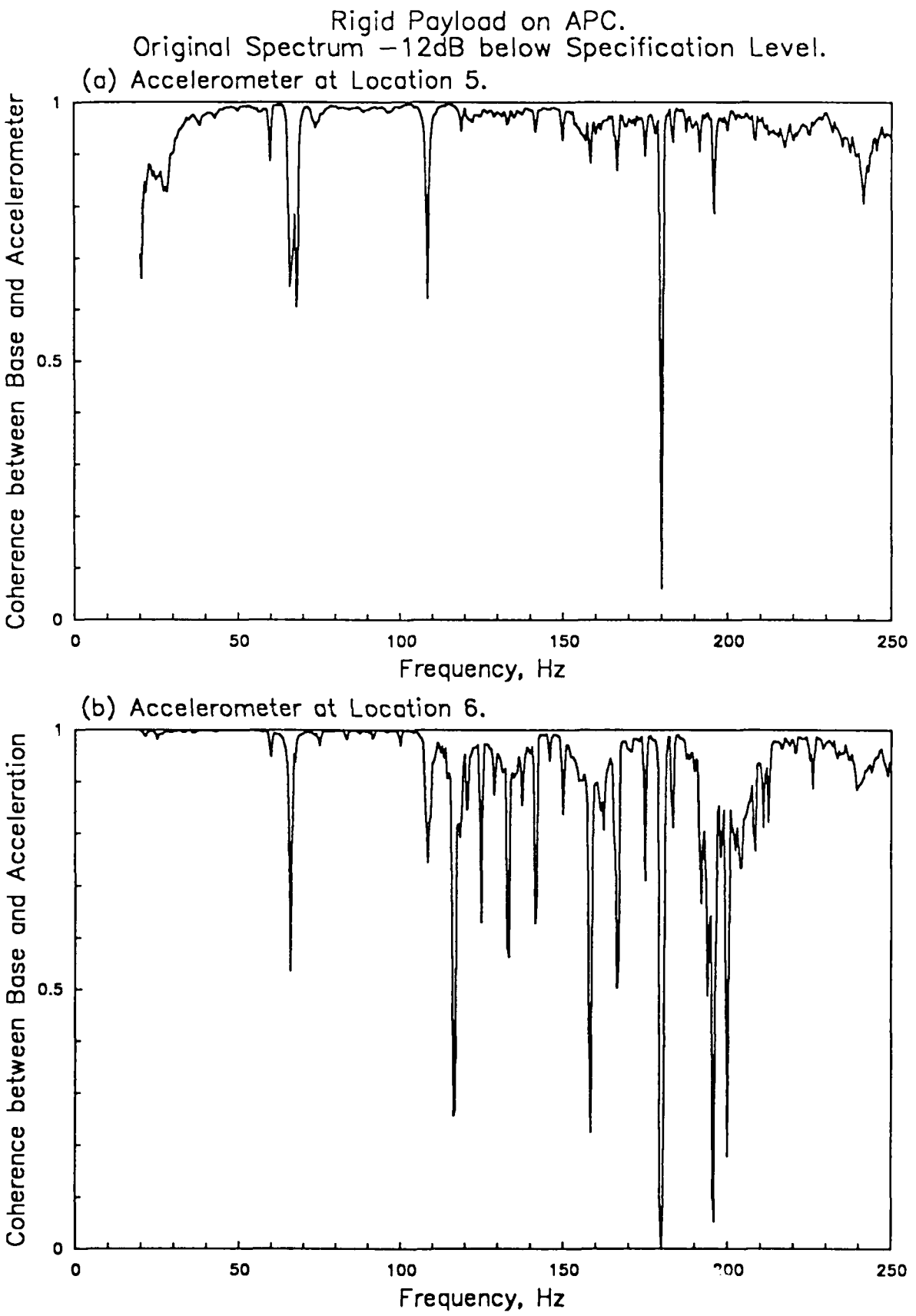

COHERENCE BETWEEN SHAKER BASE AND ACCELEROMETERS 5 AND 6.

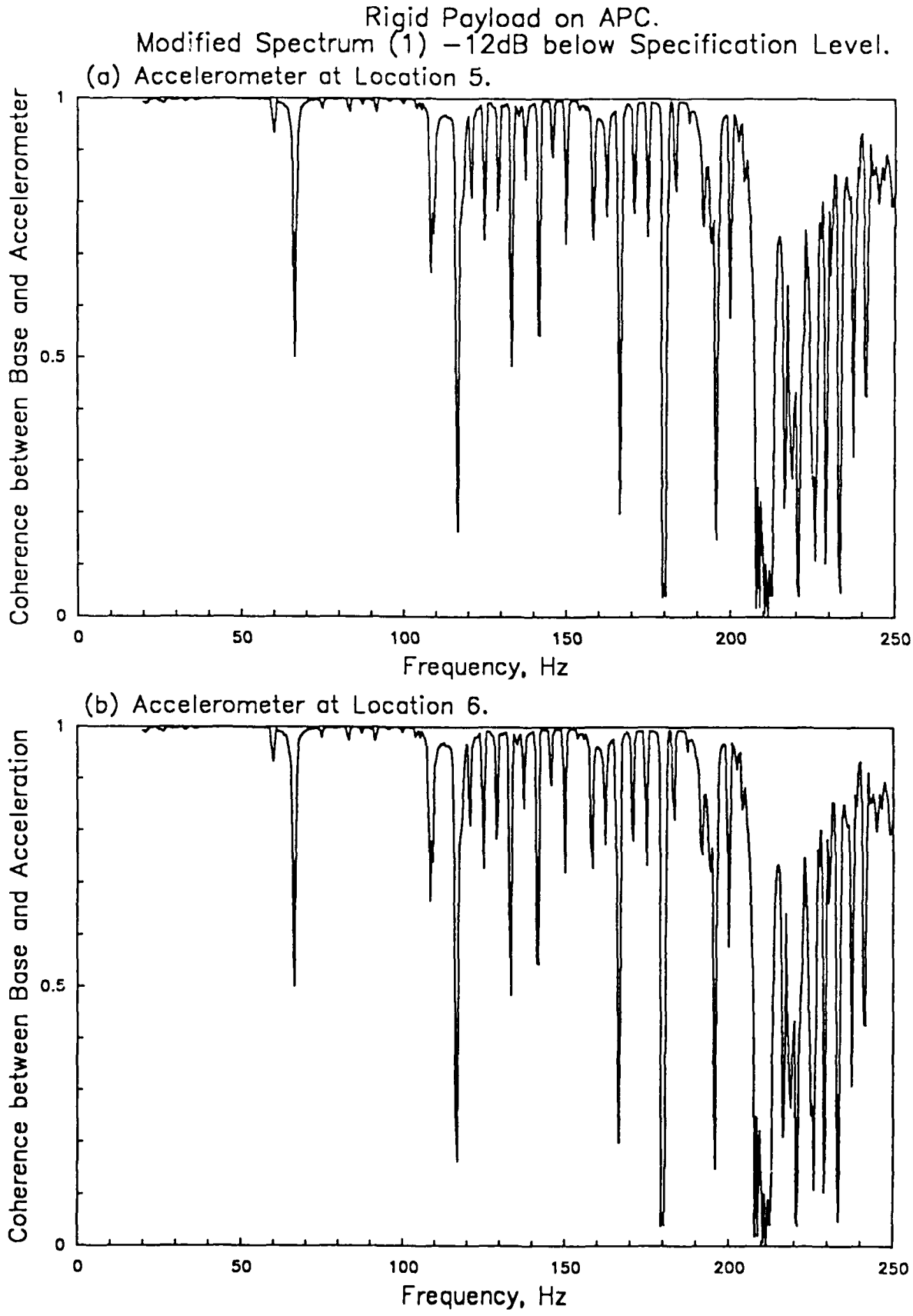

COHERENCE BETWEEN SHAKER BASE AND ACCELEROMETERS 5 AND 6.

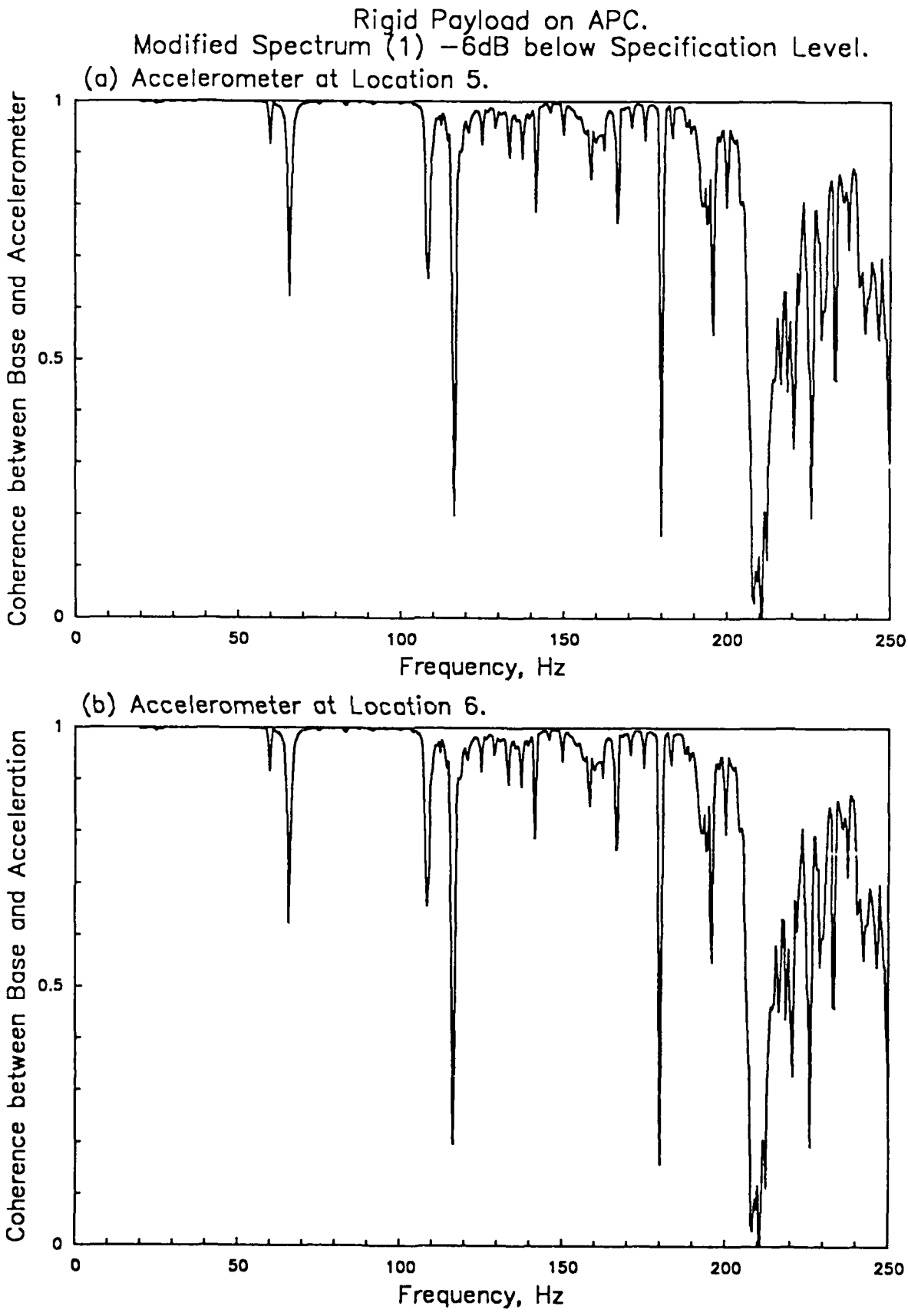

COHERENCE BETWEEN SHAKER BASE AND ACCELEROMETERS 5 AND 6.

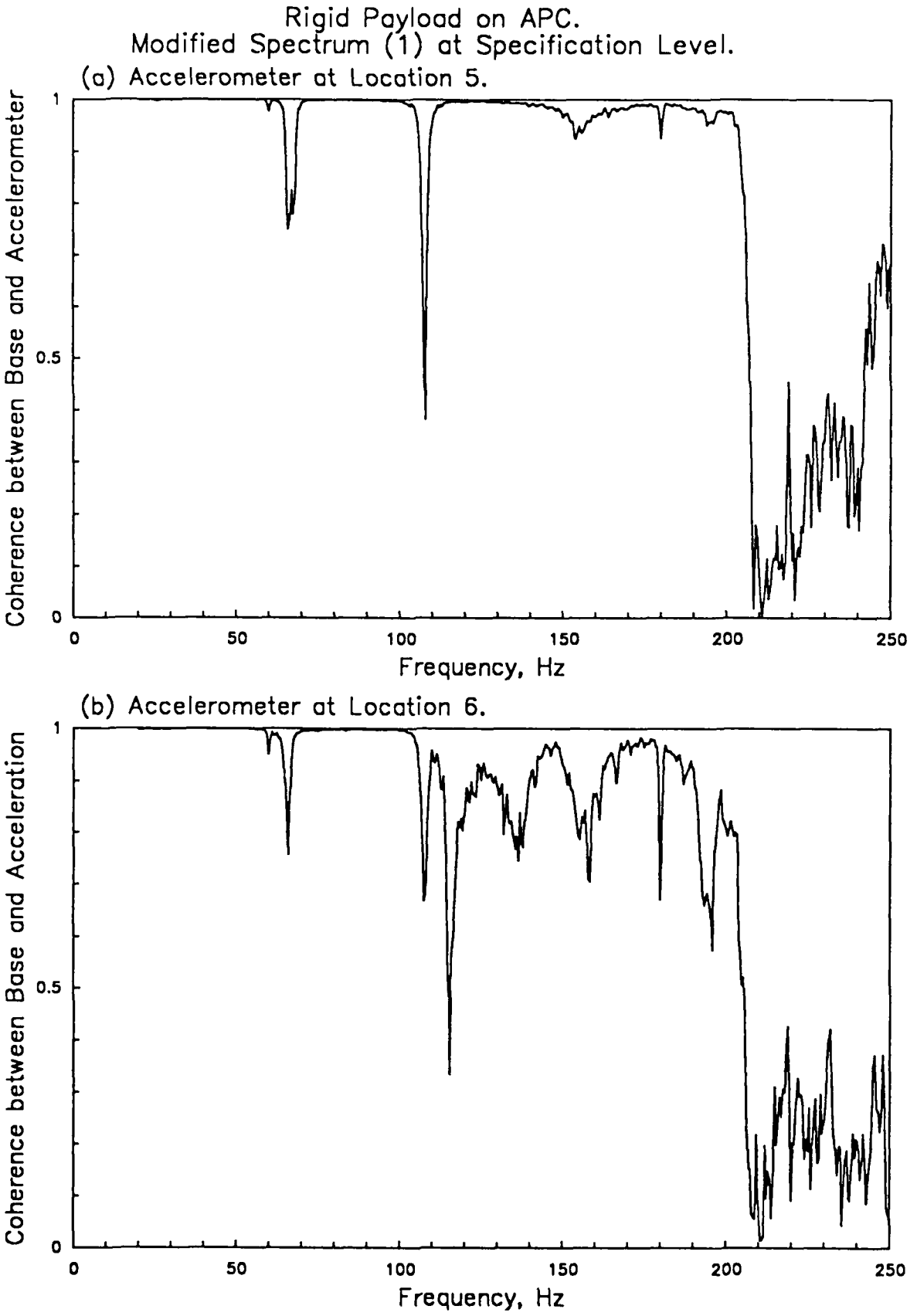

COHERENCE BETWEEN SHAKER BASE AND ACCELEROMETERS 5 AND 6.

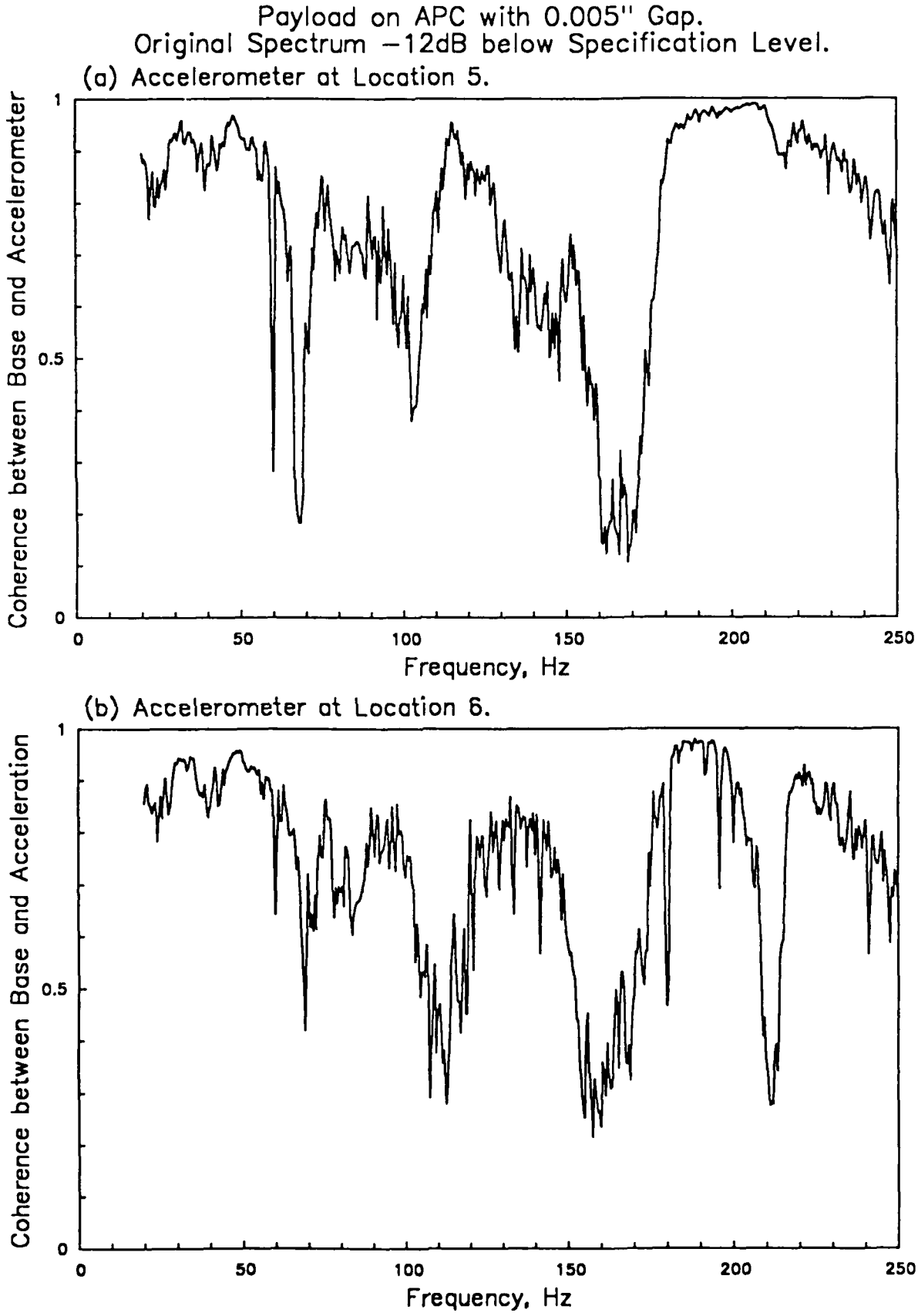

COHERENCE BETWEEN SHAKER BASE AND ACCELEROMETERS 5 AND 6.

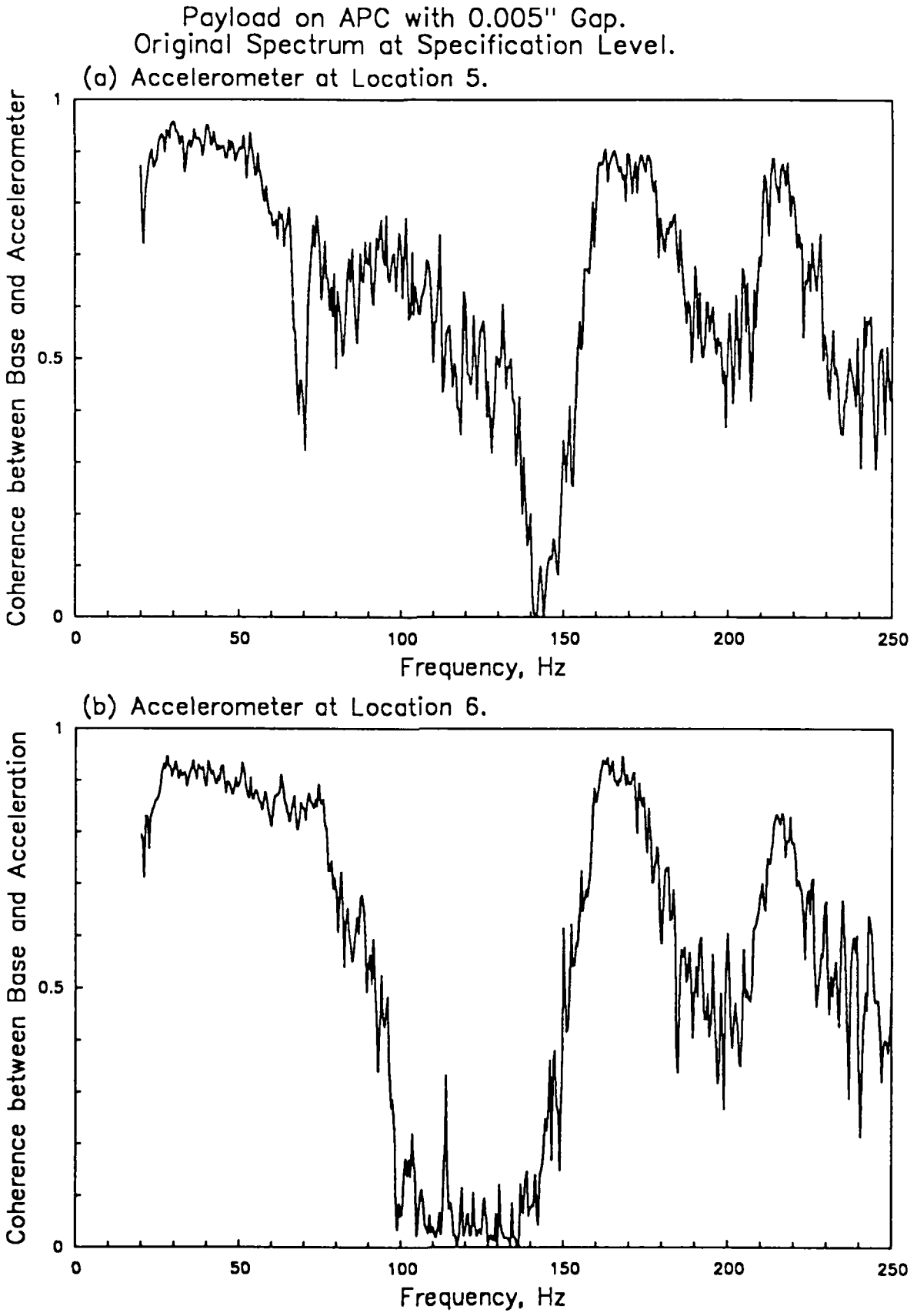

COHERENCE BETWEEN SHAKER BASE AND ACCELEROMETERS 5 AND 6.

ATTACHMENT

to Astron Report 7114-02

VIBRATION TEST SPECIFICATION FOR SSV SIDEWALL MOUNTED PAYLOADS/COMPONENTS

February 1989

Prepared by:

Astron Research and Engineering
3228 Nebraska Avenue
Santa Monica, CA 90404

Prepared for:

USAF/AFSC
HQ Space Division
Los Angeles, CA 90009-2960

Vibration Test Specification for SSV Sidewall Mounted Payloads/Components

1.0 SCOPE

This document provides test levels and durations for the random vibration testing of payloads/components mounted on the SSV cargo bay sidewall. The specified test levels and durations apply to the structure-borne vibration environment of the SSV cargo bay as defined in SD-CF-0206 [1], and do not replace or modify the required testing for the acoustic induced vibration environment detailed in SD-YV-0093 [2].

1.1 Purpose

To formally supply DoD spacecraft SPOs with a definition of the test levels and durations for the random vibration testing of payloads/components mounted on the SSV cargo bay sidewall. This information is needed to fulfill MIL-STD-1540 [3] requirements, and shall be used for developing detailed spacecraft test plans.

1.2 Background

Extensive studies have been performed [4, 5] to develop random vibration testing procedures for SSV cargo bay sidewall mounted payloads/components (hereafter referred to as test items) that account for the mounting point impedance of the sidewall structure. These procedures will suppress the over-testing inherent in conventional vibration test specifications that require a specific acceleration input to the test item without regard for the dynamic response of the test item. The procedures involve controlling the test levels based not only on the acceleration input to the test item, but also the force input to the test item as measured using the test shaker armature current. The procedures are applicable to tests performed with all commercial electrodynamic shaker systems, excluding a few large shakers that use other than a simple wire-wound armature.

2.0 SPECIFIED SHAKER INPUT LEVELS

The specified input levels from the electrodynamic shaker to the test item include two separate input parameters; (a) acceleration, and (b) force. The acceleration specification applies unless the specified force limits are exceeded.

2.1 Input Acceleration Levels

The input (shaker table) acceleration levels for the random vibration test are as specified in Figure 1, taken directly from SD-CF-0206. These input acceleration levels are applicable to all three orthogonal axes of the test item.

2.2 Input Force Levels

The input (fixture-test item interface) force level limits for the random vibration test are as specified in Figure 2. Note that different input force limits apply for the vibration test along the y and z orthogonal axis, and no input force limit applies for the vibration test along the x orthogonal axis of the test item (x, y, and z are the SSV coordinate axes). Further note that the force limits apply only below 200 Hz. The input force levels are computed using the vibration test shaker armature current. Hence, it will be necessary to intercept a signal somewhere in the shaker amplifier system that is proportional to the shaker armature current. The units of amperes (amp) will be assigned to this signal in all equations to follow. However, it is not necessary to calibrate this signal in amp; any units that are proportional to current will suffice since a proper calibration of the current in force units evolves automatically as part of the test level set-up procedure.

3.0 TEST CONFIGURATION

All test items of interest (SSV cargo bay sidewall mounted payloads/components) are designed to mount to the orbiter sidewall through an Adaptive Payload Carrier (APC) or an Increased Capacity Adaptive Payload Carrier (ICAPC), both referred to hereafter as an APC. The most accurate test simulation of the launch phase vibration environment will be achieved if the APC is included as part of the payload; i.e., the test item is attached to the vibration test shaker through the APC that will be used for its service installation. This is desirable because the APC will provide a more realistic mounting point impedance simulation for the test item that will help avoid unreasonable over-testing at resonance frequencies of the test item. However, the inclusion of the APC as part of the test item is not mandatory, and may be omitted if an appropriate APC is not available.

4.0 TEST PROCEDURE

Random vibration tests of SSV cargo bay sidewall mounted payloads/components should be performed using either the recommended procedure, or one of three alternate procedures detailed below.

4.1 Recommended Procedure

The recommended procedure requires a dual control shaker equalizer system that is designed to control both the shaker table acceleration and the input force to the test item. If a dual control equalizer system is available, perform the vibration test along each of the three orthogonal axes of the test item, as follows:

(1) For the specific electrodynamic shaker to be used for the vibration test, compute the shaker armature current-force calibration function, K(f), by the procedure detailed in the appendix to this specification.

Notes: (a). Certain large electrodynamic vibration test systems, particularly those manufactured by Unholtz-Dickie, do not use a conventional wire-wound armature and, thus, do not provide a linear relationship between the armature current and force. This recommended test procedure is not applicable to tests performed on such vibration test systems. The standard procedure in Section 4.4 must be used in these cases.

(b). The shaker armature current-force calibration need be accomplished only once for a specific shaker system. However, it is recommended that the calibration be checked at least once a year using the procedure detailed in the appendix.

(2) Mount the test item (including an APC, if possible) onto the shaker using an appropriate fixture. In most cases, this will be done as follows:

(a) For the tests along the x and z axes (in the plane of the SSV sidewall), attach the test item to the flat, horizontal surface of the moving element of a "slip-table".

(b) For the test along the y axis (normal to the SSV sidewall), attach the test item directly to the shaker table through a solid mounting plate. If the test item has widely separated mounting points, or includes an APC, it may be necessary to use an expansion fixture to properly attach the test item to the shaker table.

(c) If an APC is included as part of the test item, bolt the APC firmly to the shaker table fixture with no loose gaps, but with washers that support the APC at least 0.5 inches above the shaker table fixture.

Note: The APC attaches to the SSV cargo bay sidewall with 2-5 mil gaps at two of its three mounting points, but no effort should be made to simulate these gaps in the vibration test.

(3) Determine the total weight in pounds (denoted by W_T) of the shaker armature and all fixtures used to attach the test item to the shaker (including the moving element of a "slip-table", if used).

Note: The weight of the shaker armature is provided in the shaker manufacturer's literature.

(4) Input the acceleration control channel of the shaker equalizer system with a signal representing the shaker table motion provided by either (a) the calibrated control accelerometer mounted in the shaker table, or (b) any other calibrated accelerometer mounted at one of the test item attachment points.

(5) Input the force control channel of the shaker equalizer system with a signal representing the current in the shaker armature. The force control channel must be set-up to compute the spectrum of the shaker table-test item interface force from

$$|F(f)| = |K(f)\, C(f) - W_T\, A(f)| \qquad (1)$$

where

F(t) = Fourier transform (per unit time) of the desired force equalization signal (lb).

A(f) = Fourier transform (per unit time) of the input (shaker table) acceleration signal (g).

C(f) = Fourier transform (per unit time) of the shaker armature current signal (amp).

K(f) = Shaker armature current-force calibration function (lb/amp), as determined in the appendix.

W_T = Shaker armature and fixture weight (lb), as determined in Step (3).

Notes: (a) The current signal need not be calibrated in amp as long as it is the same signal used to determine the calibration function, K(f).

(b) The calibration function, K(f), can usually be approximated by a real valued constant, K, which simplifies the arithmetic required by Equation (1).

(6) Apply random vibration to the test item with the input acceleration power spectral density (PSD) function specified in Figure 1, except at those frequencies below 200 Hz where the interface force exceeds the limit force PSD specified in Figure 2. At all such frequencies below 200 Hz, the force limit will prevail and the shaker equalizer system will automatically control the vibration input at the force limit specified in Figure 2.

(7) Apply the input random vibration established in Step (6) to the test item for a 60 sec duration.

4.2 Alternate Procedure

If a vibration testing system with a dual control (acceleration and force) equalizer is not available, the vibration test may be performed using the alternate test procedure described in this section. The alternate procedure can be accomplished with any conventional shaker equalizer system that controls the shaker table acceleration. Using the alternate procedure, perform the vibration test along each of the three orthogonal axes of the test item, as follows:

(1) Calibrate the shaker armature current as in Step (1) in Section 4.1.

(2) Mount the test item as in Step (2) in Section 4.1.

(3) Determine the total weight as in Step (3) in Section 4.1.

(4) Establish a control accelerometer as in Step (4) in Section 4.1.

(5) Apply random vibration to the test item with the input acceleration power spectral density (PSD) function detailed in Figure 1, but with a reduced overall input vibration level of 0.83 g_{rms} (-20 dB below the specified overall test level).

(6) At the reduced input acceleration test level established in Step (5), compute the shaker interface force PSD from

$$G_{FF}(f) = |K(f)|^2 G_{CC}(f) + W_T^2 G_{AA}(f) - 2W_T \mathrm{Re}[K(f) G_{CA}(f)] \qquad (2)$$

where

$G_{CC}(f)$ = PSD of shaker armature current signal (amp^2/Hz), as defined by Equation (A.3) in the appendix.

$G_{AA}(f)$ = PSD of shaker table acceleration signal (g^2/Hz), as defined by Equation (A.7) in the appendix.

$G_{CA}(f)$ = Cross-spectral density function between the shaker armature current signal and the shaker table acceleration signal (amp-g/Hz), as defined in Equation (A.3) in the appendix.

$K(f)$ = Shaker armature current-force calibration function (lb/amp), as determined in the appendix.

W_T = Shaker armature and fixture weight (lb), as determined in Step (3).

Re[ ] = Real part of the complex number in [ ].

(7) Compare the force PSD determined in Step (6) with the input limit force PSD specified in Figure 2. If the interface force PSD exceeds 1% (-20 dB) of the limit force PSD specified in Figure 2 at any frequency below 200 Hz, reduce or "notch" the input acceleration PSD given in Figure 1 so that the interface force does not exceed 1% of the limit force at all frequencies below 200 Hz. See Figure 3 for an illustration of the procedure.

Note: If modifications are made to the Figure 1 acceleration PSD, the overall value of the reduced input acceleration will be less than the value of $0.83 g_{rms}$ originally established in Step (5).

(8) Increase the overall input acceleration level by a factor of ten (20 dB) to achieve the full test level.

Note: If modifications were made to the Figure 1 PSD in Step (7), the overall input acceleration level will be less than the specified value of 8.3 g_{rms} given in Figure 1.

(9) Apply the input acceleration PSD established in Step (8) to the test item for a 60 sec duration.

The alternate test procedure detailed above assumes the test item is linear. If there is reason to suspect the test item may have nonlinear response characteristics, Steps (5) through (7) should be repeated at an input level of 2.6 g_{rms} (10 dB below the specified overall test level) before going to the full test level.

4.3 Simplified Alternate Procedure

The recommended and alternate procedures in Section 4.1 and 4.2 will not only prevent over-testing at resonance frequencies of the test item below 200 Hz, but they will also prevent the over-testing of unusually heavy test items; i.e., they will automatically correct for mass loading of the mounting structure by the test item at all frequencies below 200 Hz. However, if the test item is not unusually heavy, the suppression of over-testing at the test item resonances alone can be achieved by a simplified alternate procedure that does not require the calculation of the cross-spectrum between the shaker armature current and the shaker table acceleration signals. Using the simplified alternate procedure, perform the vibration test along each of the three orthogonal axes of the test item as follows:

(1) Calibrate the shaker armature current as in Step (1) in Section 4.1.

(2) Mount the test item as in Step (2) in Section 4.1.

(3) Determine the total weight as in Step (3) in Section 4.1.

(4) Establish a control accelerometer as in Step (4) in Section 4.1.

(5) Apply random vibration to the test item with the input acceleration power spectral density (PSD) function detailed in Figure 1, but with a reduced overall input vibration level of 0.83 g_{rms} (20 dB below the specified overall test level).

(6) At the reduced input acceleration test level established in Step (5), compute the interface force PSD from

$$G_{FF}(f) = |K(f)|^2 G_{CC}(f) + W_T^2 G_{AA}(f) \qquad (3)$$

where

$G_{CC}(f)$ = PSD of shaker armature current signal (amp^2/Hz), as defined by Equation (A.7) in the appendix.

$G_{AA}(f)$ = PSD of shaker table acceleration signal (g^2/Hz), as defined by Equation (A.7) in the appendix.

$K(f)$ = Shaker armature current-force calibration function (lb/amp), as determined in the appendix.

W_T = Shaker armature and fixture weight (lb), as determined in Step (3).

(7) Compare the force PSD determined in Step (6) with the limit force PSD specified in Figure 2. If the interface force PSD exceeds 1% (-20 dB) of the limit force PSD specified in Figure 2 at any frequency below 200 Hz, reduce or "notch" the input acceleration PSD in Figure 1 so that the interface force does not exceed 1% of the limit force at all frequencies below 200 Hz. See Figure 3 for an illustration of the procedure.

Note: If modifications are made to the Figure 1 acceleration PSD, the overall value of the reduced input acceleration will be less than the value of $0.83 g_{rms}$ originally established in Step (5).

(8) Increase the overall input acceleration level by a factor of ten (20 dB) to achieve the full test level.

Note: If modifications were made to the Figure 1 PSD in Step (5), the overall input acceleration level will be less than the specified value of 8.3 g_{rms} given in Figure 1.

(9) Apply the input acceleration PSD established in Step (8) to the test item for a 60 sec duration.

As for the alternate test procedure in Section 4.2, the simplified alternate test procedure detailed above assumes the test item is linear. If there is reason to suspect the test item may have nonlinear response characteristics, Steps (5) through (7) should be repeated at an input level of 2.6 g_{rms} (10 dB below the specified overall test level) before going to the full test level.

4.4 Standard Test Procedure

There may be cases where the recommended or alternate test procedures in Sections 4.1 through 4.3 cannot be performed or are not desired for various reasons, including the following:

(a) The available vibration test shaker is of a type that cannot be force-calibrated because it does not provide a linear relationship between armature current and force.

(b) The test item has no resonance frequencies below 200 Hz.

(c) The test item is believed to be sufficiently rugged to withstand the possible over-testing at resonance frequencies below 200 Hz.

In these cases, a conventional input acceleration controlled random vibration test may be performed on the test item along each of the three orthogonal axes, as follows:

(1) Mount the test item onto the shaker table using an appropriate fixture, as detailed in Step 1 of Section 4.1.

(2) Using a control accelerometer mounted in the shaker table (or at one of the test item attachment points) as a measure of the input vibration level, apply random vibration with the input acceleration PSD and overall value detailed in Figure 1 for a 60 sec duration.

References

1. "Definition of SSV Structure-Borne Vibration Environment For DoD Payloads", SD-CF-0206, US Air Force Space Division, Los Angeles, CA, 12 January 1987.

2. "Acoustic Requirements For DoD Shuttle Payloads Launched From KSC", SD-YV-0093, US Air Force Space Division, Los Angeles, CA, 9 June 1982.

3. "Test Requirements For Space Vehicles", MIL-STD-1540B (USAF), 10 October 1982.

4. "Vibration Test Procedures For Orbiter Sidewall-Mounted Payloads: Phase I Final Report", Report No. 7114-01, Astron Research and Engineering, Santa Monica, CA, March 1988.

5. "Vibration Test Procedures For Orbiter Sidewall-Mounted Payloads: Phase II Final Report", Report No. 7114-02, Astron Research and Engineering, Santa Monica, CA, January 1989.

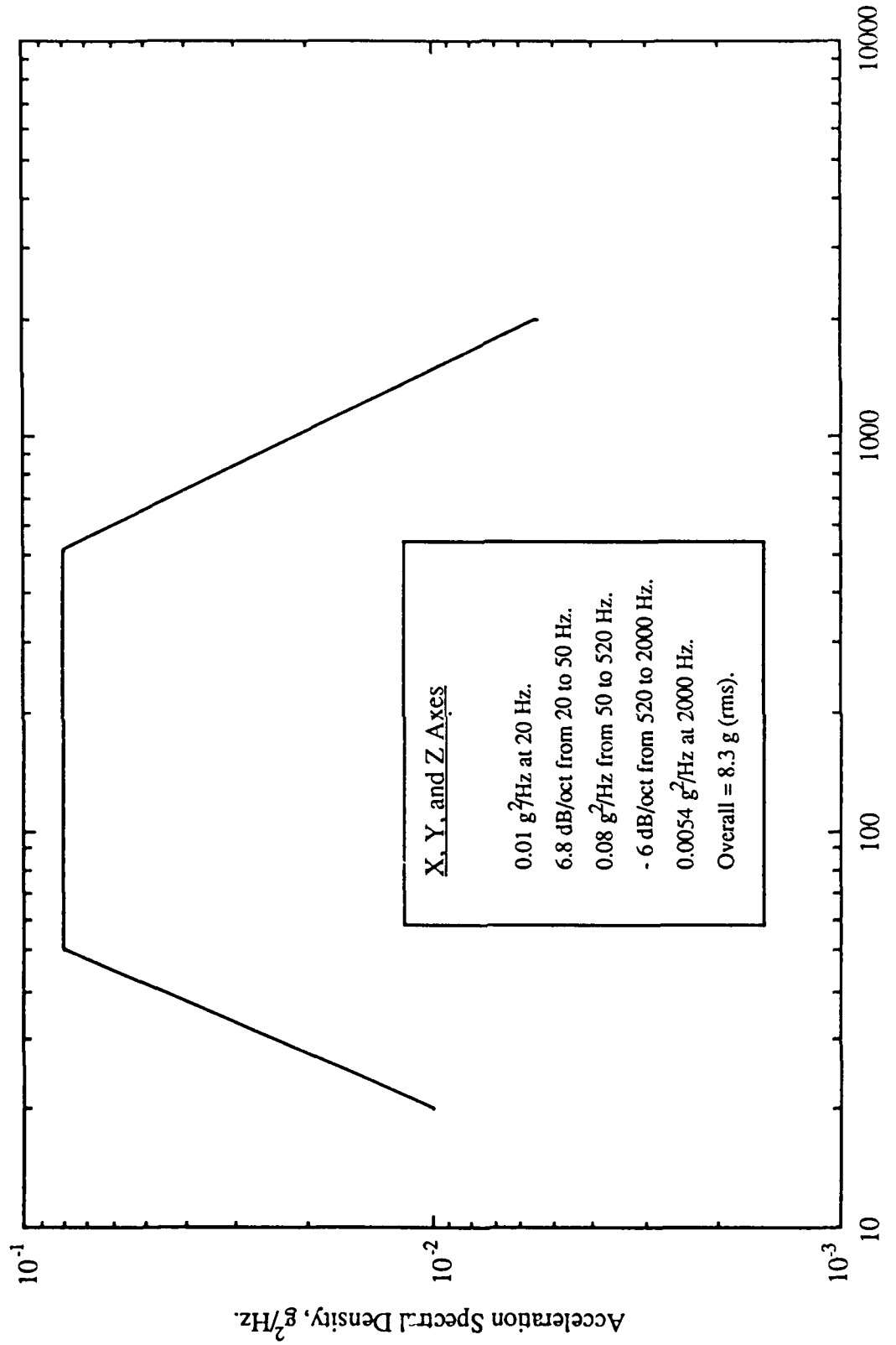

Figure 1. Acceleration Input For Vibration Testing Of SSV Cargo Bay Sidewall Mounted Payloads/Components.

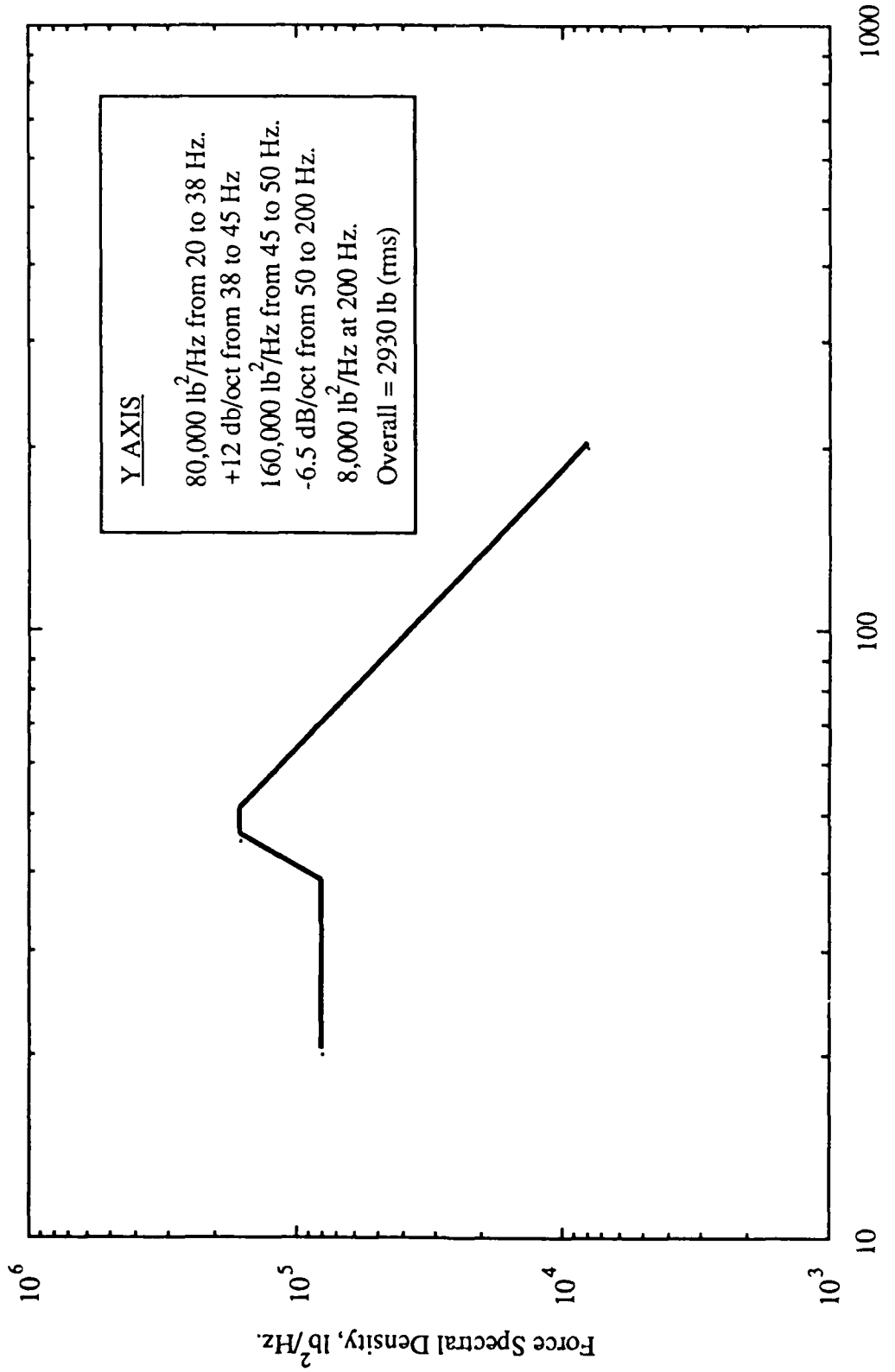

Figure 2a. Y Axis Limit Force Input For Vibration Of SSV Cargo Bay Sidewall Mounted Payloads/Components.

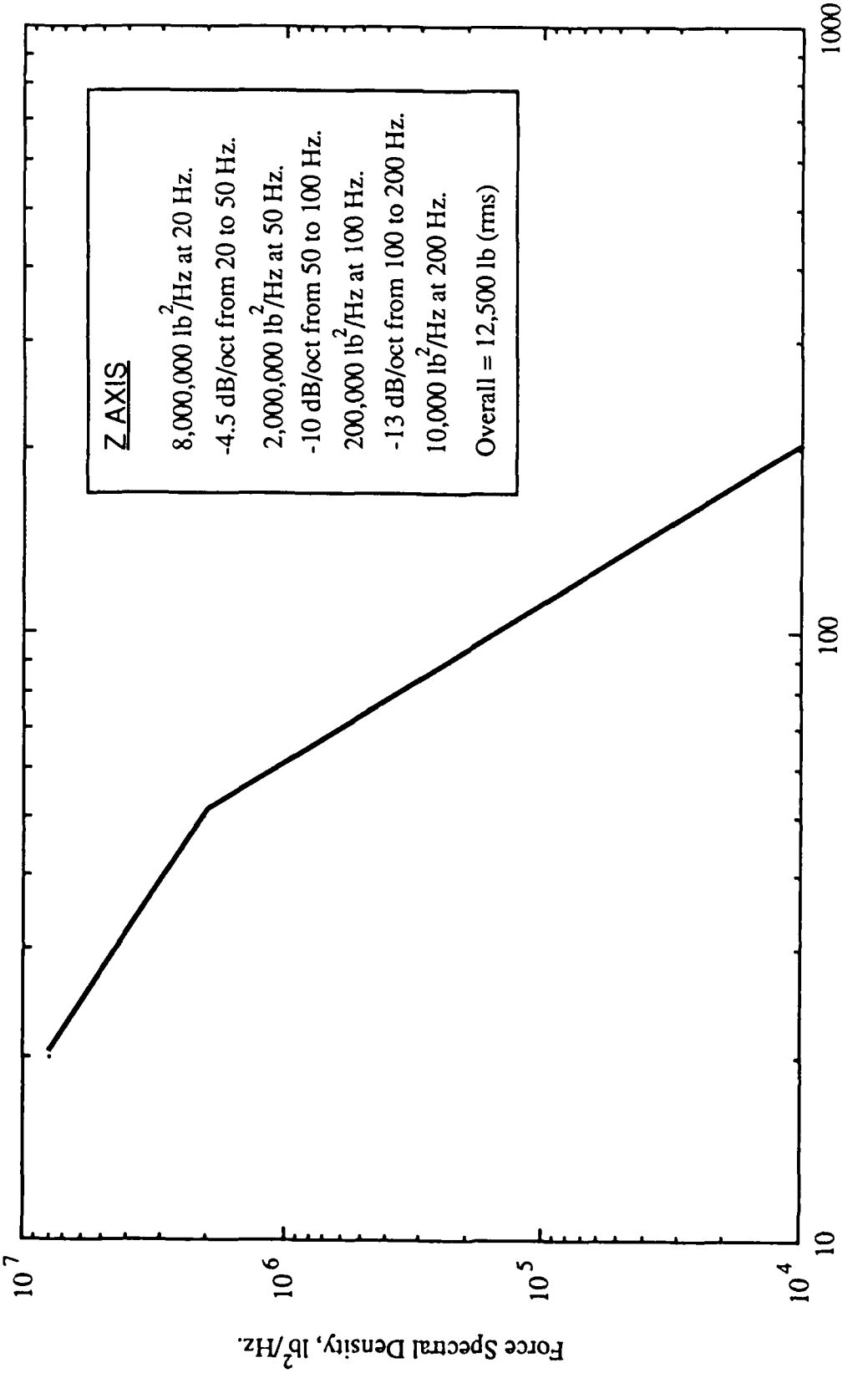

Figure 2b. Z Axis Limit Force Input For Vibration Testing Of SSV Cargo Bay Sidewall Mounted Payloads/Components.

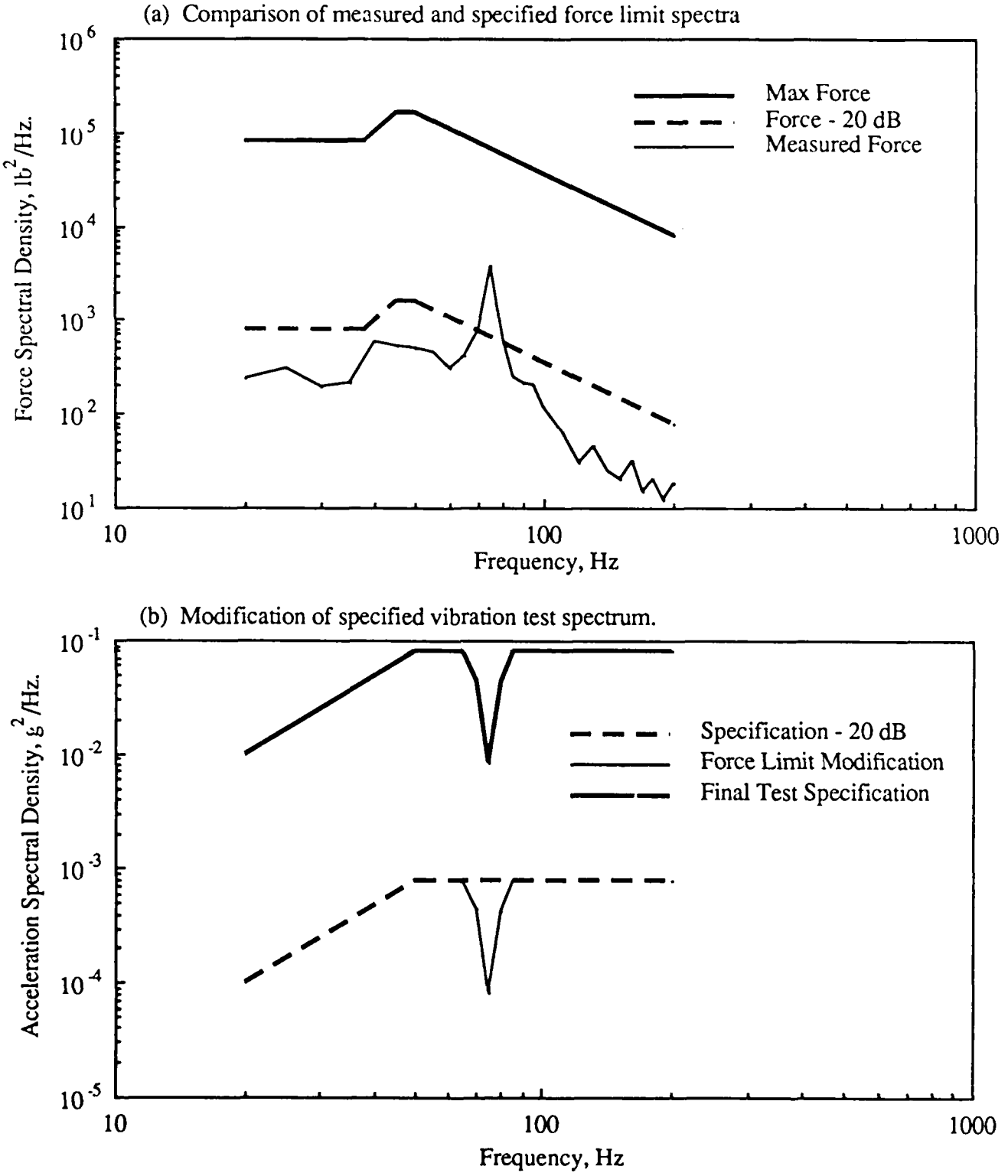

Figure 3. Illustration of Test Spectrum Modification Based Upon Alternate Test Procedure.

APPENDIX

FORCE CALIBRATION OF ELECTRODYNAMIC VIBRATION TEST SHAKER

To perform a random vibration test using force limiting procedures, it is necessary to calibrate the shaker armature current to indicate the shaker-test item interface force. This calibration can be performed on any commercial electrodynamic shaker with a wire-wound armature. For such shakers, the armature current is proportional to the force delivered by the shaker [A.1, A.2]. Assuming the shaker armature and all fixtures below the test item interface are rigid in the frequency range of interest (0 to 200 Hz), the relationship between current and interface force is given in the frequency domain (using Fourier transforms) by [A.1]

$$F(f) = K(f)C(f) - W_T A(f) \qquad (A.1)$$

where

$C(f)$ = Fourier transform of the shaker armature current (amp-sec or units proportional to amp-sec).

$A(f)$ = Fourier transform of the shaker table acceleration (g-sec).

W_T = Total weight of the shaker armature and all fixtures used to attach the test item to the shaker, including the moving element of a "slip-table", if used (lb).

$F(f)$ = Fourier transform of the shaker fixture-test item interface force (lb-sec).

$K(f)$ = Shaker armature current-force calibration function (lb/amp).

The calibration function, $K(f)$, is determined as follows:

(1) Mount rigidly to the shaker table a dead load, such as a block of steel or lead, that has no resonance frequencies below 500 Hz. The weight of the dead load should be at least 20% of the weight of the test item.

(2) Determine the total weight , W_T, of the dead load, the shaker armature, and all fixtures (including the moving element of a "slip-table", if used) that will be employed to attach the test item to the shaker. The weight of the shaker armature is provided in the shaker manufacturer's specifications.

(3) Apply a random excitation to the shaker over a frequency range exceeding 0 to 200 Hz to produce a shaker table acceleration with the autospectrum given in Figure 1.

(4) Compute the frequency response function between the shaker armature current and the shaker table acceleration given by

$$H_{CA}(f) = G_{CA}(f)/G_{CC}(f) \qquad (A.2)$$

where

$G_{CA}(f)$ = Cross-spectral density (CSD) function between the armature current and the table acceleration (amp-g/Hz).

$G_{CC}(f)$ = Power spectral density (PSD) function of the armature current (amp^2/Hz).

The CSD and PSD functions are estimated by

$$G_{CA}(f) = \sum_{i=1}^{n_d} C_i(f)A_i^*(f)/(n_dT) \quad ; \quad G_{CC}(f) = \sum_{i=1}^{n_d} C_i(f)C_i^*(f)/(n_dT) \qquad (A.3)$$

where

$C_i(f)$ = Fourier transform of the ith segment of the armature current signal (amp-sec).

$C_i^*(f)$ = Complex conjugate of $C_i(f)$

$A_i^*(f)$ = Complex conjugate of Fourier transform of the ith segment of the shaker table acceleration (g-sec).

T = Duration of each signal segment (sec).

n_d = Number of disjoint (uncorrelated) signal segments used for the averaging operations.

Note: Some textbooks (e.g., [A.3]) define the cross-spectral density function, $G_{CA}(f)$, as the average of $C_i^*(f)A_i(f)$, rather than $C_i(f)A_i^*(f)$ as shown in Equation (A.3). However, many special purpose signal analysis instruments use the convention in Equation (A.3). Since $G_{CA}(f) = G^*_{AC}(f)$, the alternate convention simply reverses the sign of the phase portion of $G_{CA}(f)$, and poses no problem in the calibration as long as the cross-spectral density function used to establish vibration test levels in Section 4.2 is calculated with the same convention.

(4) Compute the calibration function, K(f), from

$$K(f) = W_T H^*_{CA}(f) = W_T H_{AC}(f) \qquad (A.4)$$

A computed Fourier spectrum for the shaker current, C(f), can now be converted to a Fourier spectrum for the fixture-test item interface force, F(f), by

$$F(f) = K(f)C(f) \qquad (A.5)$$

(5) To check the validity of the measurements and the assumption of linearity between the shaker armature current and the shaker table acceleration, compute the coherence function between the current and acceleration signals given by

$$\gamma^2_{CA}(f) = |G_{CA}(f)|^2 / G_{CC}(f) G_{AA}(f) \quad (A.6)$$

where $G_{AA}(f)$ is the autospectral density function of the shaker table acceleration defined by

$$G_{AA}(f) = \sum_{i=1}^{n_d} A_i(f) A_i^*(f) / (n_d T) \quad (A.7)$$

All terms in Equation (A.7) are as previously defined in Equation (A.3). The coherence function, $\gamma^2_{CA}(f)$, should exceed 0.95 at all frequencies below 200 Hz for a valid force calibration of the shaker.

Reference

A.1. "Vibration Test Procedures For Orbiter Sidewall-Mounted Payloads: Phase I Final Report", Report No. 7114-01, Astron Research and Engineering, Santa Monica, CA, March 1988.

A.2. "Vibration Test Procedures For Orbiter Sidewall-Mounted Payloads: Phase II Final Report", Report No. 7114-02, Astron Research and Engineering, Santa Monica, CA, January 1989.

A.3. Bendat, J. S., and Piersol, A. G., *RANDOM DATA: Analysis and Measurement Procedures*, pp. 130-132, Wiley, New York, 1986.